THE UNIVERSITY OF ALBERTA

EXPERIMENTAL EVALUATION OF PREDICTOR CONTROL SCHEMES FOR DISTILLATION COLUMN CONTROL

BY

© CHRISTOPH B. G. MEYER

A THESIS

SUBMITTED TO THE FACULTY OF GRADUATE STUDIES AND RESEARCH

IN PARTIAL FULFILMENT OF THE REQUIREMENTS FOR THE DEGREE

OF MASTER OF SCIENCE

IN

PROCESS CONTROL (CHEMICAL ENGINEERING)

DEPARTMENT OF CHEMICAL ENGINEERING

EDMONTON, ALBERTA

FALL, 1977

UNIVERSITY OF ALBERTA

FACULTY OF GRADUATE STUDIES AND RESEARCH

The undersigned certify that they have read, and recommend to the Faculty of Graduate Studies and Research, for acceptance, a thesis entitled EXPERIMENTAL EVALUATION OF PREDICTOR CONTROL SCHEMES FOR DISTILLATION COLUMN CONTROL submitted by Christoph B. G. Meyer, Dipl. Chem.-Ing. ETH, in partial fulfilment of the requirements for the degree of Master of Science.

.....

(Supervisor)

.....

.....

.....

Date ...May 30.....1977.

ABSTRACT

Two different predictor control schemes, the Smith predictor and the analytical predictor, have been compared with conventional proportional plus integral (PI) control for the composition control of a binary distillation column. Conventional PI control, where the top composition is controlled by the reflux flow rate or the bottoms composition by means of the reboiler heat duty, is poor due to the time delays present in the process.

The performance of the control schemes has been studied for step disturbances in composition setpoint and feed flow rate. Since this study was restricted to single input, single output control schemes, only one of the product compositions was controlled in each run in order to eliminate interaction between the control loops.

The experimental evaluation was carried out using a 22.9 cm diameter, 8 tray pilot scale distillation column interfaced with an IBM 1800 digital computer. First order plus time delay transfer function models were used to represent the dynamic behaviour of the distillation column. These process models were employed in a digital simulation study of the control schemes and also served as the predictor models in the experimental application of the Smith predictor and the analytical predictor.

The simulation results showed that for the ideal case of no modelling errors a very significant improvement in the control of both product compositions was achieved by using predictor control as compared to PI control. In the experiments improved performance was obtained using the predictor control schemes in spite of serious model errors caused by the approximation of the nonlinear column dynamics by first order plus time delay predictor models. The comparison of the two predictor

control schemes showed that in the simulations the analytical predictor was superior to the Smith predictor, especially for load disturbances. In the experimental application to the pilot scale distillation column the performance of the predictor control schemes was quite similar for top composition control. For bottom composition control, however, the analytical predictor provided a significant improvement over the Smith predictor for composition setpoint and feed flow rate disturbances.

ACKNOWLEDGMENTS

The author wishes to express his gratitude to Dr. D.E. Seborg and Dr. R.K. Wood for their assistance and guidance during the project. The assistance of the staff associated with the DACS Centre, instrument and mechanical shops is also gratefully acknowledged. A special note of thanks is in order to the author's fellow graduate student, U. Simonsmeier, for the work he did in developing the automatic liquid sampling and chromatographic analysis of the bottoms composition. The financial support received from the National Research Council during much of the project is also gratefully acknowledged.

TABLE OF CONTENTS

		PAGE
CHAPTER 1:	INTRODUCTION	1
CHAPTER 2:	LITERATURE SURVEY OF PREDICTOR CONTROL SCHEMES	3
	2.1 Introduction	3
	2.2 Literature Survey	5
	2.2.1 Smith Predictor	5
	2.2.2 Analytical Predictor	7
	2.2.3 Other Predictor Control Schemes	8
CHAPTER 3:	APPLICATION OF PREDICTOR CONTROL TO A PILOT SCALE DISTILLATION COLUMN	9
	3.1 Description of the Equipment	9
	3.2 Process Models	10
	3.3 Incentives for Predictor Control	13
	3.4 Digital Predictor Control Algorithms	14
	3.4.1 Smith Predictor	14
	3.4.1.1 Smith Predictor with Load Estimation	19
	3.4.2 Analytical Predictor	22
	3.4.2.1 Optimal Controller Constants	29
	3.5 Computer Requirements	31
CHAPTER 4:	DIGITAL SIMULATION STUDY	33
	4.1 Simulation Programs	34
	4.2 Controller Tuning	35
	4.3 Top Composition Control	37
	4.3.1 The Influence of Model Errors	43
	4.4 Bottom Composition Control	51
	4.5 Discussion of Results	56
	4.5.1 Conclusions	57

TABLE OF CONTENTS (Continued)

		PAGE
CHAPTER 5:	EXPERIMENTAL EVALUATION	59
5.1	Implementation of the Control Schemes	59
5.2	Process Models for the Experimental Operating Conditions	60
5.3	Controller Tuning	66
5.4	Top Composition Control	68
5.5	Bottom Composition Control	82
5.5.1	Use of the Reboiler Temperature	107
5.6	Comparison of Experimental and Simulation Results	119
5.6.1	Simulations with the Experimental Process Models	119
5.6.2	Comparison with Experiments	129
5.7	Conclusions from the Experimental Results	136
CHAPTER 6:	CONCLUSIONS AND RECOMMENDATIONS	138
	NOTATION	141
	REFERENCES	143
	APPENDICES	
A.	A Comparison of the Smith Predictor and Conventional PI Control	148
B.	Derivation of the Proportional-Integral Analytical Predictor Algorithm	164
C.	Derivation of the Steady State Closed-loop Gain of the Proportional Analytical Predictor Control Scheme	167
D.	Digital Simulation Programs	170
E.	Implementation and Loop Record	176
F.	Control Subroutines for SP, AP, and PI Control	182
G.	Typical Steady State Operating Conditions	186
H.	T-X Diagram for the Methanol-Water System	189

LIST OF TABLES

NUMBER	TITLE	PAGE
3-1	Transfer Function Models Used in Previous Studies	12
3-2	Smith Predictor Control Algorithm	18
3-3	Smith Predictor Control Algorithm with Load Prediction	21
3-4	Proportional Analytical Predictor Algorithm	25
3-5	Proportional-Integral Analytical Predictor Algorithm	28
3-6	Digital PI Control Algorithm	28
4-1	Calculated Controller Constants for Top Composition Control	38
4-2	Simulation Results for Top Composition Control (1% Step Increase in Setpoint)	39
4-3	Simulation Results for Top Composition Control (20% Step Increase in Feed Flow)	39
4-4	Simulation Results for Top Composition Control (Series of Arbitrary Square Pulses in Feed Flow)	39
4-5	Simulation Results Illustrating the Effects of Model Errors on Top Composition Control (1% Step Increase in Setpoint)	45
4-6	Simulation Results Illustrating the Effects of Model Errors on Top Composition Control (20% Step Increase in Feed Flow)	46
4-7	Calculated Controller Constants for Bottom Composition Control	52
4-8	Simulation Results for Bottom Composition Control (1% Step Increase in Setpoint)	54
4-9	Simulation Results for Bottom Composition Control (6% Step Increase in Feed Flow)	54
5-1	Typical Steady State Operating Conditions	61
5-2	Process Models for the Distillation Column	63
5-3	Comparison of Calculated and Experimental Controller Constants	67
5-4	Summary of Experimental Results for Top Composition Control (1% Step Decrease in Setpoint)	69

LIST OF TABLES (Continued)

5-5	Summary of Experimental Results for Top Composition Control (22% Step Decrease in Feed Flow)	78
5-6	Summary of Experimental Results for Bottom Composition Control (2% Step Changes in Setpoint)	85
5-7	Summary of Experimental Results for Bottom Composition Control (17% Step Changes in Feed Flow)	86
5-8	Summary of Experimental Results for Reboiler Temperature Control (2°C Step Increase in Setpoint)	110
5-9	Summary of Experimental Results for Reboiler Temperature Control (17% Step Decrease in Feed Flow)	110
5-10	Simulation Results Using the Process Models Used in this Study Given in Table 5-2	120

LIST OF FIGURES

NUMBER	TITLE	PAGE
2-1	Block Diagram for a Continuous Feedback Control System Containing Time Delays	3
2-2	Block Diagram for a Discrete Predictor Control System Containing Time Delays	4
2-3	Block Diagram of the Continuous Smith Predictor Control Scheme	6
3-1	Schematic of the Distillation Column Control Scheme	11
3-2	Discrete Smith Predictor Control Scheme	14
3-3	Representation of Sampling Process	16
3-4	Discrete Smith Predictor with Load Prediction	19
3-5	Block Diagram of the Analytical Predictor	22
4-1	Block Diagram of the Simulated Control System	33
4-2	Comparison of SP, AP and PI Control for a 1% Step Increase in Setpoint	40
4-3	Comparison of SP, AP and PI Control for a 20% Step Increase in Feed Flow	40
4-4	Comparison of SP, AP and PI Control for a Series of Arbitrary Step Changes of ± 20% in Feed Flow	41
4-5,4-6	Influence of Model Errors on the SP for a 1% Step Increase in Setpoint	47
4-7,4-8	Influence of Model Errors on the SP for a 20% Step Increase in Feed Flow	48
4-9, 4-10	Influence of Model Errors on the AP for a 1% Step Increase in Setpoint	49
4-11, 4-12	Influence of Model Errors on the AP for a 20% Step Increase in Feed Flow	50
4-13	Comparison of SP, AP and PI Control for a 1% Step Increase in Setpoint	55
4-14	Comparison of SP, AP and PI Control for a 6% Step Increase in Feed Flow	55
5-1,5-2	Comparison of Simulated and Experimental Open-loop Responses for the Top Composition	64

LIST OF FIGURES (Continued)

5-3,5-4	Comparison of Simulated and Experimental Open-loop Responses for the Bottom Composition	65
5-5	PI Control of the Top Composition (-1% Setpoint Change)	70
5-6 to 5-8	SP Control of the Top Composition (-1% Setpoint Change)	71-73
5-9 to 5-12	AP Control of the Top Composition (-1% Setpoint Change)	74-77
5-13	PI Control of the Top Composition (-22% Feed Flow Change)	79
5-14	SP Control of the Top Composition (-22% Feed Flow Change)	80
5-15	AP Control of the Top Composition (-22% Feed Flow Change)	81
5-16	Steady State GC Measurements of the Bottom Composition at Two Different Operating Conditions of the Distillation Column	84
5-17	PI Control of the Bottom Composition (+2% Setpoint Change)	87
5-18 to 5-20	SP Control of the Bottom Composition (+2% Setpoint Change)	88-90
5-21 to 5-23	AP Control of the Bottom Composition (+2% Setpoint Change)	91-93
5-24	PI Control of the Bottom Composition (-2% Setpoint Change)	94
5-25	SP Control of the Bottom Composition (-2% Setpoint Change)	95
5-26, 5-27	AP Control of the Bottom Composition (-2% Setpoint Change)	96-97
5-28	PI Control of the Bottom Composition (+17% Feed Flow Change)	98
5-29	SP Control of the Bottom Composition (+17% Feed Flow Change)	99
5-30, 5-31	AP Control of the Bottom Composition (+17% Feed Flow Change)	100 -101
5-32	PI Control of the Bottom Composition (-17% Feed Flow Change)	102
5-33, 5-34	SP Control of the Bottom Composition (-17% Feed Flow Change)	103 -104

LIST OF FIGURES (Continued)

5-35, 5-36	AP Control of the Bottom Composition (-17% Feed Flow Change)	105 -106
5-37	PI Control of the Reboiler Temperature (+2°C Setpoint Change)	111
5-38	SP Control of the Reboiler Temperature (+2°C Setpoint Change)	112
5-39, 5-40	AP Control of the Reboiler Temperature (+2°C Setpoint Change)	113 -114
5-41	PI Control of the Reboiler Temperature (-17% Feed Flow Change)	115
5-42	SP Control of the Reboiler Temperature (-17% Feed Flow Change)	116
5-43, 5-44	AP Control of the Reboiler Temperature (-17% Feed Flow Change)	117 -118
5-45	Simulation of the Top Composition Control Using PI Control	121
5-46	Simulation of the Top Composition Control Using the SP	122
5-47	Simulation of the Top Composition Control Using the AP	123
5-48	Simulation of the Bottom Composition Control Using PI Control	124
5-49	Simulation of the Bottom Composition Control Using the SP	125
5-50	Simulation of the Bottom Composition Control Using the AP	126
5-51	Comparison of the Control Action (Reflux Flow) for a Setpoint Change of -1% in Top Composition Using PI Control and the AP	128
5-52, 5-53	Comparison of the Experimental and Simulated Responses of the Top Composition Using PI Control	130
5-54, 5-55	Comparison of the Experimental and Simulated Responses of the Top Composition Using SP Control	131
5-56, 5-57	Comparison of the Experimental and Simulated Responses of the Top Composition Using AP Control	132

LIST OF FIGURES (Continued)

5-58, 5-59	Comparison of the Experimental and Simulated Responses of the Bottom Composition Using PI Control	133
5-60, 5-61	Comparison of the Experimental and Simulated Responses of the Bottom Composition Using SP Control	134
5-62, 5-63	Comparison of the Experimental and Simulated Responses of the Bottom Composition Using AP Control	135

CHAPTER 1

INTRODUCTION

The effort that has been spent during the last years in studying the dynamics and control of distillation units is well demonstrated by the scope of the recent book by Rademaker et al. (38), but still a number of problems in this field remain to be solved.

For the pilot scale distillation column at the University of Alberta recent work has concentrated on terminal composition control using multivariable control strategies to deal with the interaction between the control variables (4,18). In industrial distillation units, however, single variable feedback control is still the most common control system encountered. Problems that arise include the deterioration of the control performance due to the inherent time delay of the process. Consequently it appears to be rewarding to investigate control techniques that compensate for time delays.

The objective of this work is to evaluate predictive control schemes for the pilot scale distillation column. The two schemes to compensate for system time delays that are considered are the Smith predictor (43, 44) and the analytical predictor (28-30). Since the first order plus time delay process models that are used as predictor models are a common representation of many chemical processes, the conclusions should be applicable to other processes as well. It should be noted that a distillation column which is inherently nonlinear, is a difficult but realistic process for the evaluation of predictor control.

The thesis is organized in three parts: Chapters 2 and 3 present the theory necessary for the application of the predictor control schemes; Chapter 4 gives simulation results for the ideal case of a perfect predictor model and the more realistic case where modelling errors are present, and Chapter 5 contains the results of the experimental application to the pilot scale distillation column. The overall conclusions concerning utilization of the two predictor control schemes are summarized in Chapter 6.

CHAPTER 2

LITERATURE SURVEY OF PREDICTOR CONTROL SCHEMES

2.1 Introduction

For a process with a time delay causing unacceptable deterioration of the control behaviour it is appropriate to devise some means to compensate for the detrimental influence on the system stability. Figure 2-1 shows the block diagram for a continuous feedback control system containing process and measurement time delays.

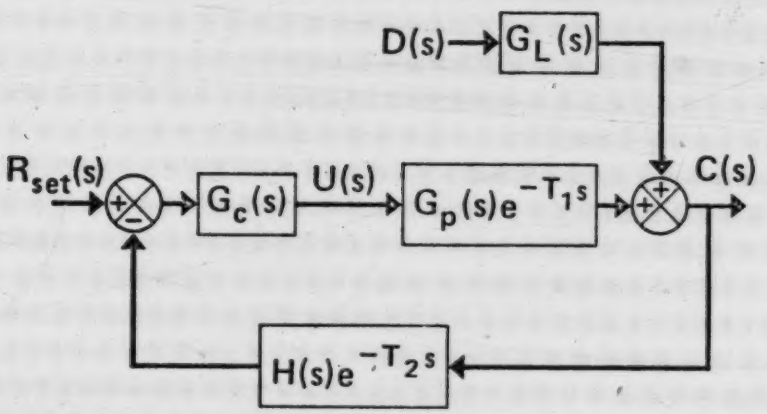

Fig. 2-1 : Block Diagram for a Continuous Feedback Control System Containing Time Delays.

The closed loop transfer function for setpoint changes for this system is:

$$\frac{C(s)}{R_{set}(s)} = \frac{G_c(s)\, G_p(s)\, e^{-T_1 s}}{1 + G_c(s)\, G_p(s)\, H(s)\, e^{-(T_1 + T_2)s}} \qquad (2.1)$$

Mathematically, the time delay term in the characteristic equation of Equation (2.1) could be eliminated by introducing a $e^{+(T_1 + T_2)s}$ term in the feedback path of Figure 2-1 (8).

Clearly an element with transfer function $e^{+(T_1 + T_2)s}$ is physically impossible because it implies knowledge of future values of the process output. However, if the dynamic model of the process is known it is possible to base control action on the estimated future output $\hat{C}_{k+\theta}$ predicted over a time interval θT_s as shown in Fig.2-2.

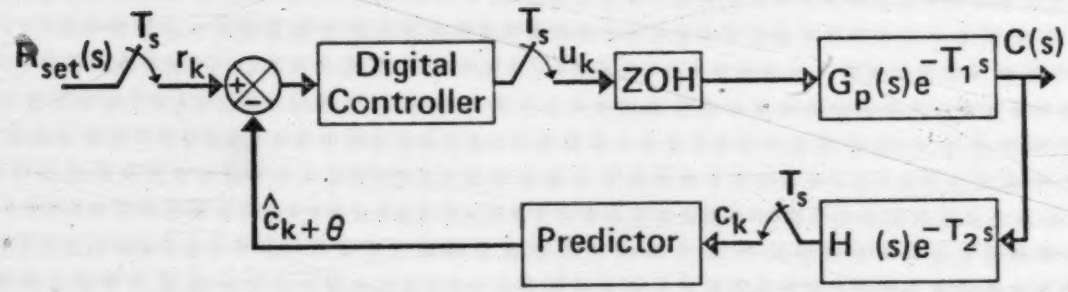

Fig. 2-2 : Block Diagram for a Digital Predictor Control System Containing Time Delays.

Prediction of future outputs is a common feature of all the control schemes that will be discussed in this chapter.

2.2 Literature Survey

Many predictor control schemes have been proposed in the literature during the past twenty years. In this investigation emphasis has been placed on methods that:

1. handle (unmeasured) disturbances using feedback control and do not require feedforward control action;

2. include some form of integral control to eliminate offset after step disturbances even in the presence of model errors, and

3. use continuous or discrete process models that can easily be obtained by dynamic testing.

2.2.1 Smith Predictor

The predictor control technique that has received the most attention is the "Smith predictor" or "Smith linear predictor" (43, 44). Several simulation and experimental studies (5,6,9,21,22,25,36,41) have demonstrated that the Smith predictor can result in significant improvement over conventional control. The sensitivity of the Smith predictor to modelling errors (5,6,11,12,23) including Padé approximations for the time delays (5,6,10) has also been considered. In recent years the Smith predictor has been extended to sampled-data systems (1,2,9,13,14,23,34) and multivariable systems (1,2,24).

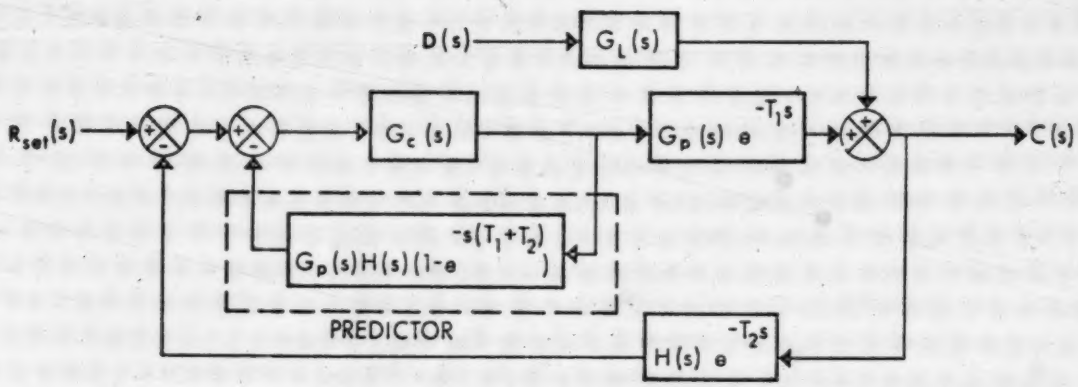

Fig. 2-3 : Block Diagram for the Continuous Smith Predictor Control Scheme.

The Smith predictor, shown in block diagram form in Figure 2-3, consists of a feedback loop around the controller, with the output of the "predictor" block representing the difference between two process models: the response of the undelayed system minus the response of the system with time delays T_1 and T_2.
It is to be noted from Figure 2-3 that for no system time delays (i.e. $T_1 = T_2 = 0$) the block diagram of the Smith predictor reduces to that of the conventional feedback control system in Figure 2-1.

For setpoint changes the closed-loop transfer function for the system of Figure 2-3 is given by:

$$\frac{C(s)}{R_{set}(s)} = \frac{G_c(s)\, G_p(s)\, e^{-T_1 s}}{1 + G_c(s)\, G_p(s)\, H(s)} \qquad (2.2)$$

Comparison of this expression with Equation (2.1) shows that the Smith predictor scheme has eliminated the time delays from the characteristic equation which will consequently allow the use of larger controller gains.

In Appendix A it is shown that the performance of the Smith predictor is significantly influenced by the load dynamics. For a relatively low value of T/τ_p where $T = T_1 + T_2$ and high value of τ_L/τ_p, use of the Smith predictor results in control performance that is inferior to PI control for step changes in load (25,32).

2.2.2 Analytical Predictor

The "analytical predictor" is a single variable predictor control scheme for sampled-data systems. It was derived by Moore (30) and evaluated by Moore et al. (28,29) who showed by simulation studies that it gives considerable improvement over conventional control. Doss and Moore (9) compared its performance with that of the Smith predictor and PI control. Doss (8) has extended the analytical predictor to first and second order discrete-time systems and reported an experimental application to a stirred tank heater (8,9). Jacobson (16) applied it to an evaporator to compensate for the effective time delay introduced by sampling. Conceptually the analytical predictor is based directly on the block diagram in Figure 2-2. It compensates for the total system time delay by predicting the process output for a time period of θT_s into the future where $\theta T_s = T_1 + T_2 + 0.5T_s$ as shown in Figure 2-2. Thus it allows for the system time delays $T_1 + T_2$ and the approximate delay of $0.5T_s$ introduced by sampling.

While the Smith predictor scheme uses standard PI or PID controllers, the proportional or proportional-integral control action in the analytical predictor scheme is derived so that the system will respond in a specified manner to disturbances, e.g. behaves as a dead-beat controller.

Since the analytical predictor can be designed to handle setpoint and load disturbances in a dead-beat fashion, it should give improved performance for load disturbances where the Smith predictor has disadvantages.

2.2.3 Other Predictor Control Schemes

Other proposed single input, single output, predictor techniques include a scheme to compensate for the sampling time delay (35); discrete time delay compensators with a single tuning parameter (15,31); a predictive feedforward control scheme (36,37) and a discrete Smith predictor for variable time delays (3).

A number of multivariable predictor control schemes based on optimal control design methods have been proposed (e.g. 17,24), but unfortunately they lead to excessively complicated control laws except for very special cases. The multivariable control scheme of Koppel and Aiken (17) is similar to the Smith predictor in the single input, single output case. However, as it does not include integral control action, it would presumably result in offset in the presence of model errors in the process gain.

CHAPTER 3

APPLICATION OF PREDICTOR CONTROL TO A PILOT SCALE DISTILLATION COLUMN

3.1 Description of the Equipment

The experimental studies were performed on a pilot scale distillation column interfaced with an IBM 1800 data acquisition and control computer. The 22.5 cm diameter column contains eight bubble cap trays on a 30.5 cm spacing. Each of the trays contains four bubble caps. The column is equipped with a total condenser and a thermosyphon reboiler. Further specific details of the column are given in the theses of Svrcek (45) and Pacey (33). At the usual operating conditions a methanol-water feed consisting of approximately 50% (by weight methanol) is separated into about 97% top product and 5% bottom product.

The column has extensive instrumentation to allow investigations in dynamics and control. Temperatures on all trays and of all product and auxiliary streams are measured as well as the flowrates of feed, reflux, top and bottom products, steam and condenser cooling water. The top product composition is measured with a capacitance probe, and the bottom composition is measured with a Hewlett-Packard model 5720A gas chromatograph using a liquid sampling system. The chromatograms are analyzed on-line by the IBM 1800 on a four minute cycle. All the measurements are transmitted to the IBM 1800 for data logging and/or control.

The column is equipped with analog controllers for all flowrates, the reboiler and condenser levels, and the feed and reflux temperatures. The principal flows, feed, reflux and steam, can also be controlled in the supervisory or direct digital control modes using the IBM 1800

computer. A detailed description of the column instrumentation is given in the theses of Svrcek (45) and Pacey (33). A simplified schematic of the column and the control configuration is shown in Figure 3-1. In this control study the top composition is controlled by the reflux flow and the bottom composition by the steam flow. The same control configuration was used in previous studies on the column by Pacey (33) and Berry (4). Liesch (18) demonstrated that for feed flow disturbances use of reflux gives superior performance compared to the direct material balance control scheme, where the top composition is controlled by manipulating the distillate flow rate.

3.2 Process Models

In order to use a predictor control scheme, a mathematical model of the process to be controlled must be available. Although the dynamics of the distillation column are inherently nonlinear, for small changes in the operating conditions the dynamics can be approximated by a first order plus time delay transfer function model. The process models used by Berry (4) and Pacey (33) to represent the dynamic behaviour of the column, expressed in SI units, are given in Table 3-1.

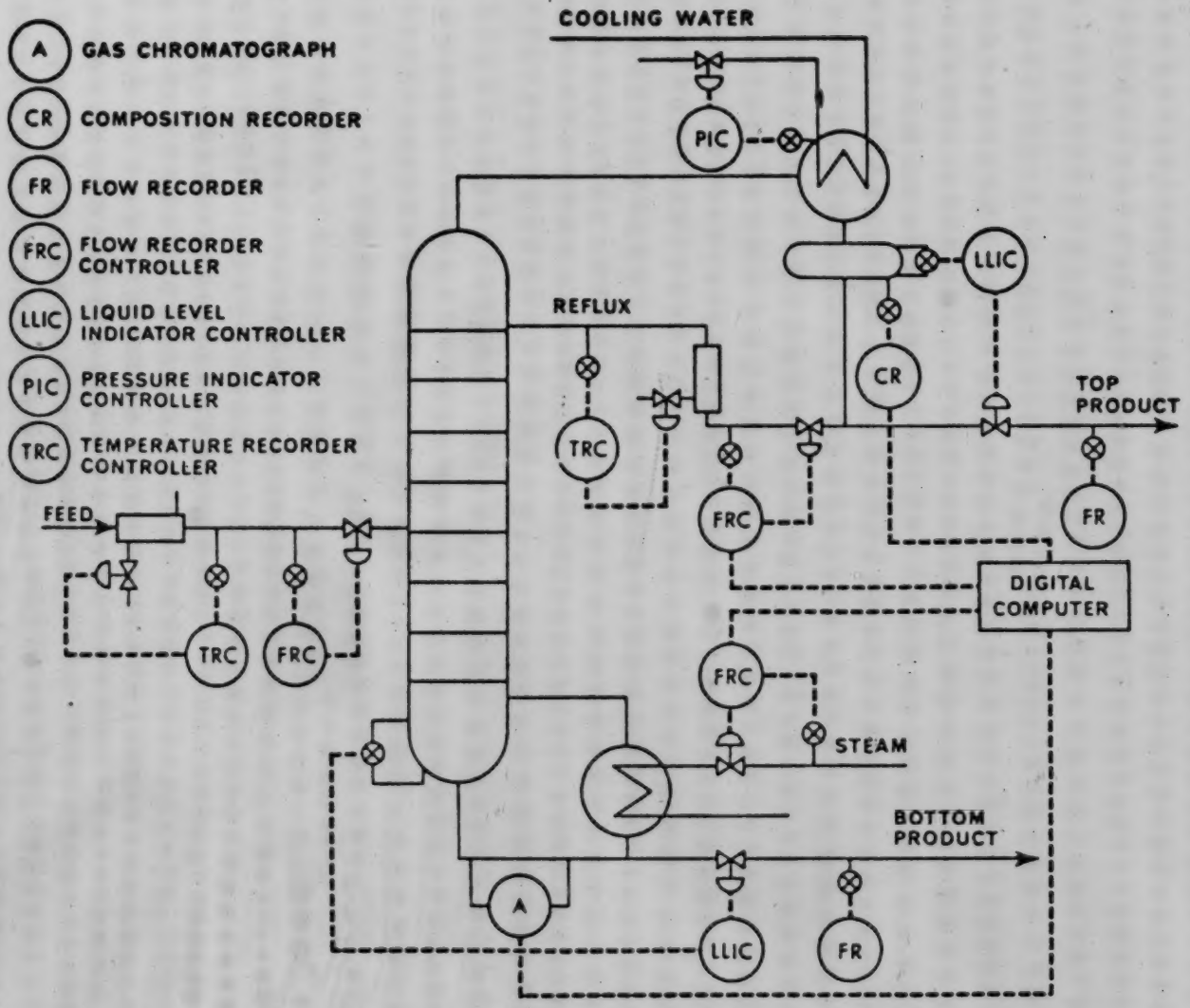

Fig. 3-1 : Schematic of the Distillation Column Control Scheme.

Table 3-1

Transfer Function Models Used in Previous Studies

Top composition (33):

$$C_D(s) = \frac{1.47e^{-51s}}{1080s + 1} R(s) + \frac{0.65e^{-360s}}{1620s + 1} F(s)$$

Bottom composition (4):

$$C_B(s) = \frac{-2.56e^{-174s}}{864s + 1} S(s) + \frac{0.65e^{-204s}}{792s + 1} F(s)$$

Flowrates are expressed in grams per second and compositions in weight percent methanol (as deviation variables). Time constants and time delays are given in seconds.

3.3 Incentives for Predictive Control

Liesch (18) noted that one factor giving rise to unsatisfactory control behaviour of the pilot scale column was the existence of time delays in the composition control loops. Generally two sources contribute to these delays: transport delays within the process and delays associated with the measurements of the controlled variables due to digital control sampling and the cycle time of the gas chromatograph analyzing bottoms composition. Top composition is measured continuously so the time delay is that of the process plus the sampling interval. Bottom composition is analyzed on a four minute cycle so the measurement contributes a four minute time delay.

With the process time delays shown in Table 3-1 there is a total time delay for the measurement and the process of approximately one minute for top composition control, compared to the time constant of 18 minutes. For the bottom composition control the combined process and measurement time delay is 7 minutes which is significant, compared to the time constant of 13 minutes.

Previous studies by Berry (4) and Liesch (18) demonstrated that PI control of the bottom composition was much less satisfactory than PI control of the top composition due to the longer time delay, and also the higher noise level in the bottom composition control loop due to the composition measurement. Consequently predictor control should be particularly effective for improving bottom composition control.

3.4 Digital Predictor Control Algorithms

The continuous first order plus time delay process models of the distillation column in Table 3-1 can be used to derive discrete Smith predictor and analytical predictor control algorithms. The discrete algorithms are more convenient for implementation on a process computer. In the derivations to follow an approach somewhat analogous to that of Moore (30) will be used.

3.4.1 Smith Predictor (SP)

A sampled-data version of the continuous SP control scheme in Figure 2-3 is shown in Figure 3-2.

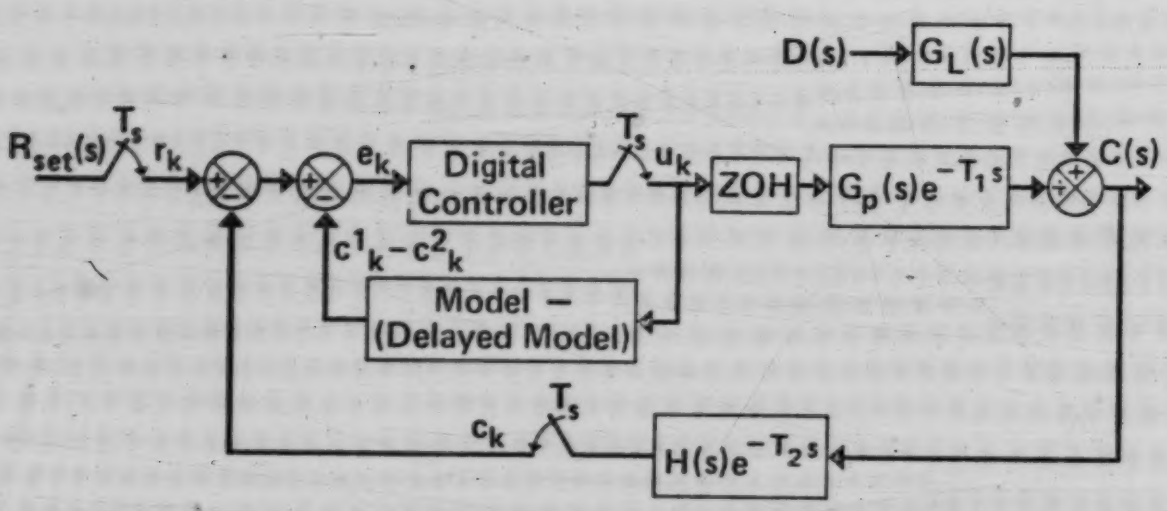

Fig. 3-2 : Digital Smith Predictor Control Scheme.

Comparison with the continuous representation shows that the predictor and the controller have been replaced by their discrete equivalents. The feedback loop around the digital controller contains a block whose output represents the difference between two model outputs: the response of a system without time delays, c_k^1, minus the response of a system which contains time delays, c_k^2. It can be seen from Figure 3-2 that in the digital case the process output is sampled and the discrete controller output is sent to the process through a zero order hold.

An expression for the quantity $c_k^1 - c_k^2$ in Figure 3-2 can be obtained by solving the differential equations corresponding to the model of the process and measurement device without time delay, $G_p(s)H(s)$, and the model including the time delays, $G_p(s)H(s)e^{-(T_1 + T_2)}$. In the following derivation, it will be assumed that $G_p(s)H(s)$ can be approximated by a first order transfer function.

For a first order process, the differential equation is given by:

$$c(t) + \tau_p \frac{dc}{dt} = K_p\, u(t) \qquad (3.1)$$

and for a first order process with total time delay, $T = T_1 + T_2$, by:

$$c(t) + \tau_p \frac{dc}{dt} = K_p\, u(t-T) \qquad (3.2)$$

If a zero order hold is used, u(t) is constant during each sampling period, and the solution of Equation (3.1) at each sampling instant is given by:

$$c_k^1 = K_p (1-B)u_{k-1} + Bc_{k-1}^1 \qquad (3.3)$$

where c_k^1 denctes the undelayed model response and $B = \exp\left(-\frac{T_s}{\tau_p}\right)$

For the solution of Equation (3.2) it may be necessary to take into account that u(t-T) will change during a sampling period if the time delay T is not an integer number of sampling times.

Consider the time interval from $(k-1)T_s$ to kT_s and a time delay $T = (N+\beta)T_s$, where $0 \leq \beta < 1$ and N is a positive integer. Then the input affecting the output during this sampling period will have the value u_{k-N-2} for a time interval of βT_s and a value u_{k-N-1} for the remaining portion $(1-\beta)T_s$ of the sampling period. This relationship is shown graphically in Figure 3-3.

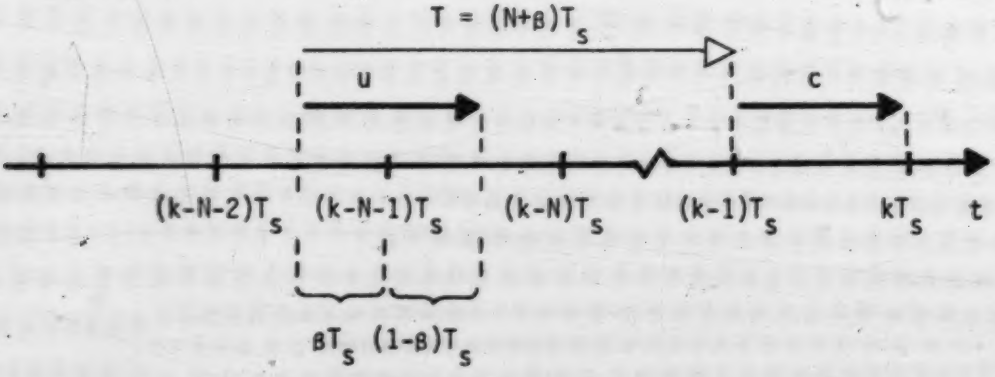

Fig. 3-3 : Representation of Sampling Process

Thus the solution for the delayed model response, denoted by c_k^2, can be obtained in two steps:

$$c_{k-1+\beta}^2 = K_p\,(1-C)u_{k-N-2} + C\,c_{k-1}^2 \qquad (3.4)$$

and

$$c_k^2 = K_p\,(1 - \frac{B}{C})u_{k-N-1} + \frac{B}{C}\;\; c_{k-1+\beta}^2 \qquad (3.5)$$

where $C = \exp\,(-\beta T_s/\tau_p)$ and

$$\frac{B}{C} = \exp\,(-(1-\beta)T_s/\tau_p)$$

Substituting Equation (3.4) into Equation (3.5) gives:

$$c_k^2 = B\,c_{k-1}^2 + B\,K_p\,(\frac{1}{C} - 1)u_{k-N-2} + K_p\,(1 - \frac{B}{C})u_{k-N-1} \qquad (3.6)$$

Equations (3.3) and (3.6) provide expressions for computing the system outputs corresponding to the model, c_k^1, and the model with time delay, c_k^2, from past control actions and the model parameters.

From Figure 3-2 it follows that:

$$e_k = r_k - c_k - (c_k^1 - c_k^2) \qquad (3.7)$$

Combining this expression with those of Equations (3.3), (3.6) and the following form of a digital PI controller,

$$u_k = K_c \left(e_k + \frac{T_s}{\tau_I} \sum_{i=0}^{k} e_i \right) \qquad (3.8)$$

yields the digital algorithm for the SP control scheme given in Table 3-2.

Table 3-2

Smith Predictor Control Algorithm

$$c_k^1 = B\, c_{k-1}^1 + K_p\,(1-B)u_{k-1}$$

$$c_k^2 = B\, c_{k-1}^2 + K_p\,(1 - \frac{B}{C})u_{k-N-1} + BK_p\,(\frac{1}{C} - 1)u_{k-N-2}$$

$$e_k = r_k - c_k + c_k^2 - c_k^1$$

$$u_k = K_c \left(e_k + \frac{T_s}{\tau_I} \sum_{i=0}^{k} e_i \right)$$

$$\text{with} \quad B = \exp(-\frac{T_s}{\tau_p})$$

$$C = \exp(-\frac{\beta T_s}{\tau_p})$$

3.4.1.1 Smith Predictor with Load Prediction

To overcome the disadvantages of the SP for load disturbances the basic scheme can be modified to include a load predictor block in the feedback path as suggested by Phillipson (34). The resulting control scheme is shown in Figure 3-4.

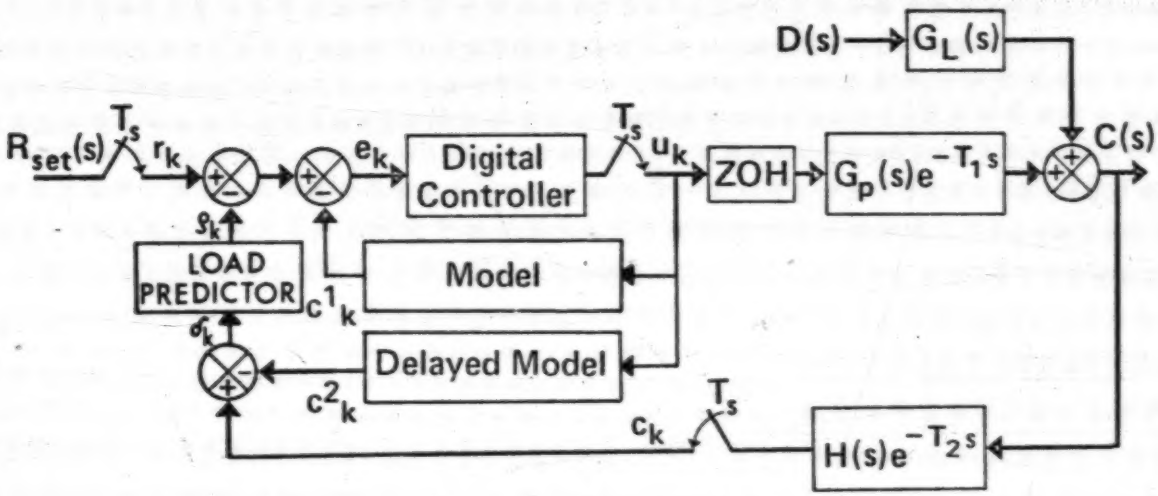

Fig. 3-4 : Digital Smith Predictor with Load Prediction.

If the load predictor block is set equal to unity, this scheme becomes equivalent to the SP scheme in Figure 3-2.

For the ideal case of a perfect process model the signal δ_k in Figure 3-4 is the portion of the system output c_k that can be attributed to load disturbances. Without load prediction the SP uses δ_k as the feedback signal and thus compensates for past disturbances. This results in sluggish responses to load changes, as shown in Appendix A.

As can be seen from Figure 3-4, for a disturbance δ_k observed at time kT_s, the change in the system output c occurred at time (kT_s-T_2), and the control action cannot affect the system output until time (kT_s+T_1). Thus there is a time delay $T = T_1+T_2$ before load disturbances can be corrected, for which the SP algorithm in Table 3-2 does not compensate. Phillipson (34) shows that an optimal control policy for this case requires load prediction. The practical difficulty, however, lies in the ignorance of the load disturbance characteristics. For fast fluctuations in load, Phillipson (34) suggests exponential filtering, which leads to the algorithm:

$$\rho_k = \delta_k + \alpha\,(\rho_{k-1} - \delta_k),\ 0 \leq \alpha < 1 \qquad (3.9)$$

For slowly changing disturbances an algorithm that extrapolates the observed load effect δ_k for a time interval θT_s where $\theta = T/T_s$ would seem to be more promising:

$$\rho_k = \hat{\delta}_{k+\theta} = \delta_k + \alpha\theta\,(\delta_k - \delta_{k-1}),\ 0 \leq \alpha < 1 \qquad (3.10)$$

In Equation (3.10) $\hat{\delta}_{k+\theta}$ denotes the load effect at time $(k+\theta)T_s$ predicted at time kT_s. Note that setting $\alpha = 0$ gives the conventional SP while $\alpha = 1$ amounts to linear extrapolation of the load effect over a time interval equal to the total system time delay T. Table 3-3 summarizes the resulting algorithm for load prediction.

Table 3-3

Smith Predictor Control Algorithm with Load Prediction

$$c_k^1 = B\, c_{k-1}^1 + K_p\,(1 - B)u_{k-1}$$

$$c_k^2 = B\, c_{k-1}^2 + K_p\,(1 - \frac{B}{C})u_{k-N-1} + B\, K_p\,(\frac{1}{C} - 1)u_{k-N-2}$$

$$\delta_k = c_k - c_k^2$$

$$\rho_k = \delta_k + \alpha\theta\,(\delta_k - \delta_{k-1})$$

$$e_k = r_k - \rho_k - c_k^1$$

$$u_k = K_c\,(e_k + \frac{T_s}{\tau_I} \sum_{i=0}^{k} e_i)$$

with B, C as defined in Table 3-2

3.4.2 Analytical Predictor (AP)

The AP, developed by Moore et al. (28-30), calculates the control signal from a prediction of the future process output $\hat{c}_{k+\theta}$, where $\theta = (T_1 + T_2)/T_s + 0.5$, rather than from the measured process output c_k . (The symbol $\wedge$ is used to denote a predicted or estimated value). Thus the total time delay $T = T_1 + T_2$ of the system as well as the effective time delay of $T_s/2$ introduced by sampling is compensated.

Figure 3-5 gives a schematic representation of the AP.

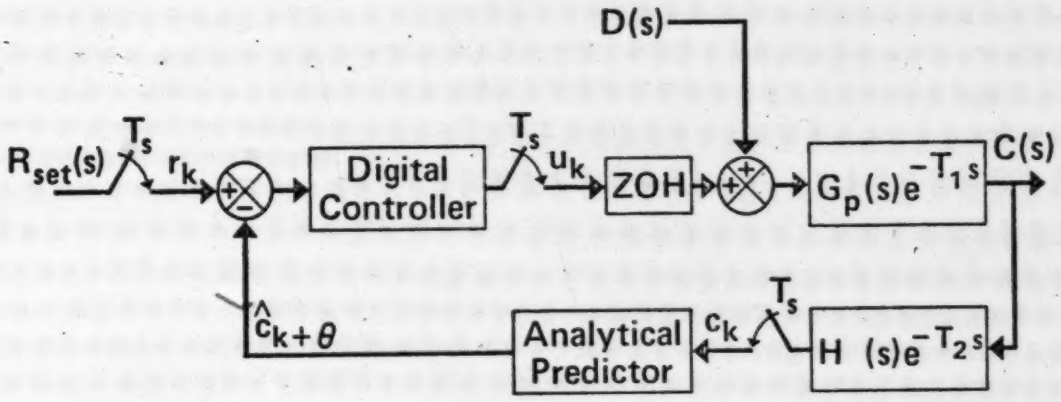

Fig. 3-5 : Block Diagram of the Analytical Predictor.

Depending on the control law used for the controller block in Figure 3-5, a proportional or proportional-integral AP control algorithm is obtained.

For proportional control action, the control law is given by:

$$u_k = K_c\ (p_k - \hat{c}_{k+\theta}) \tag{3.11}$$

where p_k is the calibrated setpoint given by Equation (3.12):

$$p_k = \frac{K_c\ K_p + 1}{K_c\ K_p}\ r_k \tag{3.12}$$

Setpoint calibration is necessary to give zero offset after setpoint changes if integral control action is not used.

An expression for $\hat{c}_{k+\theta}$ can be obtained by solving the differential equation corresponding to the model of the process and measurement device.

For a first order plus time delay model the solution for one sampling period, analogous to Equation (3.6), is:

$$c_k = B\ c_{k-1} + B\ K_p\ (\frac{1}{C} - 1)u_{k-N-2} + K_p\ (1 - \frac{B}{C})u_{k-N-1} \tag{3.13}$$

with B, C and N as previously defined in Section 3.4.1.

Employing Equation (3.13) recursively gives the predicted output N sampling times ahead as:

$$\hat{c}_{k+1} = B\, c_k + B\, K_p \left(\frac{1}{C} - 1\right) u_{k-N-1} + K_p \left(1 - \frac{B}{C}\right) u_{k-N}$$

$$\hat{c}_{k+2} = B\, \hat{c}_{k+1} + B\, K_p \left(\frac{1}{C} - 1\right) u_{k-N} + K_p \left(1 - \frac{B}{C}\right) u_{k-N+1}$$

$$\vdots$$

$$\hat{c}_{k+N} = B^N c_k + B\, K_p \left(\frac{1}{C} - 1\right) \sum_{i=1}^{N} B^{i-1}\, u_{k-i-1} \qquad (3.14)$$

$$+ K_p \left(1 - \frac{B}{C}\right) \sum_{i=1}^{N} B^{i-1}\, u_{k-i}$$

Prediction over the fractional time delay βT_s gives:

$$\hat{c}_{k+N+\beta} = C\, \hat{c}_{k+N} + K_p\, (1 - C) u_{k-1} \qquad (3.15)$$

Substituting Equation (3.14) into Equation (3.15) and rearranging gives:

$$\hat{c}_{K+N+\beta} = C\, B^N\, c_k + B^N\, K_p\, (1 - C) u_{k-N-1}$$

$$+ K_p\, (1 - B) \sum_{i=1}^{N} B^{i-1}\, u_{k-i} \qquad (3.16)$$

Predicting one half sampling period ahead yields:

$$\hat{c}_{k+\theta} = \hat{c}_{k+N+\beta+\frac{1}{2}} = A\, \hat{c}_{k+N+\beta} + K_p\, (1 - A) u_k \qquad (3.17)$$

with A defined as $A = \exp\left(-{}^{T_s}/_{2\tau_p}\right)$

Combining Equation (3.17) with the control law for the proportional AP in Equation (3.11), gives after rearrangment:

$$u_k = \frac{K_c}{1 + K_c K_p (1 - A)} (p_k - A \hat{c}_{k+N+\beta}) \qquad (3.18)$$

Equations (3.16) and (3.18) constitute the digital algorithm for the proportional AP which is given in Table 3-4.

Table 3-4

Proportional Analytical Predictor Algorithm

$$\hat{c}_{k+N+\beta} = C B^N c_k + B^N K_p (1-C) u_{k-N-1} + K_p (1-B) \sum_{i=1}^{N} B^{i-1} u_{k-i}$$

$$p_k = \frac{K_c K_p + 1}{K_c K_p} r_k$$

$$u_k = \frac{K_c}{1 + K_c K_p (1-A)} (p_k - A \hat{c}_{k+N+\beta})$$

with $A = \exp (- T_s / 2\tau_p)$

$B = \exp(- T_s / \tau_p)$

$C = \exp (- \beta T_s / \tau_p)$

$N+\beta = T / T_s$

For the case of sustained load disturbances this proportional algorithm will result in offset. To eliminate offset, integral control action needs to be included. As can be seen from Figure 3-5 a load disturbance affects the process in the same way as a control action of the same magnitude and duration. Thus a term, d_k, can be added to the control signal, u_k, resulting in the following control law:

$$u_k + d_k = K_c \, (p_k - \hat{c}_{k+\theta}) \tag{3.19}$$

As in the previous development it is assumed here that the disturbance d_k cannot be measured. However an estimate, $\hat{d}_k$, can be obtained by comparing the predicted output $\hat{c}_k$, calculated from the process model, with the actual measured output c_k and numerically integrating the difference:

$$\hat{d}_k = \hat{d}_{k-1} + K_I \, T_s \, (c_k - \hat{c}_k) \tag{3.20}$$

Using this estimate $\hat{d}_k$ for d_k in Equation (3.19) yields the control law for the proportional - integral AP.

Following a series of steps analogous to those used in deriving Equation (3.6) it is possible to establish that:

$$\hat{c}_k = Bc_{k-1} + B \, K_p \, (\frac{1}{C} - 1) \, (u_{k-N-2} + \hat{d}_{k-1})$$

$$+ K_p \, (1 - \frac{B}{C}) \, (u_{k-N-1} + \hat{d}_{k-1}) \tag{3.21}$$

In Equation (3.21) $\hat{d}_{k-1}$ is an estimate of the disturbance d_{k-1} at time $(k - 1)T_s$.

Eqn. (3.21) can be used recursively as in the derivation employed for the proportional AP to obtain the predicted process output $\hat{c}_{k+\theta}$. Finally, substituting $\hat{c}_{k+\theta}$ into Eqn. (3.19) results in the proportional-integral AP algorithm given in Table 3-5. The complete derivation of this algorithm is given in Appendix B.

The integral control action used in the AP control algorithm in Table 3-5 differs from the integral action in a conventional digitial PI controller given in Eqn. (3.8) and Table 3-6. Consider what happens when an AP control system, initially at steady state, is subjected to a setpoint change. In the absence of model errors the measured process output, c_k, will be equal to the predicted output, $\hat{c}_k$, as long as no load disturbances occur. Consequently $\hat{d}_k$, which can be regarded as the integral contribution to the control action, is zero as can be seen from Eqn. (3.20). Therefore setpoint changes are handled by proportional control action only, which is not the case for the digital PI control algorithm. It should also be noted that due to the setpoint calibration there is no offset in this case. This fact is shown in Appendix C.

If the system is subjected to load changes $\hat{d}_k$ becomes different from zero. Since in the proportional-integral form of the AP control algorithm $\hat{d}_k$ is added to the stored past control signals, a different value of the future predicted output $\hat{c}_{k+N+\beta}$ is obtained, as can be seen from Table 3-5. Consequently the control signal u_k depends on the controller tuning parameters K_C and K_I and thus contains proportional and integral control action.

Table 3-5

Proportional-Integral Analytical Predictor Algorithm

$$\hat{c}_k = B\, c_{k-1} + B\, K_p \left(\frac{1}{C} - 1\right)\left(u_{k-N-2} + \hat{d}_{k-1}\right) + K_p \left(1 - \frac{B}{C}\right)\left(u_{k-N-1} + \hat{d}_{k-1}\right)$$

$$\hat{d}_k = \hat{d}_{k-1} + K_I\, T_s (c_k - \hat{c}_k)$$

$$\hat{c}_{k+N+B} = C\, B^N c_k + B^N K_p\, (1 - C)\left(u_{k-N-1} + \hat{d}_k\right) + K_p\, (1 - B) \sum_{i=1}^{N} B^{i-1}\left(u_{k-i} + \hat{d}_k\right)$$

$$u_k = \frac{K_c}{1 + K_c\, K_p\, (1 - A)}\left(p_k - A\, \hat{c}_{k+N+B}\right) - \hat{d}_k$$

with p_k, A, B, C, N as defined in Table 3-4

Table 3-6

Digital PI Control Algorithm

$$e_k = r_k - c_k$$

$$u_k = K_c \left(e_k + \frac{T_s}{\tau_I} \sum_{i=0}^{k} e_i \right)$$

If the disturbance d can be measured, feedforward control action can be included easily (28-30). However this case will not be treated in this investigation.

3.4.2.1 Optimal Controller Constants

The controller parameters for the AP algorithm in Table 3-5 can be tuned analytically to yield a system response that meets certain performance criteria. Moore (30) has shown that the controller gain K_c can be calculated so that the system without time delay will respond in a dead-beat fashion to step changes in setpoint. The process output c_k will then show the same response delayed by the time delay T. This is the best that can be achieved considering the nature of the process.

The solution of the differential equation of the model without time delay (T=0) for one sampling period is:

$$c_{k+1} = K_p (1-B) u_k + B c_k \qquad (3.22)$$

So the AP control law for the proportional algorithm for this case is given by:

$$u_k = \frac{K_c}{1 + K_c K_p (1-A)} \left(\frac{K_c K_p + 1}{K_c K_p} r_k - A c_k \right) \qquad (3.23)$$

Using the requirement for a dead-beat controller:

$$c_{k+1} = r_k \qquad (3.24)$$

and assuming the system to be at steady state initially gives:

$$c_k = 0 \qquad (3.25)$$

From Eqns. (3.22) to (3.25) it can be shown that:

$$1 = \frac{K_p (1 - B) K_c}{1 + K_c K_p/(1 - A)} \frac{K_c K_p + 1}{K_c K_p} \tag{3.26}$$

which on rearrangement can be expressed as:

$$K_c = \frac{A}{K_p (1 - A)} \tag{3.27}$$

In a similar fashion, controller parameter K_I in the AP algorithm in Table 3-5 can be specified so that an unmeasured step disturbance can be estimated after one sampling interval. Suppose that a step disturbance of magnitude q enters the system of Fig. 3-5 at time $t = (k - 1) T_s$. Then $d_i = q$ for $i \geq k - 1$ and the response of the system without time delays is given by:

$$c_k = B c_{k-1} + K_p (1 - B) (u_{k-1} + q) \tag{3.28}$$

Since the disturbance is assumed to be zero for $t < (k - 1) T_s$, then $\hat{d}_{k-1} = 0$ and the predicted response will be:

$$\hat{c}_k = B c_{k-1} + K_p (1 - B) u_k \tag{3.29}$$

combining Eqns. (3.20), (3.28) and 3.29) gives

$$\hat{d}_k = K_I T_s (1 - B) K_p q \tag{3.30}$$

In order for the estimated disturbance to be equal to the actual disturbance after one sampling interval, the following condition must be satisfied:

$$\hat{d}_k = d_k = q \tag{3.31}$$

Combining Eqns. (3.30) and (3.31) gives the required expression for K_I,

$$K_I = \frac{1}{T_s K_p (1 - B)} \tag{3.32}$$

With the controller parameter K_c given by Eqn. (3.27) the AP becomes a dead-beat controller for any step changes in setpoint. Using the controller parameter K_I expressed by Eqn. (3.32), however, will provide dead-beat control for load disturbances only in the special case when:

1. The disturbance affects the process in the same way as a control action.

2. A step disturbance enters the system just at a sampling instant.

3.5 Computer Requirements

As can be seen from Tables 3-2 and 3-5 the algorithms for digital SP and AP control are simple and do not require excessive computer resources. The amount of computer time used will depend on the speed of the computer and the sampling frequency. For the SP, as for digital PI control, the computer time required is directly proportional to the sampling frequency since the algorithms contain a constant number of terms. In the case of the AP the number of terms in the algorithm increases with sampling frequency. If the sampling frequency is doubled for instance, N, the integer number of sampling times contained in the process time delay, is doubled as well. Consequently the summation term contains twice as many elements. For sufficiently large values of N calculation of the summation term will take up most of the computation time required for executing the algorithm. In this case the execution

time for one computation becomes proportional to N and thus the sampling frequency. For large values of N the total computer time required for AP control is consequently proportional to the square of the sampling frequency. Also, N + 1 past control signals have to be stored, as compared to two in the case of the SP.

In most practical applications, however, N will be small and the time required to execute the AP or SP algorithms will be comparable. For instance in this study N was never larger than 2, and the execution time for the algorithms on the IBM 1800 computer was negligible.

In view of the simplicity of the SP and AP control algorithms the recent advance in computer technology opens interesting possibilities for their application. Both could for instance readily be implemented using a cheap, dedicated microprocessor in place of a minicomputer.

CHAPTER 4

DIGITAL SIMULATION STUDY

A digital simulation study was undertaken to investigate the performance of SP, AP and PI control of the product compositions of the pilot scale distillation column. In most of the SP simulations the SP algorithm in Table 3-2 was used. Load prediction was included in some runs for the bottom composition control. To ensure no offset the proportional-integral version of the AP algorithm was employed. Simulations of the top composition control were made with "perfect" process models in order to study the performance of predictor control in this ideal case, and with inaccurate process models to investigate the sensitivity of the predictor control schemes to modelling errors.

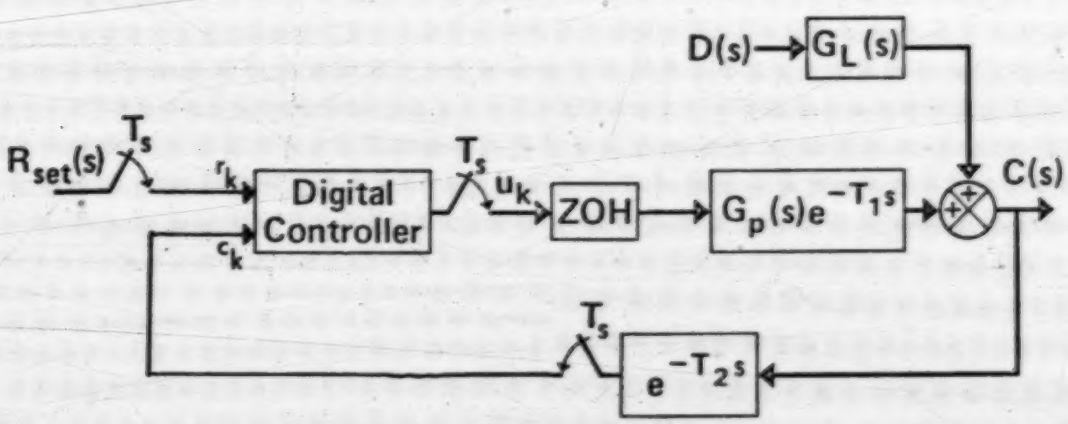

Fig. 4-1 : Block Diagram of the Simulated Control System.

4.1 Simulation Programs

The control system in Fig. 4-1 was simulated using the IBM 360 CSMP digital simulation program *. This program provides simple simulation language statements to specify standard elements of the system like time delays, first order transfer functions, sample and hold elements etc., and offers a choice of numerical integration methods and output options. In addition user written FORTRAN subroutines can be substituted for specified blocks, making the program very versatile. Listings of the programs for three simulation runs using SP, AP and PI control are given in Appendix D.

The transfer functions in Table 3-1 were used as process models. The measurement time delay T_2 in Fig. 4-1 was zero for the top composition control loop since the top composition can be measured continuously and was 4 minutes for the bottom composition, which is the cycle time of the gas chromatograph. It was found that for the rectangular integration method in CSMP an integration interval of 3 to 5 seconds was sufficiently short to ensure an accurate digital simulation of the closed-loop system. The value of the manipulated variable, u_k, was calculated every sampling instant using the control algorithms in Tables 3-2, 3-5 and 3-6. Between sampling instants, u_k was held constant using a zero order hold element. A sample time of 1 minute was chosen for the top composition control loop and of 4 minutes, equal to the cycle time of the gas chromatograph, for the bottom composition control loop.

* IBM, 360A-CX-16X, "Continuous Systems Modelling Program", Program Reference Manual.

4.2 Controller Tuning

In order to obtain a valid comparison of the performance of the three control algorithms, well tuned controllers must be used in each case. In this study the integral absolute error (IAE) was used as the performance criterion.

Since the SP scheme uses PI control action it can be tuned using the methods that are available for conventional PI controllers. For example Miller et al.(26) have developed tuning relations for first order plus time delay processes and continuous controllers using integral error performance criteria. The controller parameters are expressed in terms of the ratio of the time delay, T, to the process time constant, τ_p. Smith et al. (42) give tuning formulas that set τ_I according to available rules of thumb and adjust K_c to obtain a given percent overshoot. Some of these tuning methods have been extended to digital PI controllers (19,20,27,39). Lopez et al. (19,20) have established optimal controller constants based on ISE, IAE and ITAE integral error criteria for P, PI and PID controllers and a first order plus time delay process. However, these results are presented in graphical form and for the process parameters of the present study interpolation between the reported curves is required. Consequently, only approximate values can be obtained.
Moore et al. (27) propose an alternative approach for digital two mode controllers. They suggest that the relations for continuous controllers can be used if an effective time delay of $T' = T + T_s/2$ is employed instead of the system time delay T to account for the additional delay caused by sampling.
The agreement between constants obtained in this manner (27) and optimal constants for digital controllers (19,20) is best

for low ratios of sampling time to process time constant and for high ratios of time delay to time constant. These conditions are not satisfied for the process parameters used in this study. However, since no better tuning method was available, the approach of Moore et al. (27) was used employing the following tuning relations for continuous controllers (26):

$$K_p K_c = 0.984 \ (T'/\tau_p)^{-0.986} \tag{4.1}$$

$$\tau_I/\tau_p = 1.644 \ (T'/\tau_p)^{0.707} \tag{4.2}$$

Although the SP control scheme eliminates the time delay T from the characteristic equation, it does not compensate for the effective time delay of $T_s/2$ introduced by sampling. Thus one possibility for tuning the SP is to use controller constants calculated from Eqns. (4.1) and (4.2) based on an effective time delay of $T' = T_s/2$. The simulations showed, however, that with the controller constants calculated in this fashion the response was oscillatory for PI control and unstable for the SP. More conservative controller constants can be obtained by setting $T' = T + T_s$ for PI control and $T' = T_s$ for SP control. With these controller constants, satisfactory closed-loop responses were obtained in all cases. It should be noted that $T' = T + T_s$ corresponds to the longest possible time delay in the sampled-data system; for instance, if a load disturbance occurs immediately after a sampling instant, a time interval of $T' = T + T_s$ passes until corrective control action can affect the system output.

In the case of the AP dead-beat controller constants for the given process models and sampling times can be calculated from Eqns. (3.27) and (3.32). These values resulted in satisfactory control in the simulation study.

4.3 Top Composition Control

Simulations of the top composition control loop were made for step changes of +1% in setpoint and +20% in feed flow rate using a sampling time, T_s, of 1 minute. Feed flow rate disturbances of the same magnitude were used in a previous experimental study of the column by Pacey (33). A feed flow disturbance consisting of a series of arbitrary pulses of different duration was also employed for some simulations.

The controller constants for SP, AP and PI control were calculated using the methods discussed in Section 4.2 and are given in Table 4.1 .

In the case of the SP the controller constants based on an effective time delay of $T' = T_s/2$ ($K_c = 22.9$ and $\tau_I = 141$) led to very oscillatory responses, so more conservative settings were used in some of the reported simulation runs ($K_c = 15$ and $\tau_I = 200$). The simulation results are summarized in Tables 4-2 to 4-4. The most satisfactory responses in terms of IAE values and overshoot for setpoint changes are shown in Fig. 4-2 and the corresponding runs for feed flow changes in Figs. 4-3 and 4-4 .

The superior performance of the AP and the SP over PI control for setpoint changes is apparent from Fig. 4-2. The AP behaves as a dead-beat controller and is superior to the SP which has a small overshoot. For feed flow changes the AP gives a considerable improvement over both SP and PI control as can be seen from Fig. 4-3 and the IAE values in Table 4-3. Fig. 4-3 shows the sluggish response of the SP after a step change in feed flow. The same characteristic "tail" in the response was observed for a wide range of controller constants. The theoretical analysis of the SP, for a continuous controller, in Appendix A

Table 4-1 : Calculated Controller Constants for Top Composition Control.

CONTROL ALGORITHM	CONTROLLER CONSTANTS AND UNITS			TUNING METHOD
	K_c (g/s/%)	τ_I (s)	K_I (g/s/%s)	
PI	8.61	284	-	Eqns. (4.1) and (4.2) based on $T'=T+T_s/2$
PI	6.31	355	-	Eqns. (4.1) and (4.2) based on $T'=T+T_s$
PI	∿6.7	∿200	-	Optimal IAE constants for a discrete PI con - troller (19)
SP	22.9	141	-	Eqns. (4.1) and (4.2) based on $T'=T_s/2$
SP	11.6	230	-	Eqns. (4.1) and (4.2) based on $T'=T_s$
SP	∿12	∿100	-	Optimal IAE constants for a discrete PI con - troller (19)
AP	24.15	-	0.21	Dead-beat controller constants from Eqns. (3.27) and (3.32)

Table 4-2 : Simulation Results for Top Composition Control
(1% Step Increase in Setpoint)

RUN	K_c (g/s/%)	τ_I (s)	K_I (g/s/%s)	IAE (%s)	OVERSHOOT (%)	FIGURE
PI-2	8.61	284	-	389	0.86	-
PI-9	6.31	355	-	267	0.47	4-2
SP-1	11.6	230	-	180	0.16	4-2
SP-2	15.0	200	-	172	0.55	-
AP-1	24.15	-	0.21	142	0.0	4-2

Table 4-3 : Simulation Results for Top Composition Control
(20% Step Increase in Feed Flow)

RUN	K_c (g/s/%)	τ_I (s)	K_I (g/s/%s)	IAE (%s)	MAX. DEVIATION (%)	FIGURE
PI-4	8.61	284	-	54.0	0.17	-
PI-8	6.31	355	-	86.3	0.20	4-3
SP-8	11.6	230	-	139	0.164	4-3
SP-9	15.0	200	-	129	0.164	-
AP-6	24.15	-	0.21	18.2	0.164	4-3

Table 4-4 : Simulation Results for Top Composition Control
(Series of Arbitrary Square Pulses in Feed Flow)

RUN	K_c (g/s/%)	τ_I (s)	K_I (g/s/%s)	IAE (%s)	MAX. DEVIATION (%)	FIGURE
PI-7	6.31	355	-	338	0.356	4-4
SP-16	11.6	230	-	327	0.254	4-4
AP-15	24.15	-	0.21	91	0.218	4-4

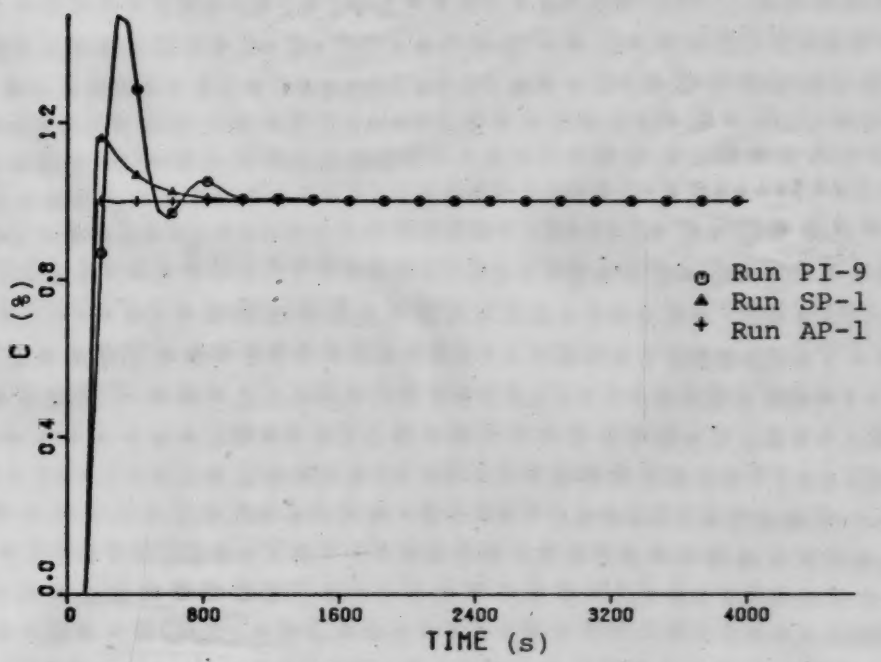

Fig. 4-2 : Comparison of SP, AP and PI Control for a 1% Step Increase in Setpoint.

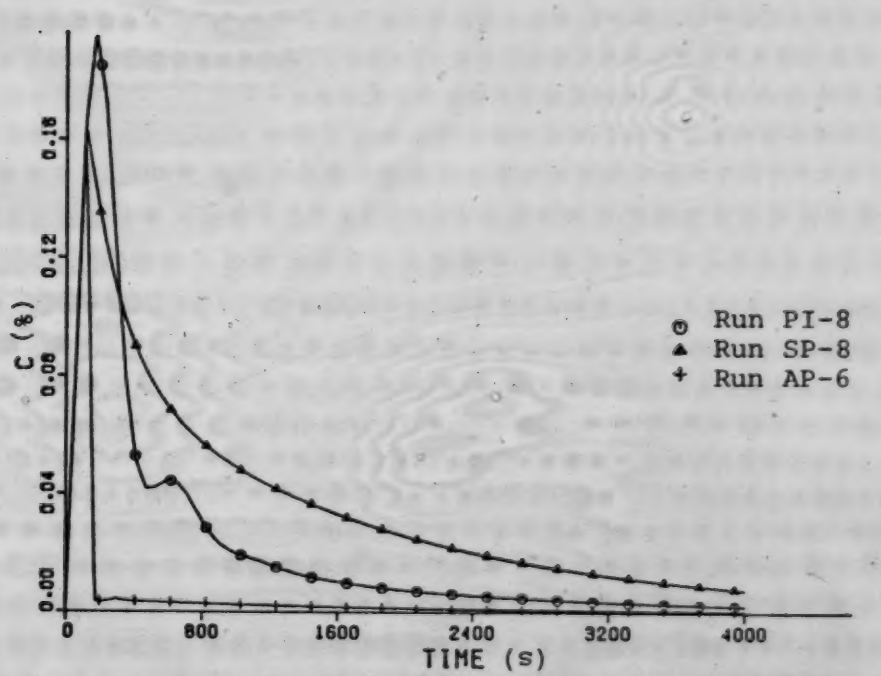

Fig. 4-3 : Comparison of SP, AP and PI control for a 20% Step Increase in Feed Flow.

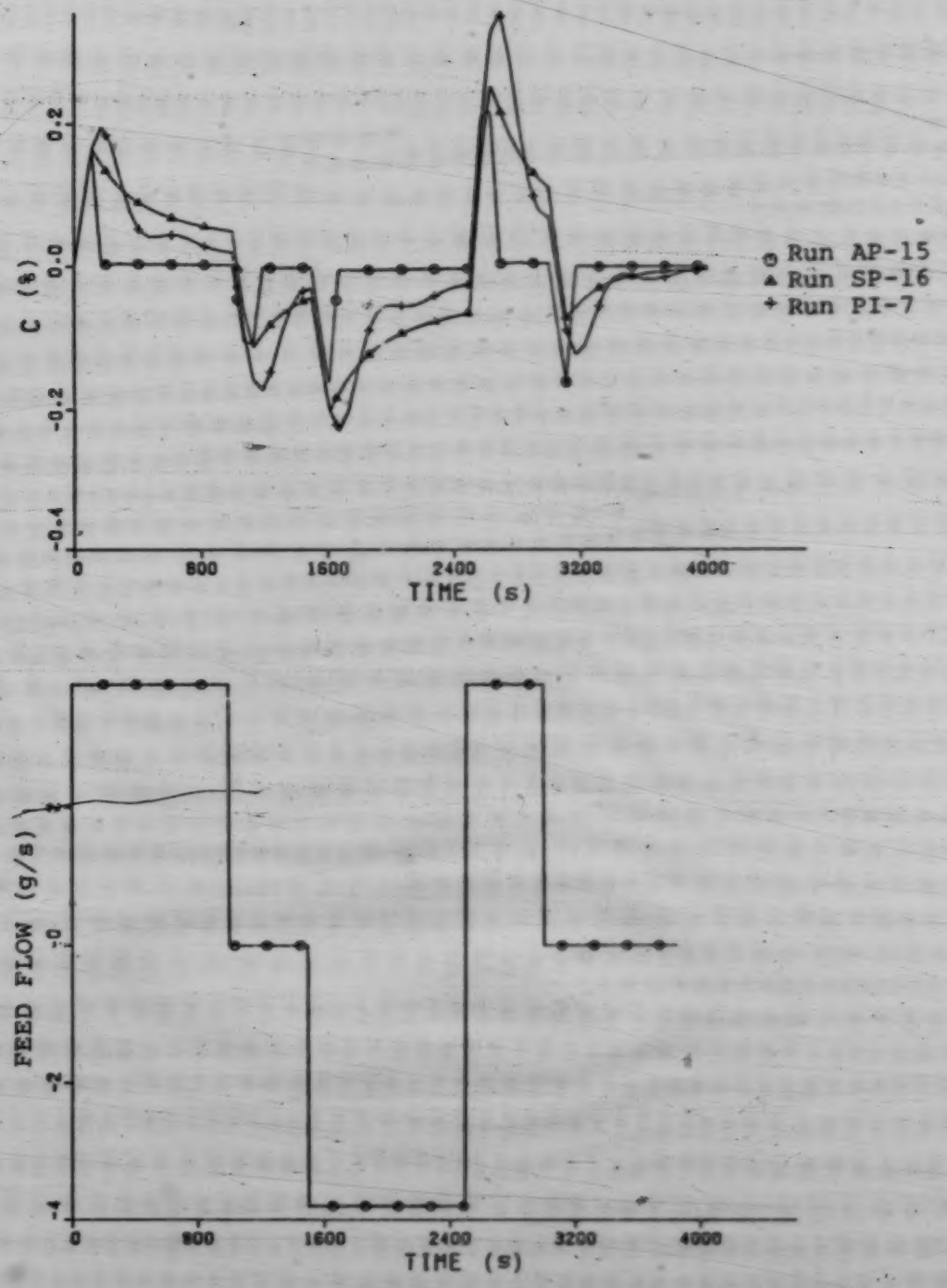

Fig. 4-4 : Comparison of SP, AP and PI Control for a Series of Arbitrary Step Changes of ± 20% in Feed Flow.

shows that this type of response can be expected if the load dynamics are slow, which was the case in the present study. For a series of arbitrary pulses in feed flow of different duration the SP shows a similar response, but in this case a new disturbance occurs before the previous transient has died out as shown in Fig. 4-4. Tables 4-3 and 4-4 show that for a step change in feed flow the SP gives considerably higher IAE values than PI control, whereas for the disturbance consisting of series of arbitrary step changes similar IAE values are obtained since the smaller maximum deviation of the SP compensates for the longer transient. Fig. 4-4 and Table 4-4 demonstrate that the AP, resulting in the lowest IAE value and the smallest maximum deviation, provides a significant improvement over SP and PI control.

4.3.1. The Influence of Model Errors

The influence of model errors on the performance of the SP and the AP was investigated by simulating the same process model but assuming values for the parameters K_p, τ_p and T_1 in the predictor model that differed by up to 30% from the process parameters. Model errors for these simulations were defined as:

$$\text{Model Error} = \frac{\text{Predictor Model Parameter-Process Parameter}}{\text{Process Parameter}} \times 100\% \quad (4.3)$$

The controller constants for the simulation runs with model errors of $\pm$ 20% K_p were calculated from the incorrect parameters in the predictor model, based on an effective time delay of $T' = T_s$ for the SP and using the equations for dead-beat control for the AP. Eqns. (4.1) and (3.27) show that this results in reduced values of K_c for model errors of +20% and increased values for model errors of -20%. Since the value of τ_I does not depend on the process gain, as can be seen from Eqn. (4.2), τ_I is the same as in the ideal case of perfect modelling. The value of K_I for the AP, however, depends on the process gain as shown in Eqn. (3.32). The controller constants of the previous case of perfect modelling are also obtained for the simulation runs with model errors in time delay, as the controller tuning relations for the SP and AP do not depend on the value of the time delay.

The simulation runs for model errors of +10% K_p, + 30% τ_p and +20%T_1 & +20% K_p were done using the controller constants for the ideal case of perfect process models, i.e. the constants were calculated from the process parameters instead of the incorrect model parameters. Note that this yields a value of K_I = 0.210 in the simulations for the AP. Due to a calculation error K_I = 0.198 was used; however, this resulted in negligible differences in the responses.

The results are summarized in Tables 4-5 and 4-6 and typical responses are shown in Figs. 4-5 to 4-12.

In the case of the SP the performance depended on the type of model error present and the disturbance used. Overestimated gains and time delays led to higher IAE values for feed flow changes, but to lower values for setpoint changes, as shown in runs SP-10, SP-11 and SP-3, SP-4. Underestimated gain and time delay on the other hand gave lower IAE values for load changes than the ideal case because the "tail" in the response curve was reduced. This fact can be appreciated by comparing runs SP-8, SP-7 and SP-12 and Figs. 4-7 and 4-8.

For the AP, model errors always led to a deterioration in control behaviour. This is demonstrated by the increase in IAE values over the ideal case of no model errors and the comparison of the transient responses in Figs. 4-9 to 4-12. Errors in the time delay, T_1, and the process gain, K_p, were found to have more severe effects than errors in the time constant, τ_p . For errors in gain K_p, underestimation is more serious than overestimation because the calculated controller constants are too large in the former case and tend to result in an oscillatory response. This can be appreciated by comparing the IAE values for runs AP-7 and AP-14 and the

Table 4-5 : Simulation Results Illustrating the Effects of Model Errors on Top Composition Control (1% Step Increase in Setpoint)

RUN	K_c (g/s/%)	τ_I (s)	K_I (g/s/%s)	IAE (%s)	OVERSHOOT (%)	MODEL ERROR	FIGURE
SP-1	11.6	230	-	180	0.16	-	4-5,4-6
SP-5	11.6	230	-	175	0.16	+10% K_p	-
SP-3	9.68	230	-	180	0.12	+20% K_p	4-5
SP-4	11.6	230	-	172	0.16	+20% T_1	4-6
SP-6	11.6	230	-	193	0.41	+30% τ_p	-
SP-13	11.6	230	-	200	0.29	+20% T_1 & +20% K_p	-
AP-1	24.15	-	0.21	142	0.0	-	4-9,4-10
AP-3	24.15	-	0.198	157	0.13	+10% K_p	-
AP-5	20.1	-	0.175	175	0.17	+20% K_p	4-9
AP-12	12.0	-	0.21	200	0.09	+20% T_1	4-10
AP-4	24.15	-	0.198	205	0.20	+30% τ_p	-

Table 4-6 : Simulation Results Illustrating the Effects of Model Errors on Top Composition Control (20% Step Increase in Setpoint)

RUN	K_c (g/s/%)	τ_I (s)	K_I (g/s/%s)	IAE (%s)	MAX. DEVIATION (%)	MODEL ERROR	FIGURE
SP-8	11.6	230	-	139	0.164	-	4-7,4-8
SP-7	14.5	230	-	112	0.164	-20% K_p	4-7
SP-10	9.68	230	-	166	0.164	+20% K_p	-
SP-12	11.6	230	-	118	0.164	-20% T_1	4-8
SP-11	11.6	230	-	161	0.164	+20% T_1	-
SP-15	11.6	230	-	186	0.167	+20% T_1 & +20% K_p	-
AP-6	24.15	-	0.21	18.2	0.164	-	4-11,4-12
AP-14	30.1	-	0.262	38.1	0.164	-20% K_p	4-11
AP-7	20.1	-	0.175	23.2	0.164	+20% K_p	-
AP-9	24.15	-	0.198	18.9	0.164	+10% K_p	-
AP-13	24.15	-	0.21	31.9	0.164	-20% T_1	4-12
AP-11	12.0	-	0.21	28.4	0.164	+20% T_1	-
AP-10	24.15	-	0.198	26.7	0.164	+30% τ_p	-

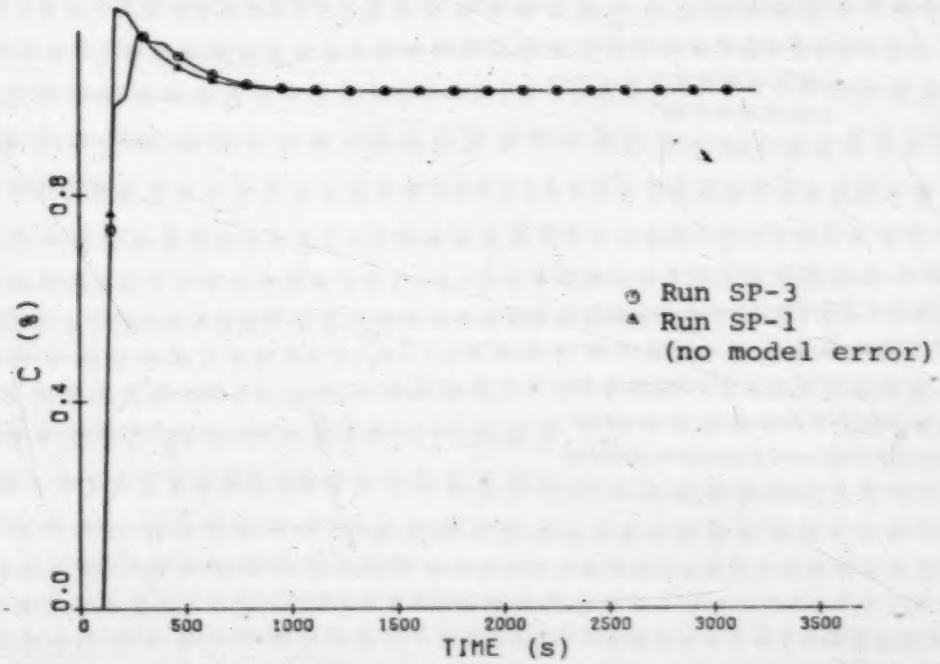

Fig. 4-5 : Influence of a Model Error of +20% in Process Gain on the SP for a 1% Step Increase in Setpoint.

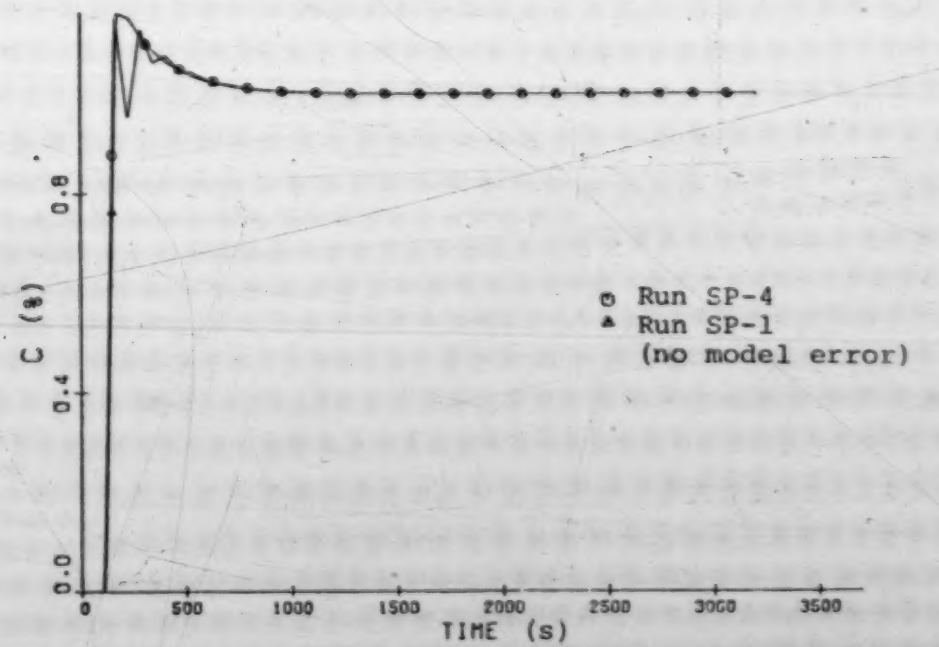

Fig. 4-6 : Influence of a Model Error of +20% in Time Delay on the SP for a 1% Step Increase in Setpoint.

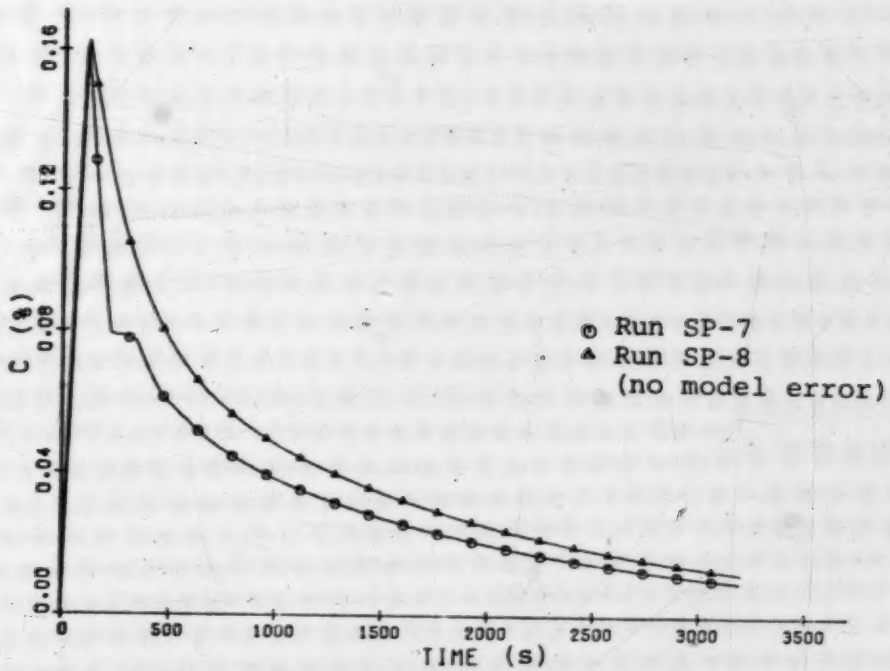

Fig. 4-7 : Influence of a Model Error of -20% in Process Gain on the SP for a 20% Step Increase in Feed Flow.

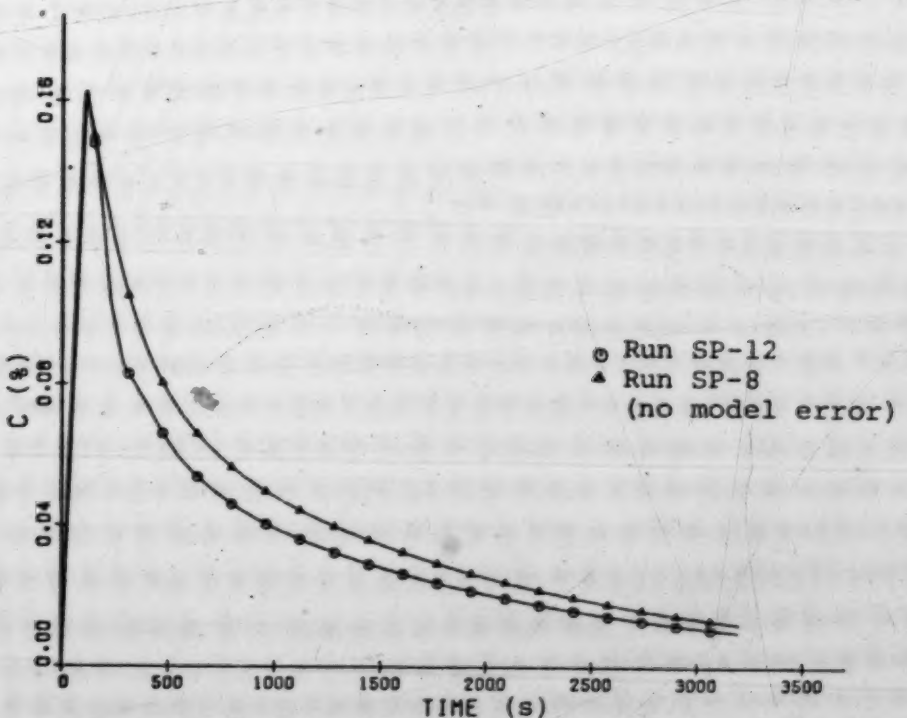

Fig. 4-8 : Influence of a Model Error of -20% in Time Delay on the SP for a 20% Step Increase in Feed Flow.

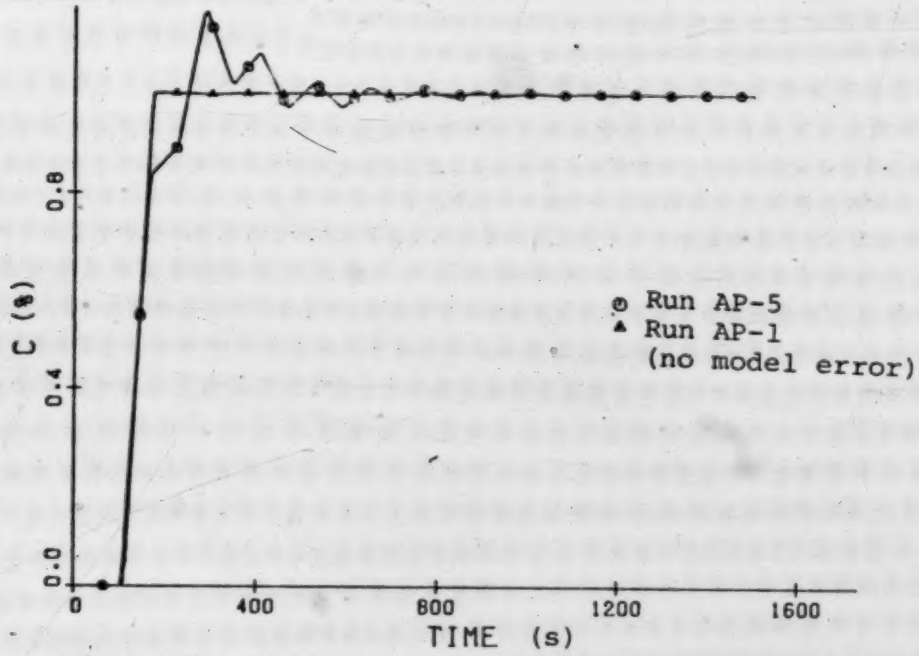

Fig. 4-9 : Influence of a Model Error of +20% in Process Gain on the AP for a 1% Step Increase in Setpoint.

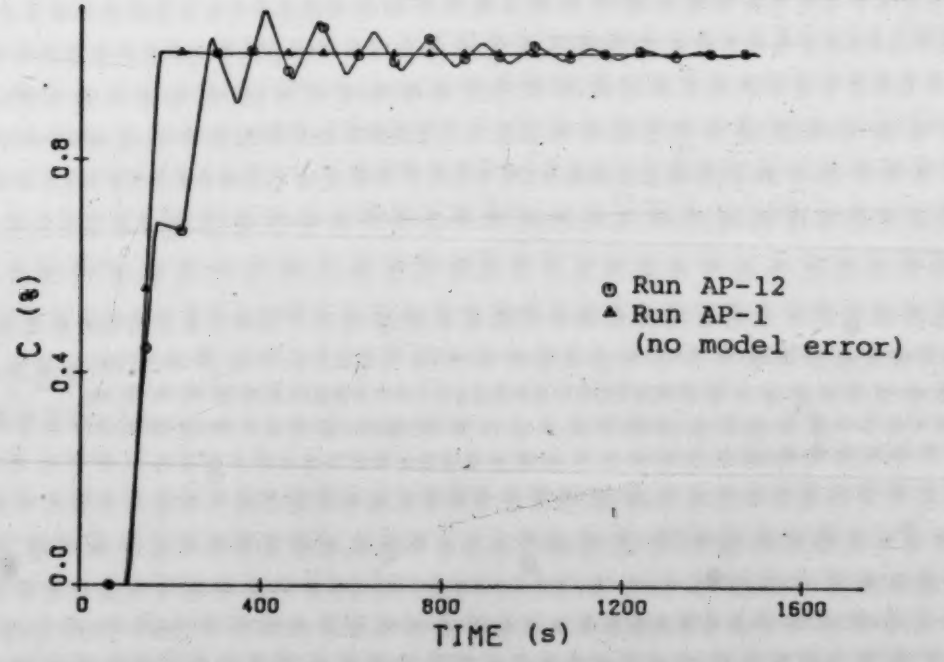

Fig. 4-10 : Influence of a Model Error of +20% in Time Delay on the AP for a 1% Step Increase in Setpoint.

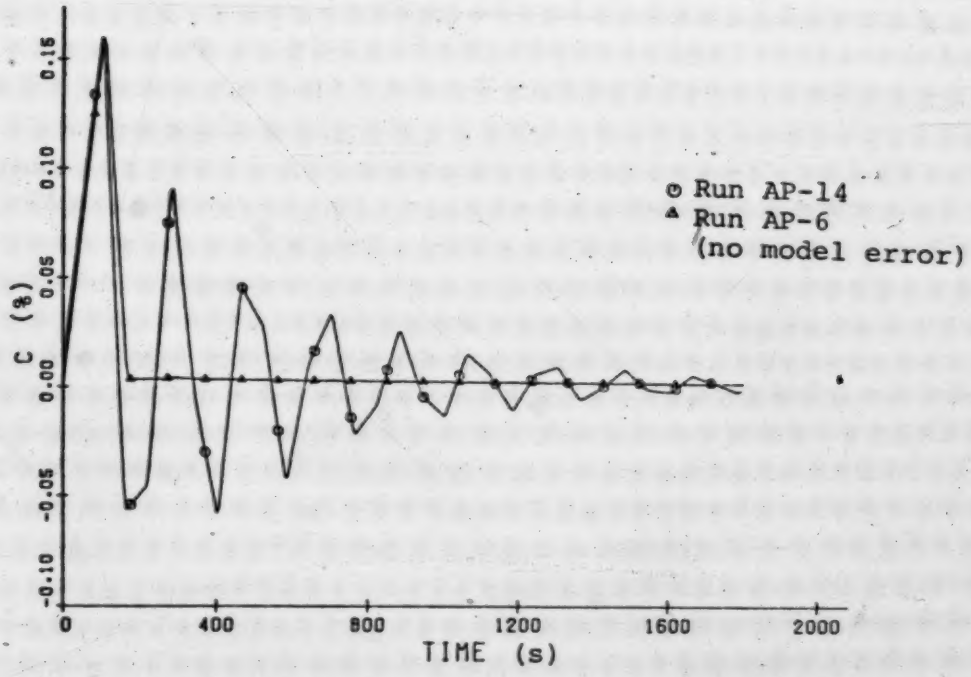

Fig. 4-11 : Influence of a Model Error of -20% in Process Gain on the AP for a 20% Step Increase in Feed Flow.

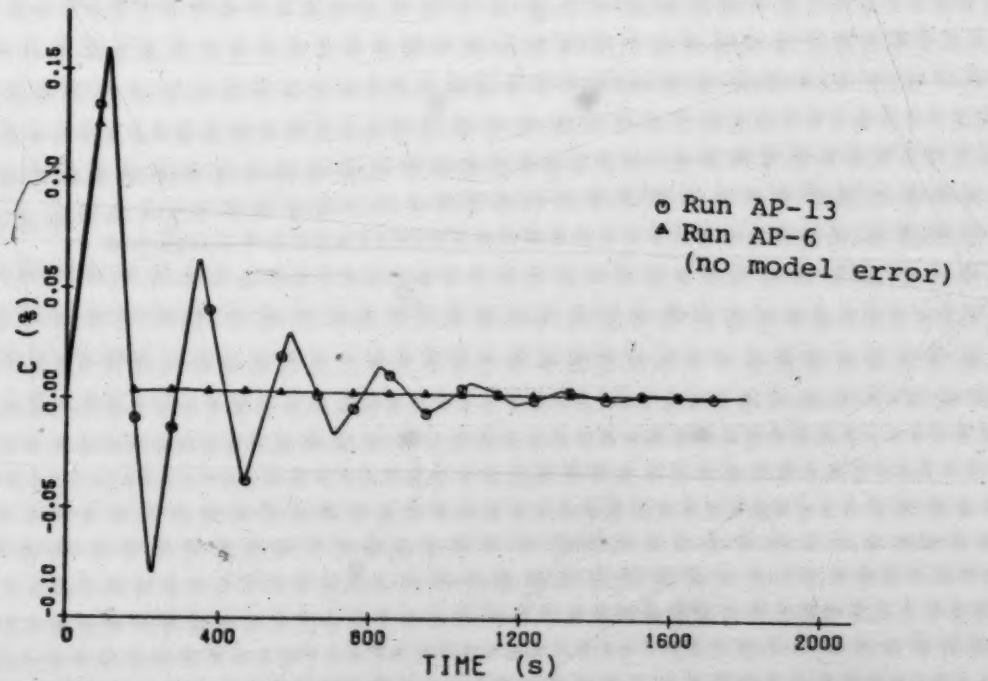

Fig. 4-12 : Influence of a Model Error of -20% in Time Delay on the AP for a 20% Step Increase in Feed Flow.

transient response in Fig. 4-11. For errors in time delay the reverse situation occurs; for an overestimated time delay (runs AP-11 and AP-12) the system was unstable and K_c had to be reduced to get a stable response as shown in Fig. 4-10. In the underestimated time delay run (AP-13) the stable but oscillatory response in Fig. 4-12 was obtained.

Evaluation of the results in Tables 4-5 and 4-6 shows that the AP is more sensitive to model errors than the SP. In the case of the AP control behaviour was always worse than for the ideal case; for the SP, a small or no decrease in control performance was observed in some cases. However, it should be noted that even with model errors the AP was still equivalent to the SP for setpoint changes and superior for feed flow changes.

4.4 Bottom Composition Control

The bottom composition control loop was simulated for step changes of +1% setpoint and +6% feed flow. Due to a program error the magnitude of the feed flow disturbances was different from 20%, the value used for the top composition simulations. However, this does not affect the comparison between the control schemes. The sampling time was 4 minutes, equal to the cycle time of the gas chromatograph. The controller constants in Table 4-7 were calculated from the process model in Table 3-1 using the methods discussed in Section 4.2.

As was the case for the top composition control the SP was unstable with the controller constants calculated using $T' = T_s / 2$ as suggested by Moore et al. (27). Consequently, the controller constants were reduced until a stable response was obtained. To determine the sensitivity of the AP to different values of the controller constants, simulations were done with the dead-beat constants as well as with controller constants which were 50% smaller.

Tables 4-7: Calculated Controller Constants for Bottom Composition Control

CONTROL ALGORITHM	CONTROLLER CONSTANTS K_c (g/s/%)	τ_I (s)	K_I (g/s/%s)	TUNING METHOD
PI	-0.620	1011	-	Eqns.(4.1) and (4.2), based on $T' = T+T_s/2$
PI	-0.506	1167	-	Eqns. (4.1) and (4.2), based on $T' = T+T_s$
PI	$\sim$ -1.06	$\sim$ 770	-	Optimal IAE constants for a discrete PI controller (19)
SP	-2.69	352	-	Eqns. (4.1) and (4.2), based on $T' = T_s/2$
SP	-1.36	574	-	Eqns. (4.1) and (4.2), based on $T' = T_s$
SP	$\sim$ -1.8	$\sim$ 330	-	Optimal IAE constants for a discrete PI controller (19)
AP	-2.62	-	-0.00671	Dead-beat controller constants from Eqns. (3.27) and (3.32)

The simulation results are summarized in Tables 4-8 and 4-9. The most satisfactory responses in terms of IAE values and overshoot for setpoint changes are shown in Fig. 4-13 and for feed flow changes in Fig. 4-14.

As expected for a system with a long time delay, PI control is not satisfactory and the superior performance of the AP and the SP for setpoint changes is seen clearly in Fig. 4-13. As was the case for top composition control, the AP behaves as a dead-beat controller with the calculated constants. A comparison of IAE values for runs AP-21 and AP-22 shows that even with suboptimal controller constants the AP is superior to PI control. Fig. 4-14 demonstrates that for feed flow changes the AP gives a considerable improvement over both SP and PI control. The sluggish response of the SP to feed flow changes that was noted for the top composition is again observed here. In this case, however, the SP gives lower IAE values than PI control.

To overcome the slow response of the SP to feed flow disturbances some simulations of the bottom composition control systems were performed using the SP algorithm with load prediction in Table 3-3. The results showed that with α=1, i.e. linear extrapolation, the system became very oscillatory and the controller constants had to be reduced to compensate for the decrease in stability. Better results were obtained by reducing α and using the controller constants calculated for the SP without load prediction. In this way the "tail" in the response curve could be reduced and the IAE value decreased from the value obtained without load prediction. However, this improvement did not seem significant enough to justify the use of a third tuning parameter (α). As the AP gave superior results with only two control modes load prediction was not persued further in this study.

Table 4-8 : Simulation Results for Bottom Composition Control (1% Step Increase in Setpoint)

RUN	K_c (g/s/%)	τ_I (s)	K_I (g/s/%s)	IAE (%s)	OVERSHOOT (%)	FIGURE
PI-21	-0.62	1011	-	1148	0.43	-
PI-22	-0.506	1167	-	955	0.16	4-13
SP-21	-1.36	574	-	564	0.20	4-13
SP-22	-2.0	440	-	936	0.92	-
AP-21	-2.62	-	-0.00671	531	0.0	4-13
AP-22	-1.30	-	-0.00671	617	0.0	-

Table 4-9 : Simulation Results for Bottom Composition Control (6% Step Increase in Feed Flow)

RUN	K_c (g/s/%)	τ_I (s)	K_I (g/s/%s)	IAE (%s)	MAX. DEVIATION (%)	FIGURE
PI-23	-0.62	1011	-	454	0.37	4-14
PI-24	-0.506	1167	-	534	0.38	-
SP-23	-1.36	574	-	372	0.37	4-14
SP-24	-2.0	440	-	322	0.37	-
AP-23	-2.62	-	-0.00671	184	0.37	4-14
AP-24	-2.62	-	-0.00335	252	0.37	-

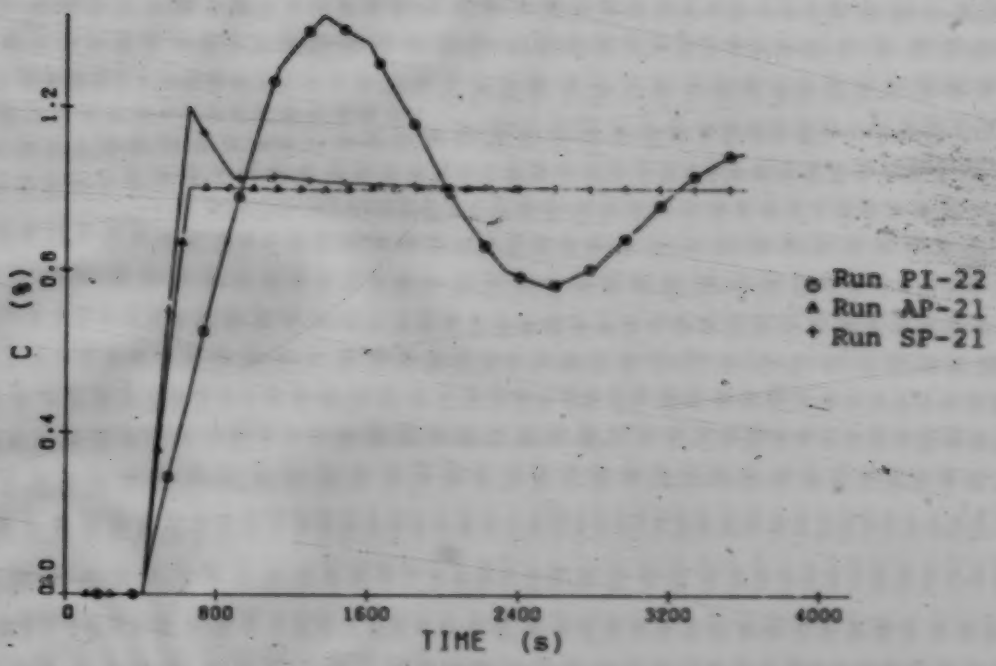

Fig. 4-13 : Comparison of SP, AP and PI Control for a 1% Step Increase in Setpoint.

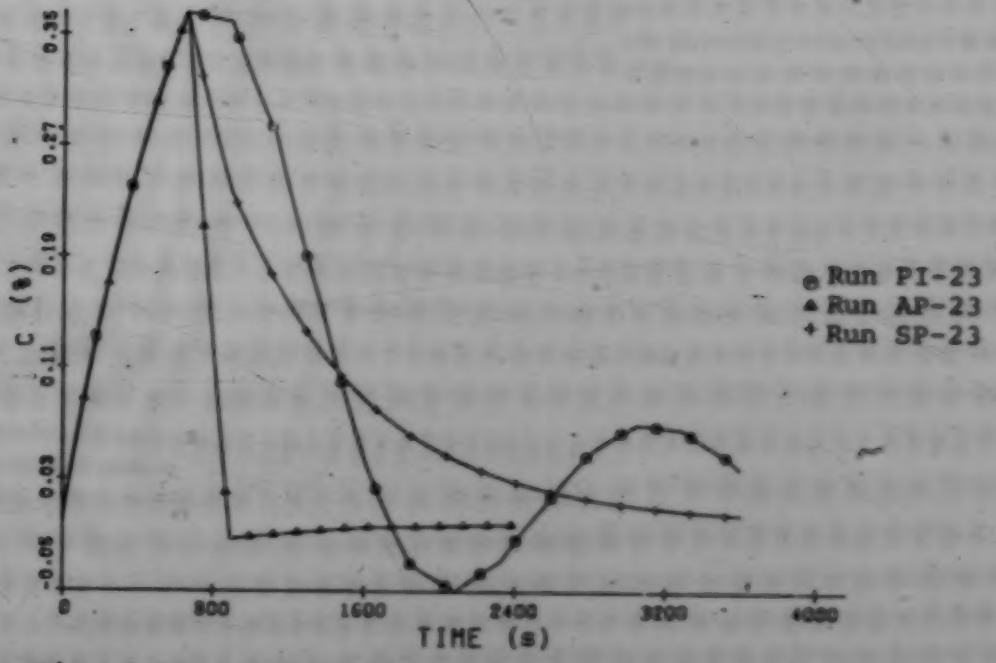

Fig. 4-14 : Comparison of SP, AP and PI Control for a 6% Step Increase in Feed Flow.

4.5 Discussion of Results

The results of the simulations for top and bottom composition control in the ideal case where no modelling errors are present show that both predictor control schemes can give an important improvement in terms of IAE values compared to PI control.

The AP was superior to the SP and PI control in all cases. With the calculated AP controller constants dead-beat control was obtained for setpoint changes, and for feed flow changes the performance came close to that of a dead-beat controller. The deviation from dead-beat control is probably due to the fact that the AP algorithm is designed for the special case where the process transfer function G_p (s) is equal to the load transfer function G_L (s), which was not the case for the distillation column model as can be seen from Table 3-1. The results of the AP for the bottom composition control, runs AP-21 to AP-24, demonstrate that even with suboptimal controller constants the performance did not deteriorate significantly. Thus the algorithm is insensitive to the controller constants, a result also noted by Doss et al. (9).

The SP gave improved results for setpoint changes for both top and bottom product control, and came close to the performance of the AP as can be seen from Figs. 4-2 and 4-13. For feed flow changes the SP gave only a slight improvement over PI control for the bottom composition and was inferior to PI control for the top composition. The simulation study of continuous SP and PI control in Appendix A demonstrated that for certain ratios of the process parameters the SP is inferior to PI control for step changes in load. In particular this

was the case for small values of the time delay to process time constant ratio, T/τ_p , where $T = T_1+T_2$, and large values of the load to process time constant ratio, τ_L/τ_p . Table 3-1 shows that these are the conditions that exist for top composition control ($T/\tau_p = 0.047$ and $\tau_L/\tau_p = 1.5$), whereas the process parameters for bottom composition control are more favorable for the SP ($T/\tau_p = 0.48$ and $\tau_L/\tau_p = 0.92$). Although the analysis used in Appendix A does not strictly apply to sampled-data systems, the SP showed the same dependency on the relative time delay and load time constant in the present simulations. Thus, better performance was obtained for bottom than for top composition control.

The simulation results in Tables 4-5 and 4-6 show that for the AP an inaccurate predictor model always led to a deterioration in performance compared to the ideal case. However, the resulting IAE values were still smaller than for PI control for both setpoint and load changes. The performance of the SP was less dependent on model errors. In some cases, especially for load disturbances, the resulting IAE values were even smaller than those obtained in the ideal case, but this may not be true for other types of load disturbances.

4.5.1. Conclusions

The simulations of the distillation column control system, using the process models in Table 3-1, for predictor control and PI control show that:

1. In the ideal case where no modelling errors are present the AP is superior to the SP and PI control for both setpoint and load changes.

2. The AP is insensitive to controller tuning. Only a small decrease in performance is obtained with suboptimal controller constants.

3. The SP is more sensitive to the controller constants used. However, it employs a PI controller and experience in PI controller tuning can be applied.

4. The SP gives good results for setpoint changes but results in sluggish responses to load changes, especially for top composition control.

5. The AP is more sensitive to modelling errors than the SP, which is demonstrated by the larger deterioration in performance when modelling errors are present. The resulting IAE values, however, are similar to those of the SP for setpoint changes and lower than those of the SP for load changes.

CHAPTER 5

EXPERIMENTAL EVALUATION

Two factors which will influence the performance of SP and AP control on an actual process were not investigated in the simulation study: the presence of noise and modelling errors involving the form of the dynamic model rather than only the magnitudes of the model parameters. The experimental study was carried out by applying the two predictor control schemes and PI control to composition control of the pilot scale distillation column at the University of Alberta. Single loop control was employed, i.e. only the top composition or only the bottom composition was controlled at one time. First order plus time delay process models of the form shown in Table 3-1 were used to describe the dynamics of the process. As these types of models apply to many industrial processes the results can be generalized and are applicable to other, similar control problems.

5.1 Implementation of the Control Schemes

In the usual operating mode of the column, the important process variables such as top composition, bottom composition etc. are monitored by the direct digital control (DDC) package of the IBM 1800 computer. The principal flows: feed, reflux and steam, are controlled using digital PI control and sampling times of 1 to 4 seconds depending on the flow control loop. These digital controllers act in the supervisory control mode, i.e. they send setpoints to the local analog flow controllers. The control algorithms in Tables 3-2, 3-5 and 3-6 were implemented as shown in Appendix E using software provided by the DDC package to get the measurements from the process and send the control signal to the process. Every sampling instant the control program obtains the latest value of the controlled variable

from the appropriate DDC measurement loop and calculates a new setpoint for the DDC reflux or steam flow control loop. This control loop in turn outputs the setpoint for the local analog flow controller. Thus the analog as well as the DDC flow control loops act as slave loops. Unless a very short sampling time T_S is specified for the master loop, the dynamics of the slave (flow control) loops are fast and can be neglected. Since sampling times of T_S = 1 minute for top composition control and T_S = 4 minutes for bottom composition control were used, this was the case. Otherwise the slave loops would effectively behave as additional lags in the master loop as noted by Dahlin (7).

For each experiment the column was controlled at the nominal steady state operating conditions for approximately one half hour before a disturbance or change in setpoint was introduced. During a run the process variables of interest were sampled every 32 seconds and the data stored on disk for later plotting and punching on cards.

5.2 Process Models for the Experimental Operating Conditions

For the experimental study it was advantageous to have operating conditions that yield top and bottom compositions that are outside the "pinch" region of the equilibrium curve since for very pure top or bottom products the process becomes highly nonlinear. However it was not possible to find operating conditions that gave low top composition and high bottom composition simultaneously since the column was designed for good separation. Thus it was necessary to strike a compromise in the selection of base operating conditions. The conditions of Table 5-1 were found to result in satisfactory product compositions. A detailed report of the operating conditions is given in Appendix G.

Table 5-1: Typical Steady-State Operating Conditions.
(Compositions in weight % methanol)

Feed, F:	18 g/s
Reflux, R:	16 g/s
Steam, S:	14-15 g/s
Feed composition, C_F:	50%
Top composition, C_D:	97%
Bottom composition, C_B:	5%
Reboiler temperature, T_R:	95° C
Distillate flow rate, D:	8.8 g/s
Bottom flow rate, B:	9.2 g/s

Berry (4) determined first order plus time delay transfer function models for the top and bottoms composition of the column from a least squares fit of experimental open loop response data. However his operating conditions were different from those used in this study and yielded lower top and bottom compositions. Experimental open loop response data for the operating conditions used in this study indicate that the process gains are quite different from Berry's gains. However the time constants and time delays remained almost unchanged. Thus in this investigation Berry's transfer function models were used to represent the process, but the experimentally determined process gains were substituted for the original gains. The process models are given in Table 5-2. Open loop responses using the first order plus time delay process models for this study were simulated for step changes in reflux, steam and feed flow. Figs. 5-1 to 5-4 show the comparison of these simulations with the experimental open loop responses obtained for the operating conditions given in Table 5-1. These figures show that:

1. The responses of the top and bottoms compositions are strongly nonlinear. This is reflected mainly in the process gain, but to a lesser degree also in the dynamics.

2. The transfer function models of Table 5-2, applicable to the operating conditions of this study, provide a reasonable approximation for both increases and decreases in reflux, steam and feed flow rates.

3. Feed flow changes cause only a very small upset in the top composition, especially for increases in feed flow.

Table 5-2 : Process Models for the Distillation Column.

For Operating Conditions Used in this Study

Top Composition :

$$c_D(s) = \frac{1.0\ e^{-60s}}{1002s + 1} R(s) + \frac{0.167\ e^{-486s}}{895s + 1} F(s)$$

Bottom Composition :

$$c_B(s) = \frac{-5.0\ e^{-174s}}{864s + 1} S(s) + \frac{2.08\ e^{-204s}}{792s + 1} F(s)$$

For Operating Conditions Used by Berry (4)

Top Composition :

$$c_D(s) = \frac{1.69\ e^{-60s}}{1002s + 1} R(s) + \frac{0.50\ e^{-486s}}{895s + 1} F(s)$$

Bottom Composition :

$$c_B(s) = \frac{-2.56\ e^{-174s}}{864s + 1} S(s) + \frac{0.65\ e^{-204s}}{792s + 1} F(s)$$

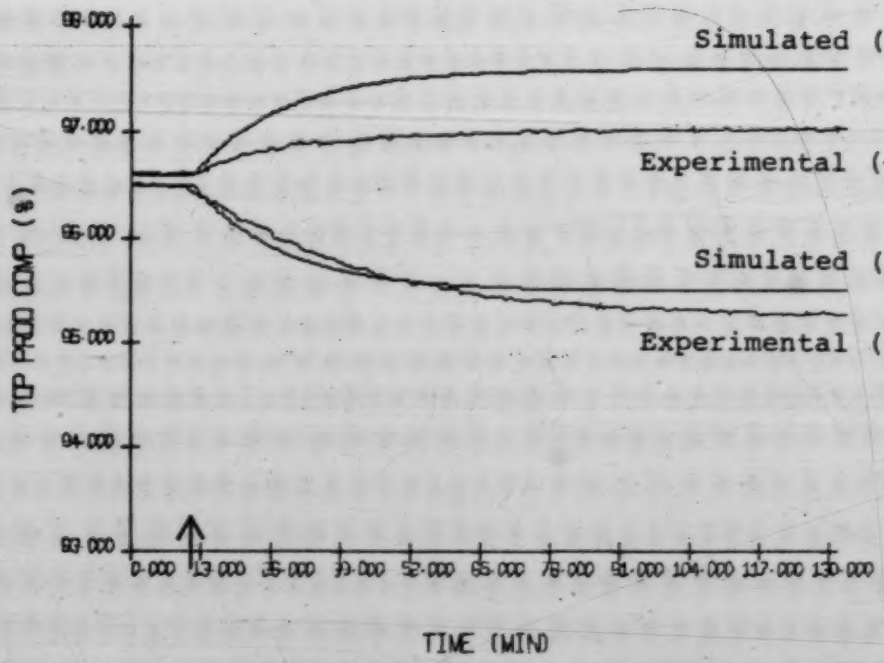

Fig. 5-1 : Comparison of Simulated and Experimental Open-loop Responses to Step Changes of +1 g/s or -1 g/s in Reflux Flow.

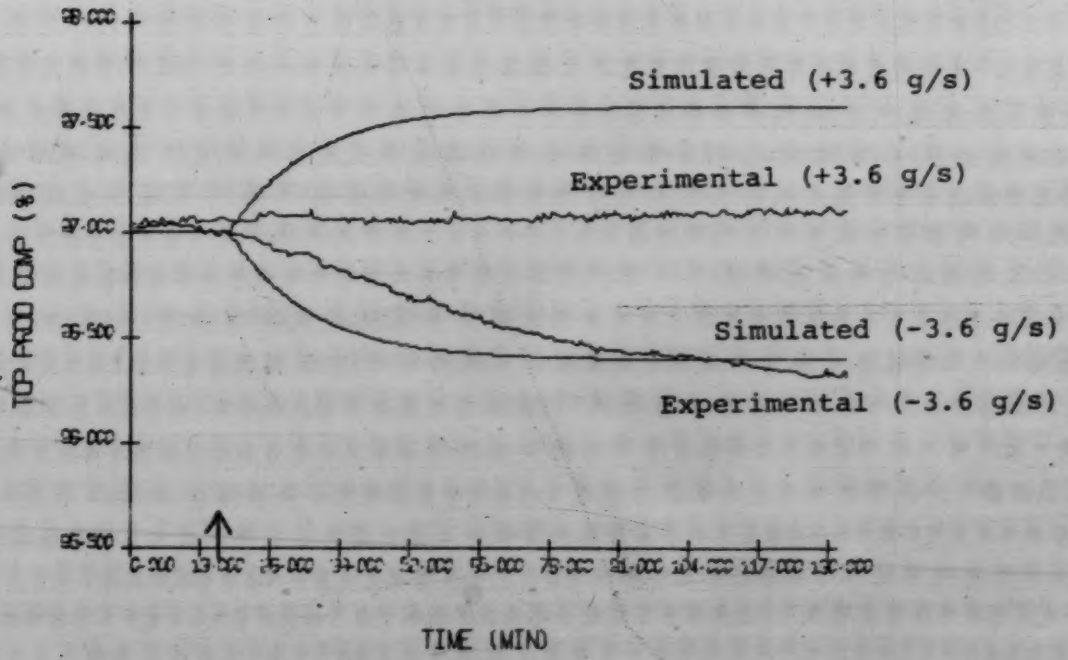

Fig. 5-2 : Comparison of Simulated and Experimental Open-loop Responses to Step Changes of +3.6 g/s or -3.6 g/s in Feed Flow.

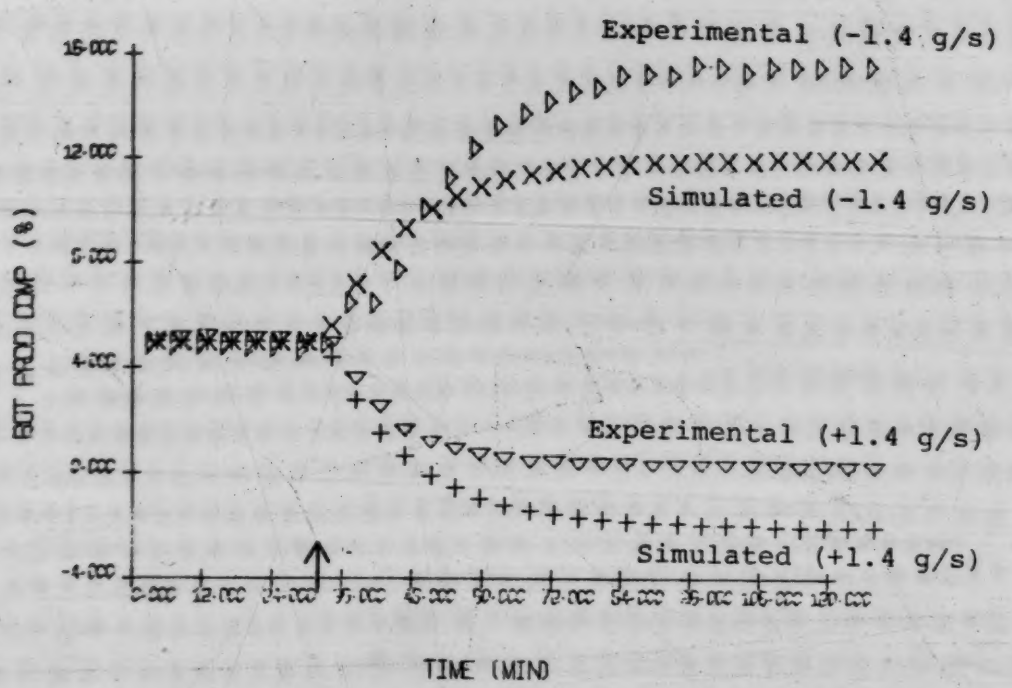

Fig. 5-3 : Comparison of Simulated and Experimental Open-loop Responses to Step Changes of +1.4 g/s or -1.4 g/s in Steam Flow.

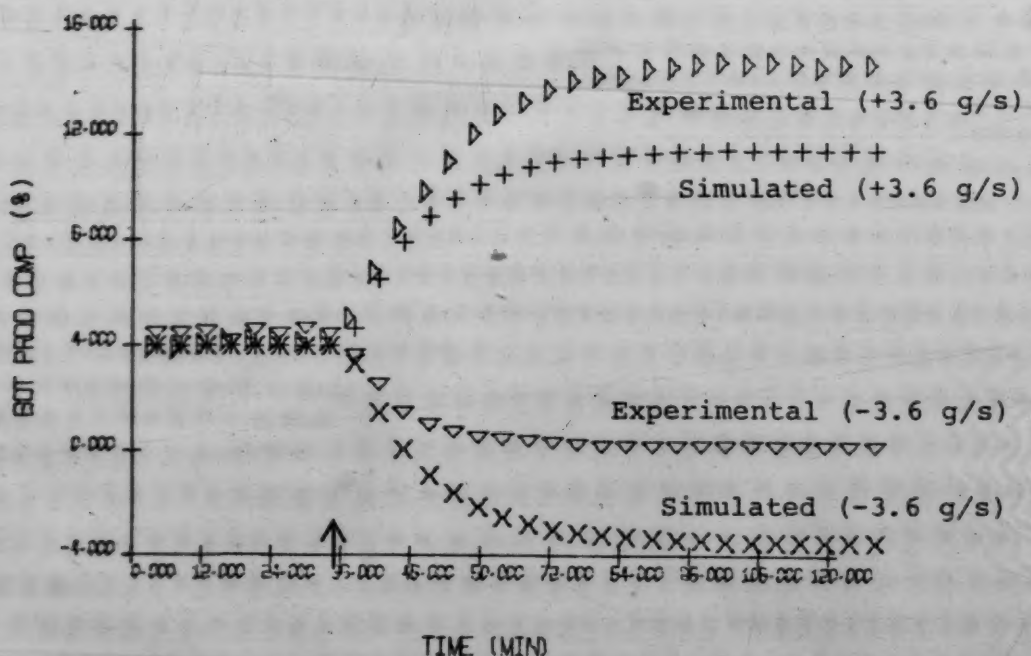

Fig. 5-4 : Comparison of Simulated and Experimental Open-loop Responses to Step Changes of +3.6 g/s or -3.6 g/s in Feed Flow.

5.3 Controller Tuning

For the process models of Table 5-2, it is possible to calculate controller constants for SP, AP and PI control using the methods described in Section 4.2. The controller constants for SP and PI control were calculated from the IAE tuning relations, Eqns.(4.1) and (4.2), based on an effective time delay of $T' = T_s$ for the SP and $T' = T + T_s$ for PI control. The constants for the AP were the calculated dead-beat constants from Eqns. (3.27) and (3.32). However the calculated controller constants resulted in unstable experimental responses so trial and error tuning became necessary. The IAE performance criterion was used as a basis for the on-line tuning. The tuned controller constants were determined for step changes in setpoint. Because of the nonlinearity of the process the direction of the applied step changes was important. Since it was found that the process gain increased for top compositions below the nominal operating conditions and bottom compositions above the nominal operating conditions, the controller constants were tuned for decreases in setpoint for the top composition and increases in setpoint for the bottom composition. This ensured that the tuned controller constants were conservative for other types of disturbances. It is not claimed that the resulting constants were those giving the optional IAE values but they are tuned well enough to allow a valid comparison between the three control schemes. Table 5-3 provides a comparison of the calculated and tuned controller constants and shows the large reductions that were necessary in order to obtain stable control.

Table 5-3 : Comparison of Calculated and Experimental Controller Constants.

CONTROL ALGORITHM	CONTROLLER CONSTANTS					
	CALCULATED			EXPERIMENTAL		
	K_c (g/s/%)	τ_I (s)	K_I (g/s/%s)	K_c (g/s/%)	τ_I (s)	K_I (g/s/%s)
Top Composition :						
PI	7.98	367	-	4.72	367	-
				10.0	250	-
SP	15.8	225	-	8.0	225	-
				10.0	-	0.06
AP	32.9	-	0.29	5.0	-	0.09
Bottom Composition :						
PI	-0.256	1167	-	-0.15	1500	-
				-0.30	1000	-
SP	-0.696	574	-	-0.20	1200	-
				-0.15	-	-0.0034
AP	-1.34	-	-0.00343	-0.20	-	-0.0020

5.4 Top Composition Control

The performance of the SP, AP and PI controllers for top composition control was evaluated at the operating conditions given in Table 5-1. Decreases in setpoint and feed flow were investigated because the top composition is very insensitive to increases in setpoint or feed flow when the composition is above 97%. Control performance was studied for step decreases of 1% in setpoint and 22% in feed flow. The IAE performance criterion was chosen as a basis for comparison with the IAE values computed for a duration of one hour after introducing the disturbance. Most experimental runs for the SP and AP were made using the process model applicable to this study given in Table 5-2 and shown below as Eqn. (5.1):

$$\frac{c_D(s)}{R(s)} = \frac{1.0\ e^{-60s}}{1002s + 1} \qquad (5.1)$$

To investigate the influence of large model errors, some runs were made using the process model established by Berry given in Eqn. (5.2):

$$\frac{c_D(s)}{R(s)} = \frac{1.69\ e^{-60s}}{1002s + 1} \qquad (5.2)$$

Although this model contains a larger process gain and leads to larger model errors at the new operating conditions, it would probably prove an adequate process model over a wider composition range, since the process gain increases for decreasing top composition. The results for setpoint changes are presented in Table 5-4 and the transient responses are shown in Figs. 5-5 to 5-12. The time at which the disturbance was introduced is denoted by an arrow on the time axis of the plots.

Table 5-4 : Summary of Experimental Results for Top Composition Control (1% Step Decrease in Setpoint)

RUN	K_C (g/s/%)	τ_I (s)	K_I (g/s/%s)	IAE (%s)	PROCESS MODEL (Equation Number)	FIGURE
PI-4	4.72	367	-	811	-	5-5
SP-5	10.0	250	-	449	5.1	5-6
SP-6	8.0	225	-	275	5.1	5-7
SP-3	6.0	250	-	644	5.2	5-8
AP-6	0.5	-	0.27	789	5.1	5-9
AP-7	5.0	-	0.09	400	5.1	5-10
AP-8	10.0	-	0.06	356	5.1	5-11
AP-4	1.0	-	0.17	767	5.2	5-12

The results for runs PI-4, SP-6 and AP-8, in Table 5-4, show that both predictors yield a significant improvement in control compared to PI control, giving a reduction in IAE values of as much as 50%. The transient responses in Figs. 5-7 and 5-11 demonstrate that with predictor control the top composition attains the new setpoint in less than 20 minutes with no overshoot, whereas with PI control the settling time is more than one hour as shown in Fig. 5-5. The performance of the SP is slightly better than that of the AP, but this could be due to better controller tuning. Controller tuning is more critical for the SP than for the AP as is demonstrated in runs SP-5, SP-6 and AP-6, AP-7 and AP-8. The small change in controller constants between the two SP runs leads to a considerable change in the IAE values and transient responses in Figs. 5-6 and 5-7 whereas with the significantly different controller constants for the AP runs, the transient response is almost the same as shown in Figs. 5-10 and 5-11. Even with the badly tuned constants in run AP-6 the control is still satisfactory and superior to PI control in terms of IAE

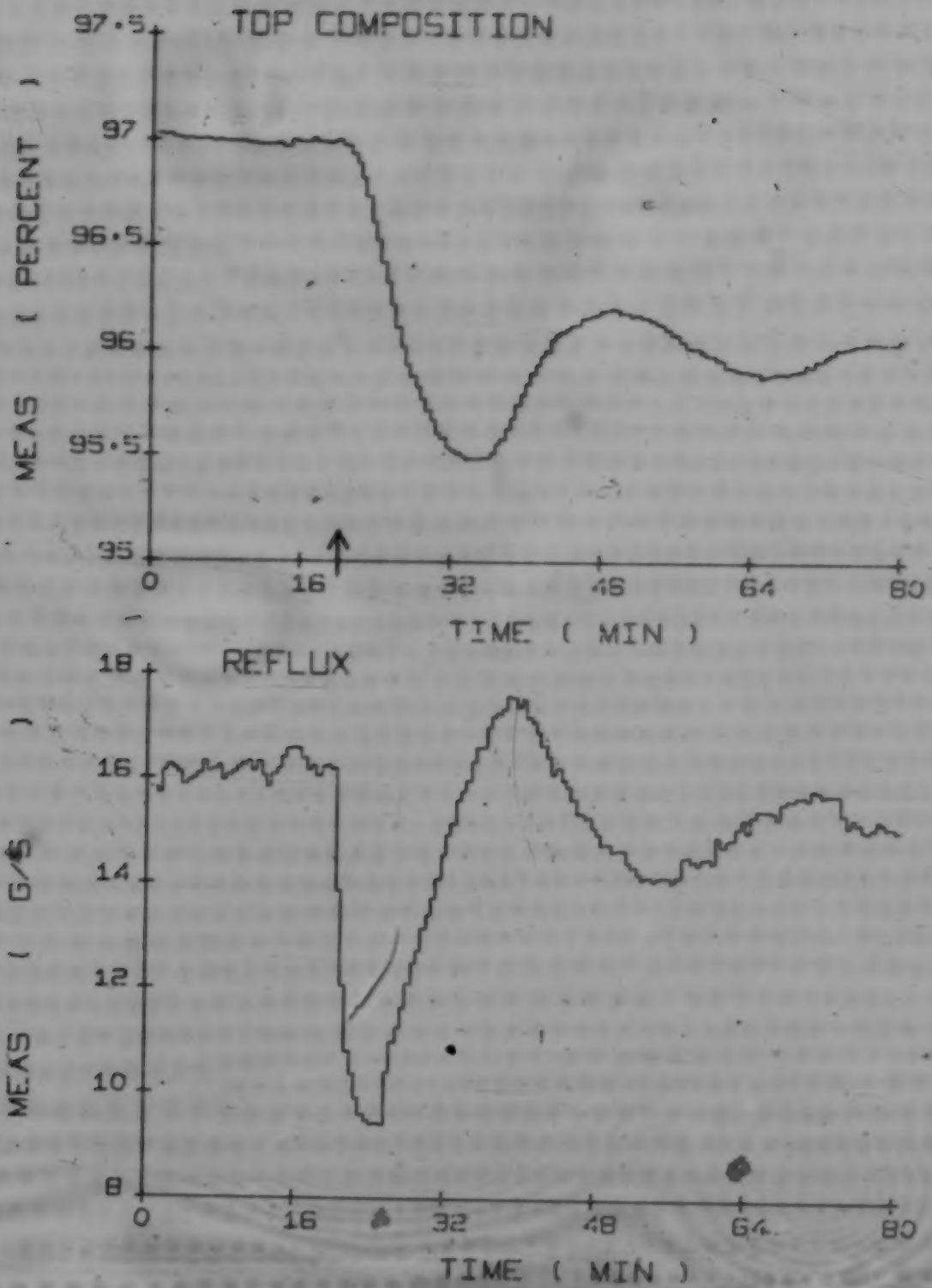

Fig. 5-5 : PI Control (-1% Setpoint Change, Run PI-4
K_c=4.72, τ_I=367)

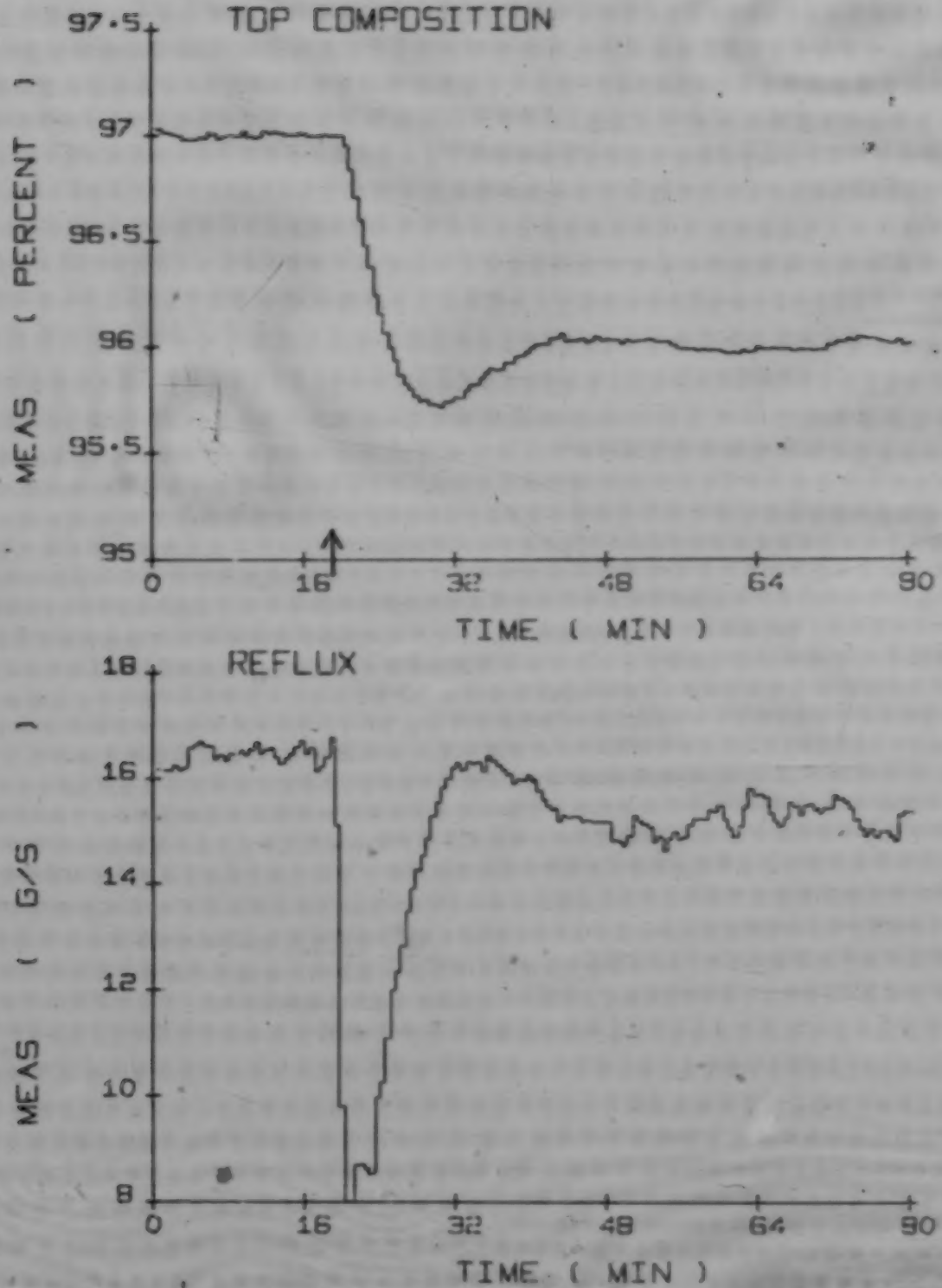

Fig. 5-6 : SP Control (-1% Setpoint Change, Run $\hat{SP}$-5
K_c=10.0, τ_I=250)

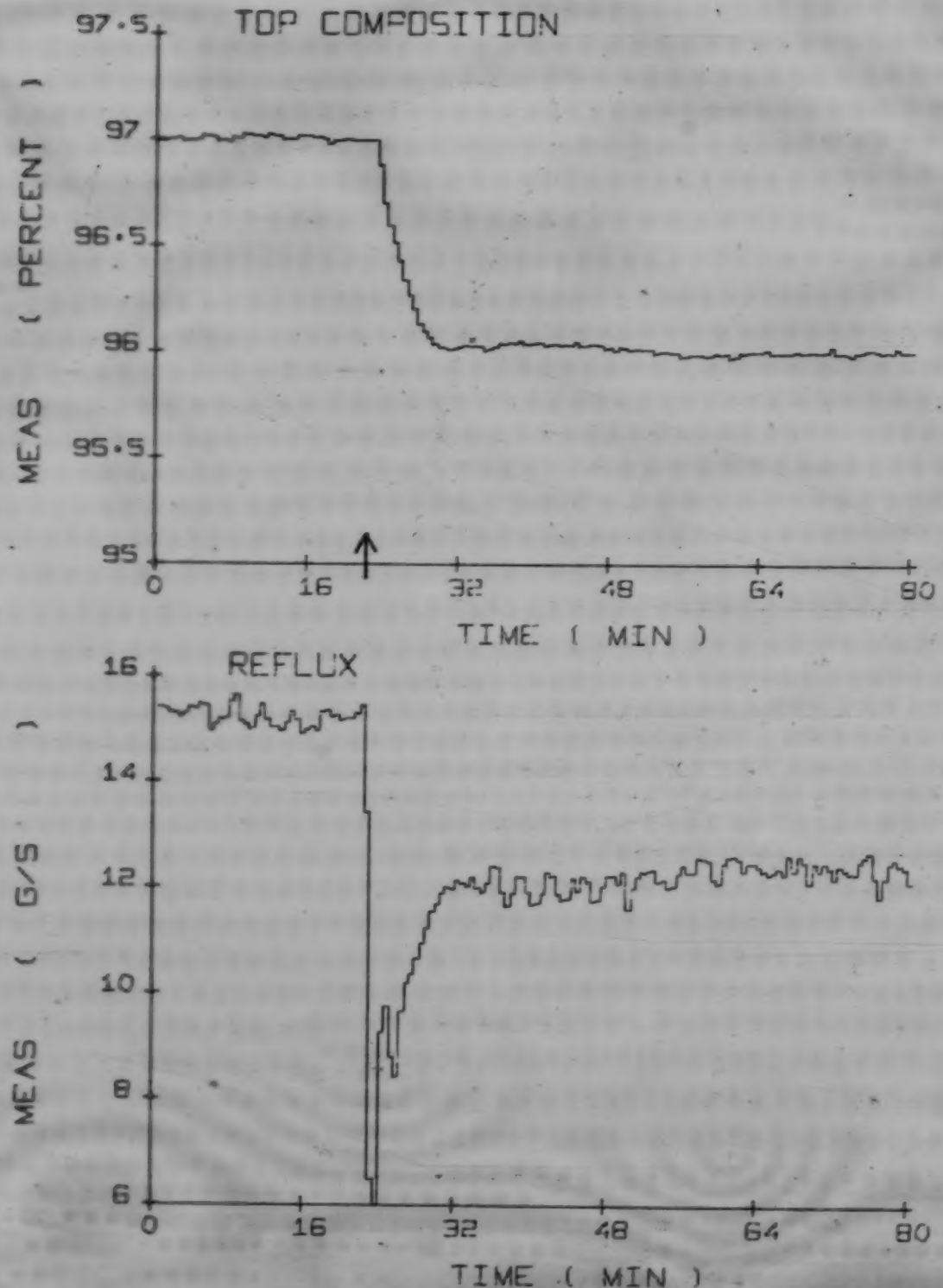

Fig. 5-7 : SP Control (-1% Setpoint Change, Run SP-6
K_c=8.0, τ_I=225)

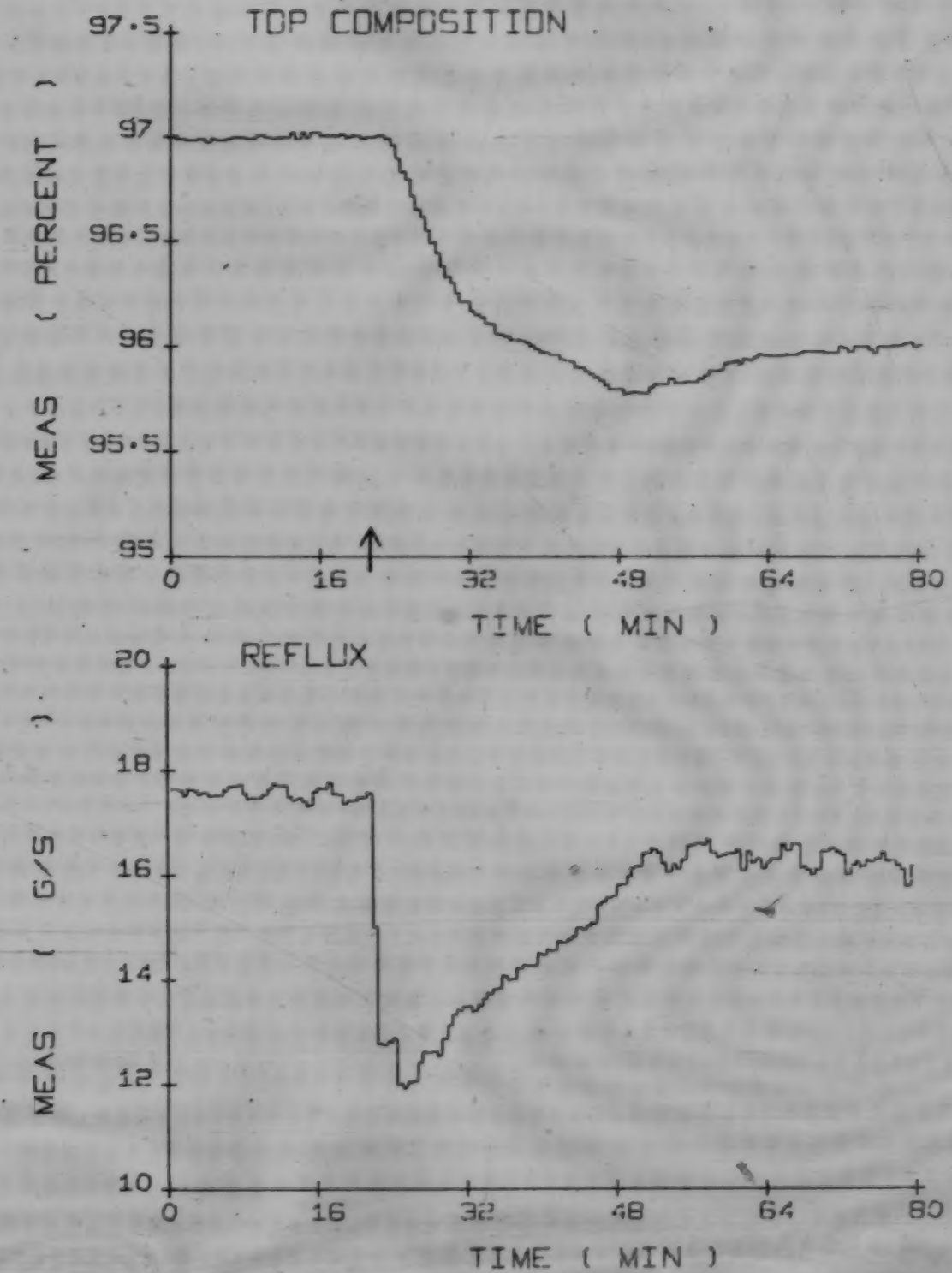

Fig. 5-8 : SP Control (-1% Setpoint Change, Run SP-3
K_c=6.0, τ_I=250)

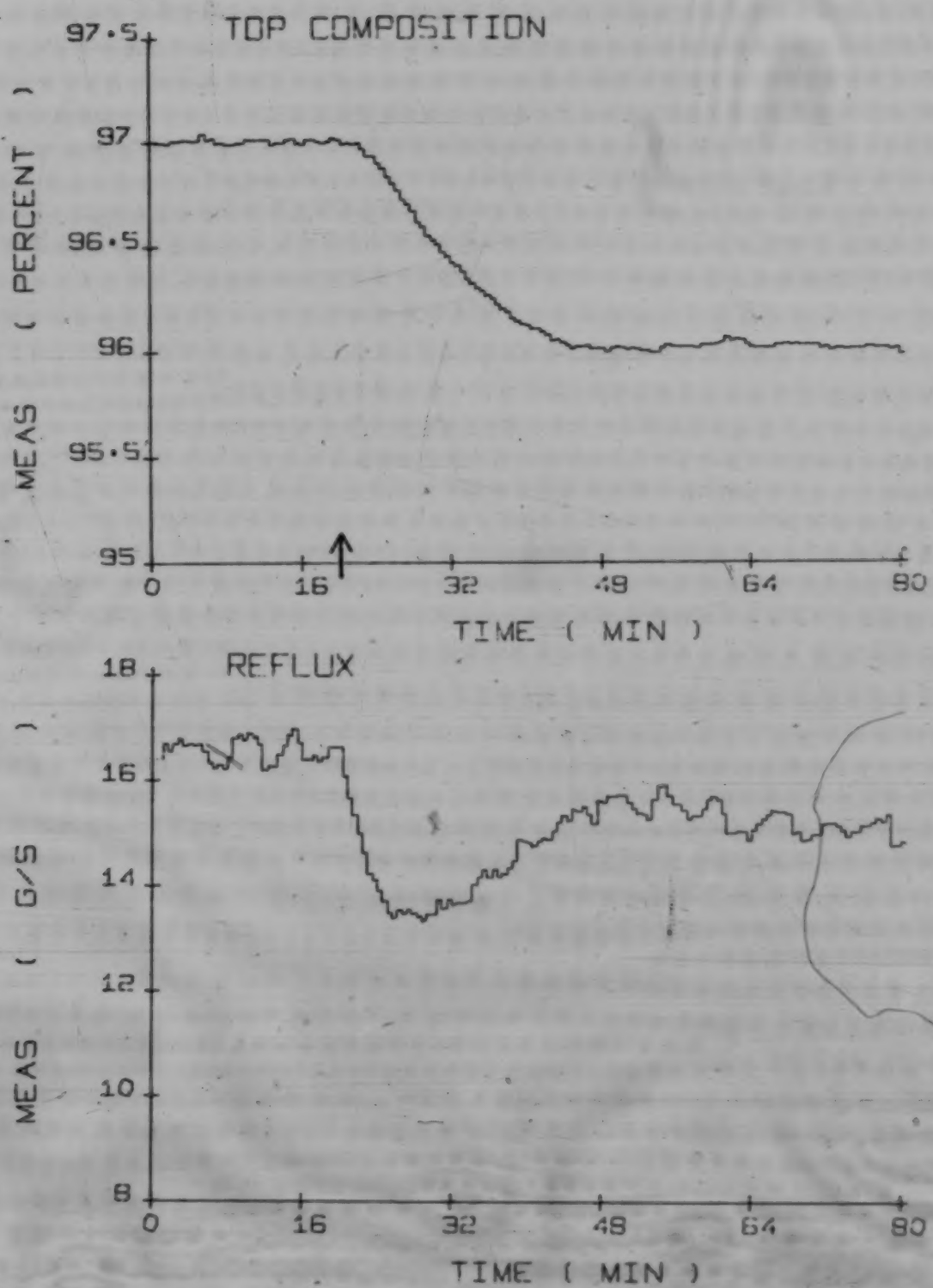

Fig. 5-9 : AP Control (-1% Setpoint Change, Run AP-6
K_c=0.5, K_I=0.27)

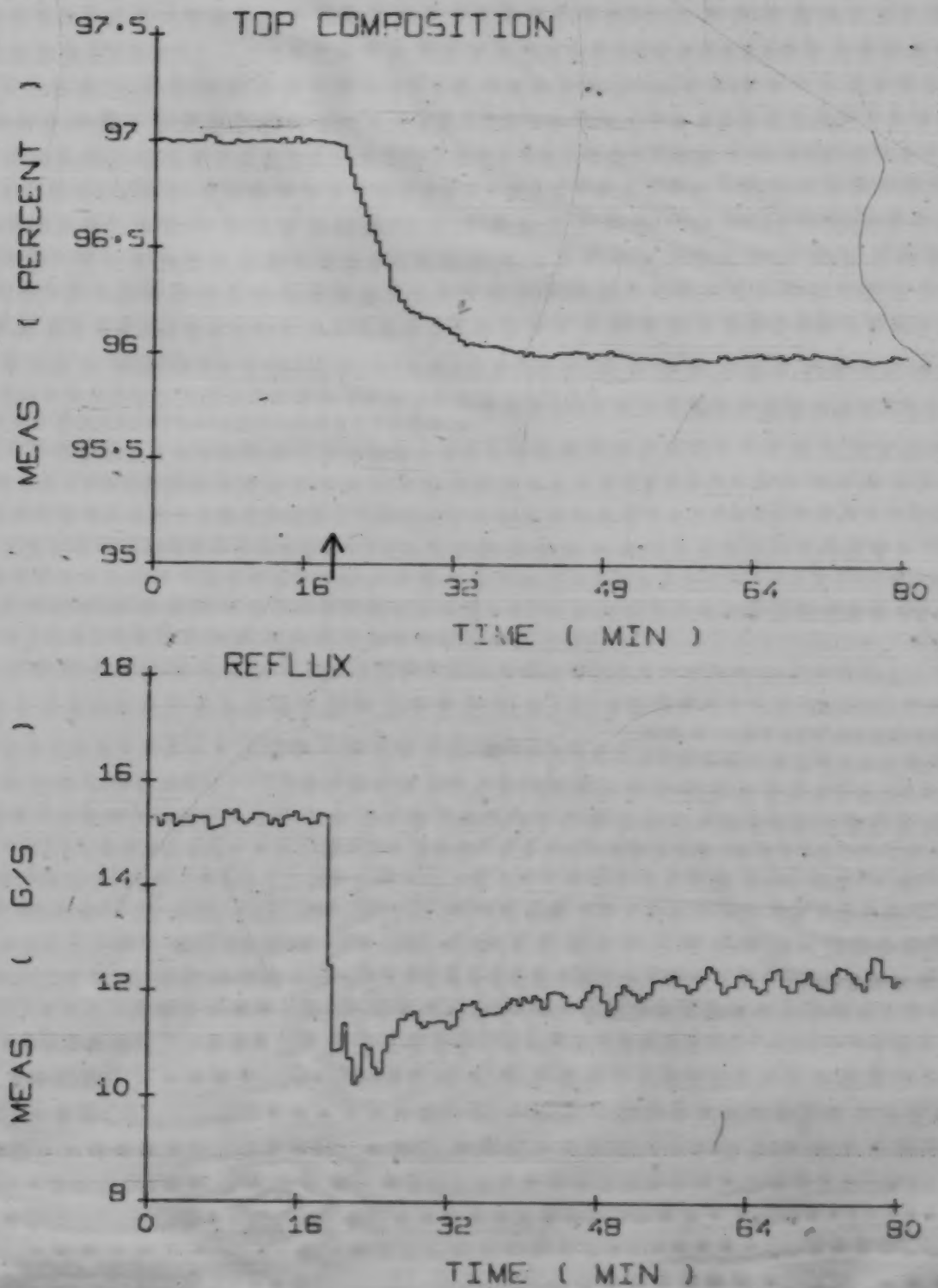

Fig. 5-10: AP Control (-1% Setpoint Change, Run AP-7
K_c=5.0, K_I=0.09)

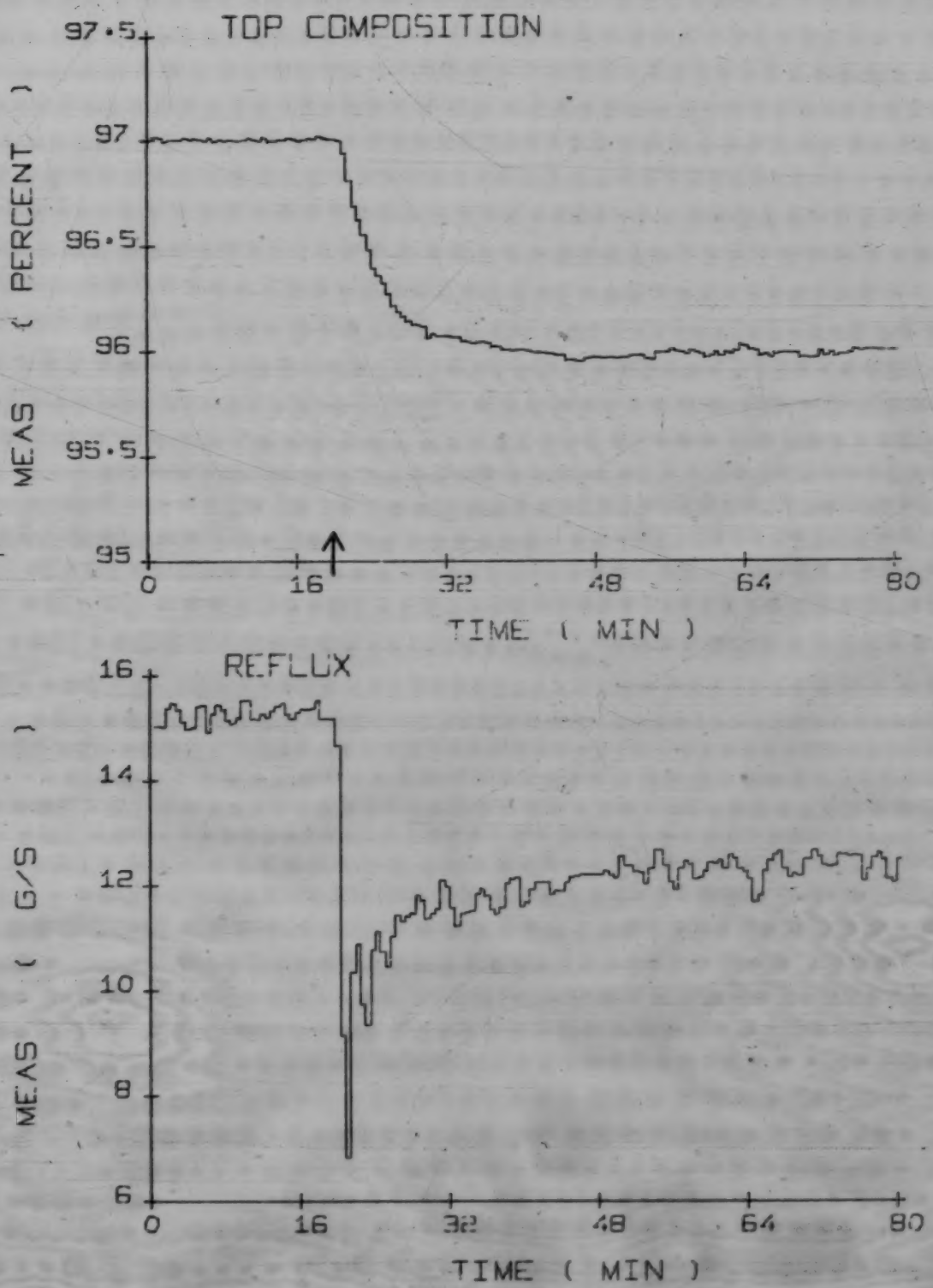

Fig. 5-11: AP Control (-1% Setpoint Change, Run AP-8
K_c=10.0, K_I=0.06)

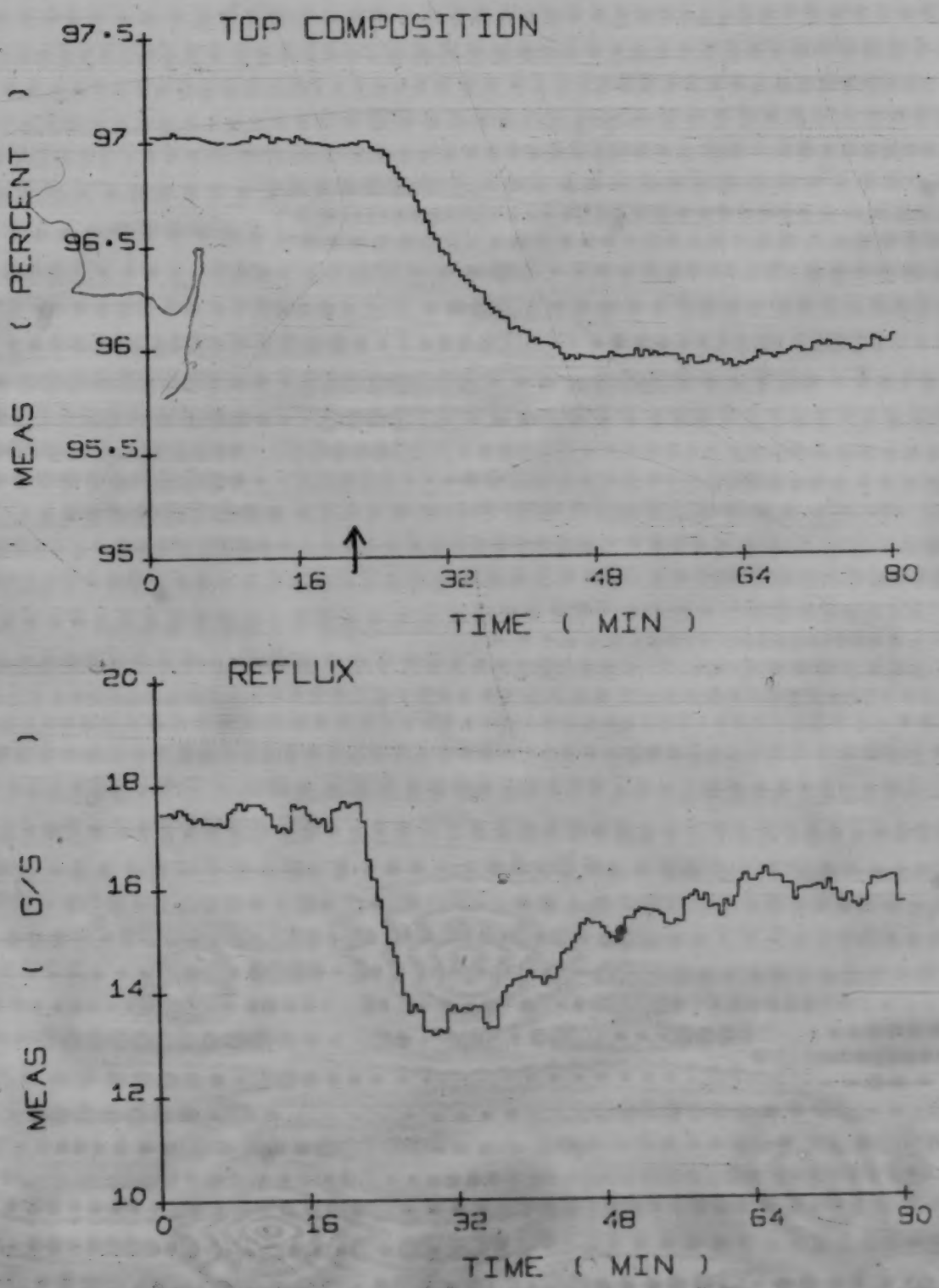

Fig. 5-12; AP Control (-1% Setpoint Change, Run AP-4
K_c=1.0, K_I=0.17)

values. When the inadequate process model of Eqn. (5.2) is employed, the performance of both predictor control schemes deteriorates considerably as shown in runs SP-3 and AP-4. The controller constants had to be reduced, compared to the runs with the model of Eqn. (5.1), in order to obtain stable control. It is to be noted that the resulting IAE values are smaller than for PI control in spite of the large modelling errors, in that the model gain is approximately 50% higher than the actual process gain. The better performance of the SP compared to the AP indicates that the SP is not as sensitive to modelling errors, as was concluded in the simulation study.

The results for feed flow changes are presented in Table 5-5 and the transient responses are shown in Figs. 5-13 to 5-15.

Table 5-5 : Summary of Experimental Results for Top Composition Control (22% Step Decrease in Feed Flow)

RUN	K_c (g/s/%)	τ_I (s)	K_I (g/s/%s)	IAE (%s)	PROCESS MODEL (Equation Number)	FIGURE
PI-5	4.72	367	-	205	-	5-13
SP-7	8.0	225	-	103	5.1	5-14
SP-4	6.0	250	-	259	5.2	-
AP-9	10.0	-	0.06	101	5.1	5-15
AP-5	1.0	-	0.17	166	5.2	-

The figures and the IAE values in Table 5-5 indicate an improvement of predictor control compared to PI control, but since the maximum deviations from steady state are very small for all three control schemes no further interpretation of the results is considered possible.

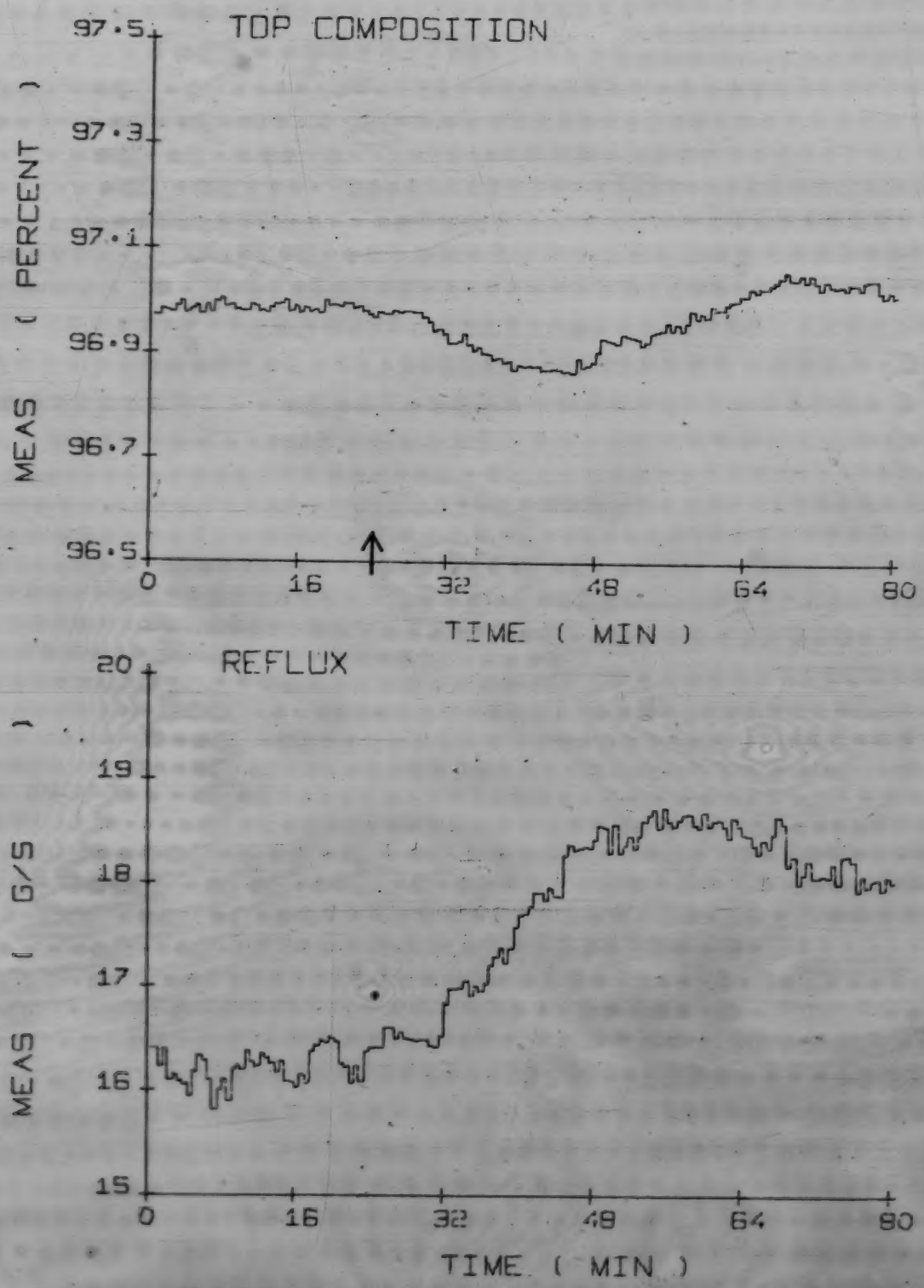

Fig. 5-13: PI Control (-22% Feed Flow Change, Run PI-5
K_c=4.72, τ_I=367)

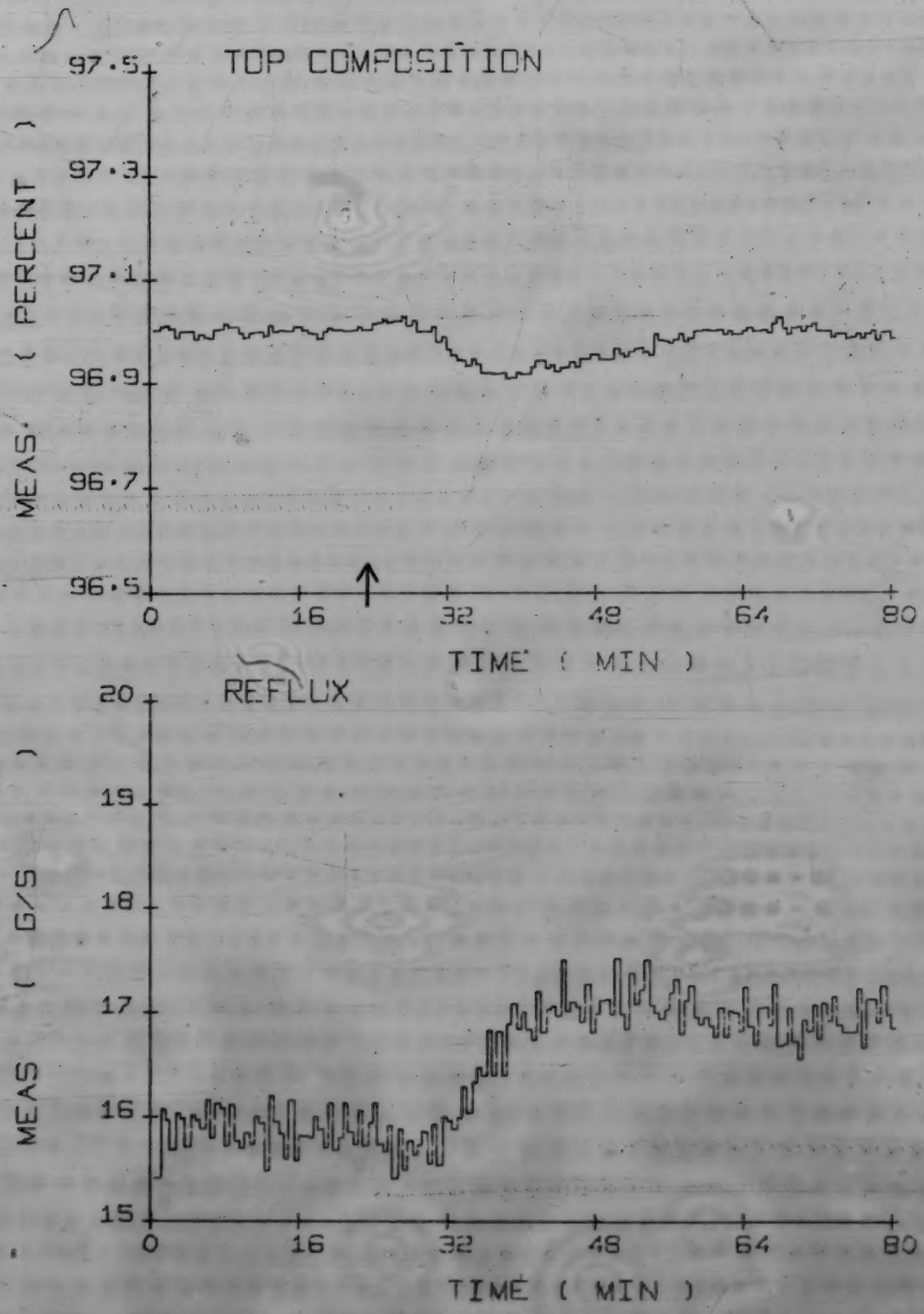

Fig. 5-14 : SP Control (-22% Feed Flow Change, Run SP-7
K_c=8.0, τ_I=225)

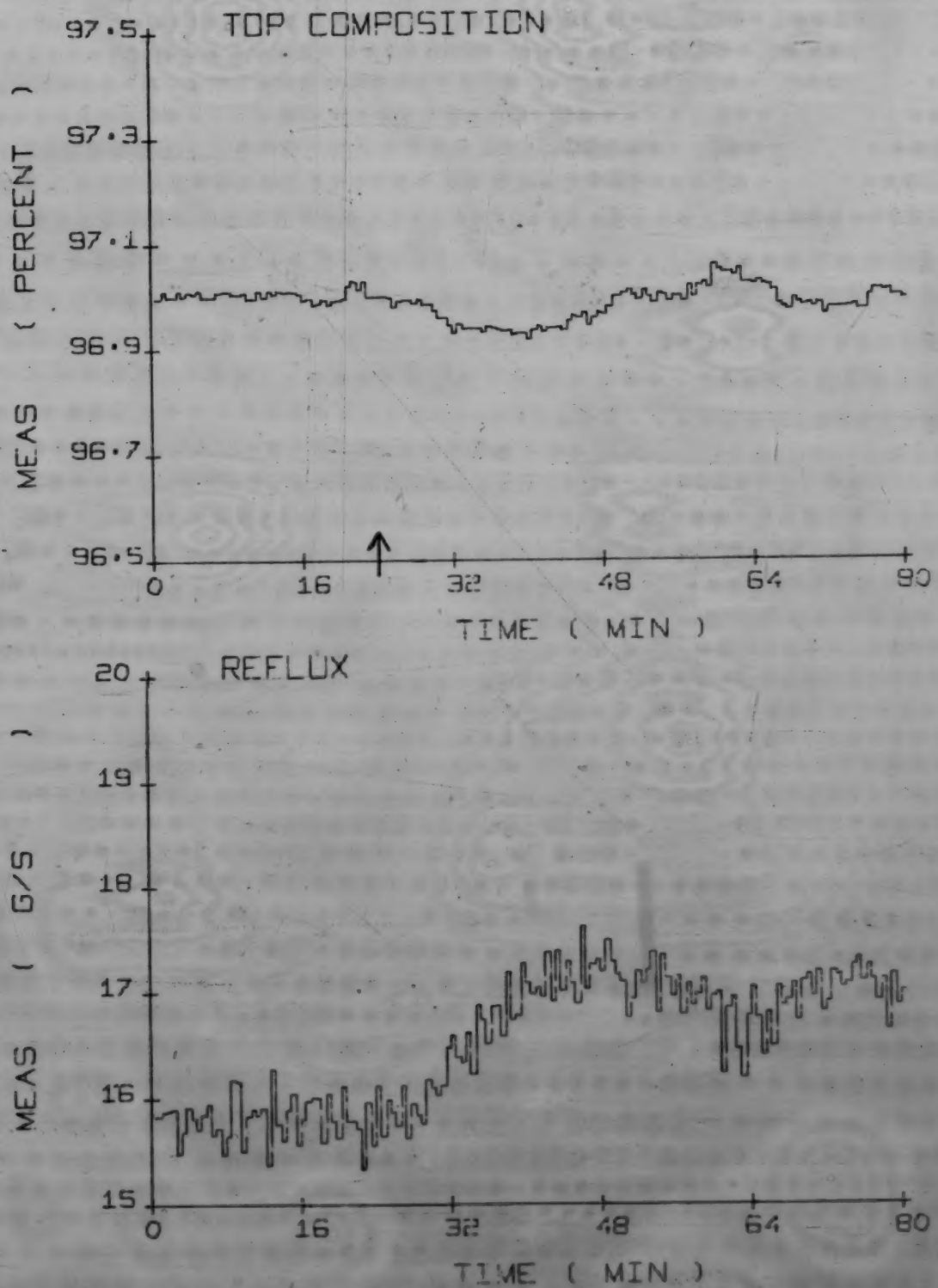

Fig. 5-15: AP Control (-22% Feed Flow Change, Run AP-9
K_c=10.0, K_I=0.06)

5.5 Bottom Composition Control

The three control schemes were compared for bottom composition control at the basic operating conditions of Table 5-1. The disturbances employed were step changes of ± 2% in composition setpoint and ± 17% in feed flow rate. The IAE performance criterion was used as the basis for comparison of the control schemes. Because the transients are longer for the bottom composition, the reported IAE values are for 2 hours duration after introducing the disturbance.

The process model of Table 5-2 given in Eqn. (5.3)

$$\frac{c_B(s)}{S(s)} = \frac{-5.0\, e^{-174s}}{864\, s + 1} \qquad (5.3)$$

was used for SP and AP control. The comparison of simulated open loop responses for this model with experimental data in Fig. 5-3 shows that Eqn. (5.3) in fact represents a compromise for increases and decreases in steam flow, due to the nonlinear column behaviour.

The bottom composition was analyzed with an on-line gas chromatograph (GC). Liquid from the reboiler was pumped through a recycle line and a liquid sample from that line was withdrawn and injected into the GC for analysis. Both the automatic liquid sampling and the chromatographic analysis were under computer control, with a cycle time of 4 minutes. This long cycle time was necessary to get a reliable composition analysis. For more details on the GC and sampling system the reader is referred to Simonsmeier (40).

The transport delay in the recycle line was found to be negligible, and consequently the total time delay associated with bottoms composition measurement was taken as the 4 minutes cycle time. The sampling time was chosen as 4 minutes, the cycle time of the GC.

The GC analysis system resulted in a rather high noise-level for the composition measurement. Figure 5-16 shows composition measurements at two different steady states and indicates that the analysis is reliable to within approximately ± 0.4 weight % methanol.

The bottom composition control runs are summarized in Tables 5-6 and 5-7 and the transient responses for setpoint changes are shown in Figs. 5-17 to 5-27 and those for feed flow changes in Figs. 5-28 to 5-36.

The responses clearly demonstrate the nonlinearity of the process. The response can be over or underdamped with the same controller constants depending on the direction of the disturbance as can be seen from Figs. 5-17 and 5-24 for PI control, and Figs. 5-23 and 5-26 for the AP. Thus constants tuned for one particular disturbance may not be well suited to other disturbances. The controller constants for all 3 control schemes were tuned for a 2% increase in bottoms composition setpoint.

A comparison of the best runs for each type of control in terms of IAE values for increases in setpoint, runs PI-22, SP-23, AP-22 and for decreases in setpoint, runs PI-24, SP-25, AP-30 shows that the AP provides a significant improvement over PI control, whereas the SP is superior to PI control for decreases in setpoint but almost identical for increases in setpoint. The fact that the AP compensates for the time delay introduced by sampling gives it an advantage over the SP since bottom composition control involves a large sampling time of 4 minutes.

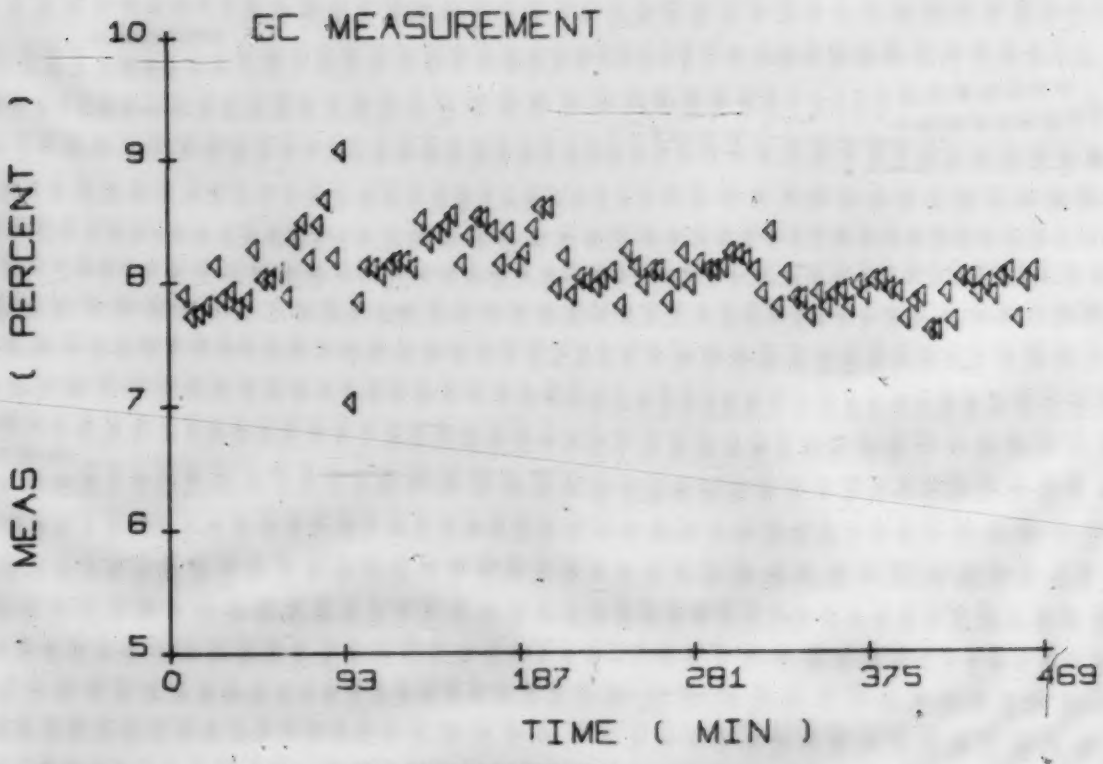

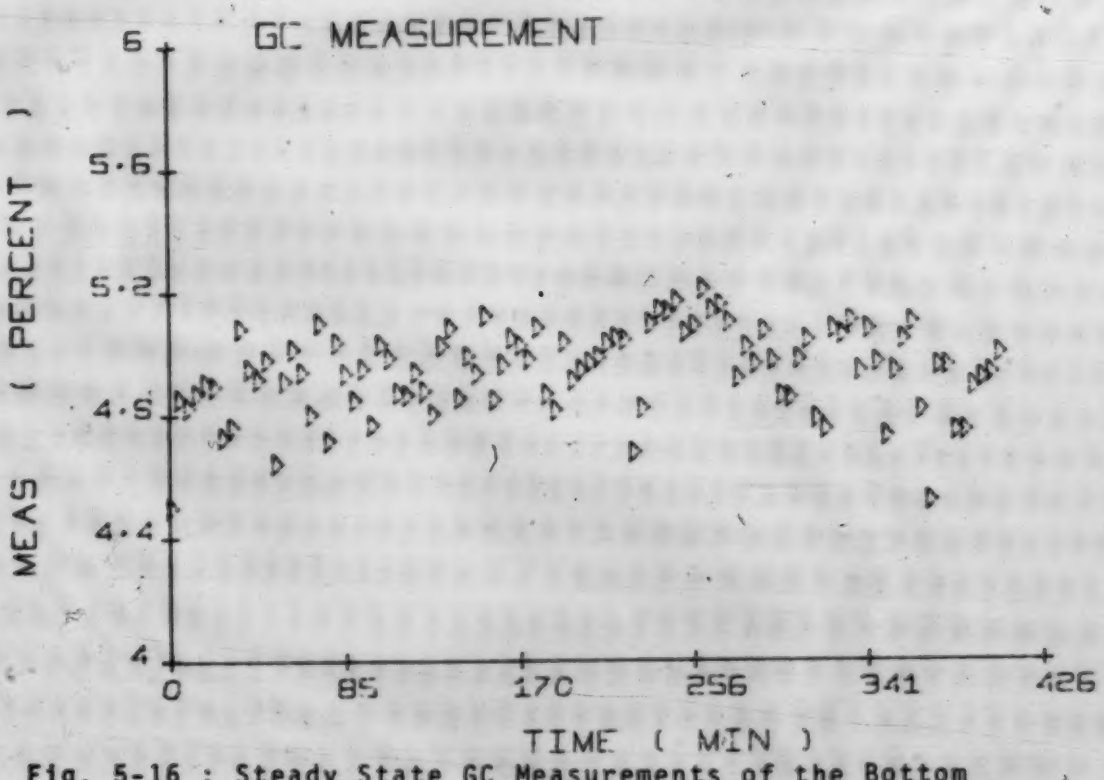

Fig. 5-16 : Steady State GC Measurements of the Bottom Composition at Two Different Operating Conditions of the Distillation Column.

Table 5-6 : Summary of Experimental Results for Bottom Composition Control
(2% Step Changes in Setpoint)

RUN	K_c (g/s/%)	τ_I (s)	K_I (g/s/%s)	IAE (%s)	FIGURE
Increases :					
PI-22	-0.15	1500	-	3250	5-17
SP-21	-0.40	800	-	4500	5-18
SP-22	-0.20	1200	-	3350	5-19
SP-23	-0.30	1000	-	3200	5-20
AP-21	-0.20	-	-0.0034	3650	-
AP-22	-0.80	-	-0.0020	2500	5-21
AP-23	-0.50	-	-0.0034	3350	-
AP-24	-0.40	-	-0.0020	3500	5-22
AP-27	-0.15	-	-0.0034	3600	5-23
Decreases :					
PI-24	-0.15	1500	-	3850	5-24
SP-25	-0.30	1000	-	2600	5-25
AP-28	-0.15	-	-0.0034	3400	5-26
AP-30	-0.80	-	-0.0020	2200	5-27

Table 5-7 : Summary of Experimental Results for Bottom Composition Control
(17% Step Changes in Feed Flow)

RUN	K_C (g/s/%)	τ_I (s)	K_I (g/s/%s)	IAE (%s)	FIGURE
Increases :					
PI-23	-0.15	1500	-	10000	5-28
SP-24	-0.30	1000	-	6600	5-29
AP-25	-0.40	-	-0.0020	7200	5-30
AP-26	-0.15	-	-0.0034	7300	5-31
Decreases :					
PI-25	-0.15	1500	-	10400	5-32
SP-26	-0.30	1000	-	8400	5-33
SP-27	-0.20	1200	-	9600	5-34
AP-29	-0.15	-	-0.0034	6900	5-35
AP-31	-0.80	-	-0.0020	7400	5-36

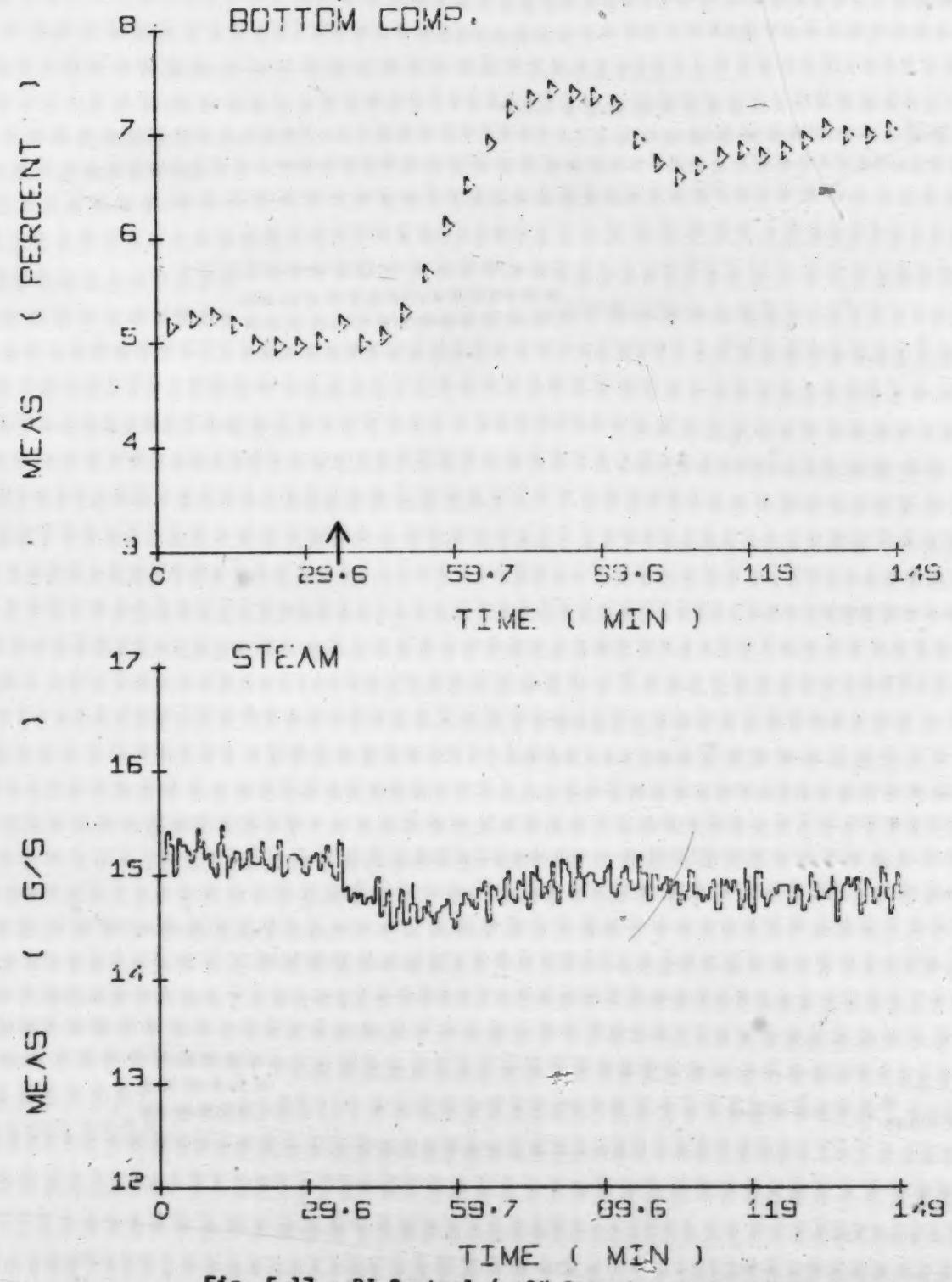

Fig. 5-17 : PI Control (+2% Setpoint Change, Run PI-22
K_c= -0.15, τ_I=1500)

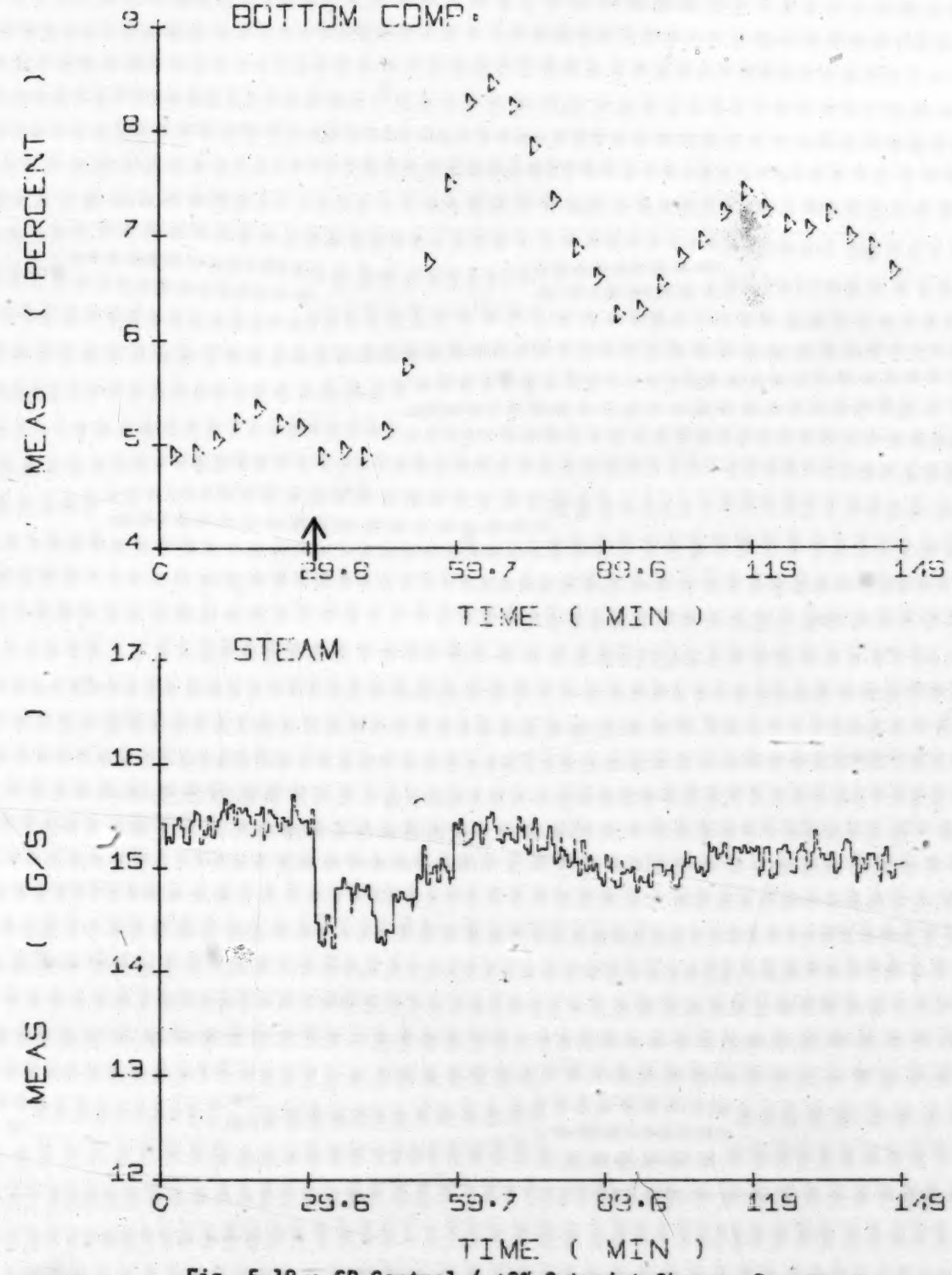

Fig. 5-18 : SP Control (+2% Setpoint Change, Run SP-21
K_c= -0.40, τ_I=800)

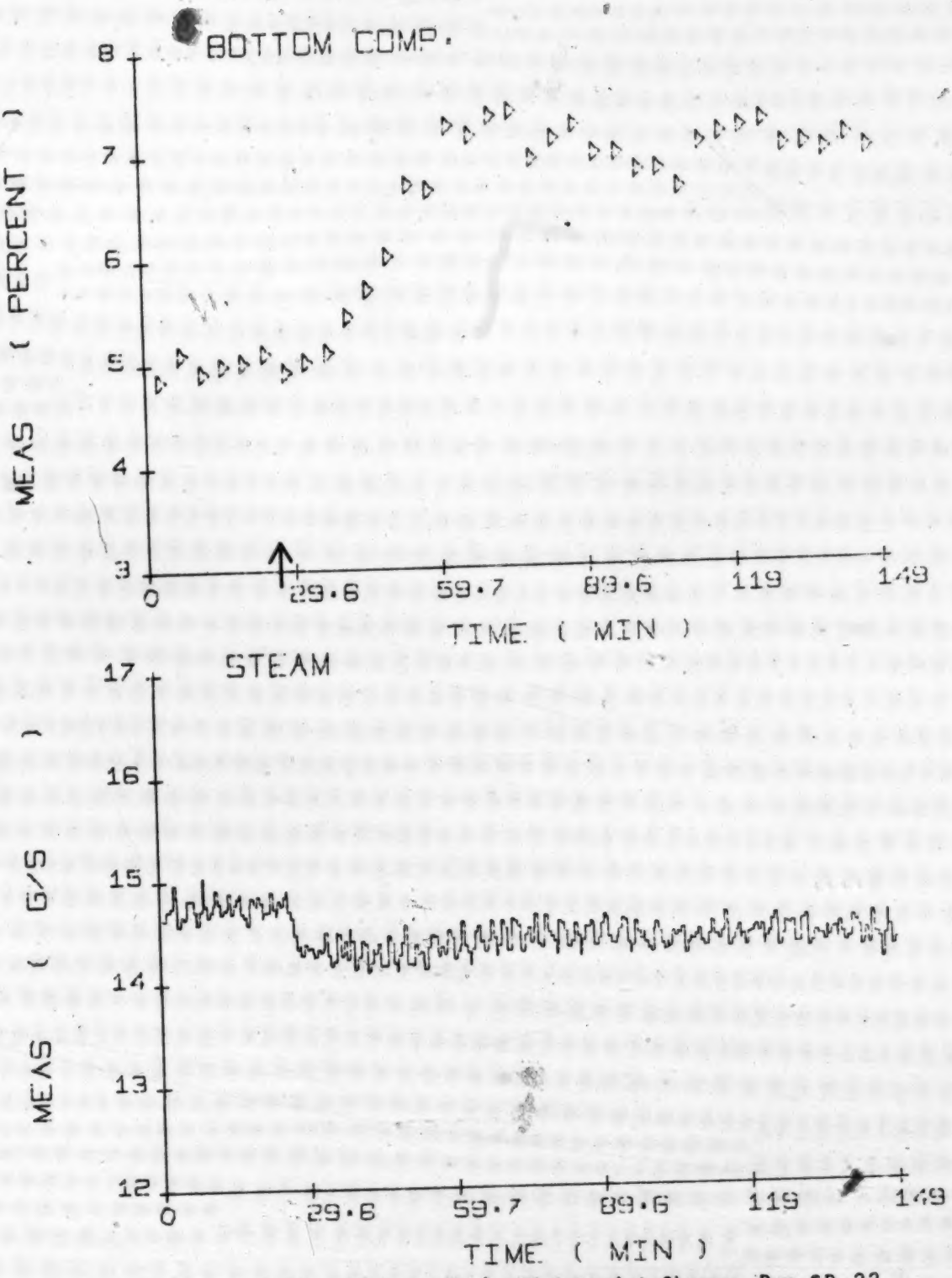

Fig. 5-19 : SP Control (+2% Setpoint Change, Run SP-22
K_c = -0.20, τ_I=1200)

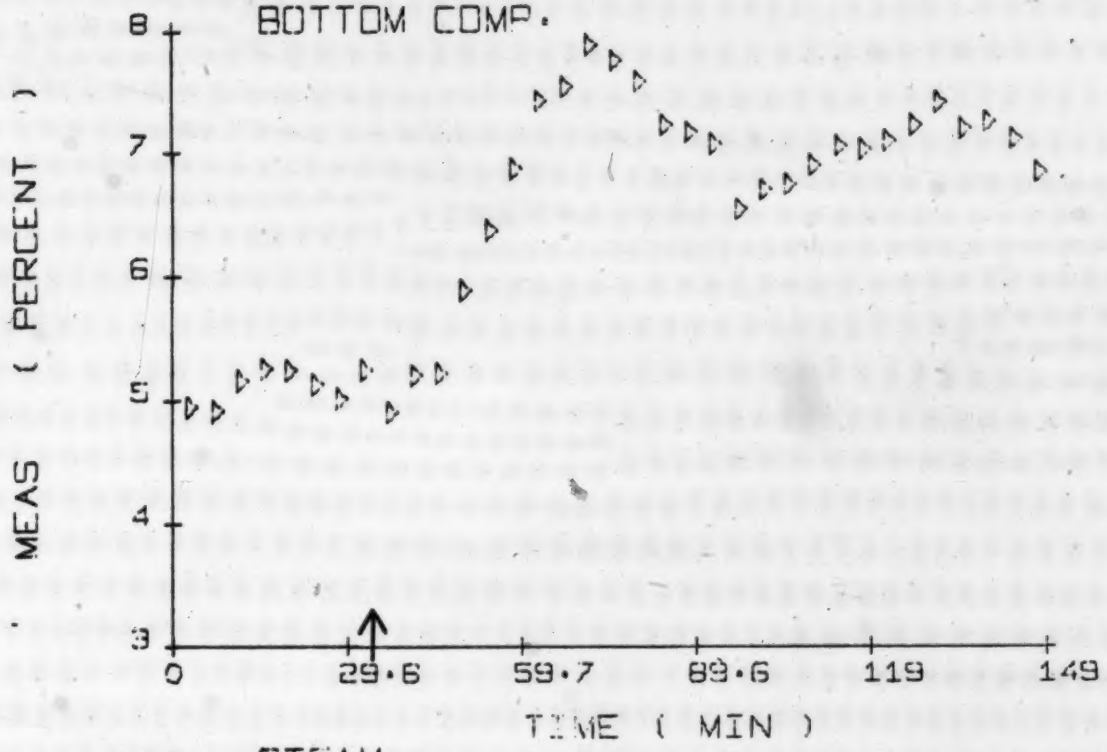

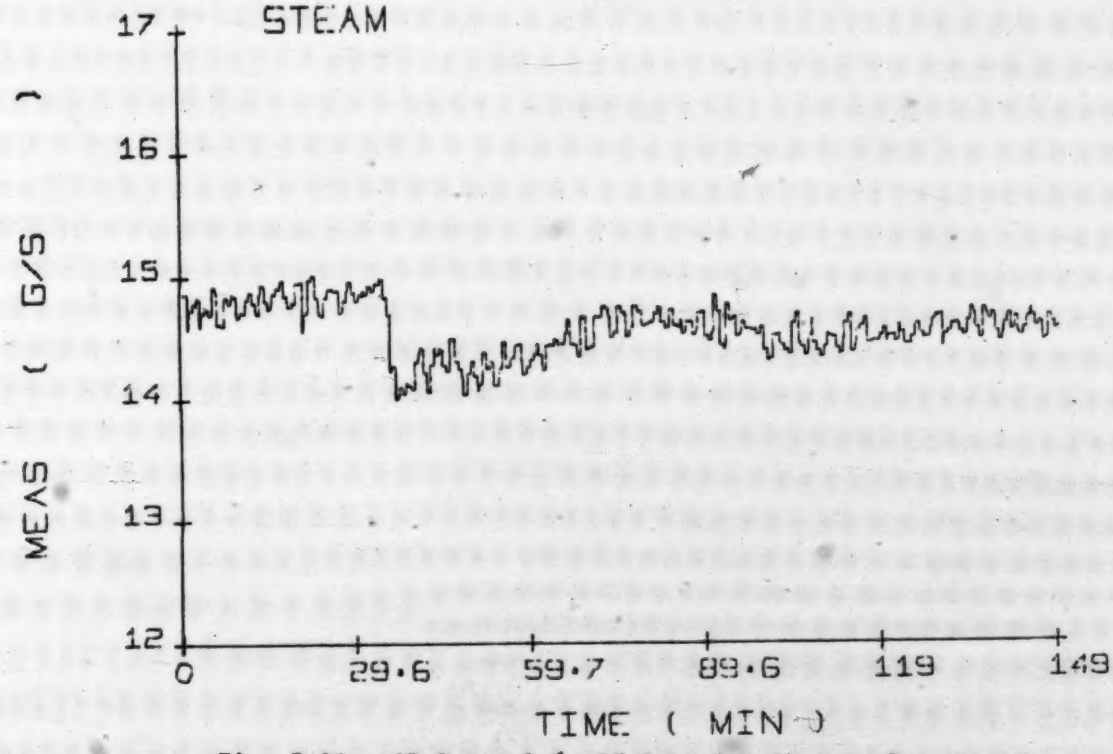

Fig. 5-20 : SP Control (+2% Setpoint Change, Run SP-23
K_c= -0.30, τ_I=1000)

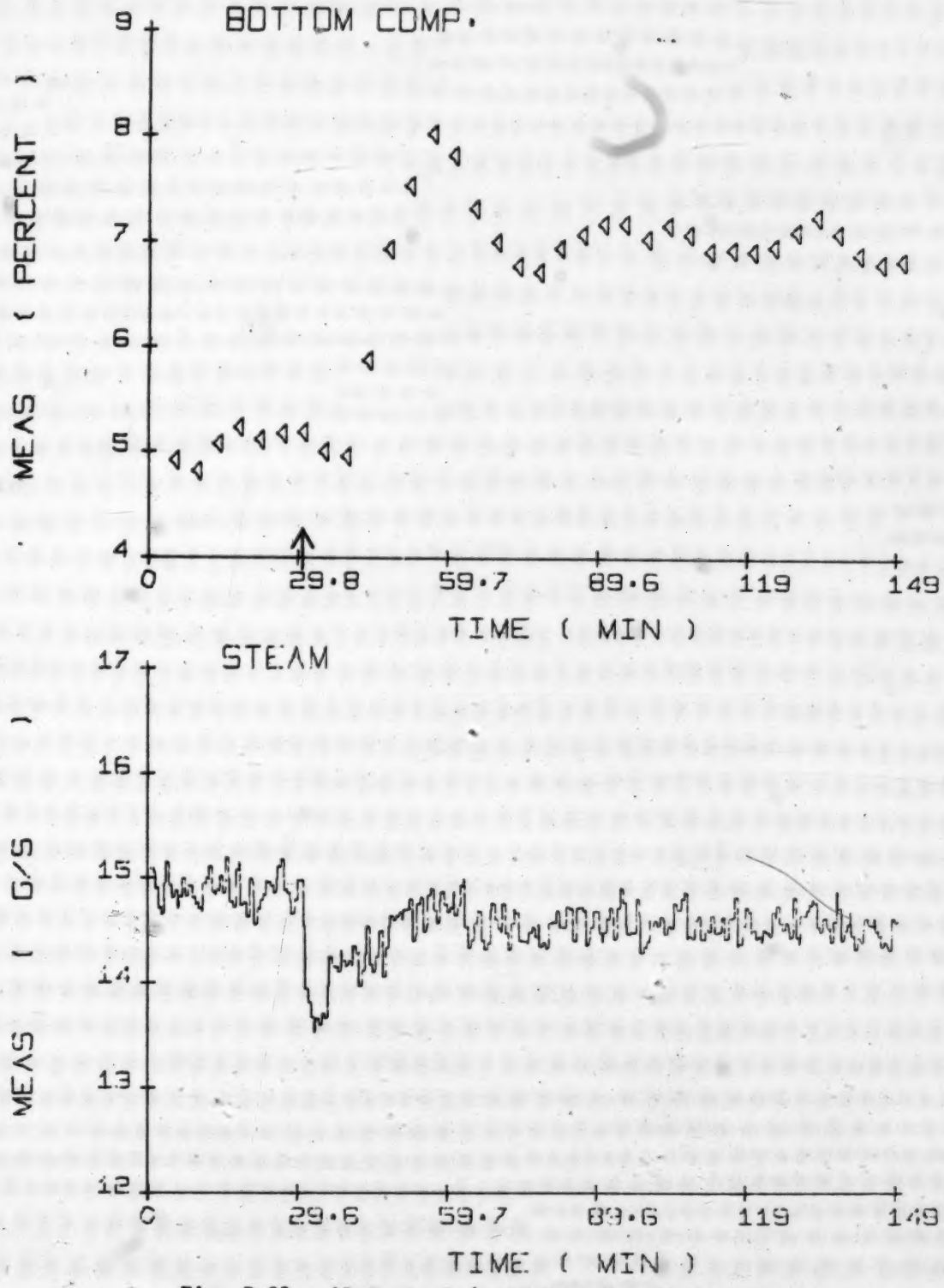

Fig. 5-21 : AP Control (+2% Setpoint Change, Run AP-22
K_C= -0.80, K_I= -0.0020)

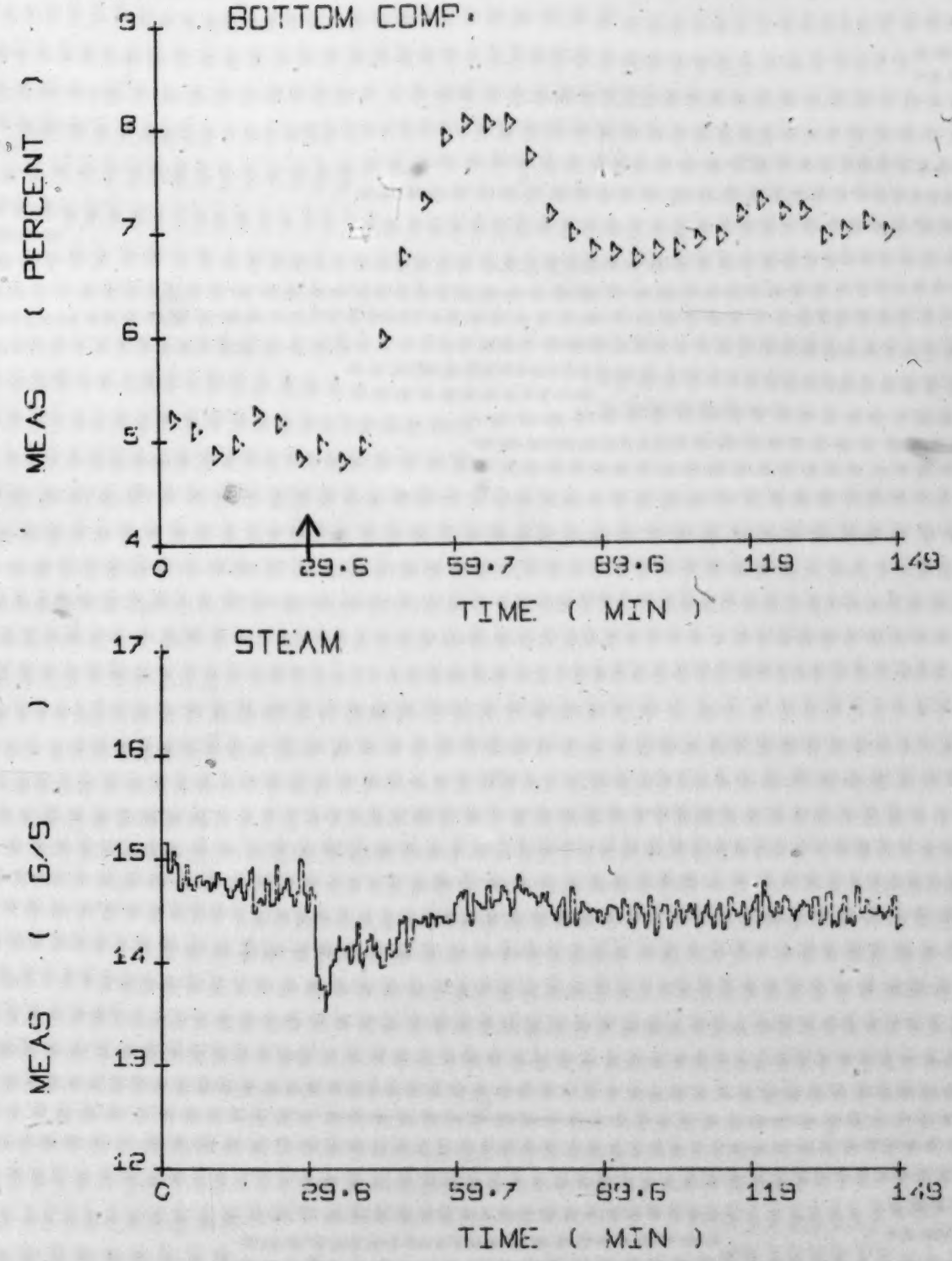

Fig. 5-22 : AP Control (+2% Setpoint Change, Run AP-24
K_c= -0.40, K_I= -0.0020)

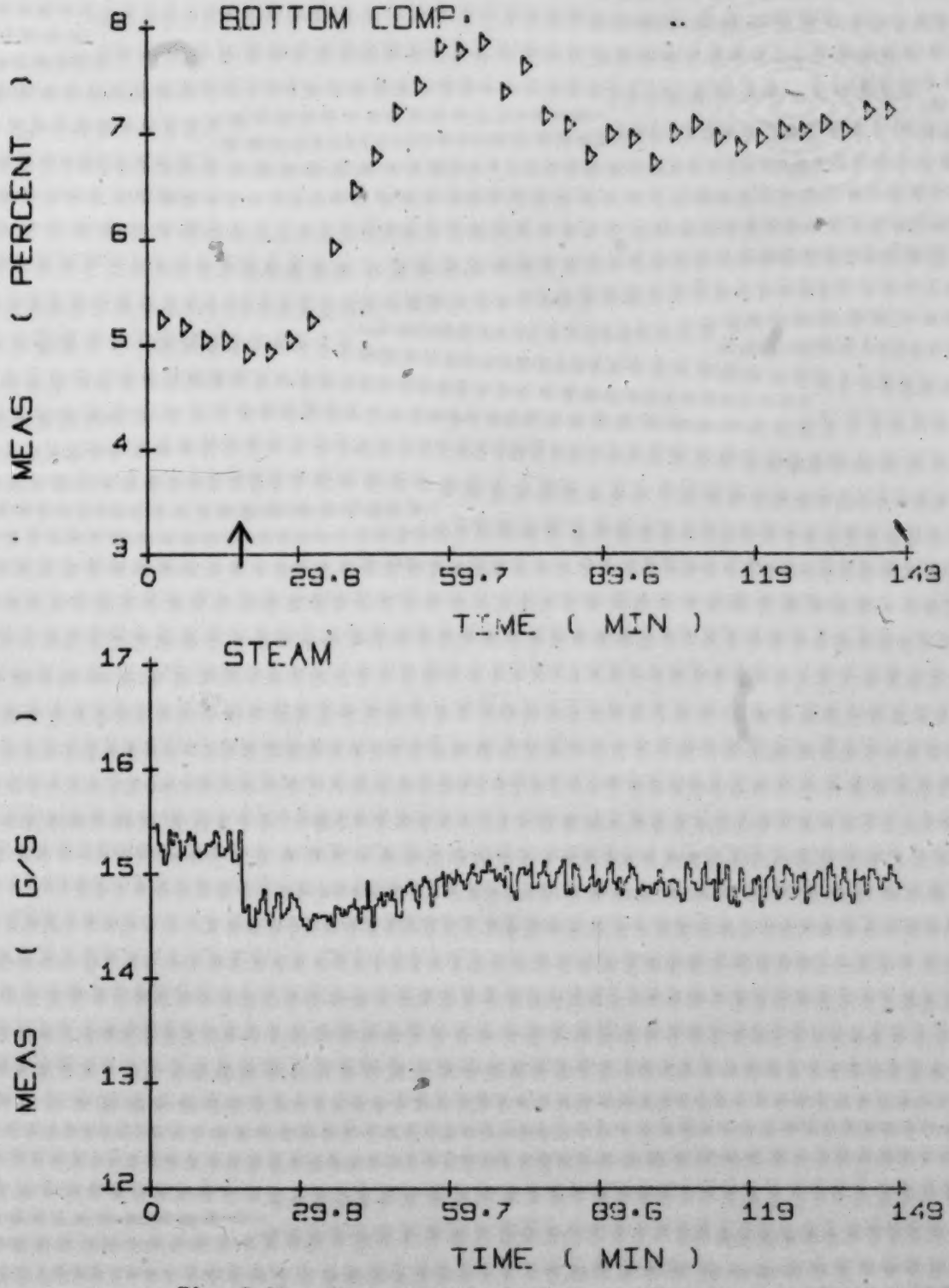

Fig. 5-23 : AP Control (+2% Setpoint Change, Run AP-27
K_c= -0.15, K_I= -0.0034)

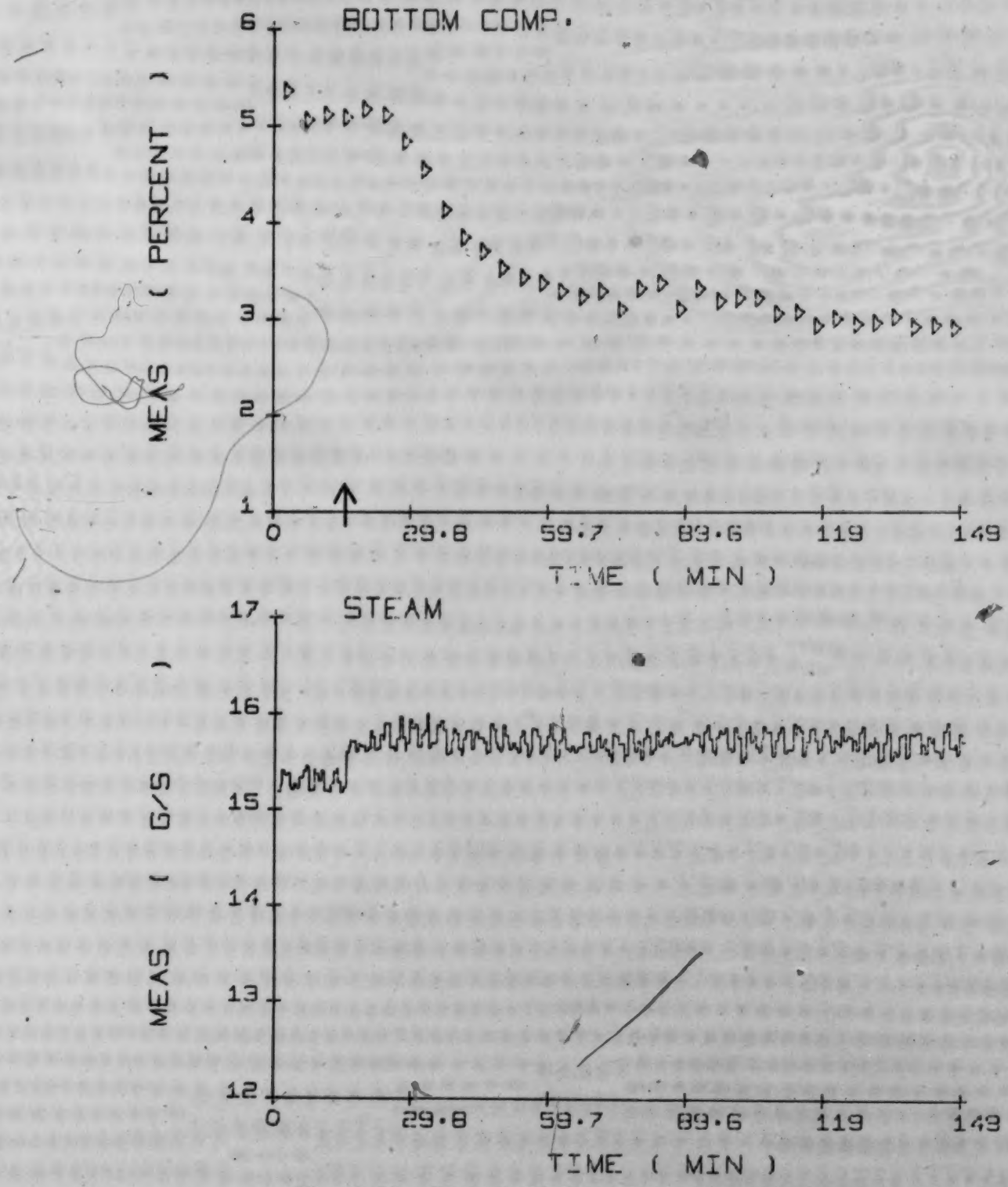

Fig. 5-24 : PI Control (-2% Setpoint Change, Run PI-24
K_c= -0.15, τ_I=1500)

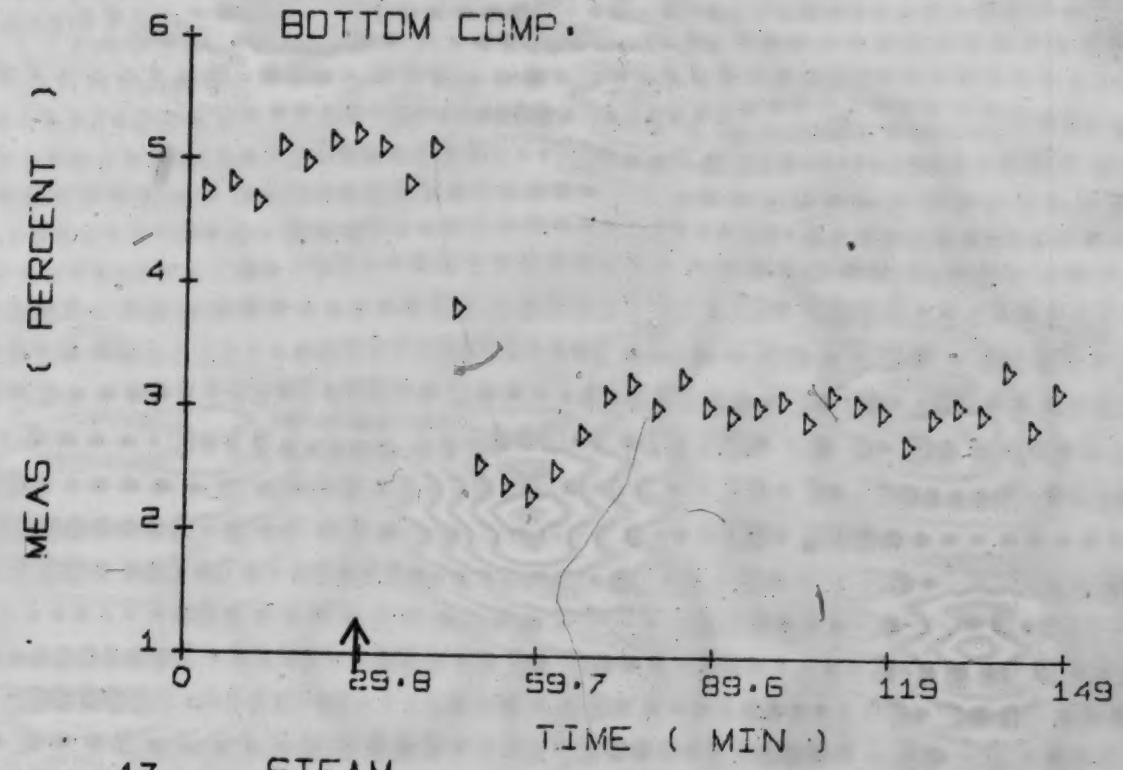

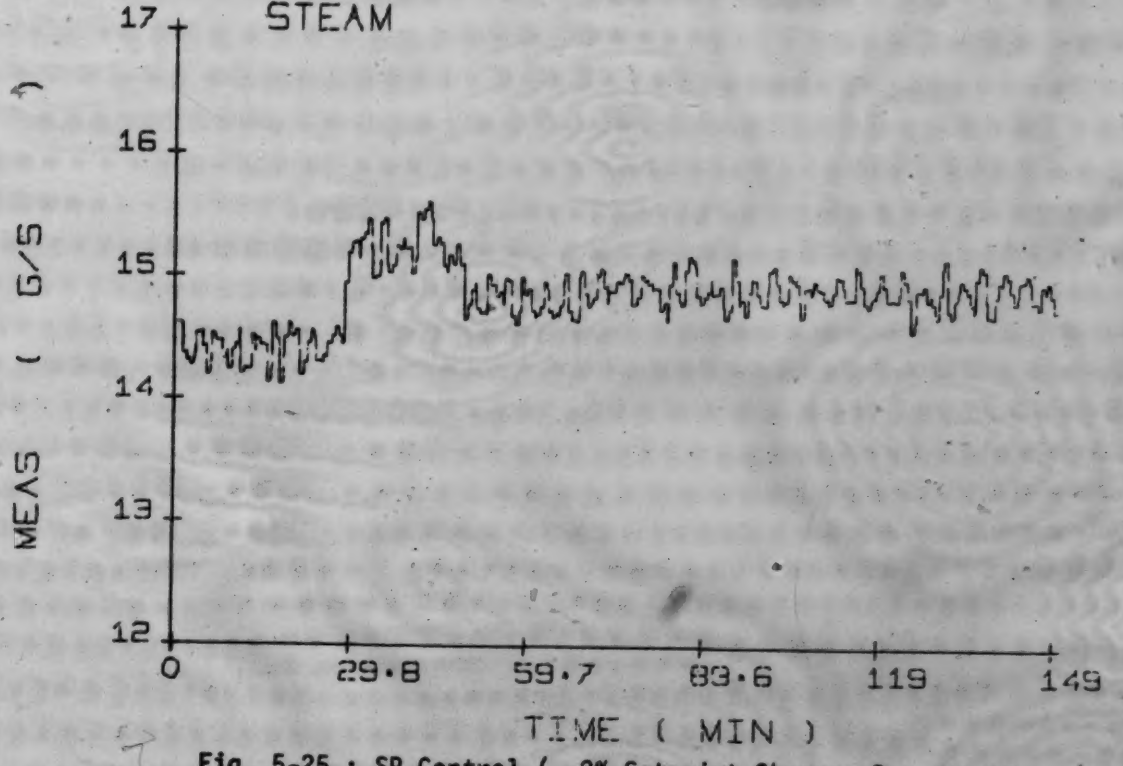

Fig. 5-25 : SP Control (-2% Setpoint Change, Run SP-25
K_c= -0.30, τ_I=1000)

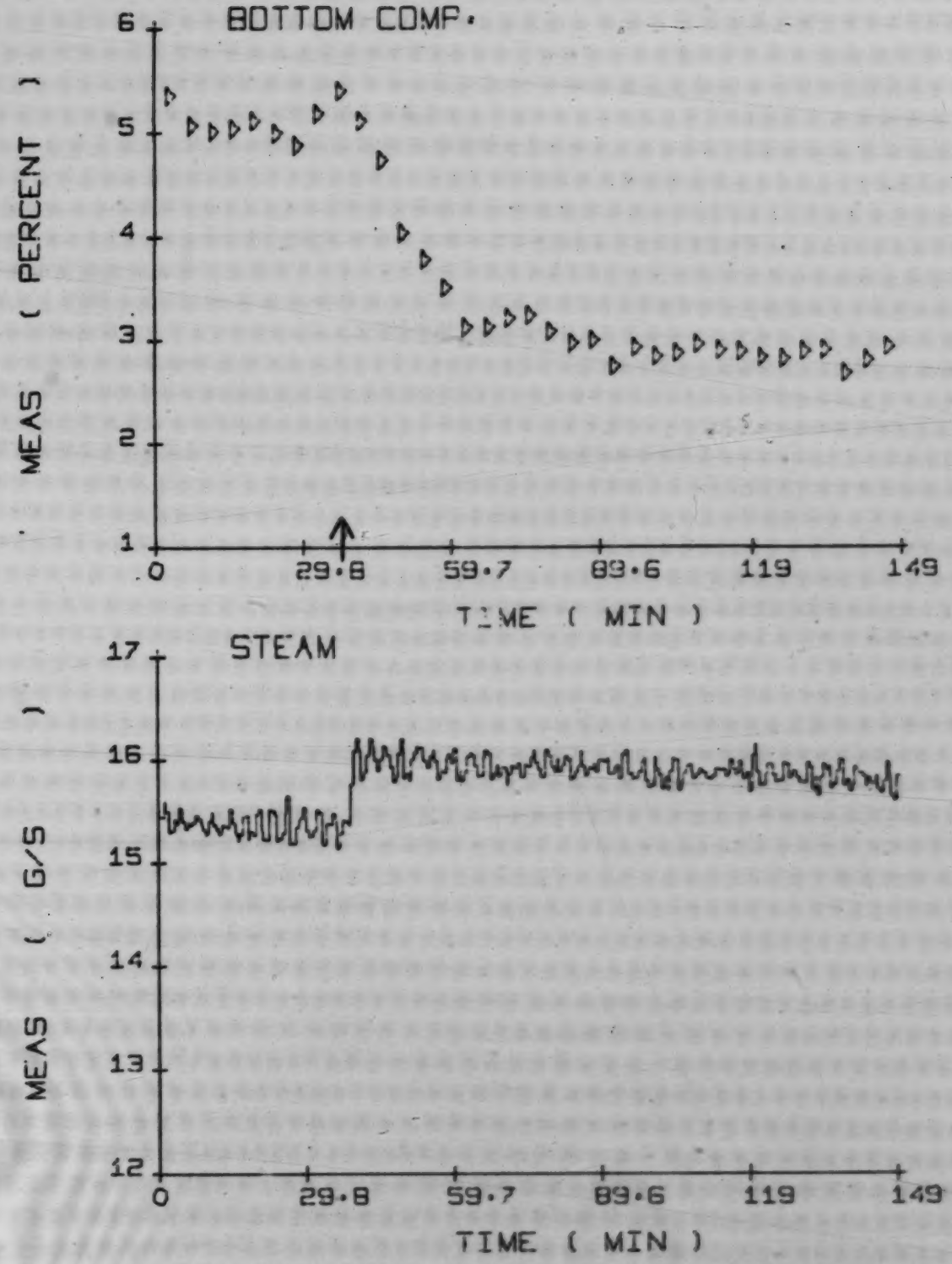

Fig. 5-26 : AP Control (-2% Setpoint Change, Run AP-28
K_c= -0.15, K_I= -0.0034)

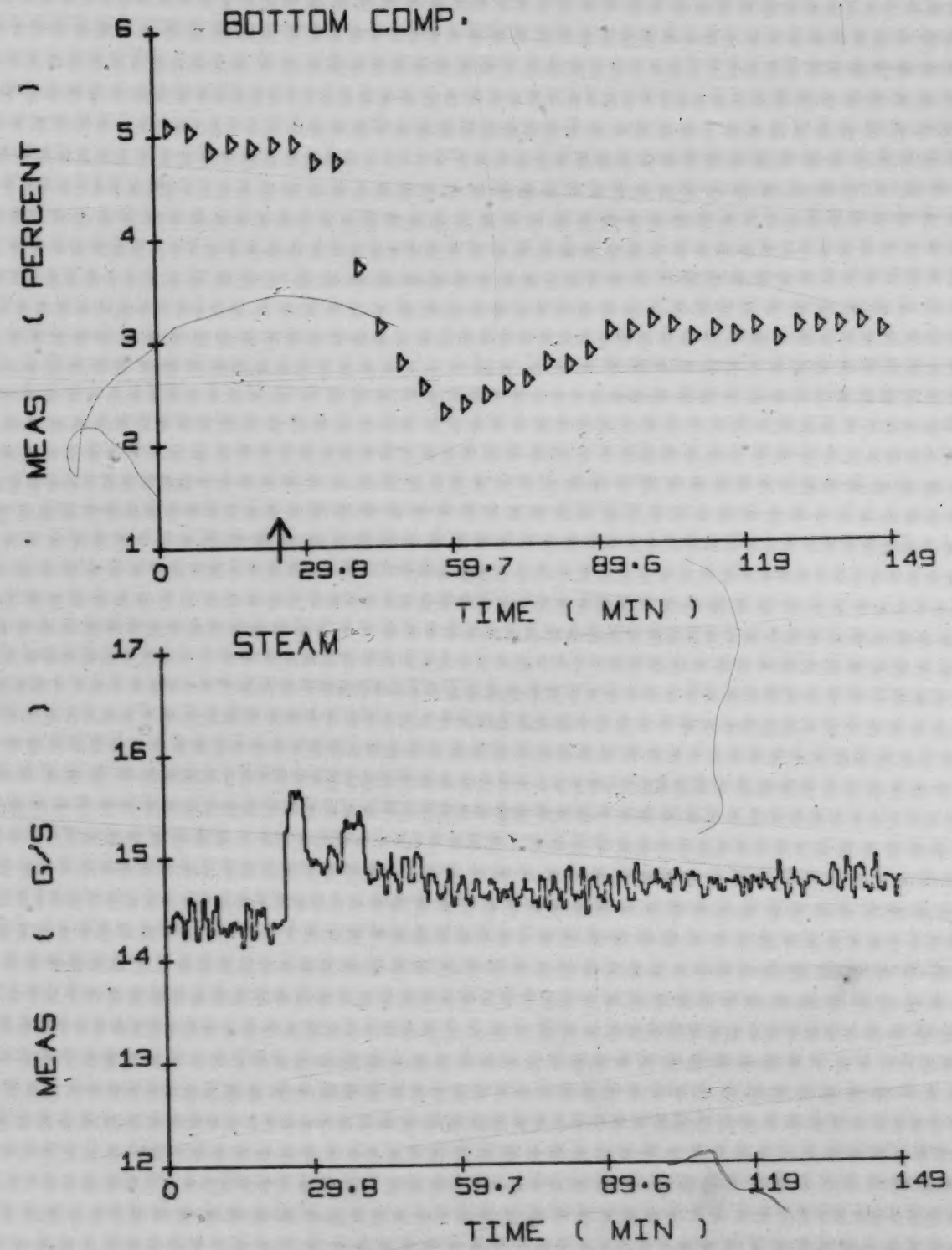

Fig. 5-27 : AP Control (-2% Setpoint Change, Run AP-30
K_c= -0.80, K_I= -0.0020)

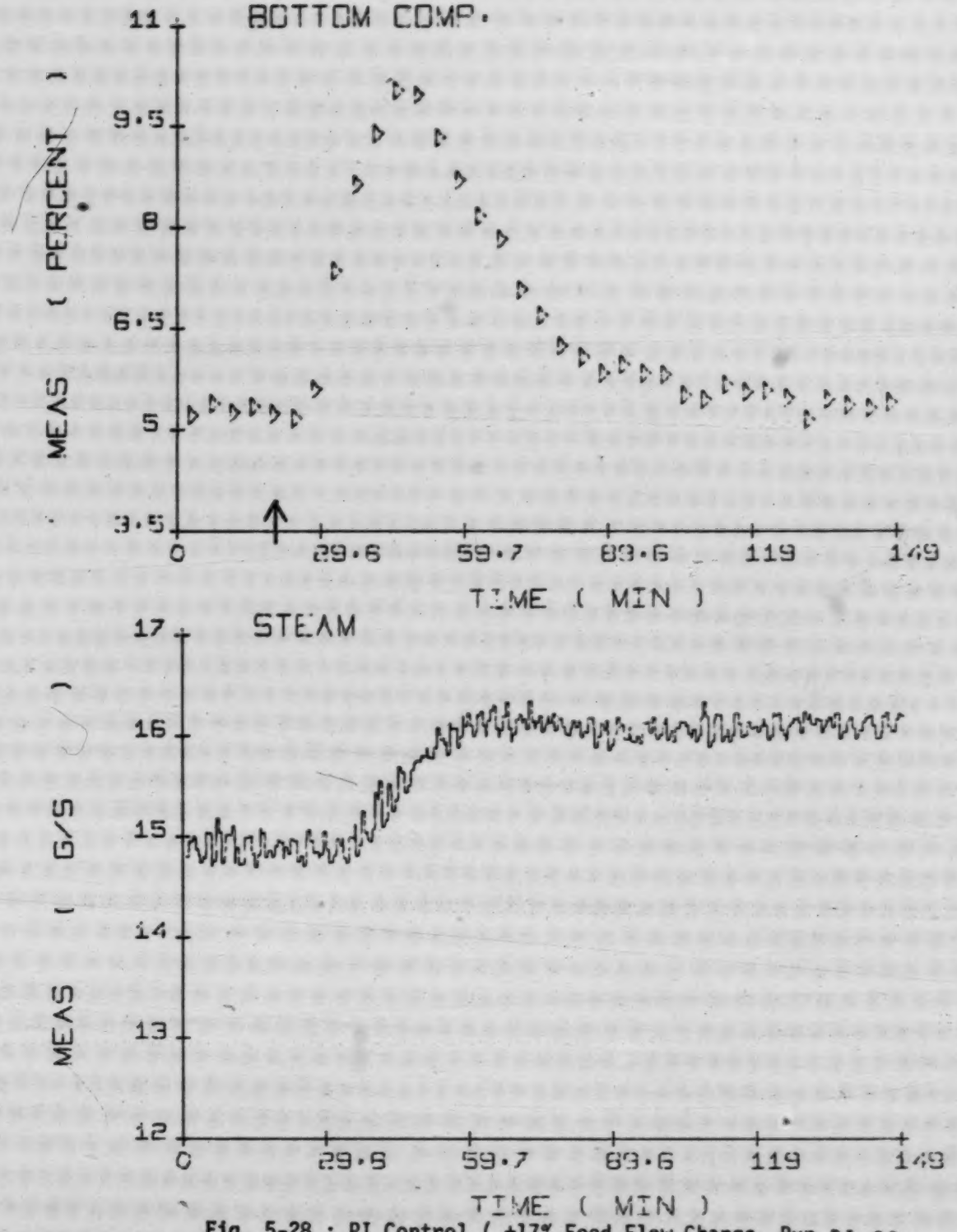

Fig. 5-28 : PI Control (+17% Feed Flow Change, Run PI-23
K_c= -0.15, τ_I=1500)

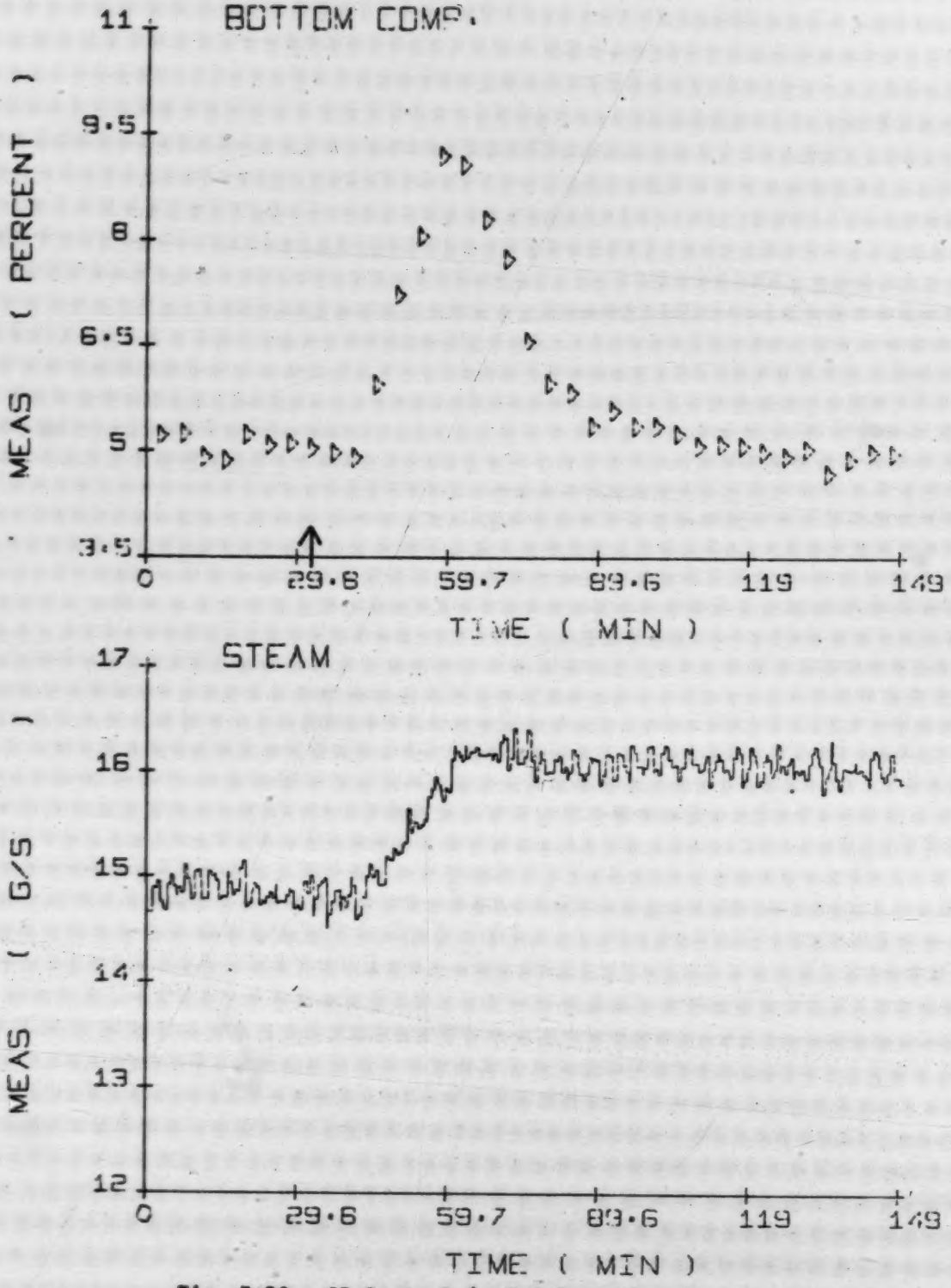

Fig. 5-29 : SP Control (+17% Feed Flow Change, Run SP-24
K_c= -0.30, τ_I=1000)

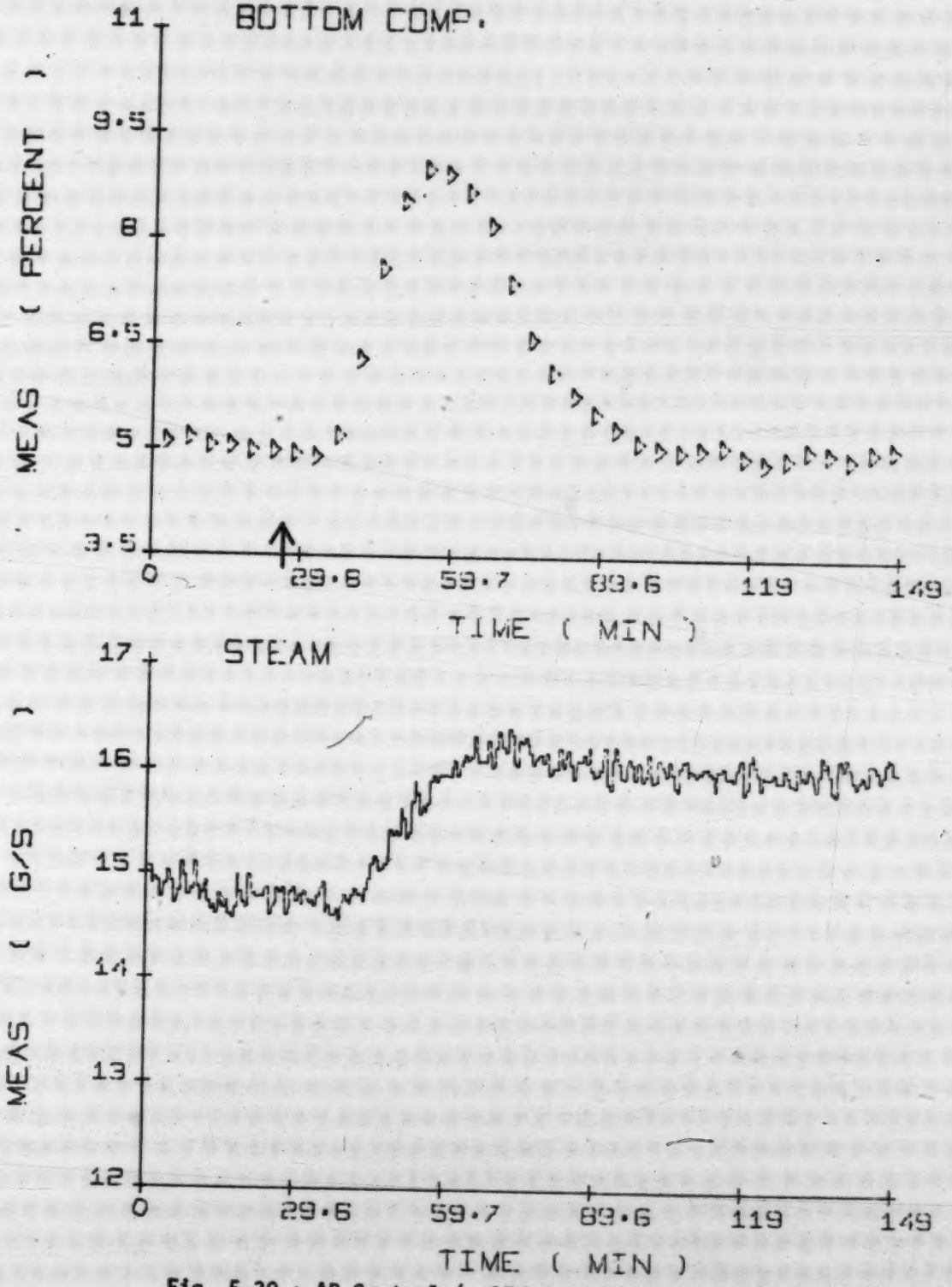

Fig. 5-30 : AP Control (+17% Feed Flow Change, Run AP-25
K_C= -0.40, K_I= -0.0020)

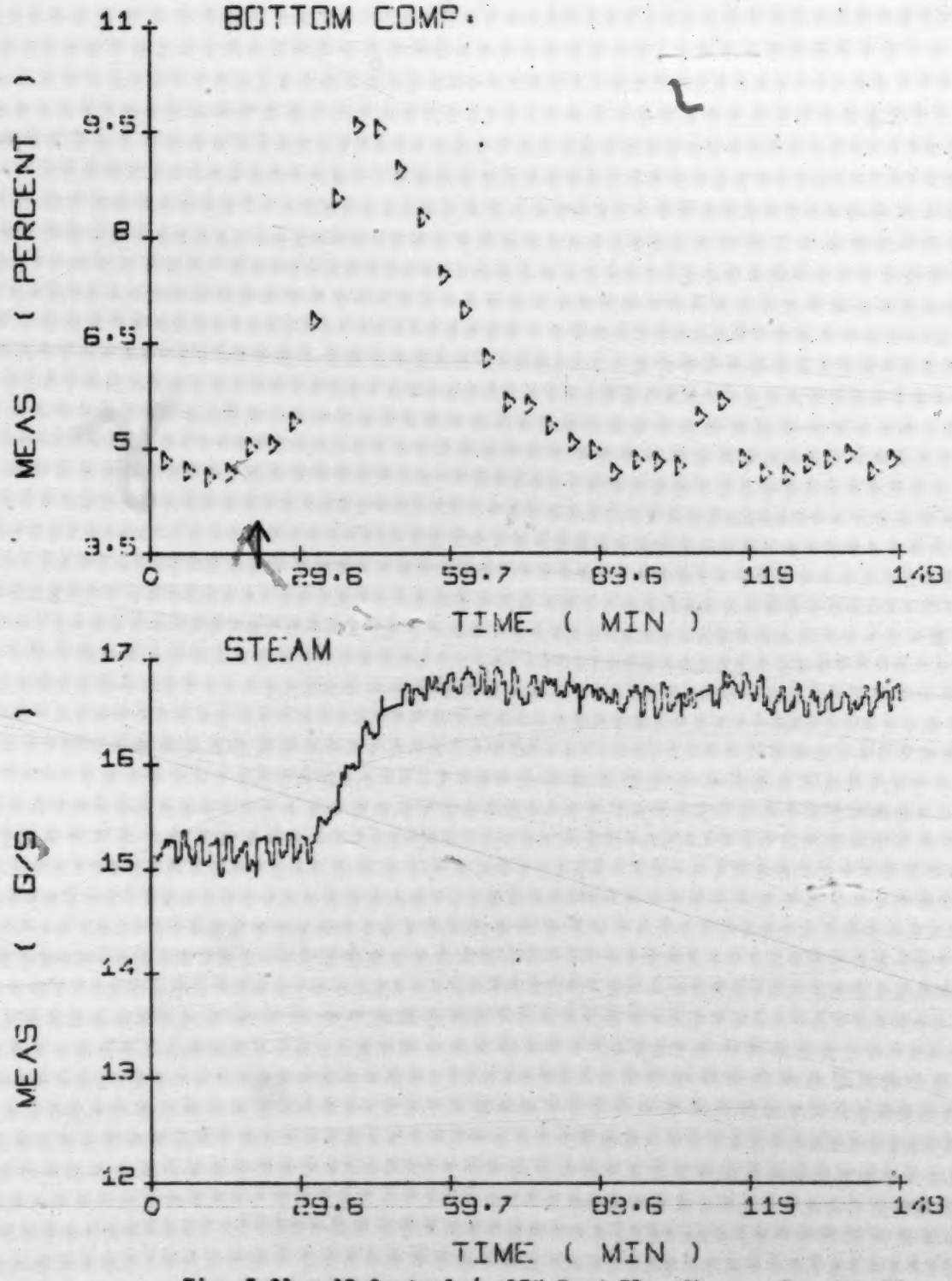

Fig. 5-31 : AP Control (+17% Feed Flow Change, Run AP-26
K_c= -0.15, K_I= -0.0034)

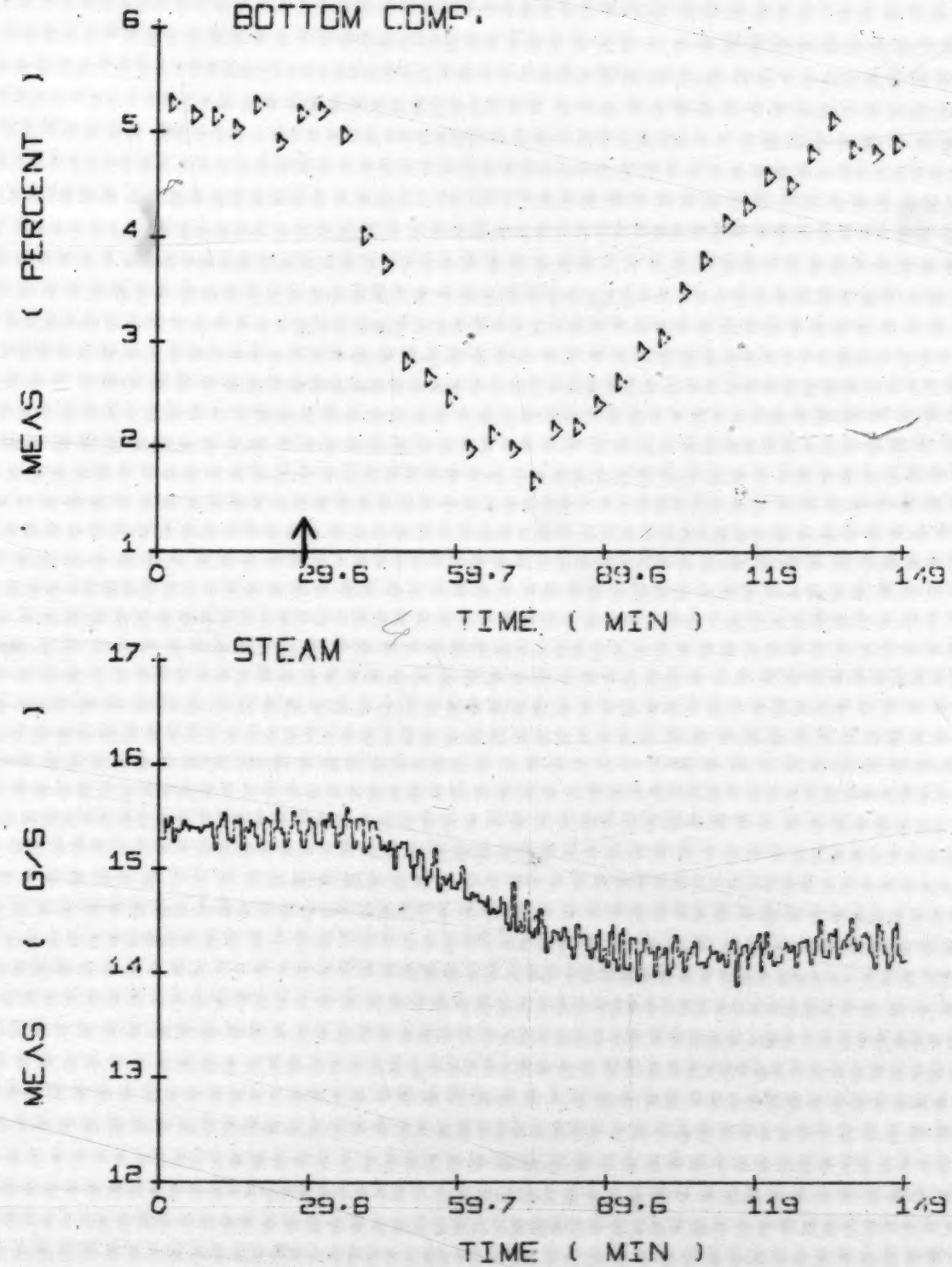

Fig. 5-32 : PI Control (-17% Feed Flow Change, Run PI-25
K_c= -0.15, τ_I=1500)

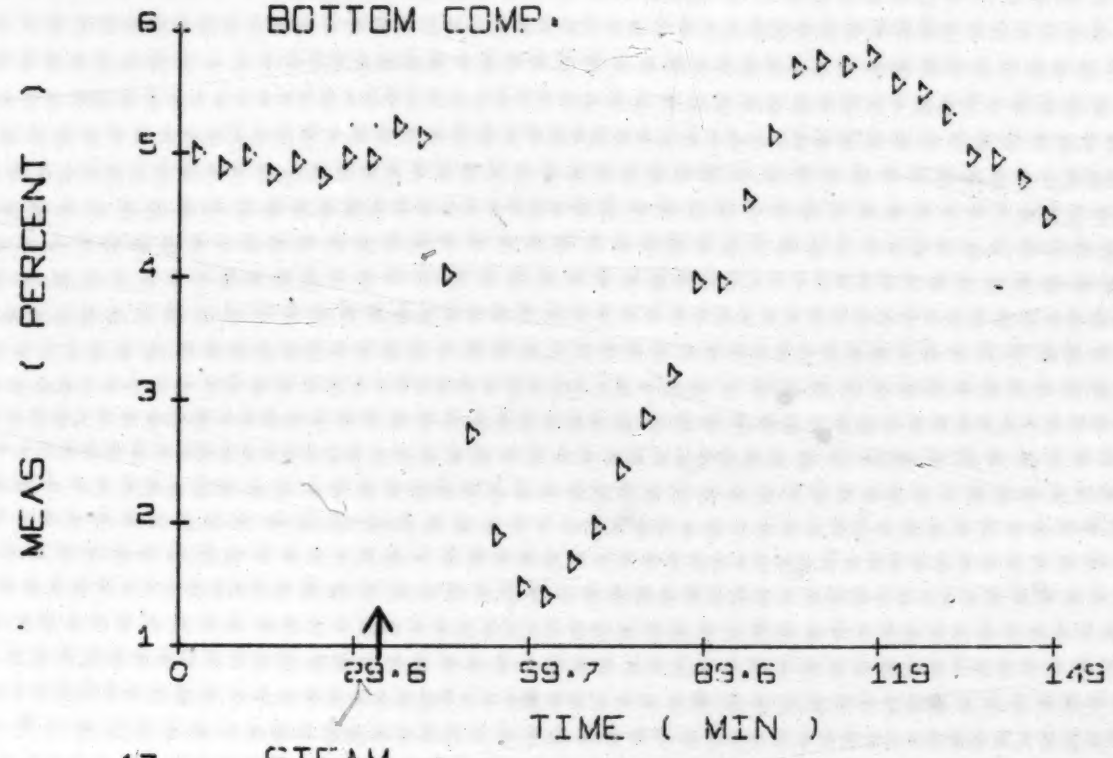

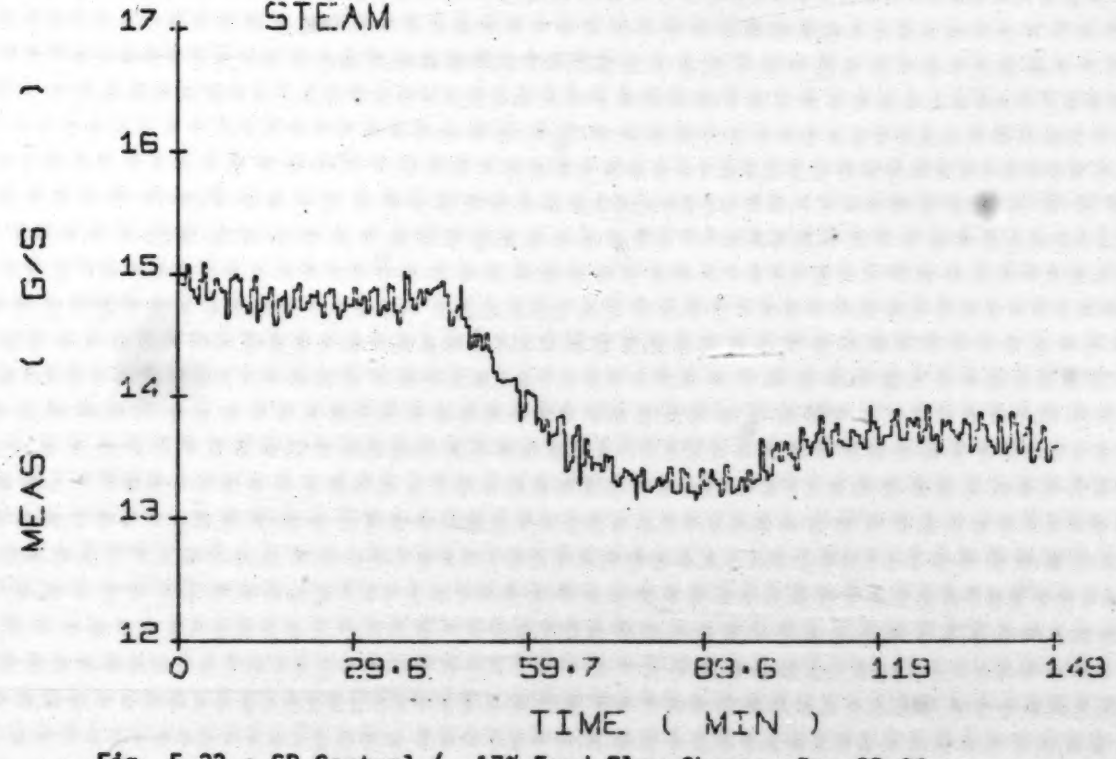

Fig. 5-33 : SP Control (-17% Feed Flow Change, Run SP-26
K_c = -0.30, τ_I = 1000)

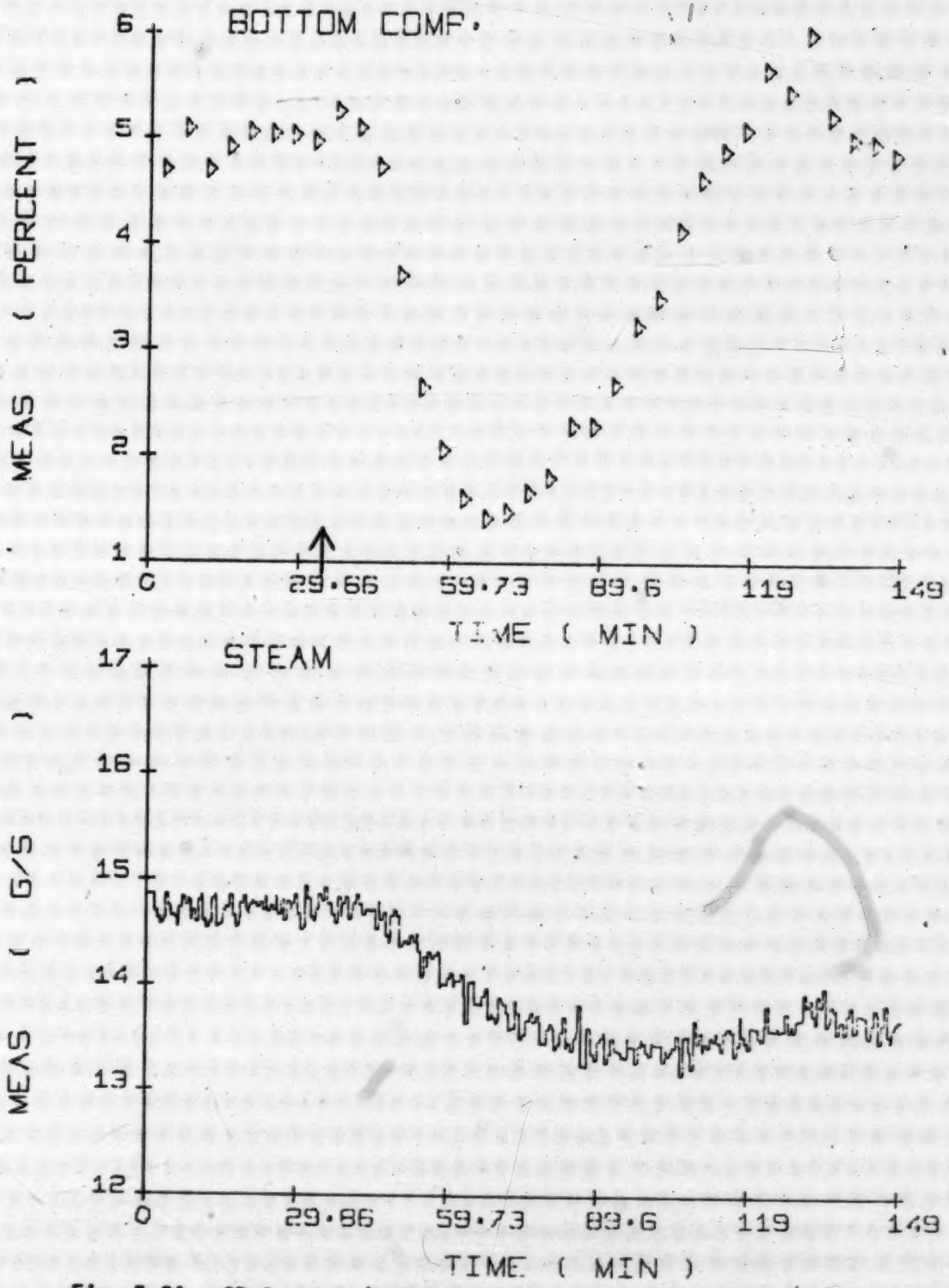

Fig. 5-34 : SP Control (-17% Feed Flow Change, Run SP-27
K_c= -0.20, τ_I= 1200)

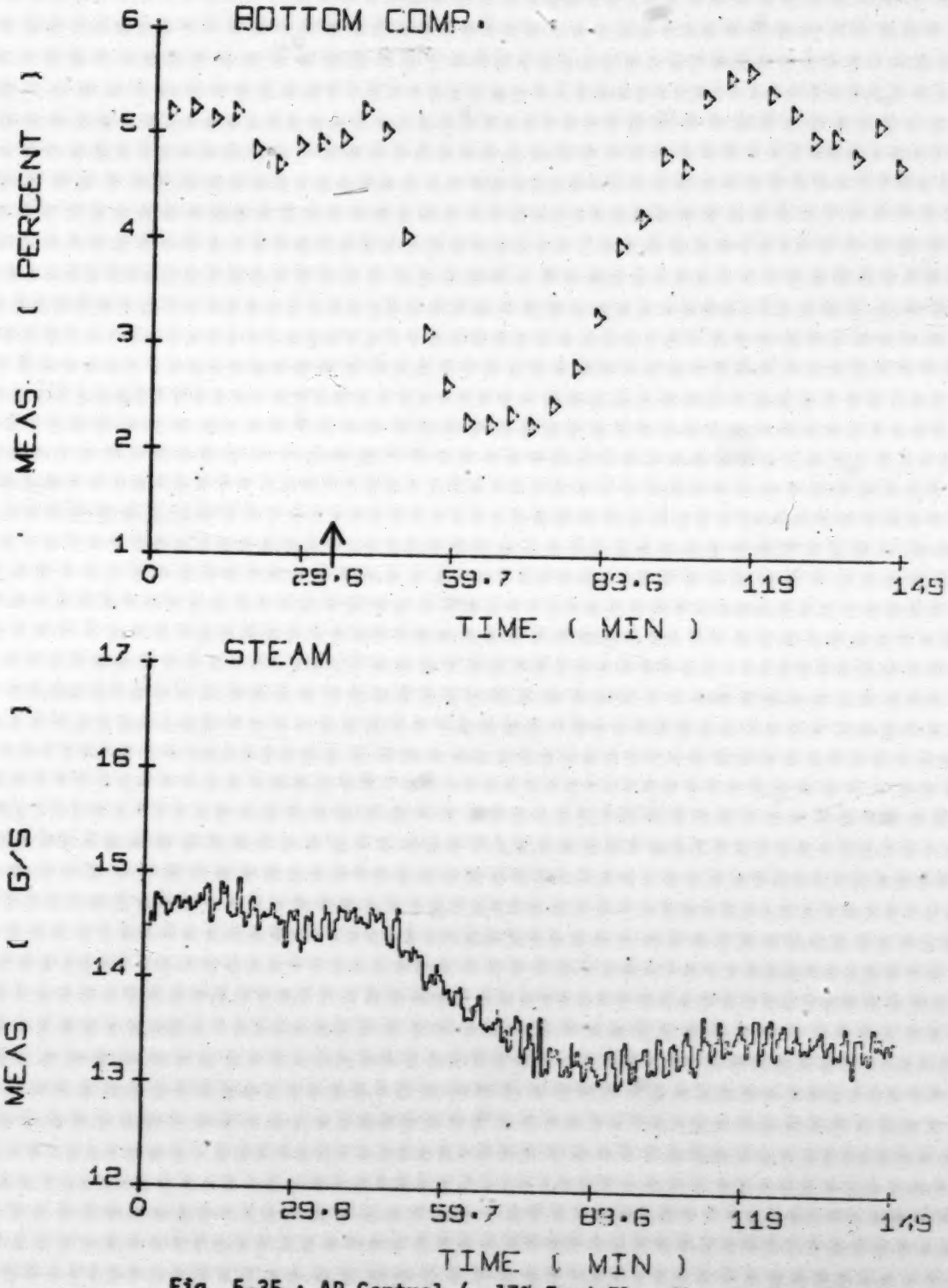

Fig. 5-35 : AP Control (-17% Feed Flow Change, Run AP-29
K_c = -0.15, K_I = -0.0034)

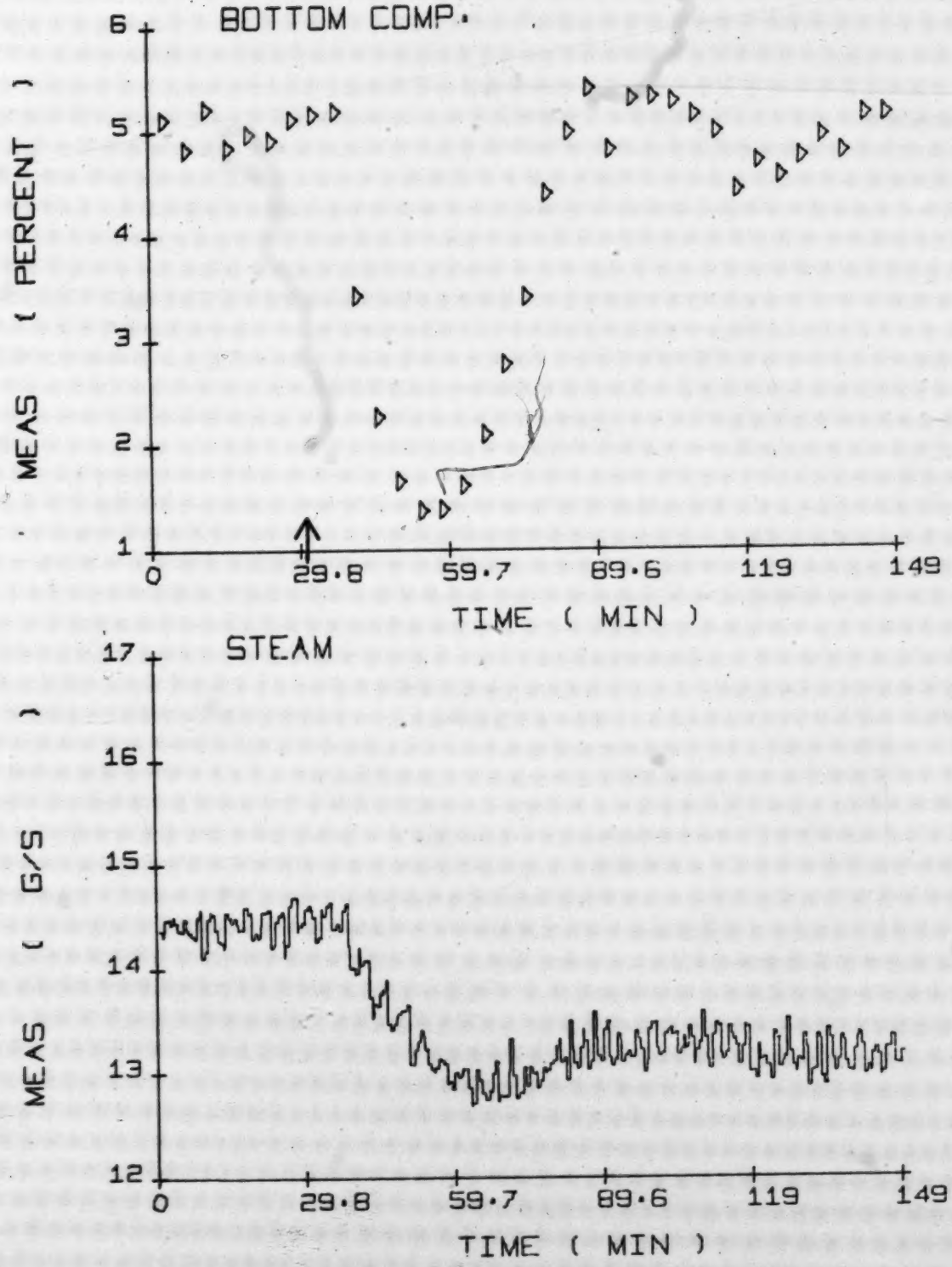

Fig. 5-36 : AP Control (-17% Feed Flow Change, Run AP-31
K_c = -0.80, K_I = -0.0020)

Runs SP-23 and SP-25 for the SP and AP-22 and AP-30 for the AP demonstrate that with predictor control better results are obtained for decreases in composition setpoint than for increases although the controller constants were tuned for increases in setpoint. The reason for this behaviour can be appreciated by realizing that for increases in composition the process gain is larger than the model gain, as can be seen in Fig. 5-3. Since underestimated gains lead to a more serious deterioration in performance than the reverse, as the simulation study demonstrated, the better results for decreases in setpoint would be explained. The tuning of the controller constants, however, would favour the runs for increases in setpoint. The net effect of these two factors is better performance for decreases as can be observed by comparison of Figs. 5-20 and 5-25 for the SP and 5-21 and 5-27 for the AP. Considering these results it appears to be advantageous for satisfactory overall performance to use a model gain closer to the maximum process gain observed in the composition range of interest rather than the average gain used in this study.

For load changes both predictor control schemes give a significant improvement over PI control which is reflected in the IAE values in Table 5-7. Quite similar responses and IAE values are obtained for the SP and the AP, and the small differences could well be due to the controller tuning.

5.5.1 Use of the Reboiler Temperature

In industrial distillation columns it is common practice to use temperature measurements for quality control, e.g. the temperature near the top or bottom of the column at some arbitrarily selected tray. For a binary mixture the composition can then be inferred from the boiling point temperature and the pressure. For the methanol-water system the relationship between composition, boiling point and pressure is given in Appendix H. Bottom

composition control, by controlling the reboiler temperature, was tested experimentally using temperature measurements at the bottom of the reboiler. In order to infer the bottom composition, the pressure at the temperature probe location has to be known and one has to assume that the liquid at this location is at the boiling point (implying perfect mixing in the reboiler). As no convenient direct pressure measurements could be made and no information regarding the mixing pattern in the reboiler was available, the relationship between the temperature measurement and the composition was established experimentally. Steady state temperature and composition measurements (by GC) were taken at different operating conditions to establish the data points shown in Fig. H-1 in Appendix H. However, the data were quite erratic, probably due to different pressures at the location of the temperature probe because of different atmospheric conditions, pressure drops and reboiler levels. Thus only approximate compositions could be inferred from the reboiler temperature measurements made in this study.

Step disturbances of +2%C in setpoint and -17% in feed flow were employed to study the performance of SP, AP and PI control using the reboiler temperature as the controlled variable. As in the previous experiments the standard operating conditions of Table 5-1 were used. The sampling time was chosen to be 1 minute.

The process model for the effect of steam on the bottoms composition, Eqn. (5.3), was used with the process gain adjusted to account for the fact that the output variable is reboiler temperature instead of composition. From Appendix H the slope of the T-X curves for the methanol-water system is approximately -0.82 ^{o}C/% so the process model for the reboiler

temperature as the controlled variable becomes:

$$\frac{T_R(s)}{S(s)} = \frac{4.1\, e^{-174s}}{864s + 1} \qquad (5.4)$$

As was the case for top and bottom composition control, controller constants could be calculated employing the methods mentioned in Section 5.3. However, the calculated controller constants had to be reduced to achieve stable control in the experimental runs for the SP and the AP. Trial and error tuning of the controller constants was done for step changes of +2°C in setpoint.

The results of the reboiler temperature control runs are presented in Tables 5-8 and 5-9 and the transient responses are shown in Figs. 5-37 to 5-44. The comparison of the IAE values for setpoint changes shows the small improvement of SP over PI control whereas the AP is inferior. For feed flow changes the SP results in a smaller overshoot, but a longer setling time in comparison with PI control as shown in Figs. 5-41 and 5-42, so that the IAE values are almost identical. The AP, with the controller constants employed for run AP-15, gives a lower IAE value than for PI or SP control in contrast to the higher IAE value using the settings corresponding to run AP-14.

In the AP control algorithm the proportional and integral control action are "separated" in the sense that in the ideal case without modelling errors the response for setpoint changes depends only on K_c, as was discussed in Section 3.4.2. This fact is demonstrated experimentally in the AP runs AP-12, AP-13 and AP-14, AP-15: for setpoint changes the lower IAE value is obtained for run AP-13 with the higher K_c and, for the sake of stability, lower K_I compared to run AP-12, whereas for feed flow changes the reverse is true.

Table 5-8 : Summary of Experimental Results for Reboiler Temperature Control
(2°C Step Increases in Setpoint)

RUN	K_C (g/s/%)	τ_I (s)	K_I (g/s/%s)	IAE (%s)	FIGURE
PI-11	0.87	564	-	1536	5-37
SP-13	2.0	300	-	1176	5-38
AP-11	0.1	-	0.04	1900	-
AP-12	0.6	-	0.02	1890	5-39
AP-13	1.2	-	0.01	1600	5-40

Table 5-9 : Summary of Experimental Results for Reboiler Temperature Control
(17% Step Decreases in Feed Flow)

RUN	K_C (g/s/%)	τ_I (s)	K_I (g/s/%s)	IAE (%s)	FIGURE
PI-12	0.87	564	-	1008	5-41
SP-12	2.0	300	-	1000	5-42
AP-14	1.2	-	0.01	1068	5-43
AP-15	0.6	-	0.02	852	5-44

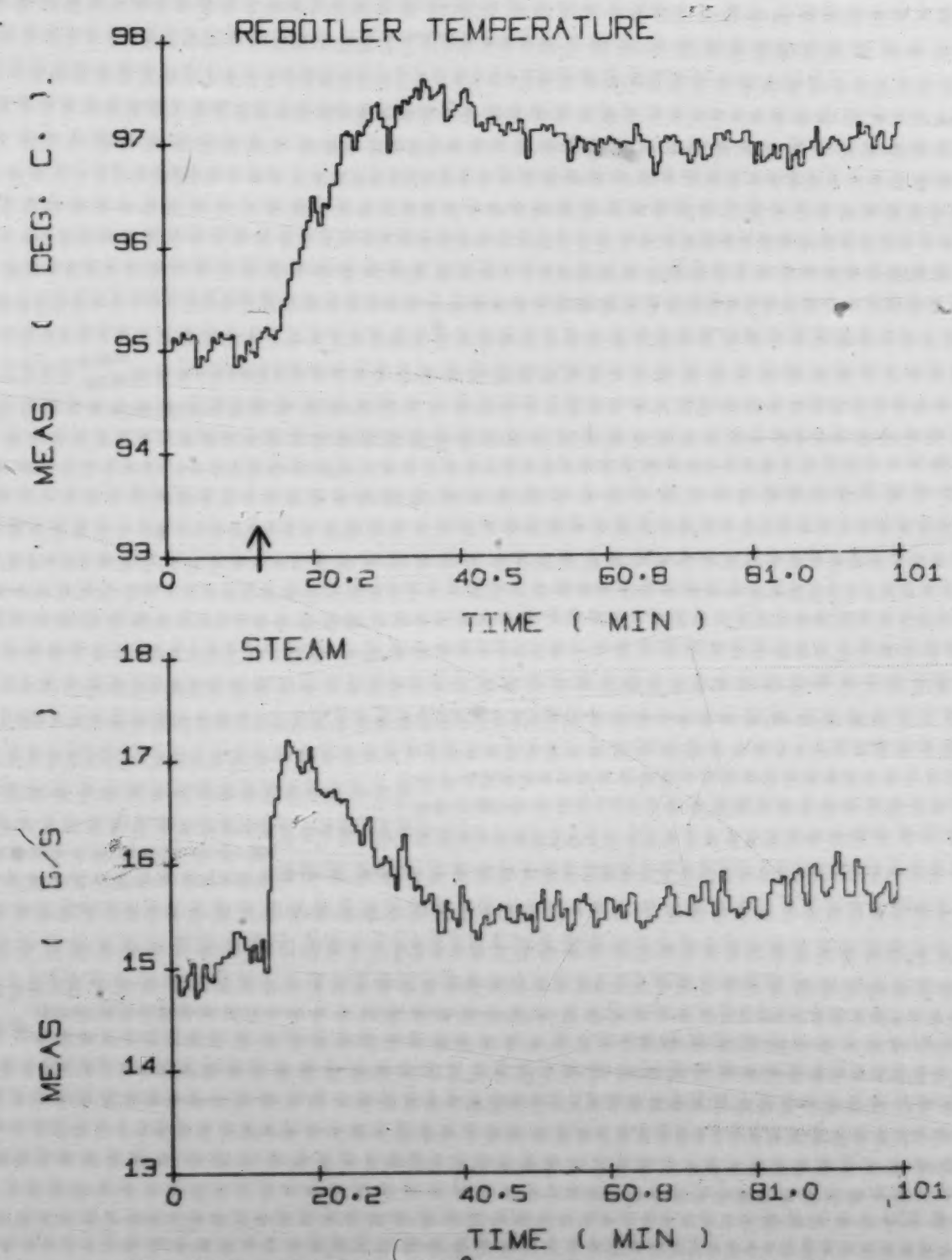

Fig. 5-37 : PI Control (+2°C Setpoint Change, Run PI-11 K_c = 0.87, τ_I = 564)

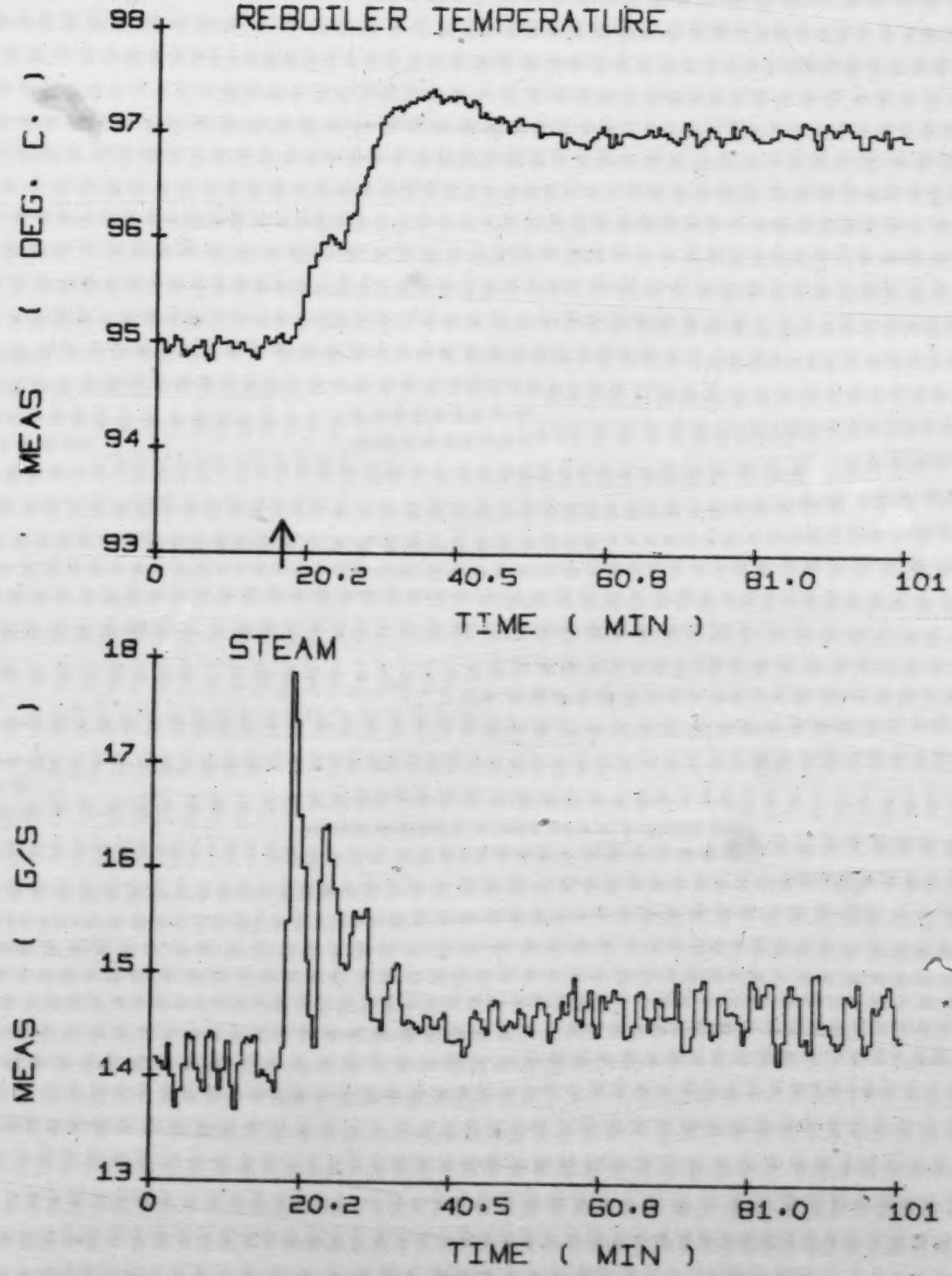

Fig. 5-38 : SP Control (+2°C Setpoint Change, Run SP-13
K_c= 2.0, τ_I= 300)

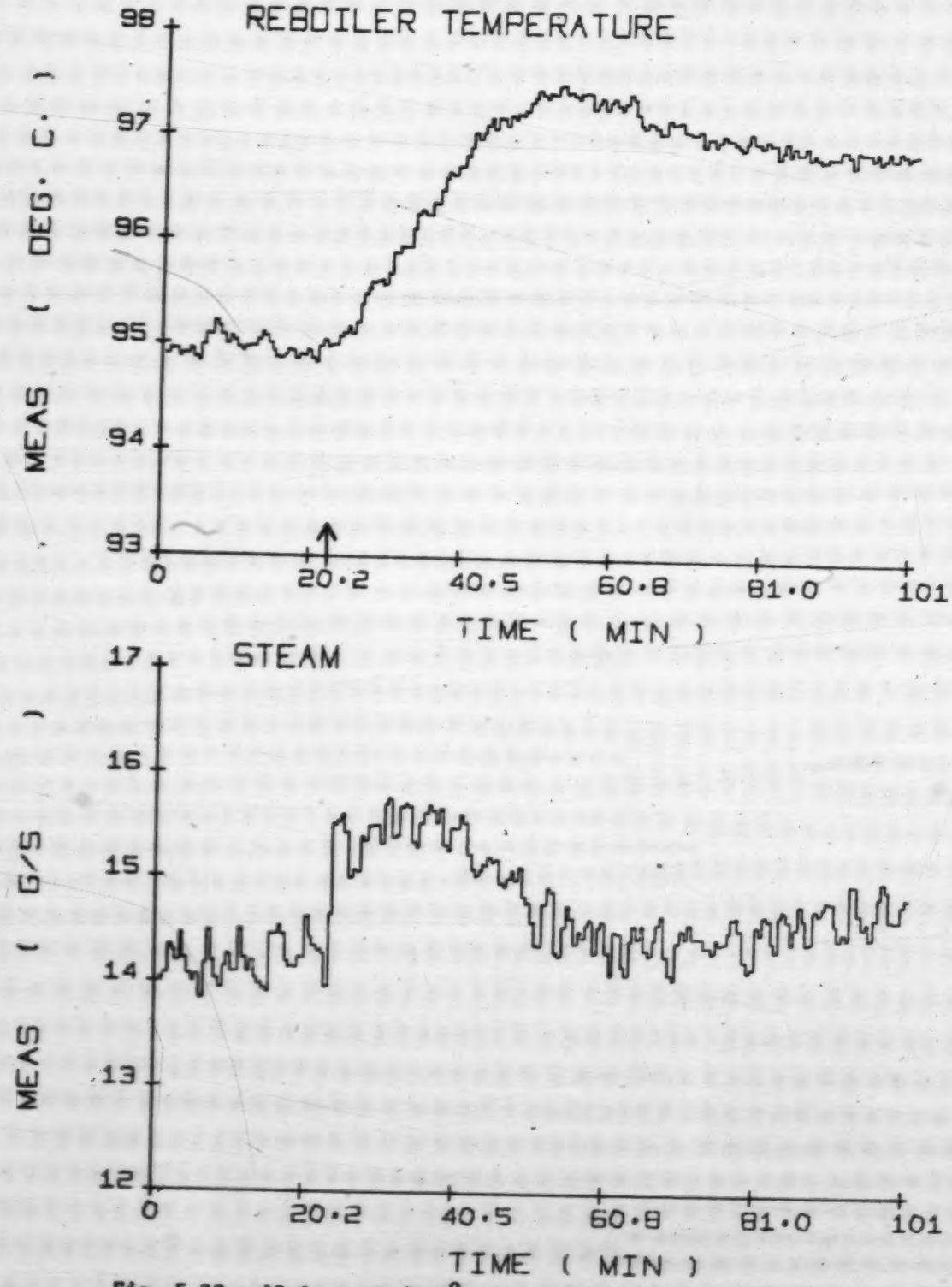

Fig. 5-39 : AP Control (+2^{o}C Setpoint Change, Run AP-12
K_C= 0.6, K_I= 0.02)

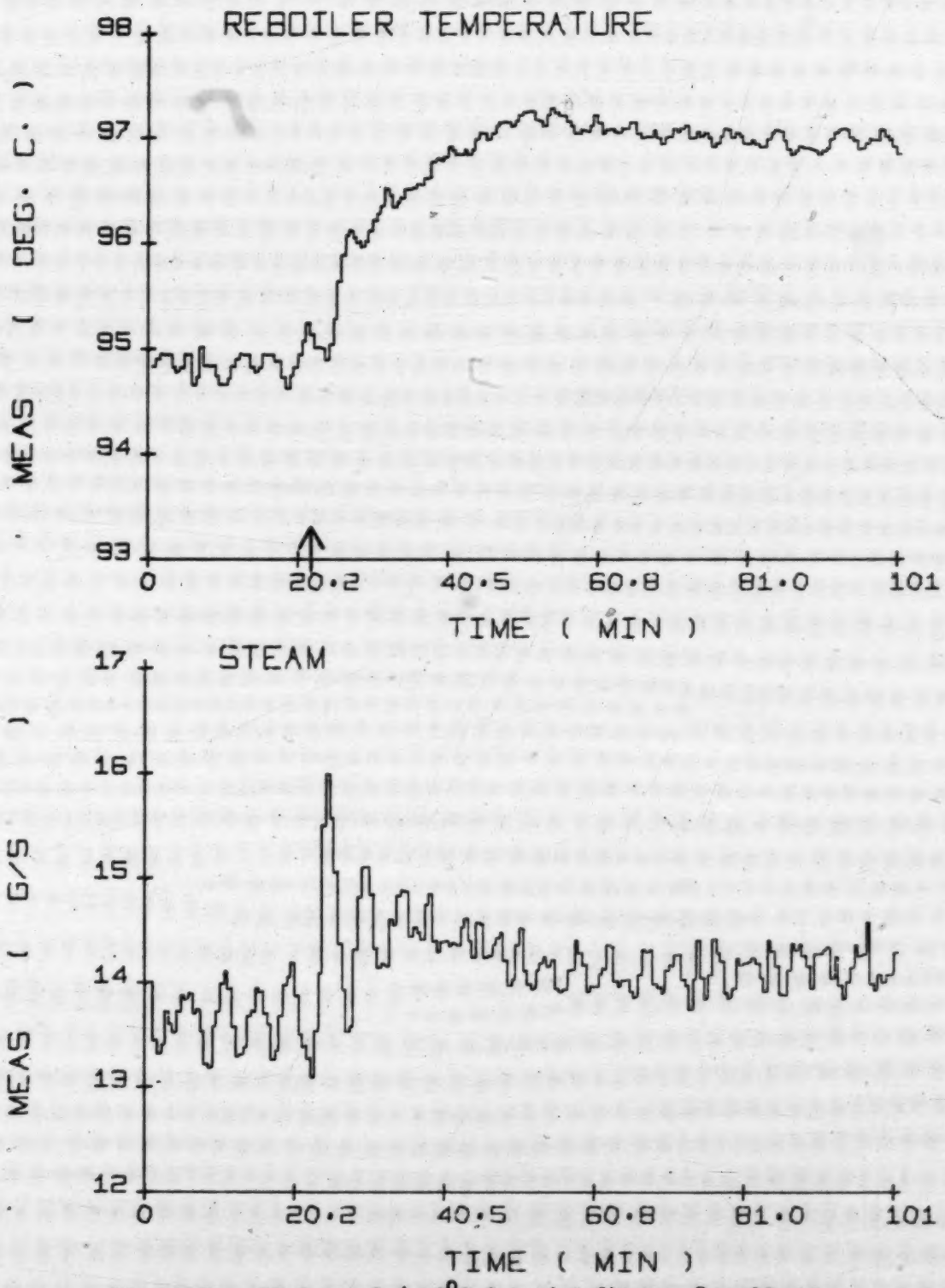

Fig. 5-40 : AP Control (+2°C Setpoint Change, Run AP-13
K_c= 1.2, K_I= 0.01)

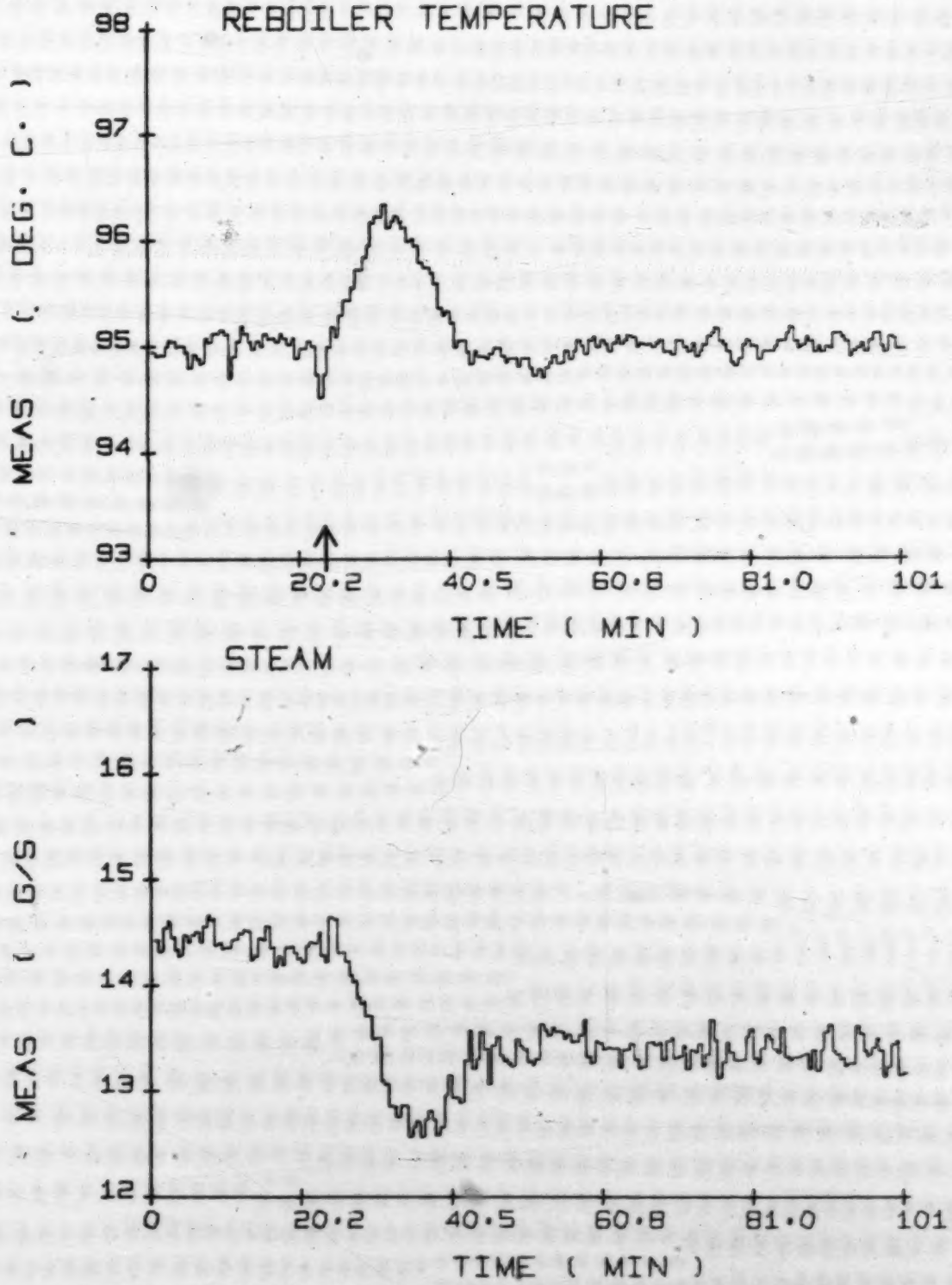

Fig. 5-41 : PI Control (-17% Feed Flow Change, Run PI-12
K_c= 0.87, τ_I=564)

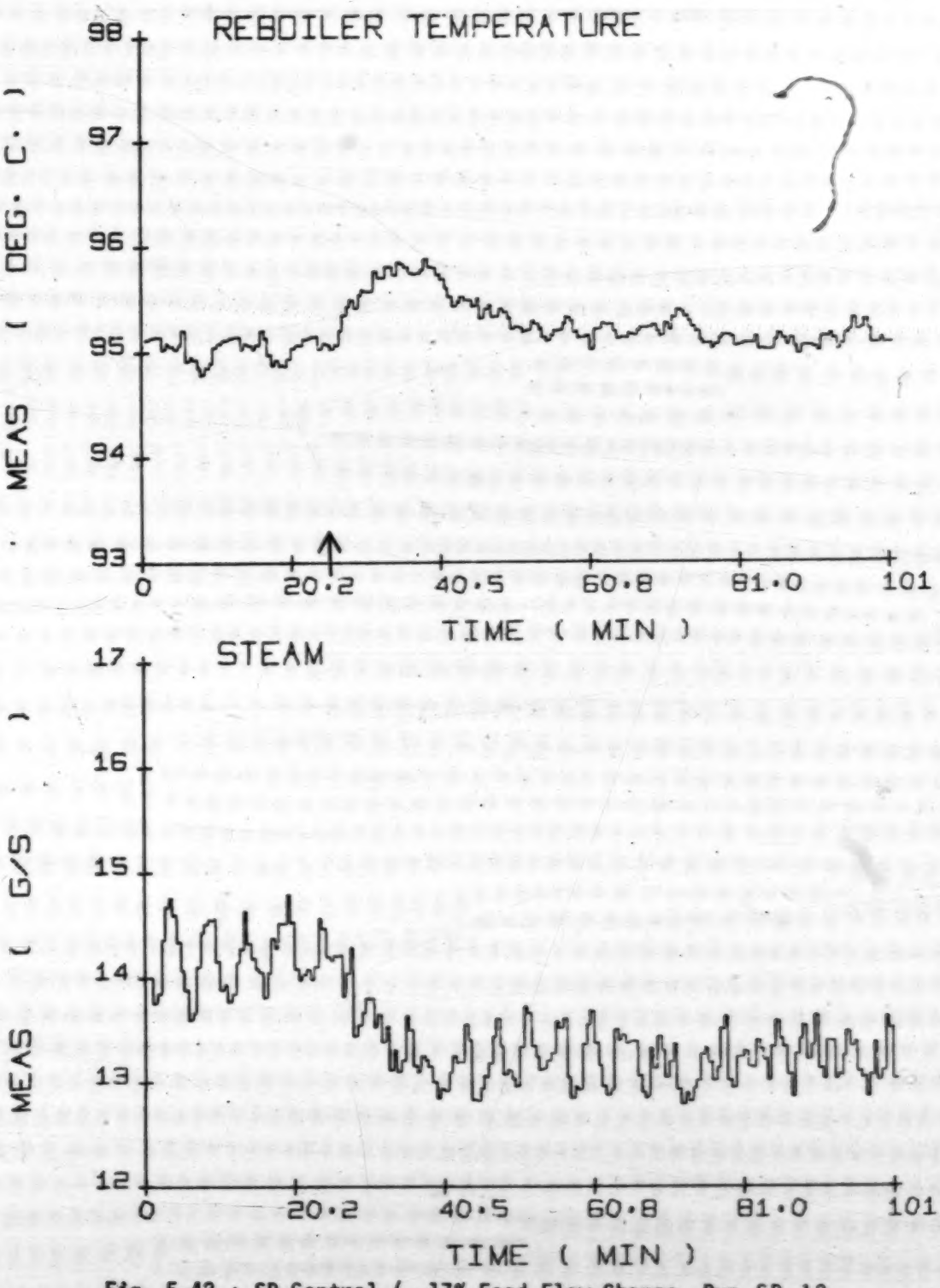

Fig. 5-42 : SP Control (-17% Feed Flow Change, Run SP-12
K_c = 2.0, τ_I = 300)

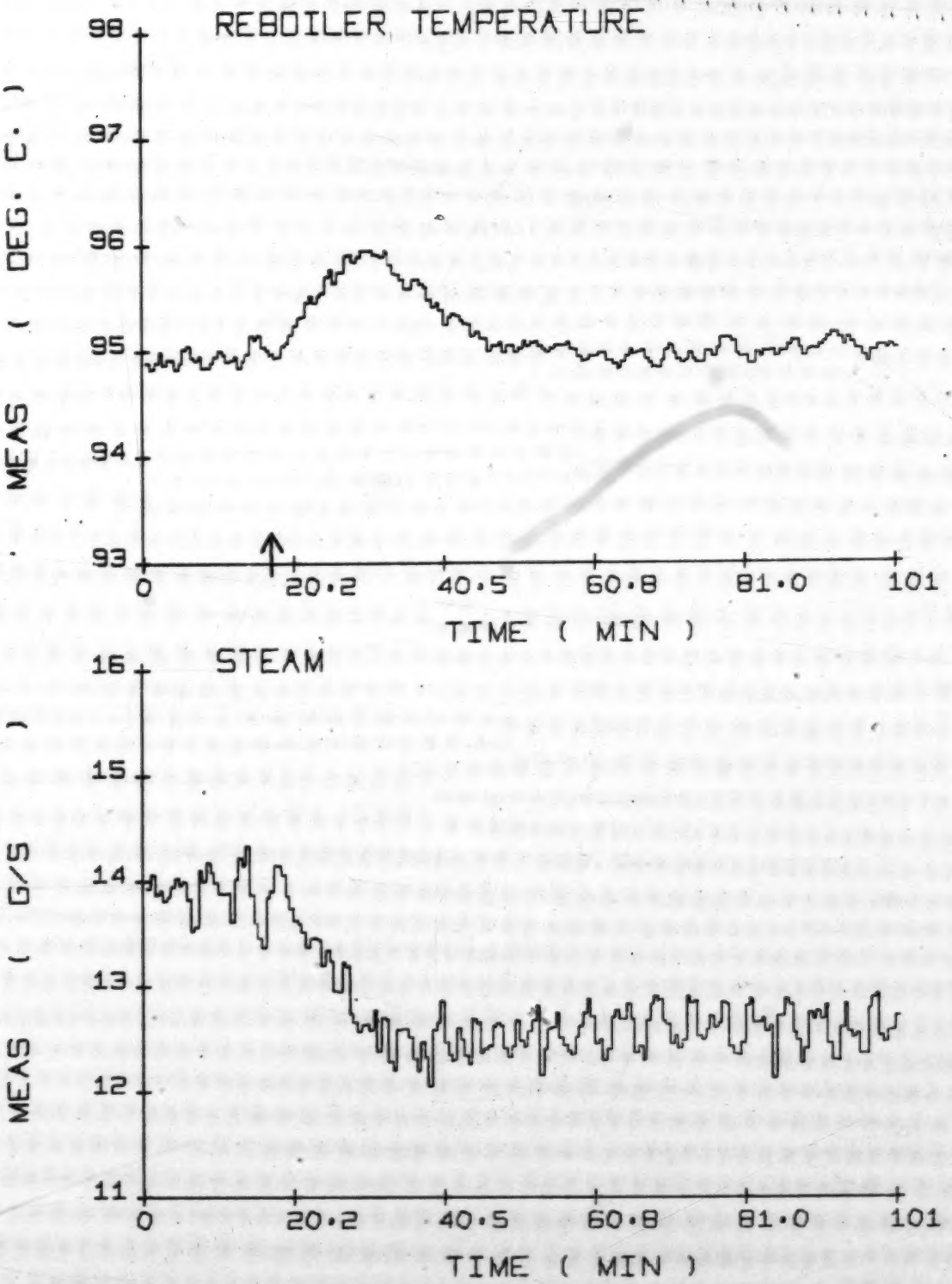

Fig. 5-43 : AP Control (-17% Feed Flow Change, Run AP-14
K_c= 1.2, K_I= 0.01)

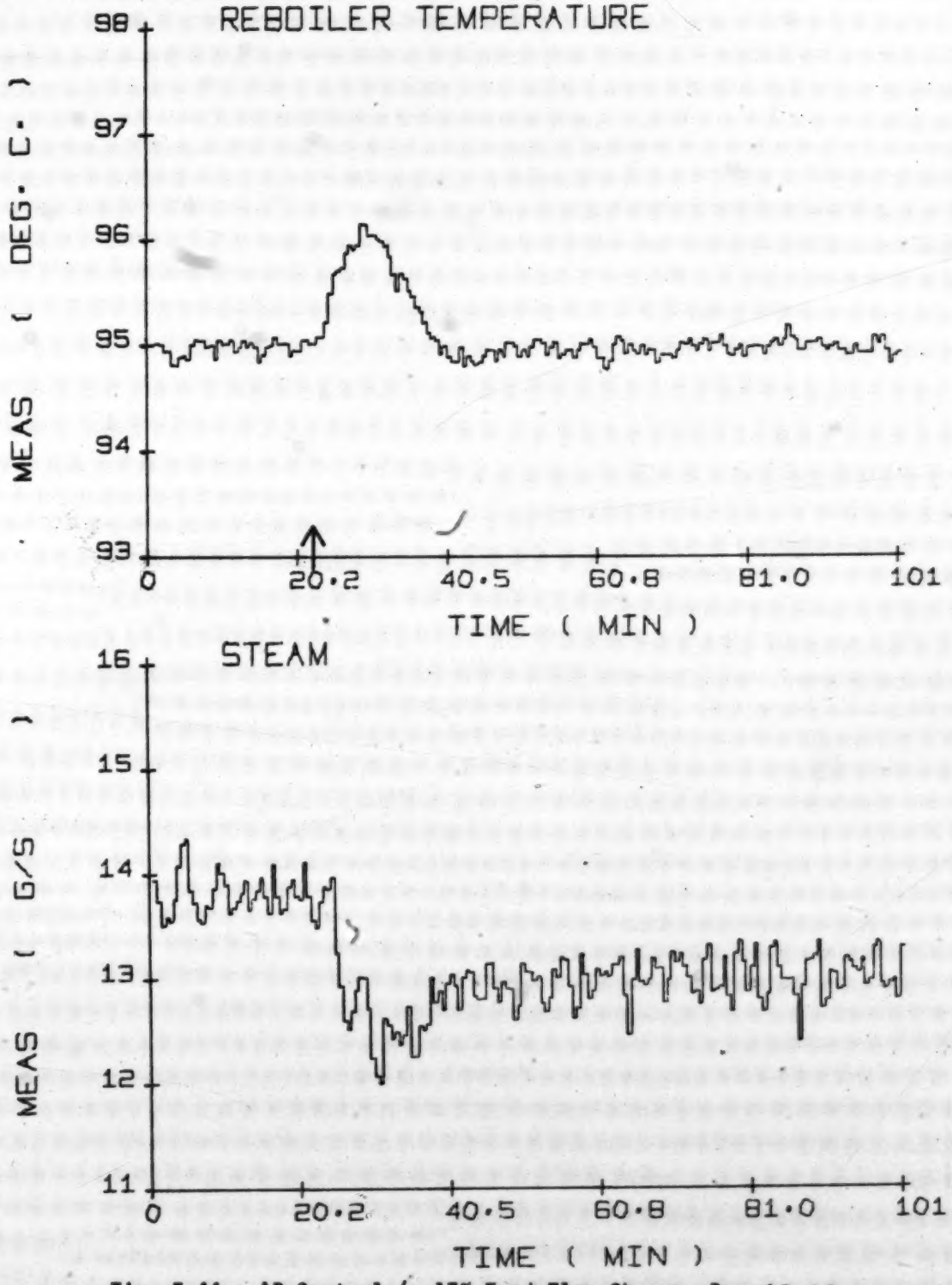

Fig. 5-44 : AP Control (-17% Feed Flow Change, Run AP-15
K_c= 0.6, K_I= 0.02)

The reason for the unsatisfactory results of predictor control for the reboiler temperature probably lies in the inadequate process model, Eqn. (5.4). Only the process gain for this model was determined experimentally; the time constant and time delay were assumed to be the same as for the model with the bottom composition as output variable, which is only a crude approximation. The time delay in particular is probably overestimated by Eqn. (5.4).

5.6 Comparison of Experimental and Simulation Results

A direct quantitative comparison of experimental results with the digital simulation results in Chapter 4 is not possible because different process models were used. In order to obtain comparable simulation results the simulations were repeated using the process models in Table 5-2, for the operating conditions used in this study, with the same step disturbances that were used in the experimental study.

5.6.1 Simulations Based on the Experimental Process Models

Top and bottom composition control of the column using SP, AP and PI control was simulated for the ideal case where no modelling errors are present. Simulations were performed using not only the calculated controller constants, but also the controller constants used in the experimental tests that resulted in the smallest IAE values. The controller constants are summarized in Table 5-3 and the results of the simulations are presented in Table 5-10. Figs. 5-45 to 5-50 show the corresponding transient responses. In all the simulations the step disturbances were introduced at time zero.

Table 5-10 : Simulation Results Using the Process Models Used in this Study given in Table 5-2. (N.B. The Runs with Odd Run Number Employed the Experimental Controller Constants)

RUN	K_c (g/s/%)	τ_I (s)	K_I (g/s/%s)	IAE (%s)	FIGURE
1% Decrease in Top Composition Setpoint					
PI-41	4.72	367	-	321	5-45(a)
PI-42	7.98	367	-	273	
SP-41	8.0	225	-	240	5-46(a)
SP-42	15.8	225	-	208	
AP-41	10.0	-	0.06	213	5-47(a)
AP-42	32.9	-	0.29	152	
22% Decrease in Feed Flow for the Top Composition					
PI-43	4.72	367	-	56.3	5-45(b)
PI-44	7.98	367	-	32.2	
SP-43	8.0	225	-	58.0	5-46(b)
SP-44	15.8	225	-	49.0	
AP-43	10.0	-	0.06	39.4	5-47(b)
AP-44	32.9	-	0.29	8.3	
2% Increase in Bottom Composition Setpoint					
PI-45	-0.15	1500	-	3610	5-48(a)
PI-46	-0.256	1167	-	1970	
SP-45	-0.20	1200	-	2960	5-49(a)
SP-46	-0.696	574	-	1136	
AP-45	-0.80	-	-0.0020	1190	5-50(a)
AP-46	-1.34	-	-0.00343	1073	
17% Decrease in Feed Flow for the Bottom Composition					
PI-47	-0.15	1500	-	11800	5-48(b)
PI-48	-0.256	1167	-	5700	
SP-47	-0.20	1200	-	9900	5-49(b)
SP-48	-0.696	574	-	3630	
AP-47	-0.80	-	-0.0020	2490	5-50(b)
AP-48	-1.34	-	-0.00343	1800	

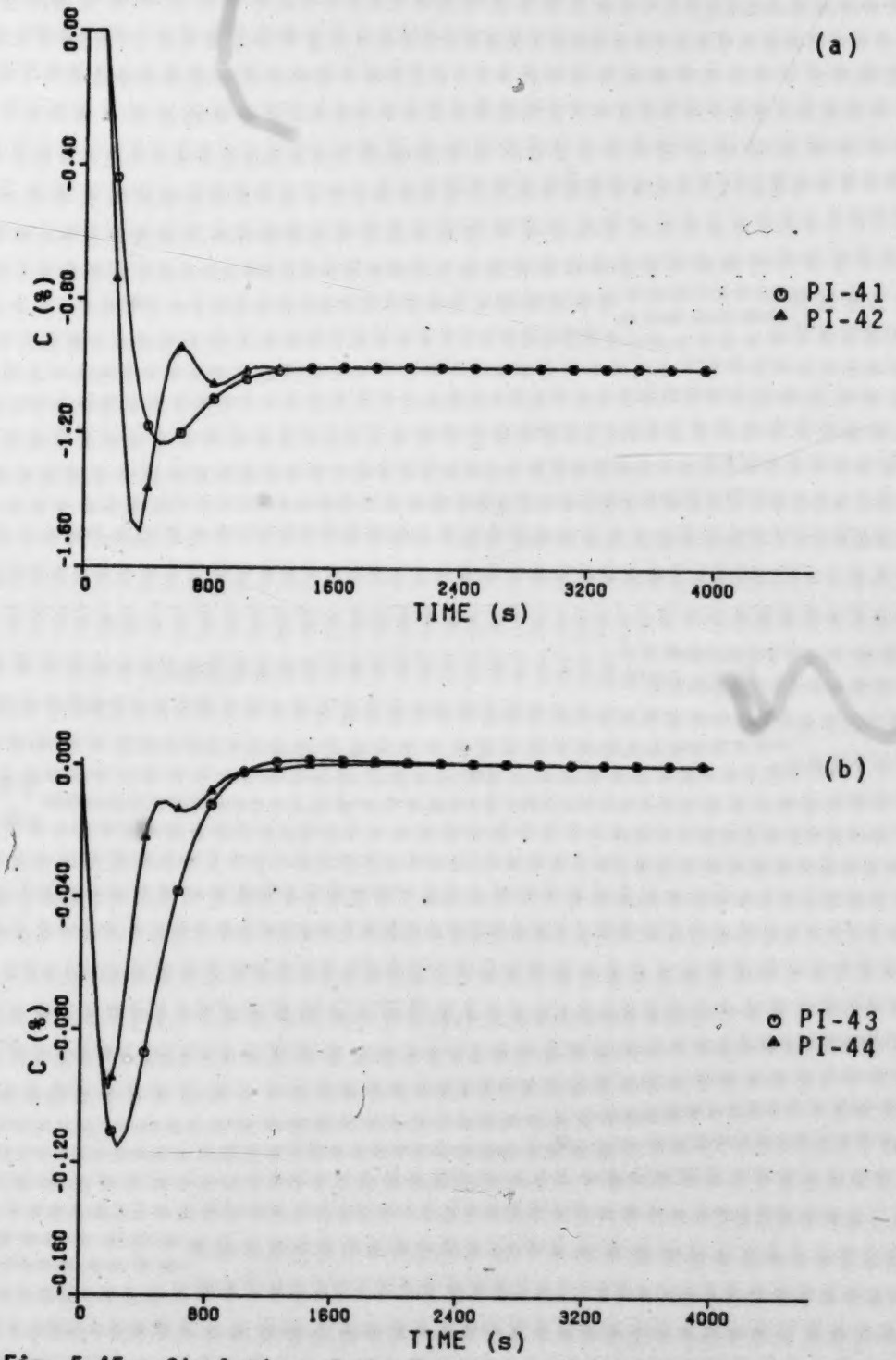

Fig. 5-45 : Simulation of the Top Composition Control for a Setpoint Change of -1% (a) and a Feed Flow Change of -22% (b) using PI Control.

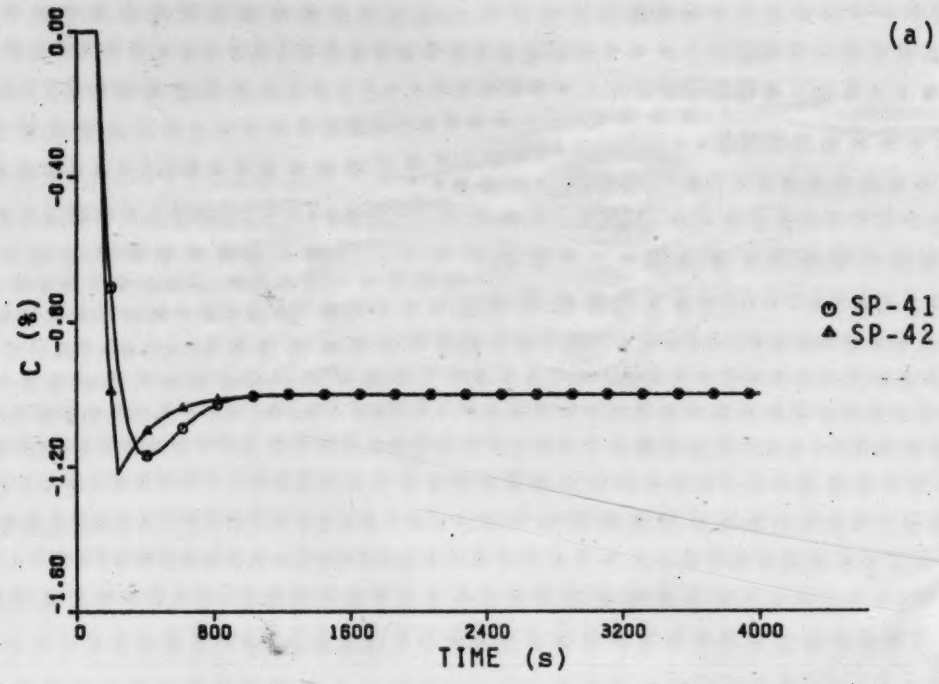

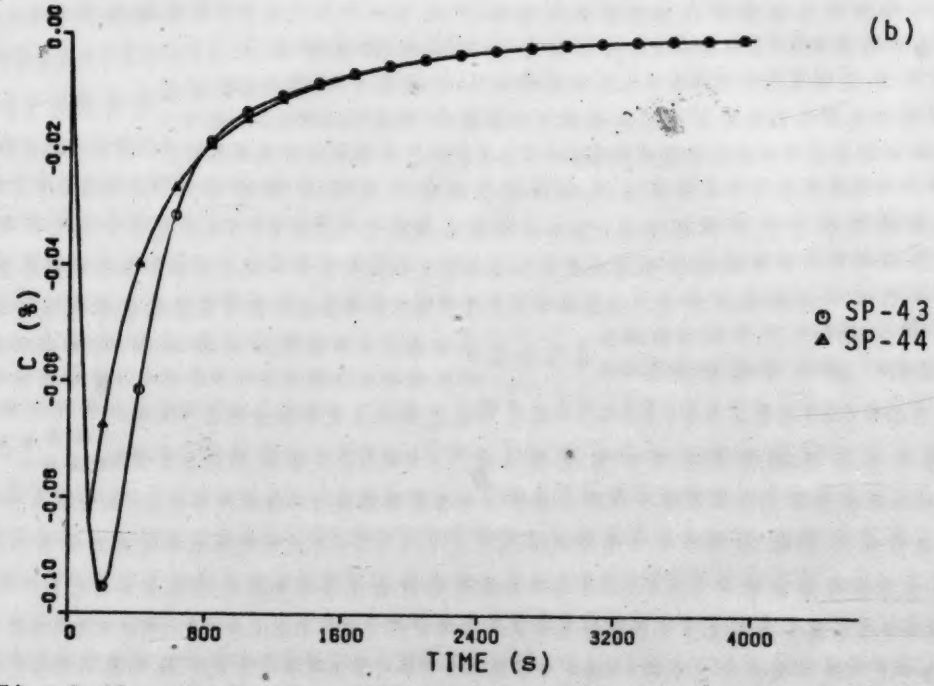

Fig. 5-46 : Simulation of the Top Composition Control for a Setpoint Change of -1% (a) and a Feed Flow Change of -22% (b) using the SP.

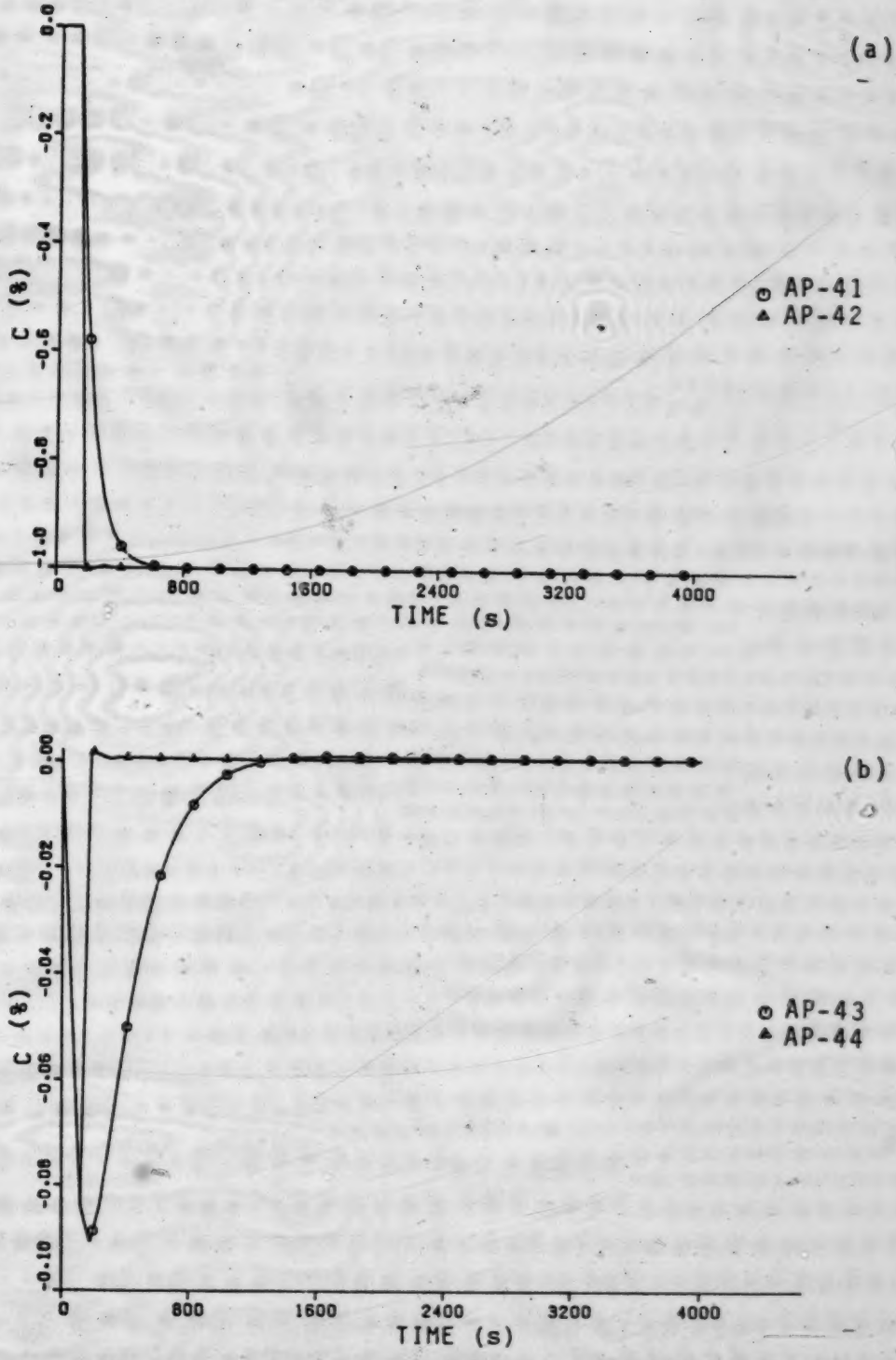

Fig. 5-47 ; Simulation of the Top Composition Control for a Setpoint Change of -1% (a) and a Feed Flow Change of -22% (b) using the AP.

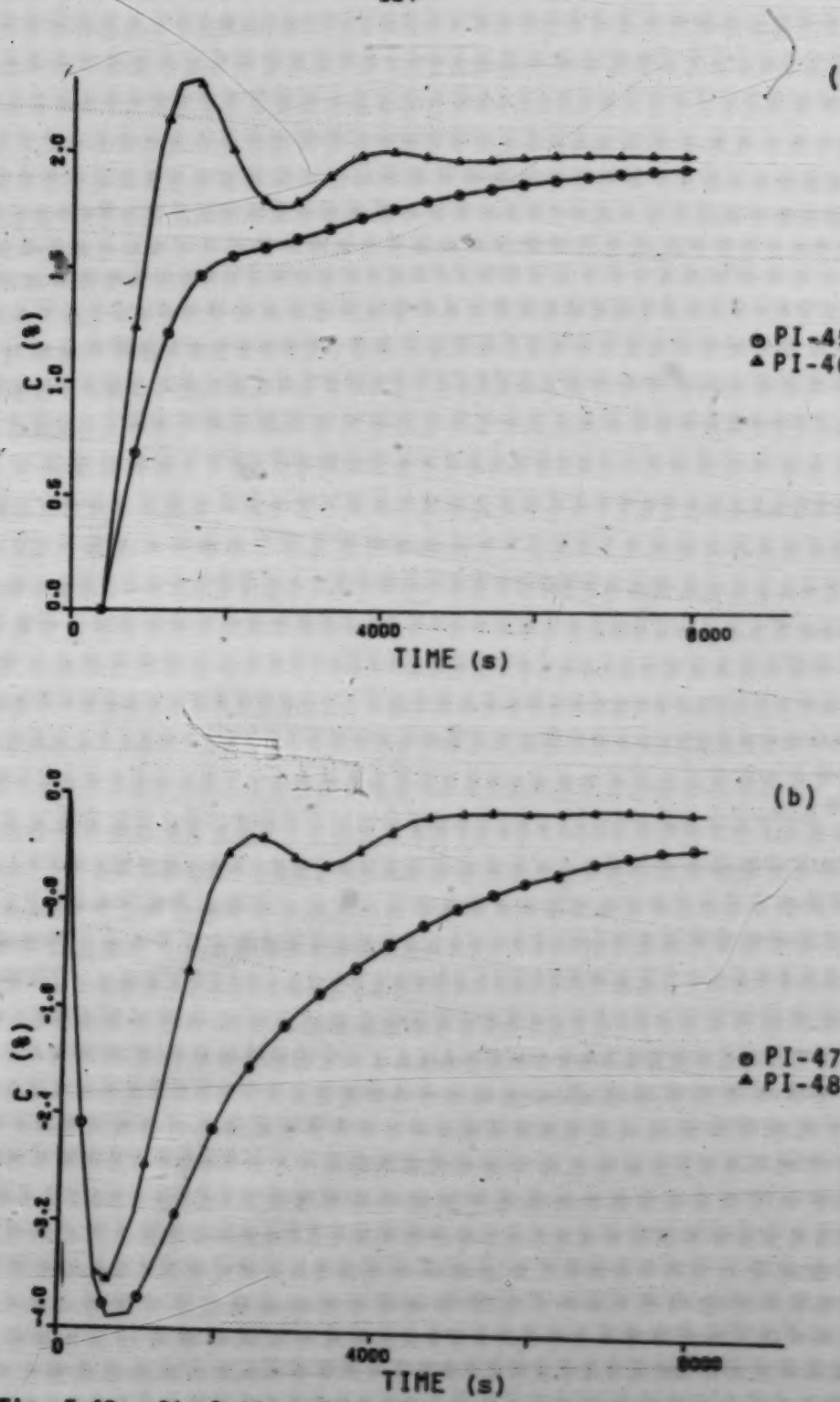

Fig. 5-48 : Simulation of the Bottom Composition Control for a Setpoint Change of +2% (a) and a Feed Flow Change of -17% (b) using PI Control.

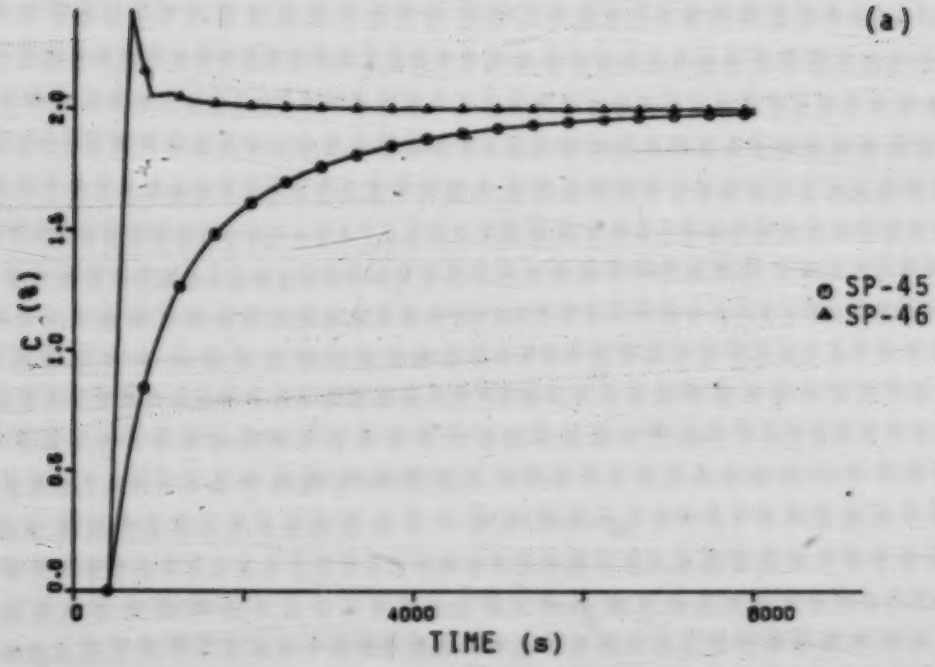

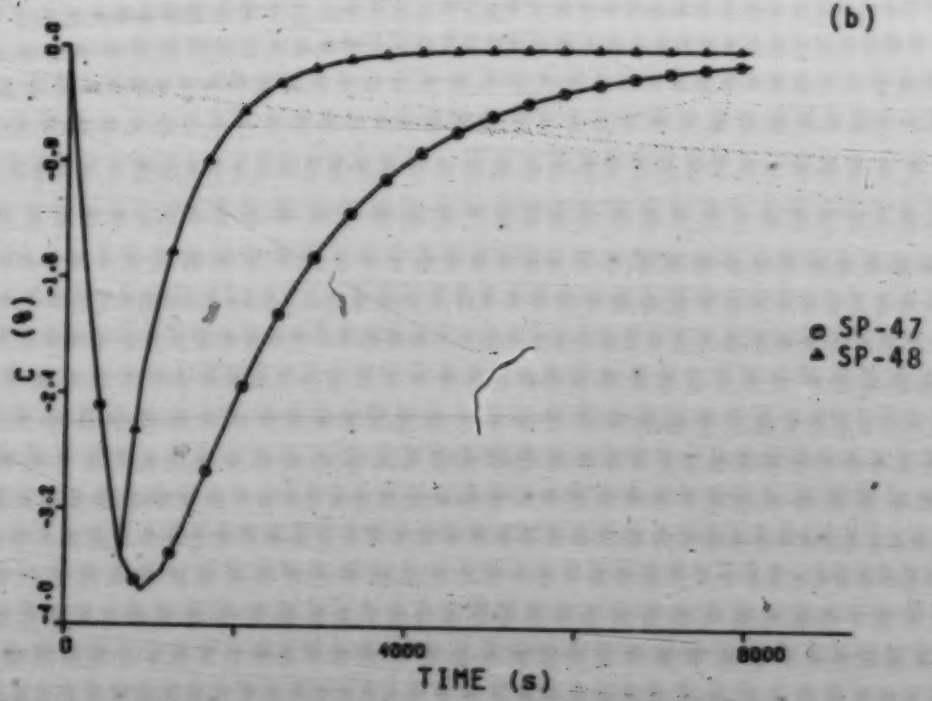

Fig. 5-49 : Simulation of the Bottom Composition Control for a Setpoint Change of +2% (a) and a Feed Flow Change of -17% (b) using the SP.

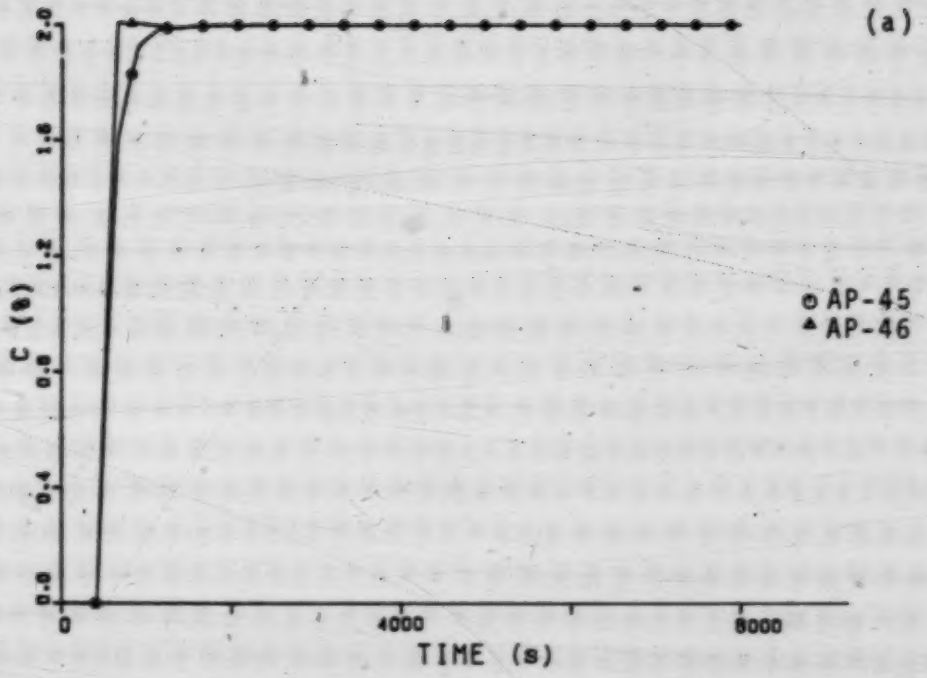

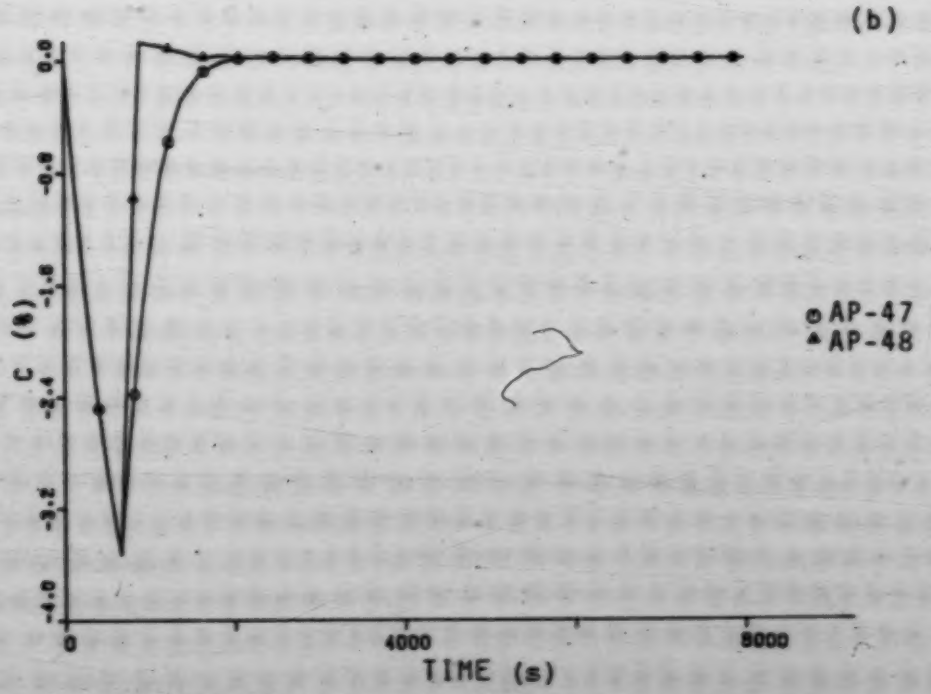

Fig. 5-50 : Simulation of the Bottom Composition Control for a Setpoint Change of +2% (a) and a Feed Flow Change of -17% (b) using the AP.

The simulations with the calculated controller constants (i.e. the runs with even run numbers in Table 5-10) confirm the conclusions of the digital simulation study in Chapter 4 as far as the performance of the three control schemes in the ideal case of no modelling errors is concerned. The AP is superior to SP and PI control in each case. The SP gives a significant improvement over PI control for setpoint changes but exhibits a sluggish response for feed flow changes as shown in Figs. 5-46(b) and 5-49(b).

The runs with the experimental controller constants (i.e. the simulations with odd run numbers in Table 5-10) demonstrate the deterioration of the control performance due to the smaller constants which had to be used to obtain satisfactory control experimentally. Particularly noticeable are the slow responses of the bottom composition for SP and PI control in Figs. 5-48 and 5-49.

The results in Fig. 5-50 again demonstrate the insensitivity of the AP to tuning. Only a small decrease in control performance results by using the experimental constants as compared to the calculated dead-beat controller constants.

Fig. 5-51 shows the behaviour of the manipulated variable, reflux flow, corresponding to the top composition control runs for setpoint changes using PI and AP control. Obviously use of the AP, with dead-beat constants, requiring that the output be brought to the new setpoint in one sampling period requires large changes in the manipulated variable. For the steady state value of the reflux flow of approximately 16 g/s, the change of more than 16 g/s for run AP-42 shown in Fig. 5-51(b) would not be physically possible. However with the experimentally determined controller constants, the required control action was always within the physical constraints.

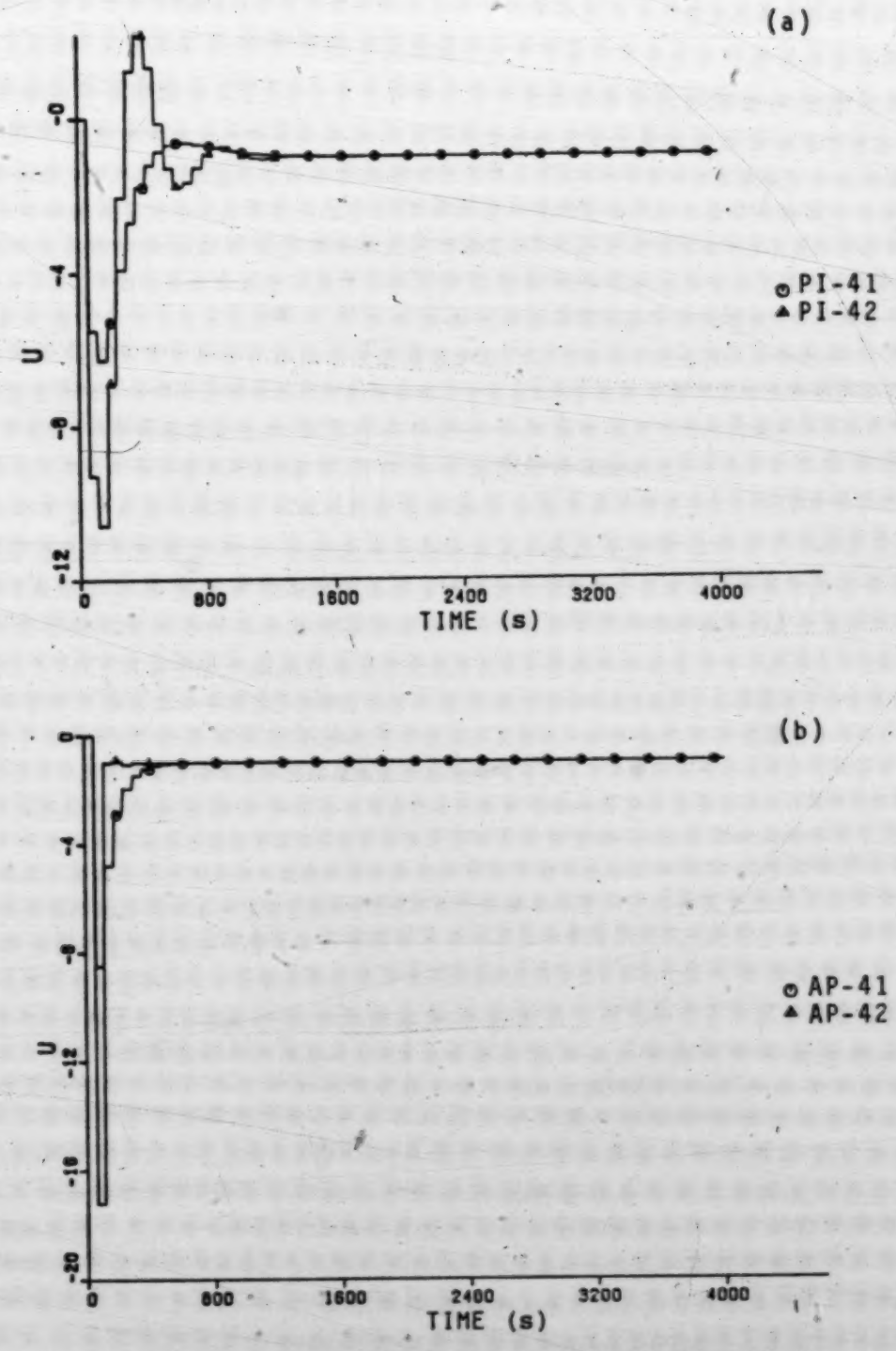

Fig. 5-51 : Comparison of the Control Action (Reflux Flow) for a Setpoint Change of -1% in Top Composition using PI Control (a) and the AP (b).

5.6.2 Comparison with Experiments

A comparison of the simulation results in Section 5.6.1 with the experimental results in Sections 5.4 and 5.5 provides a means for investigating the influence of modelling errors, nonlinearities of the process and noise on the control behaviour. The simulations were carried out using the controller constants and process models used in the experiments but for the ideal case where no modelling errors or noise are present. Consequently deviations between the experimental and simulated responses can be attributed to these factors.

The results shown in Figs. 5-52 to 5-63 demonstrate the deterioration of the control performance that was obtained experimentally. The responses of the top composition in Figs. 5-52 to 5-57 are slower experimentally than in the simulations indicating that the process has slower dynamics than was assumed in the model. This could be due to incorrect model structure, namely the fact that other smaller time constants were neglected to obtain a first order plus time delay process model. Fig. 5-52 shows that the experimental response with PI control is more oscillatory than predicted by the simulation. This result can be explained by the nonlinear nature of the process: as the process gain increases for decreasing composition any overshoot to smaller compositions will be amplified, thus leading to oscillations.

The experimental responses for the bottom composition control exhibit more overshoot than the simulated responses for increases in composition as is demonstrated in Figs. 5-58, 5-60 and 5-62. This can again be explained by the nonlinearity of the process, which results in an increase in gain with increasing composition as shown in Fig. 5-3. The higher

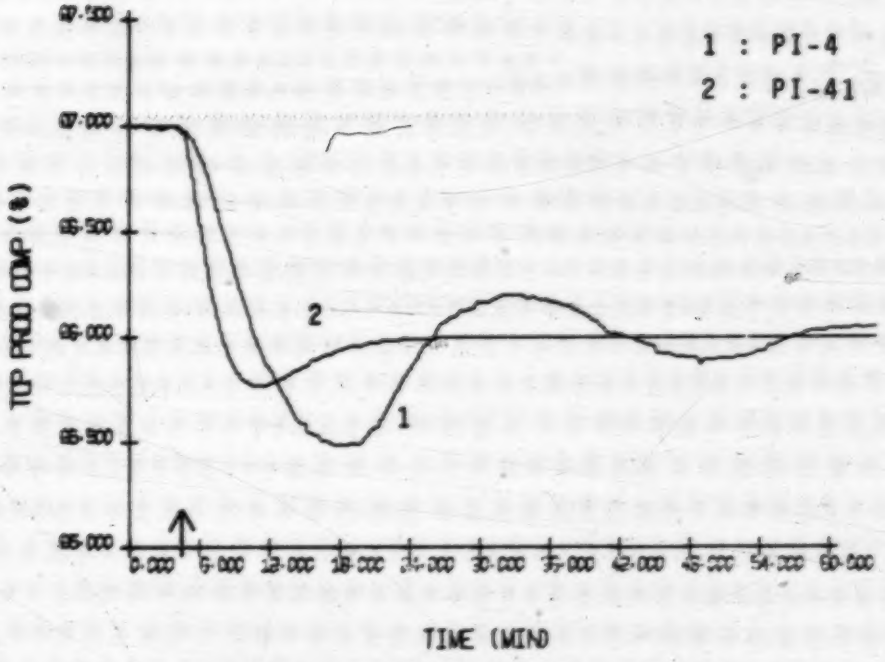

Fig. 5-52 : Comparison of the Experimental (1) and Simulated (2) Responses of the Top Composition for a -1% Setpoint Change Using PI Control.

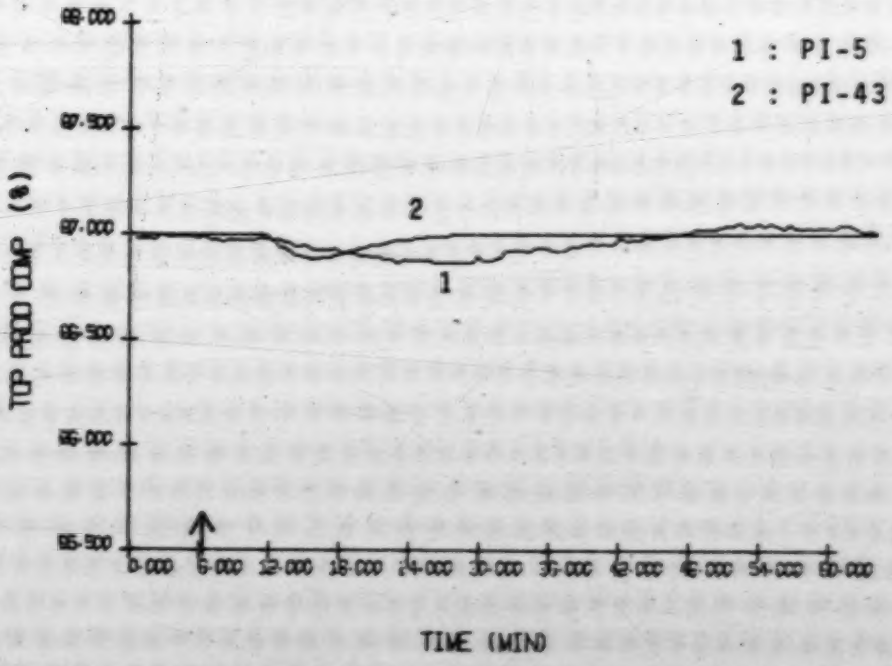

Fig. 5-53 : Comparison of the Experimental (1) and Simulated (2) Responses of the Top Composition for a -22% Feed Flow Change Using PI Control.

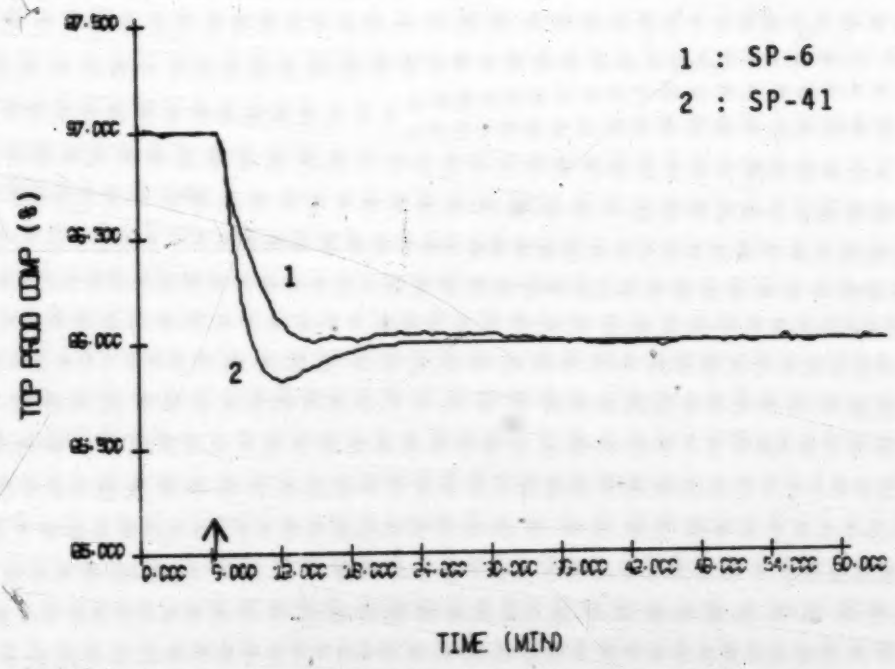

Fig. 5-54 : Comparison of the Experimental (1) and Simulated (2) Responses of the Top Composition for a -1% Setpoint Change Using SP Control.

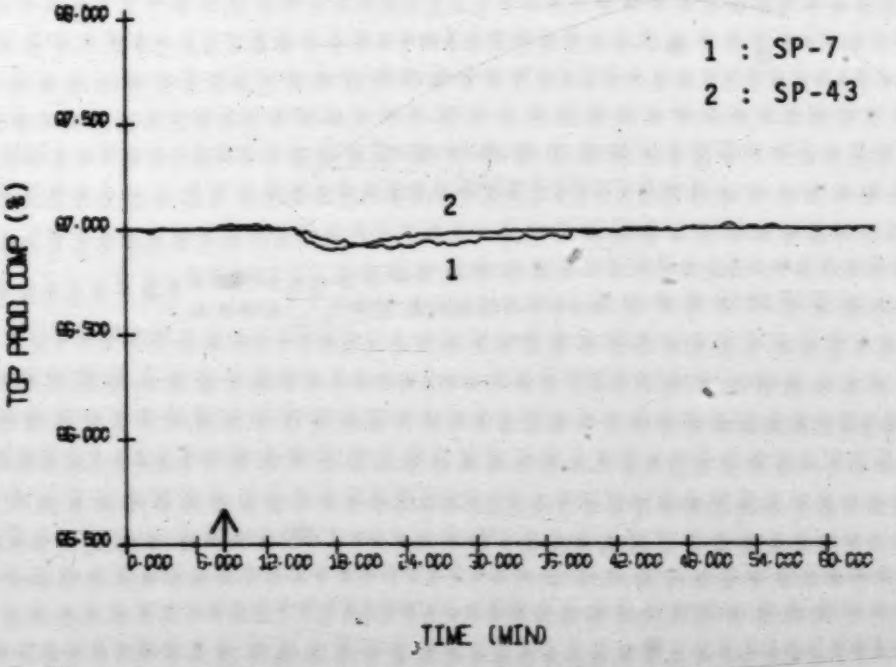

Fig. 5-55 : Comparison of the Experimental (1) and Simulated (2) Responses of the Top Composition for a -22% Feed Flow Change Using SP Control.

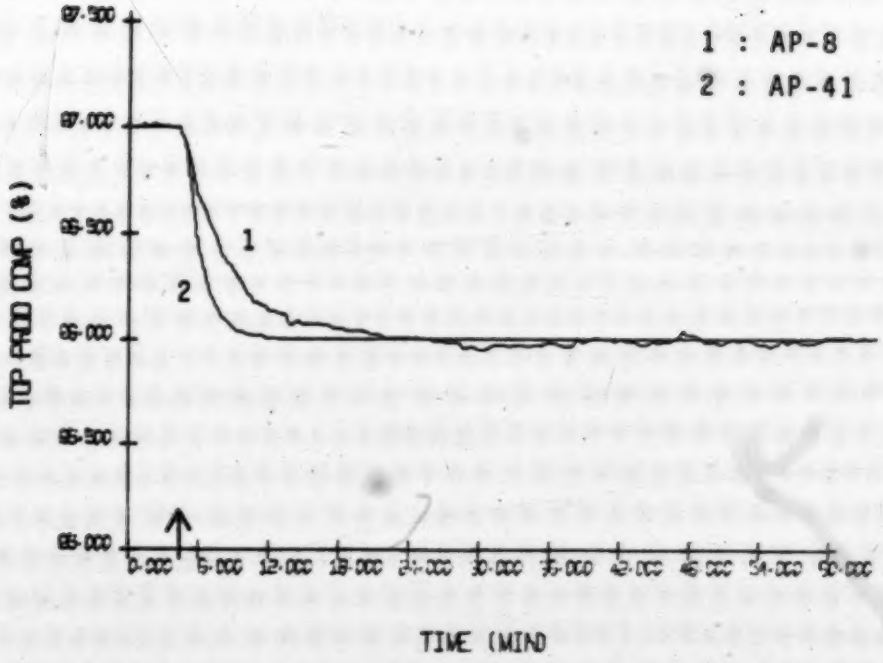

Fig. 5-56 : Comparison of the Experimental (1) and Simulated (2) Responses of the Top Composition for a -1% Setpoint Change Using AP Control.

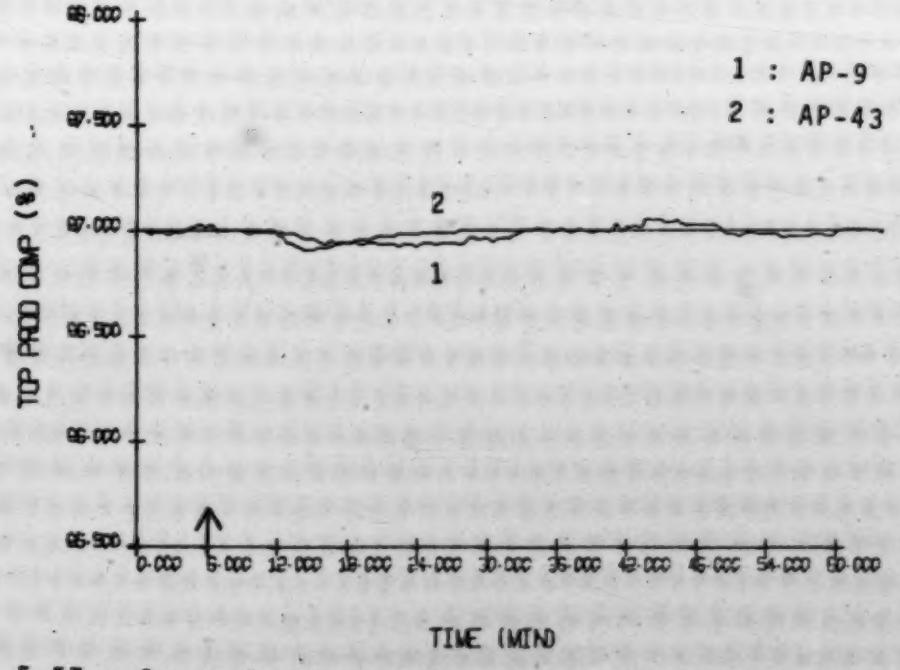

Fig. 5-57 : Comparison of the Experimental (1) and Simulated (2) Responses of the Top Composition for a -22% Feed Flow Change Using AP Control.

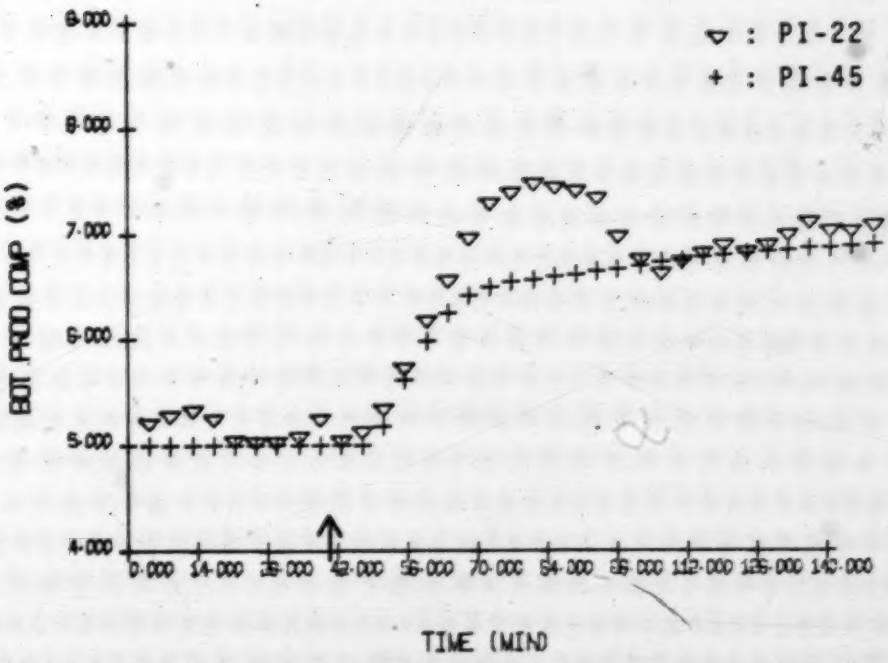

Fig. 5-58 : Comparison of the Experimental (▽) and Simulated (+) Responses of the Bottom Composition for a 2% Setpoint Change Using PI Control.

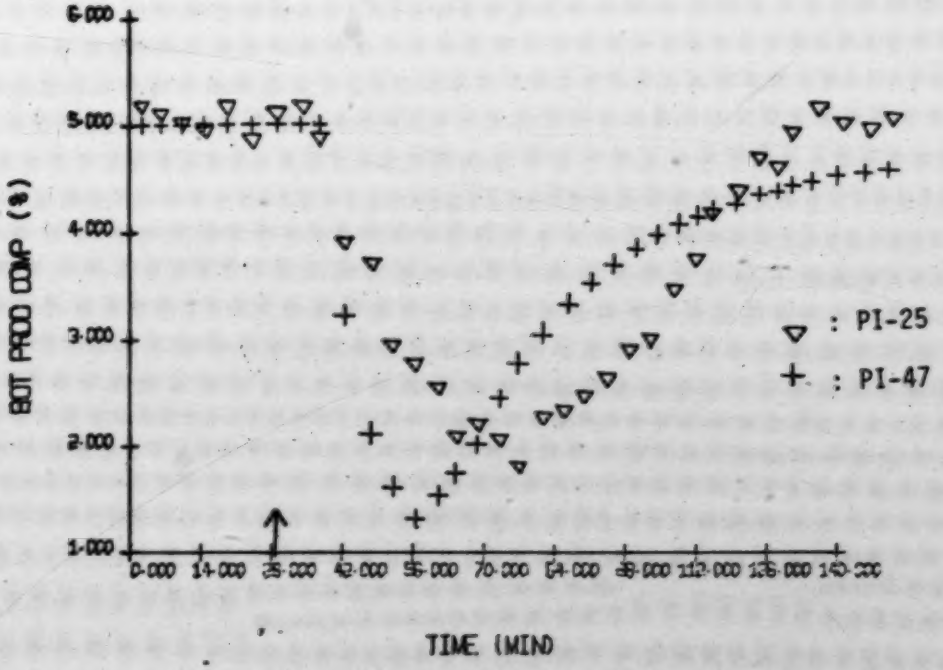

Fig. 5-59 : Comparison of the Experimental (▽) and Simulated (+) Responses of the Bottom Composition for a 17% Feed Flow Change Using PI Control.

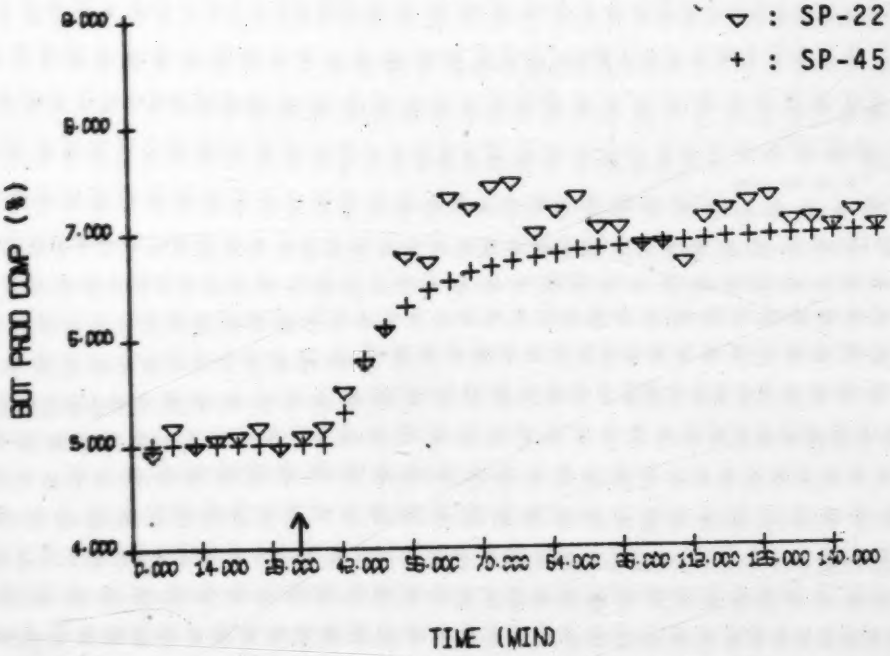

Fig. 5-60 : Comparison of the Experimental (▽) and Simulated (+) Responses of the Bottom Composition for a 2% Setpoint Change Using SP Control.

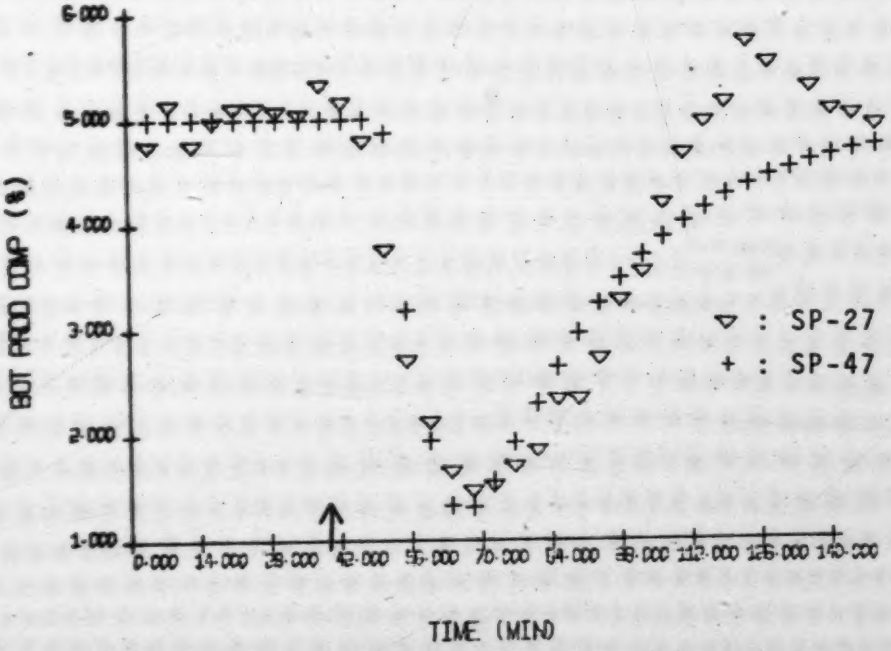

Fig. 5-61 : Comparison of the Experimental (▽) and Simulated (+) Responses of the Bottom Composition for a -17% Feed Flow Change Using SP Control.

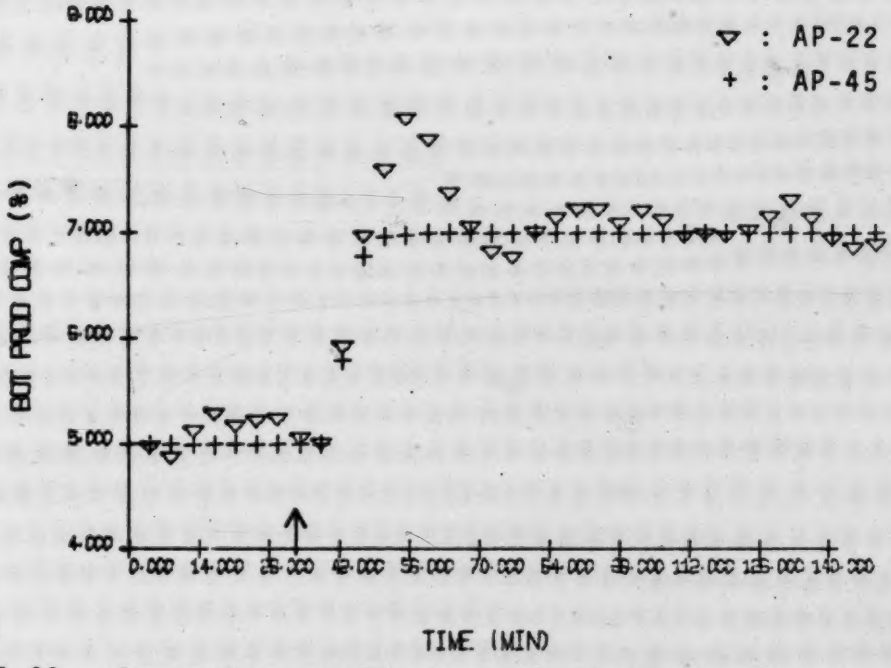

Fig. 5-62 : Comparison of the Experimental (▽) and Simulated (+) Responses of the Bottom Composition for a 2% Setpoint Change Using AP Control.

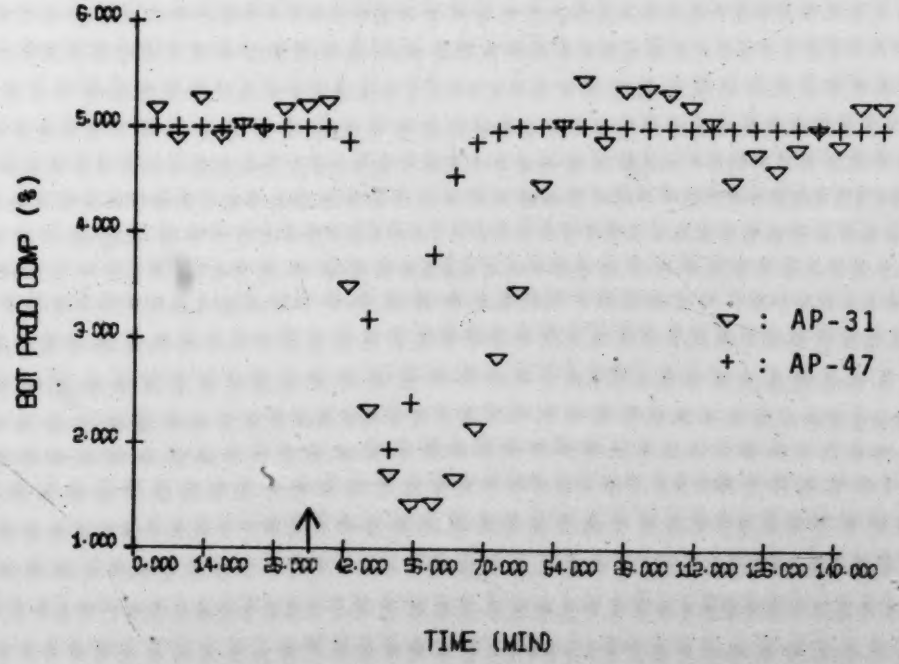

Fig. 5-63 : Comparison of the Experimental (▽) and Simulated (+) Responses of the Bottom Composition for a -17% Feed Flow Change Using AP Control.

sensitivity of the AP to modelling errors compared to the SP is clearly demonstrated in Figs. 5-60 to 5-63. Whereas the simulated and experimental responses for the SP in Figs. 5-60 and 5-61 agree remarkably well, the experimental responses for the AP in Figs. 5-62 and 5-63 show a significantly deteriorated control behaviour. Initially the experimental responses of the SP and the AP for decreases in feed flow are quite similar to the simulated responses as shown in Figs. 5-61 and 5-63 , and demonstrate that the dynamics assumed in the model agree well with the dynamics of the process. In contrast, the experimental response with PI control is slower than the simulated response, as shown in Fig. 5-59. The reason for this behaviour remains unclear; a plugged sample valve in the on-line GC may have been the cause.

5.7 Conclusions from the Experimental Investigation

The results for top composition control using SP, AP and PI control demonstrate that for setpoint changes:

1. Both predictors give a significant improvement over PI control. This is demonstrated by IAE values which are less than one half of the values for PI control.

2. Both predictors can handle very severe model errors. Even when a process model with a 50% error in the gain is employed the control is still stable, though only marginally superior to PI control.

Since the top composition is insensitive to feed flow changes, only very small deviations from the steady state were obtained. The results indicate the superior performance of the predictors over PI control but are not conclusive for this reason.

The following conclusions can be drawn from the results for the bottom composition control for setpoint and feed flow changes:

1. Both predictors resulted in an improvement over PI control.

2. Better performance of the predictors was obtained for decreases in setpoint or feed flow, since in this case the process gain is smaller than the model gain. For an increase in setpoint or feed flow the reverse is true, leading to oscillatory responses.

3. For setpoint changes the AP was superior to the SP.

4. For feed flow changes the SP and the AP performed in a similar fashion and gave a significant improvement over PI control.

Reboiler temperature control for setpoint and feed flow changes showed only a marginal improvement of predictor control over PI control presumably because of the inadequate process models that were used. This demonstrates the fact that careful process modelling is a prerequisite to obtain satisfactory results using predictor control.

Controller constants calculated from the process models resulted in very oscillatory responses in the experimental tests for all three control schemes, requiring on-line tuning of the controller constants. For SP and PI control a moderate reduction of the calculated controller constants resulted in satisfactory control performance. The AP required a larger reduction of the calculated controller constants to provide stable control. Once the range of satisfactory controller settings was found, however, the AP was quite insensitive to the controller constants used.

CHAPTER 6

CONCLUSIONS AND RECOMMENDATIONS

The analytical and Smith predictor control schemes have been successfully used to control the top and bottoms composition of a pilot scale, methanol-water distillation column. The first order plus time delay predictor models provided a satisfactory representation of the column dynamics for control purposes. The experimental results indicate that both the analytical and Smith predictors give a significant improvement over PI control for both setpoint and feed flow changes. For top composition control the Smith predictor provided slightly better control than the analytical predictor. However the analytical predictor performance was superior for bottoms composition control. Initial experimental tests of the three control schemes with calculated controller constants resulted in very oscillatory responses, so trial and error tuning became necessary. The analytical predictor showed a marked insensitivity to different controller constants used in these experiments.

The simulation study demonstrated that both predictor control schemes provide a significant improvement over PI control for setpoint changes. For load changes the analytical predictor performance was superior to that of the Smith predictor which resulted in very sluggish responses. The simulation study showed also that both the analytical and Smith predictors exhibit a satisfactory degree of insensitivity to modelling errors. However, the performance of the analytical predictor deteriorated more compared to the ideal case of a perfect process model.

In this investigation the analytical predictor was superior to the Smith predictor in the simulations and in most experiments. In other practical applications, the better performance of the analytical predictor will have to be balanced against its higher sensitivity to modelling errors.

Some recommendations for future work suggested by this study include the following:

1. The unsatisfactory performance of the Smith predictor for load disturbances might be improved. A possible approach is given in Section 3.4.1.1., where load prediction has been included in the control algorithm.

2. The Smith predictor algorithm could be modified to compensate for the time delay introduced by sampling in a fashion similar to that used in the analytical predictor. Prediction of the future process output over a time interval equal to one half of the sampling interval could be included in the algorithm for the response of the system without time delay. The algorithm for the system with time delay should not be modified, however, since it is designed to cancel the measured process output in the ideal case of a perfect process model and no disturbances.

3. The improved control performance achieved using the analytical predictor suggests that a theoretical investigation of the possibilities for generalizing this approach would be meaningful. In particular, extensions to the multivariable case and the case of a load transfer function different from the process transfer function could be studied.

4. The nonlinear dynamics of distillation columns imply that predictor control will only be satisfactory over a small range of operating conditions. It would appear worthwhile to include a variable process gain in the predictor model which could be adjusted for the level of composition. Alternatively one could consider an adaptive predictor control

strategy, which could identify the parameters in the predictor model on-line. This approach would allow use of the predictor scheme over a wide range of operating conditions and furthermore would eliminate the need for a priori accurate process models.

NOTATION

B:	bottoms flow rate
C, c:	system output
c^1:	output of system without time delay
c^2:	output of system with time delay
c_B:	bottom composition
c_D:	top composition
c_F:	feed composition
D:	distillate flow rate
D, d:	load disturbance
e:	controller input
F:	feed flow rate
G_C:	controller transfer function
G_L:	load transfer function
G_p:	process transfer function
H:	measurement transfer function
k:	positive integer number
K_C:	controller gain
K_I:	integral controller constant
K_p:	process gain
N:	integer number of sampling times
p:	calibrated setpoint
R:	reflux flow rate
R_{Set}, r:	setpoint
S:	steam flow rate
s:	Laplace operator
T, T', T_1, T_2:	time delays
T_R:	reboiler temperature
T_s:	sampling time
U, u:	control action

Greek symbols

α:	constant, $0<\alpha<1$
β:	fractional number of sampling time, $0<\beta<1$
δ:	observed effect of a load disturbance
θ:	dimensionless time delay
ρ:	predicted effect of a load disturbance
τ_I:	reset time
τ_L:	load time constant
τ_p:	process time constant

Subscripts:

k:	denotes a discrete variable

Superscripts:

$\wedge$:	denotes a predicted value

Abbreviations:

AP:	analytical predictor
GC:	gas chromatograph
IAE:	integral absolute error
PI:	proportional-integral
SP:	Smith predictor
ZOH:	zero order hold

REFERENCES

1. Alevisakis, G., Seborg, D.E., "An Extension of the Smith Predictor Method to Multivariable Linear Systems Containing Time Delays", Int. J. Control, 3, 541-551 (1973).

2. Alevisakis, G., Seborg, D.E., "Control of Multivariable Systems Containing Time Delays Using a Multivariable Smith Predictor", Chem. Eng. Sci., 29, 373-380 (1974).

3. Bakke, R.M., "Direct Digital Control with Self-Adjustment for Processes with Variable Dead Time and/or Multiple Delays", Instr. Soc. of America, Preprint No. 30.1-1-65, 20th Ann. ISA Conf., Los Angeles (1965).

4. Berry, M.W., "Terminal Composition Control of a Binary Distillation Column", M.Sc. Thesis, Department of Chemical Engineering, The University of Alberta, Edmonton (1973).

5. Buckley, P.S., "Automatic Control of Processes with Dead Time", Proc. 1st IFAC Congress, Moscow (1960).

6. Buckley, P.S., "Techniques of Process Control", Wiley, New York (1964).

7. Dahlin, E.B., "Designing and Tuning Digital Controllers", Instr. and Control Systems, 41, No. 6, 77-83 (1968).

8. Doss, J.E. "The Design and Application of a Discrete Predictive Dead Time Compensator for Direct Digital Control", Ph. D. Thesis, Department of Chemical Engineering, The University of Tennessee (1974).

9. Doss, J.E., Moore, C.F., "Comparison of Dead Time Compensation Techniques in DDC", 74th Nat. AIChE Mtg., New Orleans (1973).

10. Eisenberg, L., "Analysis of Smith Linear Predictor Control Systems", ISA Trans., 6, No. 4, 329-334 (1967).

11. Garland, B. Marshall, J.E., "Sensitivity Considerations of Smith's Method for Time-Delay Systems", Electron. Lett., 10, No. 15, 308-309 (1974).

12. Garland, B., Marshall, J.E., "Application of the Sensitivity Points Method to a Linear Predictor Control System", Int. J. Control, 21, 681-688 (1975).

13. Gray, J.O., Hunt, P.W.B., "State-Feedback Controller with Linear Predictor for Systems with Dead Time", Electron. Lett., 7, No. 12, 335-337 (1971).

14. Gray, J.O., Hunt, P.W.B., "State-Feedback Controller for Systems with Dead Time", Electron. Lett. 7, No. 516, 131-133 (1971).

15. Higham, J.D., "Single-term Control of First and Second-order Processes with Dead Time",Control, 12, No. 2, 136-140 (1968).

16. Jacobson, B.A., "Multiloop Computer Control of an Evaporator", M. Sc. Thesis, Department of Chemical Engineering, The University of Alberta (1970).

17. Koppel, L.B., Aiken, P.M., "A General Process Controller", I & EC Process Design and Development, 8, No. 2, 174-184 (1969).

18. Liesch, D.W., "Decoupled Feedforward-Feedback Control of a Binary Distillation Column", M. Sc. Thesis, Department of Chemical Engineering, The University of Alberta (1974).

19. Lopez, A.M., Murrill, P.W., Smith, C.L., "Tuning PI and PID Digital Controllers", Instr. and Control Systems, 42, No. 2, 89-95 (1969).

20. Lopez, A.M., Murrill, P.W., Smith, C.L., "Optimal Tuning of Proportional Digital Controllers", Instr. and Control Systems, 41, No. 10, 97-102 (1968).

21. Lupfer, D.E., Oglesby, M.W., "Applying Dead-Time Compensation for Linear Predictor Process Control", ISA Journal, 8, No. 11, 53-57 (1961).

22. Lupfer, D.E., Oglesby, M.W., "The Application of Dead-Time Compensation to a Chemical Reactor for Automatic Control of Production Rate", ISA Trans., 1, No. 1, 72-80 (1962).

23. Marshall, J.E., "Extension of O.J. Smith's Method to Digital and Other Systems", Int. J. Control, 19, 933-939 (1974).

24. Mee, D.H., "An Extension of Predictor Control for Systems with Control Time-Delays" Int. J. Control, 18, 1151-1168 (1973).

25. Meyer, C., Seborg, D.E., Wood, R.K., "A Comparison of the Smith Predictor and Conventional Feedback Control", Chem. Eng. Sci., 31, 775-778 (1976).

26. Miller, J.,Lopez, A.M., Smith, C.L., Murril, P.W., "A Comparison of Controller Tuning Techniques", Control Eng., 14, No. 12, 72-75 (1967).

27. Moore, C.F., Smith, C.L., Murrill, P.W., "Simplifying Digital Control Dynamics for Controller Tuning and Hardware Lag Effects", Instr. Pract., No. 1, 45-49 (1969).

28. Moore, C.F., Smith, C.L., Murrill, P.W., "Improved Algorithm for Direct Digital Control", Instr. and Control Systems, 43, No. 1, 70-74 (1970).

29. Moore, C.F., Smith, C.L., and Murrill, P.W., "Improving Performance of Digital Control Loops", 4th LSU Workshop on Digital Computers in Process Control, Baton Rouge, La. (1969).

30. Moore, C.F., "Selected Problems in the Design and Implementation of Direct Digital Control", Ph. D. Thesis, Department of Chemical Engineering, Louisiana State University (1969).

31. Mori, M., "Discrete Compensator Controls Dead Time Process", Control Eng., 9, No. 1, 57-60 (1962).

32. Nielsen, G., "Control of Systems with Time Delay", Proc. 4th IFAC Congress, Warsaw (1969).

33. Pacey, W.C., "Control of a Binary Distillation Column", M. Sc. Thesis, Department of Chemical Engineering, The University of Alberta, Edmonton (1973).

34. Phillipson, P.H., "Optimum Regulation of Sampled-data Processes", Int. J. Control, 21, 785-793 (1975).

35. Pracht, C.P., McVey, E.S., "Near Ideal Digital Predictive Compensation", IEEE Trans. Aut. Contr., AC-15, 471-474 (1970).

36. Prasad, C.C., Krishnaswamy, P.R., "Control of Pure Time Delay Processes", Chem. Eng. Sci., 30, 207-215 (1975).

37. Prasad, C.C., Krishnaswamy, P.R., "A Dual-loop Predictor for pH Control", Instr. Tech., No. 7, 53-57 (1975).

38. Rademaker, O., Rijnsdorp, J.E., Maarleveld, A., "Dynamics and Control of Continuous Distillation Units", Elsevier Scientific Publishing Company, New York (1975).

39. Roberts, P.D., Dallard, K.E., "Discrete PID Controller with a Single Tuning Parameter", Measurement and Control, 7, 469-473 (1974).

40. Simonsmeier, U., M. Sc. Thesis, Department of Chemical Engineering, The University of Alberta, Edmonton (in preparation).

41. Smith, C.A., Groves, F.R., "Dead Time Compensation Based on Empirical Nonlinear Process Models", Proc. 28th Ann. ISA Conf., Houston, Tex. (1973).

42. Smith, C.L., Corripio, A.B., Martin, J., "Controller Tuning from Simple Process Models", Instr. Tech., No. 12, 39-44 (1975).

43. Smith, O.J.M., "Closer Control of Loops with Dead Time", Chem. Eng. Progr., 53, No. 5, 217-219 (1957).

44. Smith, O.J.M., "A Controller to Overcome Dead Time", ISA Journal, 6, No. 2, 28-33 (1959).

45. Svrcek, W.Y., "Dynamic Response of a Binary Distillation Column", Ph. D. Thesis, Department of Chemical and Petroleum Engineering, The University of Alberta, Edmonton (1967).

APPENDIX A

A COMPARISON OF THE SMITH PREDICTOR AND CONVENTIONAL FEEDBACK CONTROL*

1. INTRODUCTION

The detrimental effects of time delays in feedback control loops are well known. Of the special control techniques proposed for processes with time delays, the "Smith predictor" or "Smith linear predictor" (1,2) has probably received the most attention. Several simulation and experimental studies (3-7) have demonstrated that the Smith predictor can result in significant improvements over conventional control. The sensitivity of the Smith predictor to modelling errors (7-9) including Padé approximations to the time delays (7,10) have also been considered. In recent years the predictor has been extended to sampled-data systems (5,9,11,12,14, 15) and multi-variable systems (13-15) .

Nielsen (16) has compared the performance of the Smith predictor and conventional PI, PID and integral controllers for simulated processes described by first and second order transfer functions plus time delays. He reported that the Smith predictor is superior to conventional controllers for setpoint changes if the "Integral Absolute Error" is used as the performance index. However, for load changes Nielsen's simulated results indicate that the Smith predictor gives better control only if large time delays are present; for relatively small time delays, the conventional controllers are better. Nielsen's analysis assumes that the load variable and the manipulated variable affect the controlled variable in the same fashion (i.e. the special case when the load and process transfer functions are identical).

* Appendix A is in the form of a draft for a publication (25).

In this investigation it is demonstrated that a comparison of the Smith predictor and conventional feedback controllers must take into account the relative dynamics of the load and process transfer functions.

2. THEORETICAL ANALYSIS

The block diagram of the closed loop system including the Smith predictor is shown in Figure 1. The predictor consists of a feedback loop around the controller with the output of the "predictor" block representing the difference between two process models: the response of the undelayed system minus the response of the system with time delays T_1 and T_2. If there are zero time delays (i.e. $T_1 = T_2 = 0$) or if the predictor block is omitted, the block diagram in Figure 1 reduces to the diagram for a conventional feedback control system.

For load disturbances, the closed-loop transfer function for the system in Figure 1 is given by:

$$\frac{C(s)}{U(s)} = \frac{G_L(s)[1 + G_c(s)G_p(s)H(s)\ [1 - e^{-s(T_1+T_2)}]]}{1 + G_c(s)G_p(s)H(s)} \quad (1)$$

The characteristic equation for this system is

$$1 + G_c(s)G_p(s)H(s) = 0 \quad (2)$$

which is also the characteristic equation for the system in Figure 1 when the time delays are zero. Thus the Smith predictor eliminates the time delays from the characteristic equation and consequently allows larger controller gains to be used.

For purposes of illustration the following transfer functions will be considered:

$$G_c(s) = K_c \left[1 + \frac{1}{\tau_I s}\right] \qquad G_p(s) = \frac{K}{\tau_p s + 1}$$

$$H(s) = 1 \qquad G_L(s) = \frac{K_L}{\tau_L s + 1}$$

Then the characteristic equation is second order and the closed-loop system in Figure 1 is stable for all positive values of K_c and τ_I. (Note that this is not the case when the Smith predictor is omitted, due to the presence of the time delays in the characteristic equation.)

Equation (1) can be rearranged to give

$$\frac{C(s)}{U(s)} = G_L(s) \left[1 - \frac{G_c(s)G_p(s)H(s)\ e^{-s(T_1 + T_2)}}{1 + G_c(s)G_p(s)H(s)}\right] \qquad (3)$$

Suppose that $G_c(s) \to \infty$, which can be realized by letting $K_c \to \infty$ and/or $\tau_I \to 0$. Then the closed-loop system remains stable and Equation (3) reduces to

$$\frac{C(s)}{U(s)} = G_L(s) - G_L(s)\ e^{-s(T_1 + T_2)} \qquad (4)$$

The inverse Laplace transform of Equation (4), with $c(t) = \mathcal{L}^{-1}[C(s)]$, can be expressed as

$$c(t) = \mathcal{L}^{-1}[G_L(s)U(s)] - \mathcal{L}^{-1}[G_L(s)U(s)\ e^{-s(T_1 + T_2)}] \qquad (5)$$

Equation (5) can be written as

$$c(t) = c_{OL}(t) - c_{OL}(t - T_1 - T_2) \tag{6}$$

where $c_{OL}(t)$ denotes the open-loop response to an arbitrary input, $u(t)$. Figure 2 shows that $c(t)$ attains its steady-state value of zero when $c_{OL}(t - T_1 - T_2)$ reaches its steady-state value, $\bar{c}_{OL}$.

For the situation where $c_{OL}(t)$ is a monotonic function (as shown in Figure 2), an analytical expression for the Integral Absolute Error (IAE) performance criterion can be derived. If only load changes are considered, then

$$IAE = \int_0^\infty |c(t)|dt = \int_0^\infty |c_{OL}(t) - c_{OL}(t - T_1 - T_2)|dt \tag{7}$$

Since $c_{OL}(t)$ is assumed to be a monotonic function, this integral can be evaluated by integrating with respect to c rather than t. This is especially convenient since Figure 2 illustrates that the horizontal distance between $c_{OL}(t)$ and $c_{OL}(t - T_1 - T_2)$ is a constant, $T_1 + T_2$. Thus the integral in Equation (7) can be written as

$$IAE = \int_0^{\bar{c}_{OL}} (T_1 + T_2)dc \tag{8}$$

which reduces to

$$IAE = (T_1 + T_2)\bar{c}_{OL} \tag{9}$$

The expression for the IAE criterion in Equation (9) has been derived for the asymptotic case where $G_c(s) \to \infty$ and the open-loop response is a monotonic function (e.g. response to a step disturbance). However, this expression also provides a lower limit to the IAE value that can be obtained for the more realistic situation where $G_c(s) < \infty$.

A similar analysis can be made for setpoint changes. Here, the closed-loop transfer function is

$$\frac{C(s)}{R(s)} = \frac{G_c(s)G_p(s)\ e^{-sT_1}}{1 + G_c(s)G_p(s)H(s)} \tag{10}$$

Letting $G_c(s) \to \infty$ gives

$$\frac{C(s)}{R(s)} = e^{-sT_1} \tag{11}$$

Taking the inverse Laplace transform of Equation (11) with $r(t) = \mathcal{L}^{-1}[R(s)]$ gives

$$c(t) = r(t - T_1) \tag{12}$$

The corresponding IAE expression is

$$IAE = \int_0^\infty |r(t) - r(t - T_1)|dt \tag{13}$$

If r(t) is a monotonic function, then Equation (13) reduces to

$$IAE = T_1\bar{r} \tag{14}$$

where $\bar{r}$ is the new steady state value of the setpoint. The expression in Equation (14) provides a lower limit to the IAE value that can be obtained using the Smith predictor when $G_c(s) < \infty$.

3. SIMULATION RESULTS

To illustrate the effect of system parameters on the relative performance of the Smith predictor and a conventional PI controller, the system shown in Figure 1 was simulated using the IBM CSMP/1130 simulation program (17). For convenience, the total time delay of the system will be denoted by $T = T_1 + T_2$. Representative simulation results are shown in Table 1 for a unit step change in the load disturbance with the control behaviour characterized in terms of the ratio IAE/IAE_{min}. The IAE_{min} value denotes the theoretical minimum value of Equation (9), that is, $IAE_{min} = (T_1 + T_2)\,\bar{c}_{OL}$.

The values in parentheses are for controller constants $K_c = 20$ and $\tau_I = 1/3$, while the other values are for $K_c = 10$ and $\tau_I = 1/3$. Clearly, even with only moderately high values of K_c and τ_I the performance of the Smith predictor comes close to the best that can be expected theoretically, with the exception of the case $\tau_L/\tau_p = 0$ (no load transfer function) and $T/\tau_p = 0.1$ (relatively small time delay). However, even for these conditions using $K_c = 100$ and $\tau_I = 1/3$ reduces the value of IAE/IAE_{min} to 1.13. The numerical values given in Table 1 were obtained with $\tau_p = 10$. However, other values of τ_p gave essentially the same IAE/IAE_{min} values provided that T/τ_p and τ_L/τ_p were held constant.

The effect of the magnitude of the load time constant on the control behavior is significant as can be seen from the simulation results given in Figure 3 for a step change in the load disturbance. Clearly, as the ratio of the load time constant to the process time constant increases, there is a deterioration in control behavior. It should be noted that these results are for arbitrary controller parameters $K_c = 20$, $\tau_I = 1/3$ and that values of IAE/IAE_{min} closer to one could probably be obtained by

controller tuning. Since the Smith predictor performance does not deterioriate markedly when only moderately high values of K_c and $1/\tau_I$ are employed, similar results can be expected for other systems where $G_p(s)$ is not first order.

In order to assess if there is an advantage in using the Smith predictor, the same process and a conventional PI controller were simulated. The PI controller settings were tuned to yield the lowest IAE value after a unit step change in load (cf. Table 2).[9] Note that the numerical values given in Table 2 are IAE values normalized by dividing by IAE_{min}, the theoretical minimum for the Smith predictor when $G_c(s) \rightarrow \infty$. Consequently, when the value is less than one, the conventional PI controller is superior to the Smith predictor while a value greater than one implies that the Smith predictor yields a better control behavior. As can be observed from Table 2, conventional PI control is preferred for small time delays and relatively slow load dynamics (i.e. large values of τ_L/τ_p).

Closed-loop responses for the Smith predictor and conventional PI control are shown in Figure 4. These results were obtained using controller settings that minimized the IAE value for a unit step change in the load disturbance. For small values of T/τ_p, there is little advantage in utilizing the Smith predictor. However, when $T/\tau_p = 1.0$ the Smith predictor is better as indicated by the shorter response times in Figure 4 and lower IAE values.

The superiority of the Smith predictor over conventional control for setpoint changes is illustrated in Figure 5. It can be seen that the Smith predictor results in a much shorter response time and a lower IAE value in comparison with conventional PI control. This same conclusion is also apparent

from the asymptotic analysis in Equations (11) - (14). After a step change in setpoint, the closed-loop response attains the new setpoint in a period of time equal to the time delay, T_1, and results in an IAE value of $T_1\bar{r}$ (cf. Equation (14)). Clearly, this rapid response and small IAE value cannot be achieved with conventional PI control because a finite controller gain must be used to ensure closed-loop stability.

Note that the IAE/IAE_{min} value for a setpoint change is identical to the value for a load disturbance if $\tau_L/\tau_p = 0$ and there is no time delay in the feedback path. This relationship can be appreciated from analyzing the block diagram in Figure 1.

5. CONCLUSIONS

The simulation results have clearly demonstrated that for a system containing a time delay, use of a Smith predictor will not always give rise to improved control performance. For a process consisting of a first order system plus time delay, improved control behaviour can always be achieved for setpoint changes, but if the disturbance to this system is a load upset then there may not be any advantage in employing a Smith predictor. The predictor is effective provided that the ratio T/τ_p is large while τ_L/τ_p is small, implying its success for systems with large time delays and negligible load transfer function dynamics. Although the conclusions concerning the effectiveness of the Smith predictor are based on the analysis of a relatively simple process, the same general conclusions are also expected for higher order systems. That is, improved regulatory control behaviour can result by employing a Smith predictor provided there is a significant time delay and the load transfer function dynamics are relatively fast.

NOTATION

C = Output variable

E = Error

G_c = Controller transfer function

G_L = Load transfer function

G_p = Process transfer function

H = Measurement transfer function

IAE = Integral Absolute Error

K = Process gain

K_c = Controller gain

K_L = Load gain

PI = Proportional plus integral

R = Setpoint

s = Laplace operator

t = Time

T_1, T_2 = Time delays

T = $T_1 + T_2$

U = Load disturbance

Greek

θ = t/τ_p

τ_I = Integral time

τ_L = Load time constant

τ_p = Process time constant

Subscripts and Superscripts

OL = Open loop

min = Minimum

$-$ = Steady state

REFERENCES

(1) SMITH O.J.M., Chem. Eng. Progr. 1957, 53, 217.

(2) SMITH O.J.M., ISA Journal, 1959, 6, 28.

(3) LUPFER D.E. and OGLESBY M.W., ISA Trans. 1962, 1, 72.

(4) SMITH C.A. and GROVES F.R., Proc. 28th Ann. ISA Conf., Houston, 1973.

(5) DOSS J.E. and MOORE C.F., 74th Nat. AIChE Mtg., New Orleans, March, 1973.

(6) CHANDRA PRASAD C. and KRISHNASWAMY P.R., Chem. Eng. Sci., 1975, 30, 207.

(7) BUCKLEY P.S., Proc. 1st. IFAC Congress, Moscow, 1960.

(8) GARLAND B. and MARSHALL J.E., Electron. Lett., 1974, 10, 308.

(9) MARSHALL J.E., Int. J. Control, 1974, 19, 933.

(10) EISENBERG L., ISA Trans., 1967, 6, 329.

(11) GRAY J.O. and HUNT P.W.B., Electron. Lett., 1971, 7, 131.

(12) GRAY J.O. and HUNT P.W.B.,'Electron. Lett., 1971, 7, 335.

(13) MEE D.H., Int. J. Control, 1973, 18, 1151.

(14) ALEVISAKIS G. and SEBORG D.E., Int. J. Control, 1973, 17, 541.

(15) ALEVISAKIS G. and SEBORG D.E., Chem. Eng. Sci., 1974, 29, 373.

(16) NIELSEN G., Proc. 4th IFAC Congress, Warsaw, 1969.

(17) IBM, 1130-CX-13X, 1130 Continuous Systems Modeling Program, Program Reference Manual.

Table 1 : Effect of Time Delay and Load Time Constant on the IAE/IAE_{min} Value for the Smith Predictor.

T/τ_p \ τ_L/τ_p	0.0	0.5	1.0	2.0
0.1	2.13	1.03	1.03	1.02
	(1.61)	(1.02)	(1.01)	(1.00)
1.0	1.11	1.00	1.00	1.00
	(1.06)	(1.00)	(1.00)	(1.00)

Table 2 : Values of IAE/IAE_{min} Using Conventional Control.

T/τ_p \ τ_L/τ_p	0.0	0.5	1.0	2.0
0.1	2.9	0.76	0.42	0.32
1.0	1.92	1.79	1.55	1.18

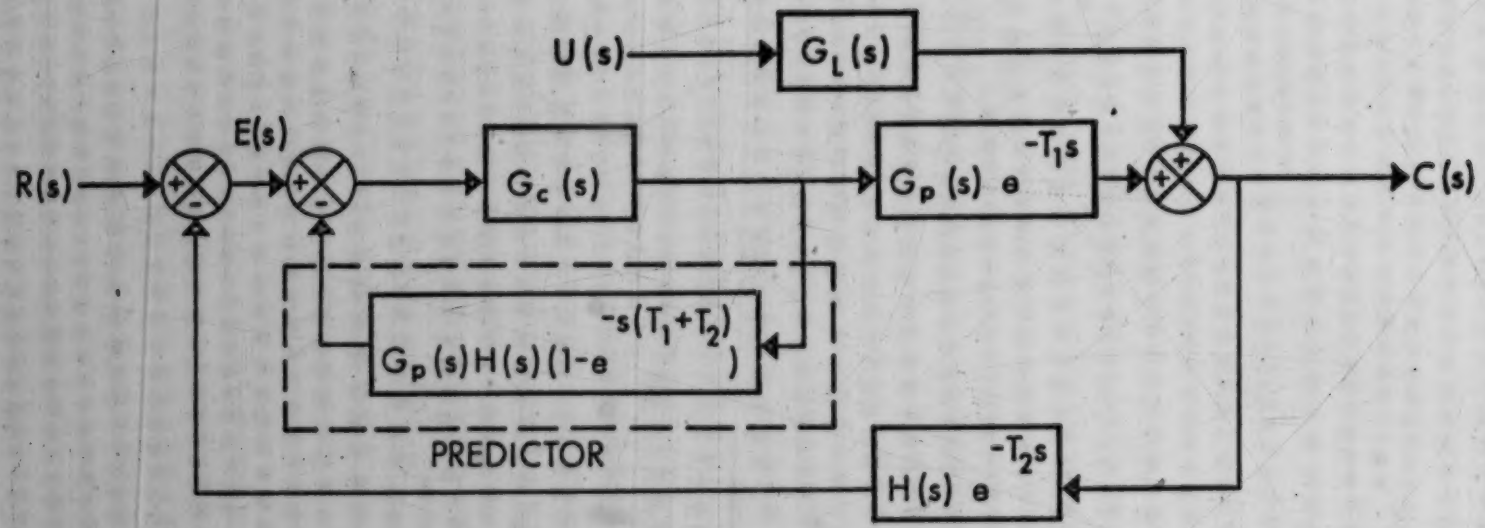

Figure 1. Block diagram of a Smith predictor control scheme.

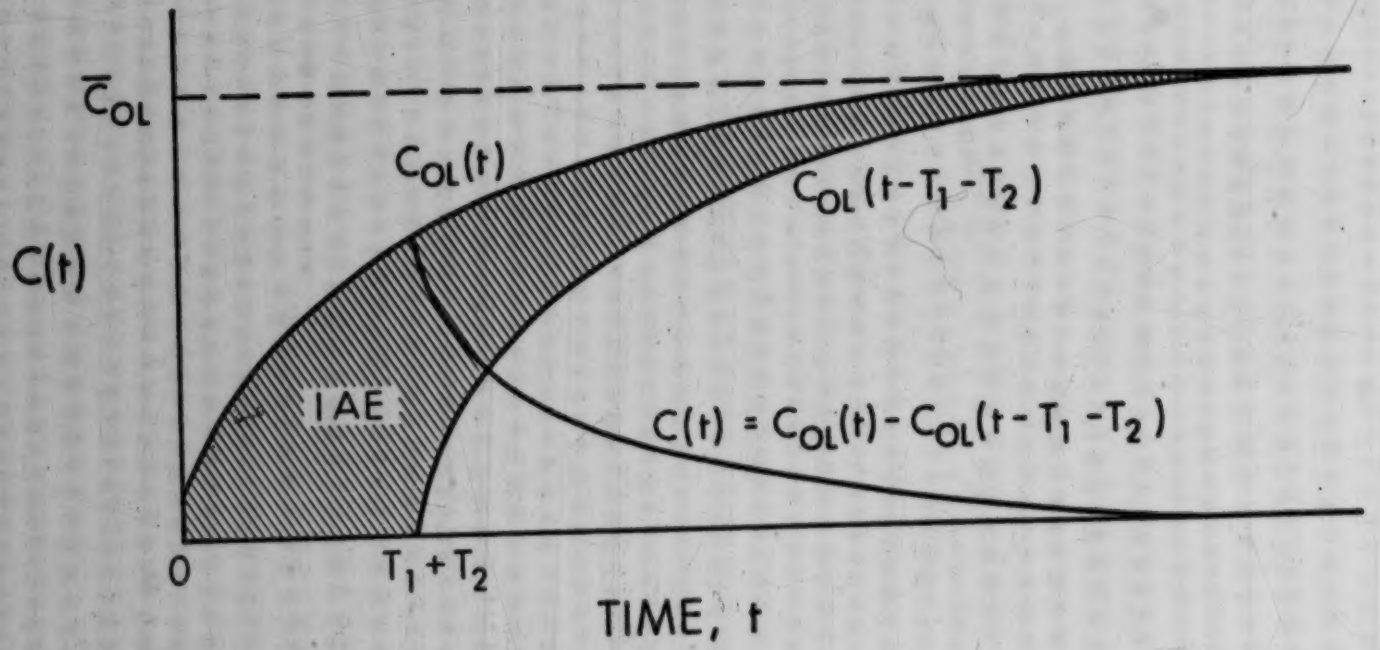

Figure 2. Closed-loop response, c(t), for the ideal case where $G_c(s) \to \infty$.

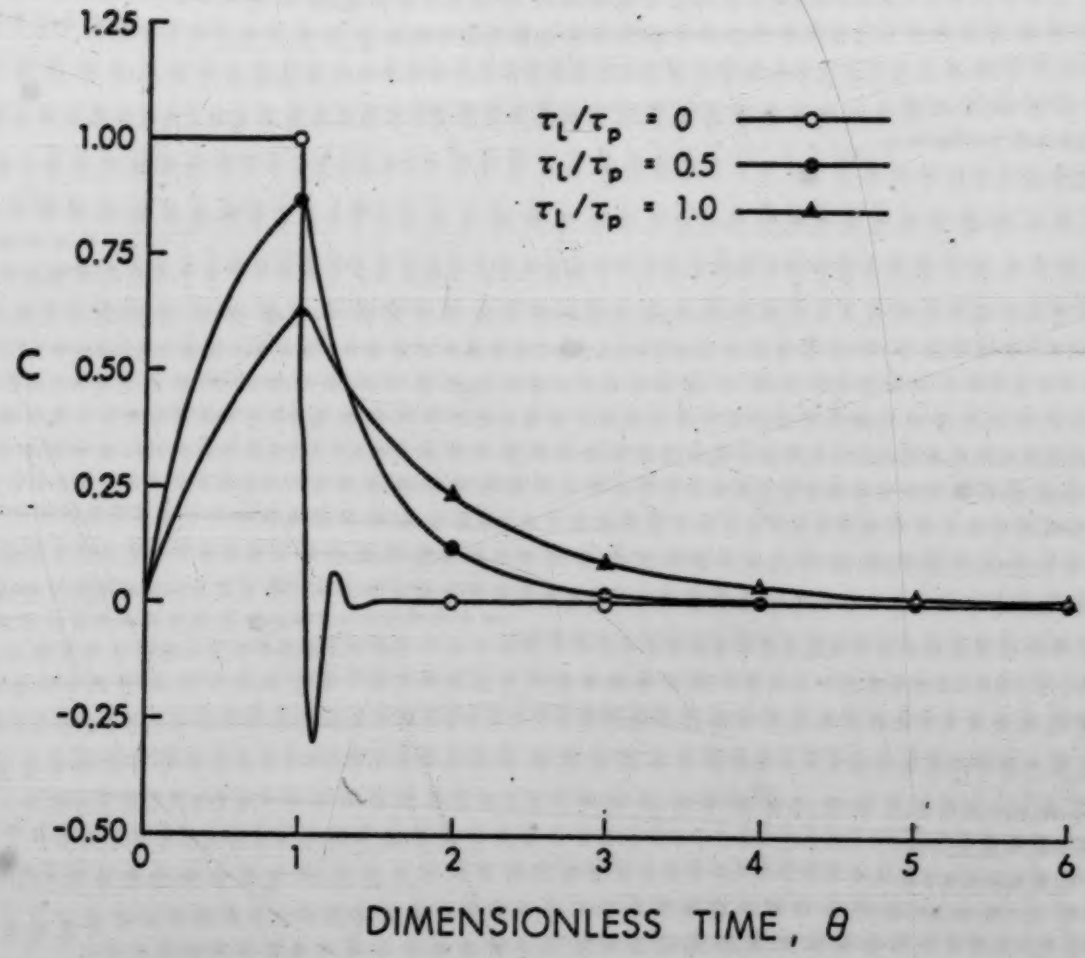

Figure 3. Effect of load time constant on the closed-loop response of the Smith predictor control system for a step change in load disturbance.

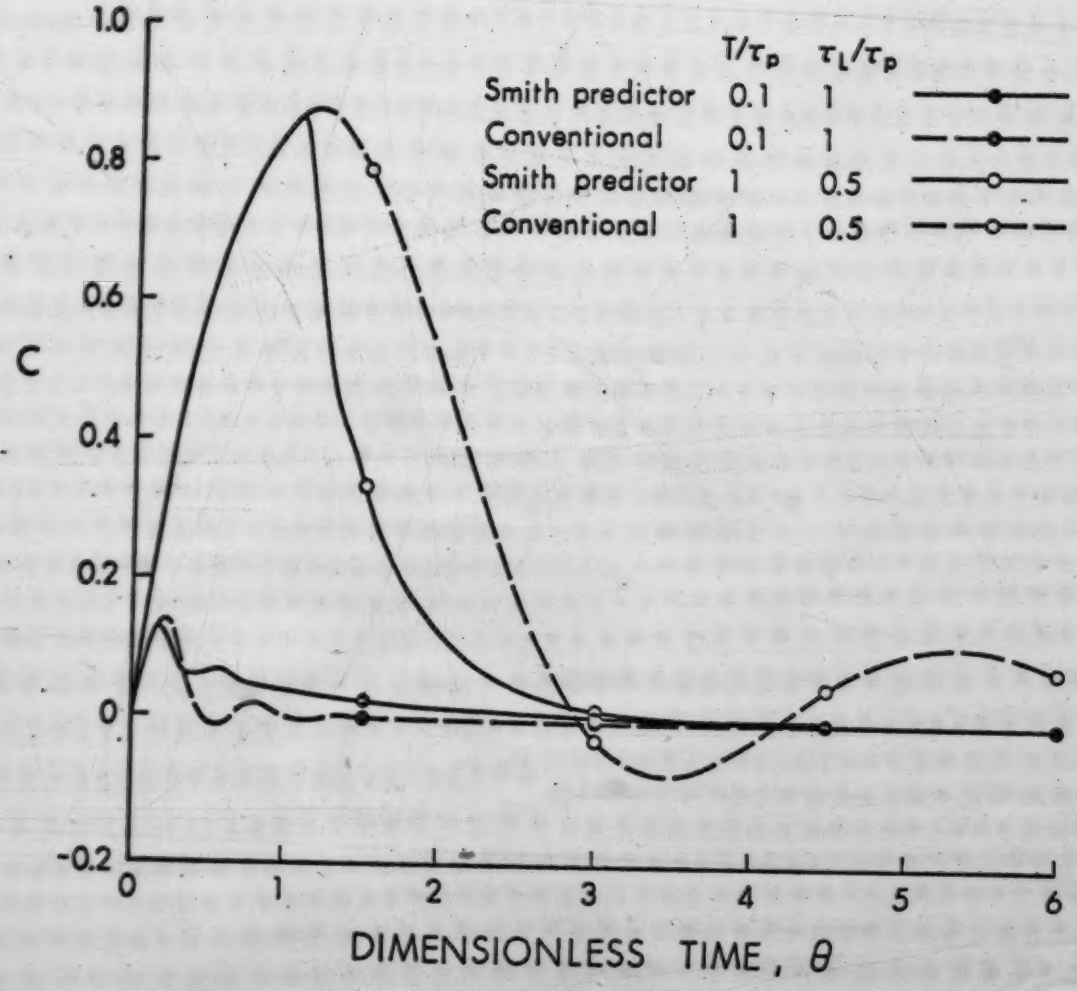

Figure 4. A comparison of the Smith predictor and a conventional PI controller for a unit step change in load disturbance.

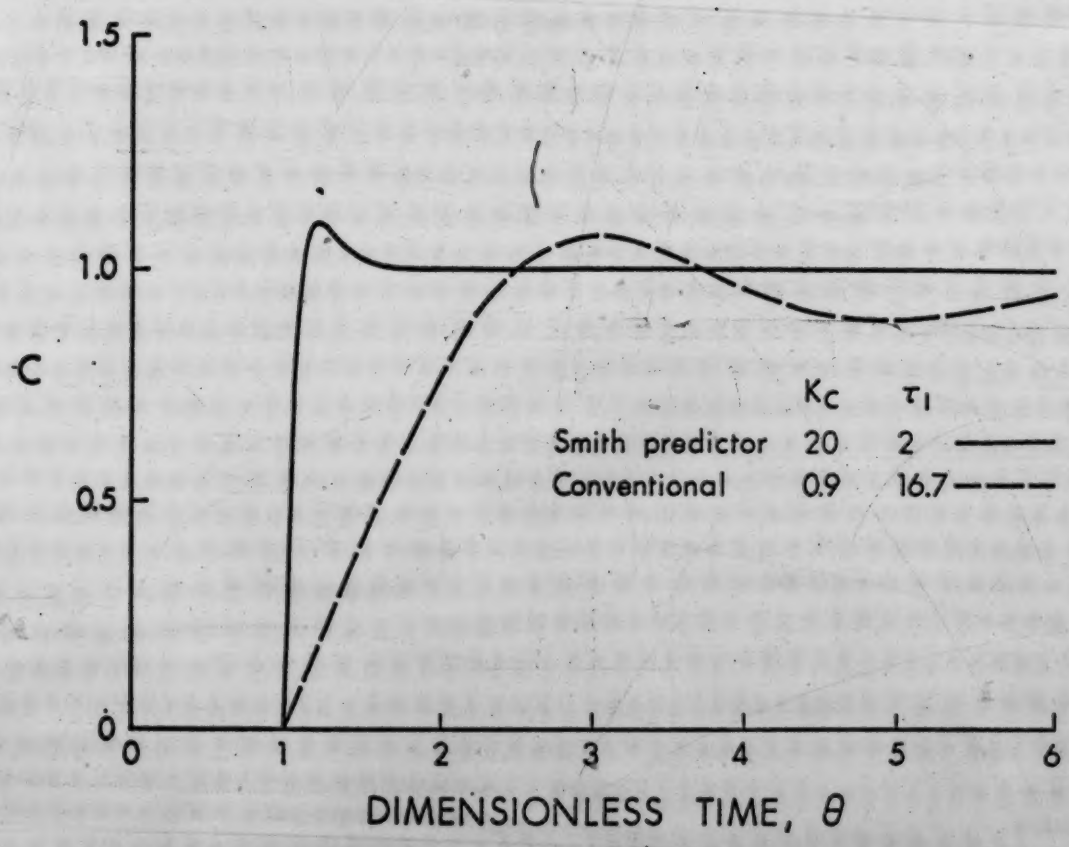

Figure 5. A comparison of the Smith predictor and a conventional PI controller for a unit step change in setpoint.

APPENDIX B

DERIVATION OF THE PROPORTIONAL-INTEGRAL ANALYTICAL PREDICTOR CONTROL ALGORITHM

This Appendix contains a derivation of the proportional-integral form of the AP control algorithm developed by Moore (30). The control law for this algorithm is given by:

$$u_k + d = K_c\,(p_k - \hat{c}_{k+\theta}) \tag{B.1}$$

where d is a constant, unmeasured disturbance affecting the process in the same way as a control action as shown in Fig. 3.5. p_k is the calibrated setpoint:

$$p_k = \frac{K_c K_p + 1}{K_c K_p}\, r_k \tag{B.2}$$

An expression for the predicted future output $\hat{c}_{k+\theta}$ can be obtained from the differential equation of the process. For a first order plus time delay model, the solution for one sampling period is:

$$\hat{c}_{k+1} = B\,c_k + BK_p\left(\frac{1}{C} - 1\right)(u_{k-N-1}+d) + K_p\left(1 - \frac{B}{C}\right)(u_{k-N}+d) \tag{B.3}$$

Using Eqn. (B.3) recursively gives:

$$\hat{c}_{k+2} = B\hat{c}_{k+1} + BK_p\left(\frac{1}{C} - 1\right)(u_{k-N}+d) + K_p\left(1 - \frac{B}{C}\right)(u_{k-N+1}+d)$$

$$\vdots$$

$$\hat{c}_{k+N} = B^N c_k + BK_p\left(\frac{1}{C} - 1\right)\sum_{i=1}^{N} B^{i-1}\,(u_{k-i-1}+d)$$

$$+ K_p\left(1 - \frac{B}{C}\right)\sum_{i=1}^{N} B^{i-1}\,(u_{k-i}+d) \tag{B.4}$$

Prediction over the fractional time delay βT_s yields:

$$\hat{c}_{k+N+\beta} = C\hat{c}_{k+N} + K_p\,(1-C)\,(u_{k-1}+d) \tag{B.5}$$

Substituting Eqn. (B.4) into Eqn. (B.5) and rearranging gives:

$$\hat{c}_{k+N+\beta} = CB^N c_k + B^N K_p\,(1-C)\,(u_{k-N-1}+d) + K_p\,(1-B)\sum_{i=1}^{N} B^{i-1}\,(u_{k-i}+d) \tag{B.6}$$

For prediction one half sampling time ahead it follows that

$$\hat{c}_{k+\theta} = A\hat{c}_{k+N+\beta} + K_p\,(1-A)\,(u_k+d) \tag{B.7}$$

Combining Eqns. (B.1) and (B.7) gives:

$$u_k = \frac{K_c}{1+K_cK_p(1-A)}\,(p_k - A\,\hat{c}_{k+N+\beta}) - d \tag{B.8}$$

An estimate of the disturbance d can be obtained by comparing the process output c_k with the predicted output $\hat{c}_k$:

$$\hat{d}_k = \hat{d}_{k-1} + K_I T_s\,(c_k - \hat{c}_k) \tag{B.9}$$

where $\hat{d}_k$ is the estimate of d at time kT_s, and K_I is a tuning parameter. $\hat{c}_k$ in Eqn. (B.9) is obtained analogous to Eqn. (B.3), with d replaced by $\hat{d}_{k-1}$, the estimate at time $(k-1)\,T_s$:

$$\hat{c}_k = \hat{c}_{k-1} + BK_p \left(\frac{1}{C} - 1\right)(u_{k-N-2} + \hat{d}_{k-1}) + K_p \left(1 - \frac{B}{C}\right)(u_{k-N-1} + \hat{d}_{k-1}) \qquad \text{(B.10)}$$

Eqns. (B.6) and B.8), with the disturbance d replaced by the current estimate $\hat{d}_k$, together with Eqns. (B.9) and (B.10) provide the algorithm for the proportional-integral AP given in Table 3-5.

APPENDIX C

DERIVATION OF THE STEADY STATE CLOSED-LOOP GAIN OF THE PROPORTIONAL ANALYTICAL PREDICTOR CONTROL SCHEME

In order to eliminate offset after setpoint changes with proportional control action only the AP control algorithm uses setpoint calibration. Moore (30) notes that the calibration factor $(K_cK_p+1)/K_cK_p$ results in a closed-loop gain of the proportional AP control scheme equal to unity and consequently no offset occurs after step changes in setpoint. That this is the case is not obvious, so it will be demonstrated in this Appendix.

From the algorithm in Table 3-4, the expression for the calibrated setpoint is:

$$p_k = \frac{K_cK_p + 1}{K_cK_p} r_k \tag{C.1}$$

and the control action is given by:

$$u_k = \frac{K_c}{1+K_cK_p(1 - A)}(p_k - A\hat{c}_{k+N+\beta}) \tag{C.2}$$

At steady state, the control action is constant and $u_k = u_{k-1} = \ldots = u_{k-N} = u_{k-N-1}$. Consequently the equation for the predicted future output $\hat{c}_{k+N+\beta}$ can be simplified to give:

$$\hat{c}_{k+N+\beta} = CB^N c_k + u_k \left(B^N K_p(1-C) + K_p(1-B) \sum_{i=1}^{N} B^{i-1} \right) \tag{C.3}$$

The process output at steady state is given by:

$$c_k = K_p u_k \tag{C.4}$$

From Eqns. (C.3) and (C.4) it follows that

$$\begin{aligned}\frac{\hat{c}_{k+N+s}}{c_k} &= CB^N + \frac{1}{K_p}\left(B^N K_p(1-C) + K_p(1-B)\sum_{i=1}^{N} B^{i-1} \right) \\ &= CB^N + B^N - B^N C + \sum_{i=1}^{N} B^{i-1} - \sum_{i=1}^{N} B^i \\ &= B^N + (1-B) + (B-B^2) + (B^2-B^3) + \ldots + (B^{N-1}-B^N) \\ &= 1 \end{aligned} \tag{C.5}$$

Combining Eqns. (C.2), (C.4) and (C.5) gives, after rearranging:

$$\begin{aligned} c_k &= \frac{\dfrac{K_c}{1 + K_c K_p (1-A)} K_p p_k}{1 + \dfrac{K_c}{1 + K_c K_p (1-A)} K_p A} \\ &= \frac{K_c K_p p_k}{1 + K_c K_p (1-A) + K_c K_p A} \\ &= \frac{K_c K_p}{1 + K_c K_p} p_k \end{aligned} \tag{C.6}$$

Eqn. (C.6) provides an expression for the closed-loop gain of the proportional AP control scheme. From Eqns. (C.1) and (C.6) it follows that

$$\frac{\bar{c}_k}{r_k} = 1 \qquad (C.7)$$

which is the result noted by Moore (30).

APPENDIX D

DIGITAL SIMULATION PROGRAMS

Appendix D shows listings for 3 CSMP simulation runs using SP, AP and PI control. To simulate different runs only the PARAMETER statements and the statements specifying the disturbance in the DYNAMIC section of the programs had to be changed. The 3 examples shown are the programs used to simulate arbitrary step changes in feed flow, runs SP-16, AP-15 and PI-7. For more details on the simulation package the reader is referred to the IBM 360 CSMP manual *.

* IBM, 360A-CX-16X, "Continuous Systems Modelling Program", Program Reference Manual.

```
TITLE     DISCRETE DATA CONTROL SYSTEM
*
*         SP CONTROL
*
INITIAL
      KTD=TD/TS
      BETA=TD/TS-KTD
DYNAMIC
          U=ZHOLD(X1,X2)
          C1=REALPL(IC,TAUP,U)
          C2=C1*KP
          L6=STEP(T0)
          L2=STEP(1000.)
         L3=STEP(1500.)
         L4=STEP(2500.)
         L5=STEP(3000.)
         LO=L6-L2-L3+2*L4-L5
         LOAD=LO*3.8
          C3=DELAY(13,TD,C2)
           L=KL*L1
           L1=REALPL(IC,TAUL,LOAD)
           C=C3+L
           X1=IMPULS(0.,TS)
HISTRY SMITH(100)
  X2=SMITH(R,C,CM1,CM2,NC,TS,ALPHA,KTD,TAUM,GM,SUM,KC,TI,BETA,X1)
          ABSC=ABS(R-C)
          IAE=INTGRL(0,ABSC)
PARAMETER  TAUP=1080. , KP=1.47 , TD=52.
PARAMETER  TAUM=1080. , GM=1.47
PARAMETER  KC=11.6 , TI=230. , TS=60.
PARAMETER  T0=0. , ALPHA=0. , R=0.
PARAMETER  TAUL=1620. , KL=0.65
*
INCON      SUM=0. , IC=0. , NC=0
INCON       CM1=0. , U=0. , X2=0. , CM2=0.
FIXED NC,KTD
TIMER      DELT=4. , FINTIM=4000. , OUTDEL=8. , PRDEL=400.
*
PREPARE   U,C,LO
PRINT   U,C,L,IAE,CM1,CM2,SUM,X1
*
LABEL      SP CONTROL
*
METHOD     RECT
*
END
STOP
      FUNCTION SMITH(K,P,CX,CM1,CM2,NC,TS,ALPHA,KTD,TAUM,GM,SUM,KC,
     & TI,BETA,X1)
COMMON MEM
      REAL KC
      EQUIVALENCE (C(1),TIME)
      IF(X1.GT.0.)GOTO 3
      RETURN
```

```
      3 CONTINUE
        I=K+KPT1
C     J = INDEX OF U KTD+1 SAMPLING TIMES BACK
C     NC = CURRENT STORAGE LOCATION OF U
        IF(TIME.GT.0.)GOTO 31
        DO 32 KK=1, 100
     32 SYMB(I+KK-1)=0.
        U=0.
        DOLD=0.
        SMITH=0.
        RETURN
     31 CONTINUE
        J=NC-KTD-1
        IF(J.LT.0)J=100+J
        JJ=J-1
        IF(JJ.LT.0)JJ=100+JJ
        UPAST=SYMB(I+J)
        U2PAST=SYMB(I+JJ)
C     PREDICTOR
        B=EXP(-TS/TAUM)
        CE=EXP(-BETA*TS/TAUM)
        CM2=CM2*B+R*GM*(1./CE-1.)*U2PAST+GM*(1.-B/CE)*UPAST
C     MODEL
        CM1=CM1*B+GM*(1.-E)*U
C     LOADPREDICTOR
        D=CM2-CX
        P=D+ALPHA*TS*(KTD+BETA)*(D-DOLD)
        DOLD=D
C     CONTROL
        E=R-CM1+P
        SUM=SUM+E
        U=KC*(E+TS/TI*SUM)
        UH=15.
        UL=-15.
        IF(U.GT.UH)U=UH
        IF(U.LT.UL)U=UL
C     STORES NEW U
        SYMB(I+NC)=U
        NC=NC+1
        IF(NC.EQ.100)NC=0
        SMITH=U
        RETURN
        END
ENDJOB
```

```
TITLE    DISCRETE DATA CONTROL SYSTEM
*
*     AP CONTROL
INITIAL
     KTD=TD/TS
    BETA=TD/TS-KTD
DYNAMIC
          U=ZHOLD(X1,X2)
          C1=REALPL(IC,TAUP,U)
          C2=C1*KP
          L2=STEP(0.)
         L3=STEP(1000.)
        L4=STEP(1500.)
         L5=STEP(2500.)
         L6=STEP(3000.)
        LO=L2-L3-L4+2*L5-L6
         LOAD=LO*3.8
          C3=DELAY(13,52.,C2)
           L=KL*L1
           L1=REALPL(IC,TAUL,LOAD)
           C=C3+L
           X1=IMPULS(0.,TS)
HISTRY ANPRE(100)
       X2=ANPRE(R,C,CM,CP,CXO,NC,SUM,TS,TD,KTD,TAUM,GM,DK,KC,KI,BETA,X1)
          ABSC=ABS(R-C)
          IAE=INTGRL(0,ABSC)
PARAMETER  TAUP=1080. , KP=1.47 , TD=52.
PARAMETER  TAUM=1080. , GM=1.47
PARAMETER  KC=24.15 , KI=0.21 , TS=60.
PARAMETER  T0=0. , R=0.
PARAMETER  TAUL=1620. , KL=0.65
*
INCON       IT=0 , IC=0. , NC=0
INCON       CM=0. , CXO=0. , CP=0. , DK=0.
FIXED NC,KTD,IT
TIMER      DELT=4. , FINTIM=4000. , OUTDEL=8. , PRDEL=400.
*
PREPARE   U,C,LOAD
*
LABEL  AP-CONTROL
PRINT   U,C,L,IAE,CM,CP,DK,SUM
*
METHOD     RECT
*
END
STOP
     FUNCTION ANPRE(K,R,CX,CM,CP,CXO,NC,SUM,TS,TD,KTD,TAUM,GM,DK,KC,KI,
    & BETA,X1)
COMMON MEM
      INTEGER IT
      REAL KC,KI,LOWL
      EQUIVALENCE (C(1),TIME)
      IF(X1.GT.0.)GOTO 3
      RETURN
```

```
      3 CONTINUE
        UPL=32.
        LOWL=-32.
        I=K+KPT1
C  J = INDEX OF U KTD+1 SAMPLING TIMES BACK
C  NC = CURRENT STORAGE LOCATION OF U
C  SYMB = STORAGE FOR PAST U VALUES
        J=NC-KTD-1
        IF(J.LT.0)J=100+J
        JI=J-1
        IF(JI.LT.0)JI=100+JI
C  INITIALIZES
        IF(TIME.GT.0.)GOTO 12
        DO 14 M=1,100
     14 SYMB(I+M-1)=0.
        U=0.
        ANPRE=0.
        RETURN
     12 CONTINUE
        B=EXP(-TS/TAUM)
        CE=EXP(-TS*BETA/TAUM)
        A=EXP(-TS/(2.*TAUM))
C  PREDICTOR
        CM=B*CXO+GM*(1-B/CE)*(SYMB(I+J)+DK)+GM*B/CE*(1-CE)
       & *(SYMB(I+JI)+DK)
        CXO=CX
C  INTEGRAL TERM
        DK=DK+KI*TS*(CX-CM)
C  PREDICTED OUTPUT
        IF(KTD.EQ.0)GOTO 6
        SUM=0.
        DO 7 L=1,KTD
        NP=NC-L
        IF(NP.LT.0)NP=100+NP
      7 SUM=SUM+B**(L-1)*(SYMB(I+NP)+DK)
        CP=CX*CE*B**KTD+GM*(1-B)*SUM+GM*(1-CE)*B**KTD
       & *(SYMB(I+J)+DK)
        GOTO 8
C  FOR FRACTIONAL DEADTIME
      6 CP=CX*CE+GM*(1-CE)*(U+DK)
C  CONTROL
      8 PK=R*(1+1/(KC*GM))
        U=KC/(1+KC*GM*(1-A))*(PK-A*CP)-DK
        IF(U.GT.UPL)U=UPL
        IF(U.LT.LOWL)U=LOWL
C  STORES NEW U
        SYMB(I+NC)=U
        NC=NC+1
        IF(NC.EQ.100)NC=0
        ANPRE=U
        RETURN
        END
ENDJOB
```

```
TITLE     DISCRETE DATA CONTROL LOOP
*
*         PI CONTROL
*
DYNAMIC
          U=ZHOLD(X1,X2)
          C1=REALPL(IC,TAUP,U)
          C2=C1*KP
          R1=STEP(0.0)
          R2=STEP(1000.)
         R3=STEP(1500.)
         R4=STEP(2500.)
        R5=STEP(3000.)
       LO=R1-R2-R3+2*R4-R5
         LOAD=LO*3.8
          C3=DELAY(13,TD,C2)
           L=KL*L1
           L1=REALPL(IC,TAUL,LOAD)
           C=C3+L
          X1=IMPULS(0.0,TS)
           ABSC=ABS(R-C)
           IAE=INTGRL(0,ABSC)
*
PROCEDURE    X2,OUTSUM = BLO(TIME,X1,C,KC,TI,R,SUM,TS,IT)
      IF(TIME.EQ.0.0)GOTO 5
      IF(X1.GT.0.)GOTO 4
      GOTO 5
  4   CONTINUE
* PI  CONTROL
      ERR=R-C
      SUM=SUM+ERR
      OUTSUM=SUM
      X2=KC*(ERR+TS/TI*SUM)
   5  CONTINUE
ENDPRC
*
INCON   IC=0. , U=0.0 , SUM=0.
PARAMETER  TAUP=1080. , KP=1.47 , TD=52.
PARAMETER  KC=6.31 , TI=355. , TS=60.
PARAMETER  TC=0. , R=0.
PARAMETER  TAUL=1620. , KL=0.65
FIXED IT
*
TIMER      DELT=4. , FINTIM=4000. , OUTDEL=8. , PRDEL=400.
*
PREPARE   U,C,LO
PRINT IAE,C
*
LABEL      PI CONTROL
*
METHOD     RECT
*
END
STOP
ENDJOB
```

APPENDIX E

IMPLEMENTATION AND LOOP RECORDS

Appendix E describes the implementation of the control schemes and the data acquisition used in this study. The SP, AP and PI control algorithms were implemented in the supervisory control mode. The DDC software was used to obtain the measurements from the process and send the control action to the process as shown in Fig. E-1. Note that the sampling time for the DDC flow control loops is 1 to 4 seconds (1 s for the feed and steam and 4 s for the reflux flow loop) and thus much shorter than the sampling time of the control program (1 minute for top composition control, 4 minutes for bottom composition control). The distillation column was monitored and the feed flow (loop 0601), reflux flow (loop 0602) and steam flow (loop 0603) controlled using the IBM 1800 DDC package. Loops 0601 to 0635 are the pertinent measurement and data acquisition records. A diagram showing the measured variables and the associated loops can be found in the thesis of Liesch (18).

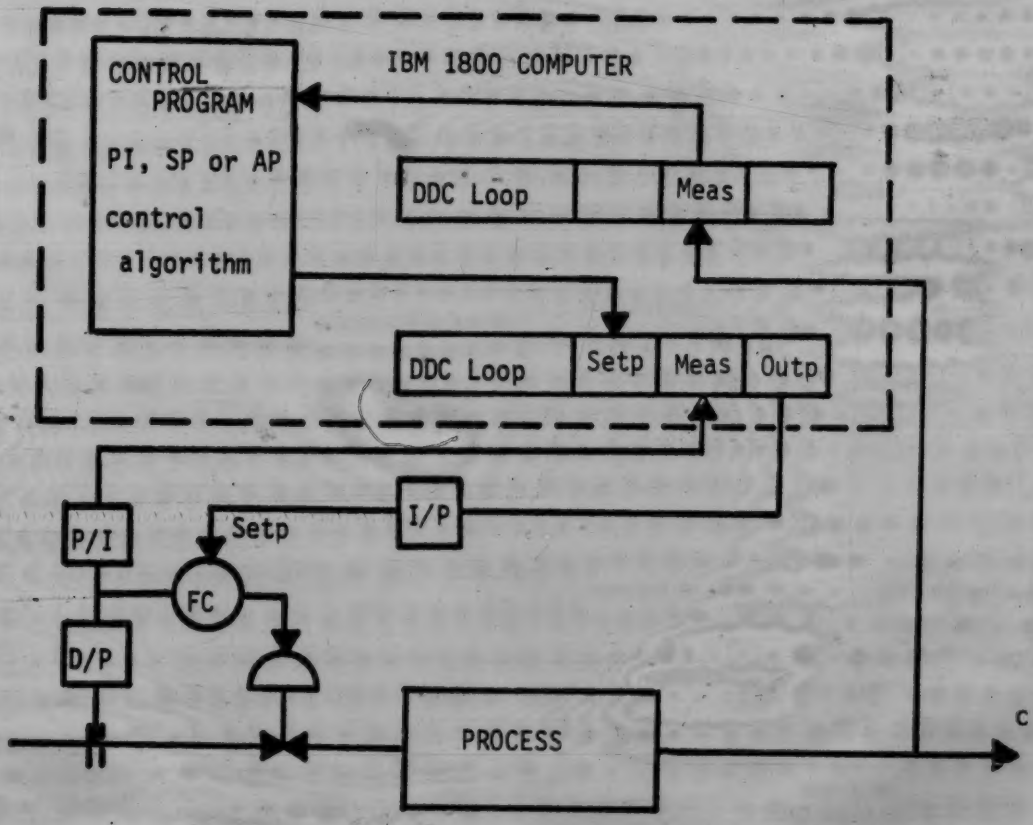

Symbols:

D/P : Differential pressure cell

P/I : Pressure to current converter

I/P : Current to pressure converter

FC : Analog flow controller

Setp: Setpoint

Meas: Measurement

Outp: Output

Fig. E-1 : Implementation of the Control Schemes.

LOOP RECORD 0601

```
0601  E218  005C  1006  3800  9E40  14A0  0000  5728  5745
7FFF  7FFF  2000  7FFF  0000  2000  7FFF  0000  2000  106A
3801  C080  0000  37E8  0080  0066  FF8E
```

LOOP RECORD 0602

```
0602  E218  205C  1005  1800  9E40  188C  FE95  435C  432C
7FFF  7FFF  0000  7FFF  0000  0029  7FFF  0000  2110  116A
2148  C380  0000  214A  1000  0800  FFFC
```

LOOP RECORD 0603

```
0603  F218  005C  1004  3800  9E40  1050  FDF3  478D  4796
7FFF  7FFF  2000  7FFF  0FA4  2000  7FFF  0000  2000  126A
2628  C080  0000  2624  0B00  0066  FFC1
```

LOOP RECORD 0604

```
0604  E218  204F  100A  0000  9100  0850  2422  28DF  3138
7FFF  7FFF  2550  35E8  0000  0000  7FFF  0000  0000  0602
550B  2020  0000  5385  1F40  001F  FFDB
```

LOOP RECORD 0605

```
0605  E218  005E  1007  3340  9E40  0C54  000E  5ABC  3C7F
7FFF  7FFF  2000  7FFF  0000  2000  7FFF  0000  0000  0000
0000  0000  0000  0000  0000  0000  0000
```

LOOP RECORD 0606

```
0606  E010  205F  1008  1000  9EC0  0E50  0000  2849  0000
7FFF  7FFF  2110  7FFF  0000  2110
```

LOOP RECORD 0607

```
0607  A010  507F  0608  3800  9180  4E20  0000  0799  01FB
7FFF  7FFF  2110  7FFF  0000  2110
```

LOOP RECORD 0608

```
0608  8010  C00F  0000  0000  9180  4E20  0000  0704  01FB
7FFF  7FFF  2110  7FFF  0000  2110
```

LOOP RECORD 0609

```
0609  A010  707F  0629  3000  91A0  4E20  0000  FEB9  4666
7FFF  0000  8000  0000  0000  800C
```

LOOP RECORD 0610

```
0610  F010  0000  F091  3800  A280  2868  FF4E  3005  0000
7FFF  7FFF  2110  7FFF  0000  2110
```

LOOP RECORD 0611

```
0611  F010  21BF  F083  3800  A0C0  2B68  FF4E  1726  0000
7FFF  7FFF  2110  7FFF  0000  2110
```

LOOP RECORD 0612

```
0612  F010  21BF  F084  3800  A0C0  2B68  FF4E  15C5  0000
7FFF  7FFF  2110  7FFF  0000  2110
```

LOOP RECORD 0613

```
0613  F010  21BF  F085  3800  A0C0  2B68  FF4E  33D4  0000
7FFF  7FFF  2110  7FFF  0000  2110
```

LOOP RECORD 0614

```
0614  F010  21BF  F086  3800  A0C0  2B68  FF4E  14DC  0000
7FFF  7FFF  2110  7FFF  0000  2110
```

LOOP RECORD 0615

```
0615  F010  21BF  F087  3800  A0C0  2B68  FF4E  1402  0000
7FFF  7FFF  2110  7FFF  0000  2110
```

LOOP RECORD 0616

```
0616  F010  21BF  F088  3800  A0C0  2B68  FF4E  133D  0000
7FFF  7FFF  2110  7FFF  0000  2110
```

LOOP RECORD 0617

```
0617  F010  21BF  F089  3800  A0C0  2B68  FF4E  1338  0000
7FFF  7FFF  2110  7FFF  0000  2110
```

LOOP RECORD 0618

```
0618  F010  21BF  F08A  3800  A0C0  2B68  FF4E  12ED  0000
7FFF  7FFF  2110  7FFF  0000  2110
```

LOOP RECORD 0619

```
0619  F010  21BF  F08B  3800  A0C0  2B68  FF4E  127C  0000
7FFF  7FFF  2110  7FFF  0000  2110
```

LOOP RECORD 0620

```
0620  F010  21BF  F093  3800  A0C0  2B68  FF4E  1242  0000
7FFF  7FFF  2110  7FFF  0000  2110
```

LOOP RECORD 0621

```
0621  F010  21BF  F092  3800  A0C0  2B68  FF4F  1530  0000
7FFF  7FFF  2110  7FFF  0000  2110
```

LOOP RECORD 0622

```
0622  F010  21BF  F095  3800  A0C0  2B68  0000  076C  0000
7FFF  7FFF  2110  7FFF  0000  2110
```

LOOP RECORD 0623

```
0623  F010  21BF  F096  3800  A0C0  2B68  FF4E  0C7C  0000
7FFF  7FFF  2110  7FFF  0000  2110
```

LOOP RECORD 0624

```
0624  E010  200F  2097  0000  A100  F2F0  02D0  0006  0000
0000  7FFF  3000  7FFF  0000  3000
```

LOOP RECORD 0625

```
0625  E010  200F  100D  0000  9940  350C  E512  5472  0000
7FFF  7FFF  3000  7FFF  0000  3000
```

LOOP RECORD 0626

```
0626  E010  200F  100C  0000  9940  BF28  1F40  4572  0000
7FFF  7FFF  3000  7FFF  0000  3000
```

LOOP RECORD 0627

```
0627  E010  205F  1009  3340  AEC0  3520  FA56  4F1D  0000
7FFF  7FFF  2110  7FFF  0000  2110
```

LOOP RECORD 0628

```
0628  F010  21BF  F091  3800  A0C0  2B68  FF4F  19AD  0000
7FFF  7FFF  2110  7FFF  0000  2110
```

LOOP RECORD 0629

```
0629  8010  800F  0000  0000  91A0  4E20  0000  FEB9  0000
0000  0000  8000  0000  0000  800C
```

LOOP RECORD 0630

```
0630  8620  5000  0601  0014  032A  FF01  5709  5740  5776
579F  56FE  5707  5713  5758  5775  5785  5779  56F7  56F7
578F  577D  5738  5735  570F  5785  5757  5793  5796  573D
573F  56EA
```

LOOP RECORD 0631

0631 8620 5000 0602 100C 032A E101 43BF 436A 4384
43AB 4347 42F2 4304 42EB 42BB 4364 4392 4375 4309
437C 42CD 4334 42DF 4302 42D5 42C8 4236 430E 432F
43B6 42EF

LOOP RECORD 0632

0632 8620 5000 0603 000F 032A E101 45DF 44CB 4532
47AE 475C 47BE 47F0 41BB 4152 4168 417A 411E 416C
4255 4324 4276 422A 42BF 42DD 4282 429A 4573 459B
447D 4592

LOOP RECORD 0633

0633 8620 5004 0604 0012 032A E101 2A77 2A0B 29D2
29AF 299B 297A 295C 2939 290F 290A 2803 2AEA 2AF7
2ABB 2AA1 2ABD 2A97 2ABB 2AB6 2AAB 2A8D 2AA6 2A60
2A60 2A54

LOOP RECORD 0634

0634 8620 8000 0607 0012 0329 FF1D 0549 045C 04E4
038C 031A 009F 01BF 0327 050E 070C 07AF 0221 0221
0221 0221 0221 0221 0221 0221 0221 0221 0221 0414
055E 0497

LOOP RECORD 0635

0635 8620 8000 0609 000D 0329 FF1D FEB9 FEB9 FEB9
FEB9 FEB9 FEB9 FEB9 FEB9 FEB9 FEB9 FEB9 FEB9 FEB9
FEB9 FEB9 FEB9 FEB9 FEB9 FEB9 FEB9 FEB9 FEB9 FEB9
FEB9 FEB9

LOOP RECORD 0636

0636 8620 5004 0628 0008 032A E101 19AA 1915 1913
1912 1912 1910 1910 190D 1917 191C 1924 192E 1930
1935 1939 193E 1948 194A 1959 1963 1973 1978 1988
198E 199E

APPENDIX F

CONTROL SUBROUTINES FOR SP, AP AND PI CONTROL

The control algorithms were implemented as shown in Fig. E-1 in Appendix E. The current value of the controlled variable was obtained every sampling instant from the appropriate DDC loop, the control action calculated using one of the subroutines shown in Appendix F and output to the DDC flow control loop. SMITH contains the algorithm for SP, ANPRE for AP and PICO for PI control. The FORTRAN listings show that neither the SP nor the AP require an excessive amount of computation.

```
      SUBROUTINE SMITH(U,CX,CM1,CM2,SUM,KC,TI,TS,R,B,CE,GM,BETA,ALPHA,
     + DOLD,NC,KTD,JS,USS,OUTL)
      REAL KC
      DIMENSION SYMB(40)
C  J = INDEX OF U KTD+1 SAMPLING TIMES BACK
C  NC = CURRENT STORAGE LOCATION OF U
      READ(38'JS)(SYMB(I),I=1,40)
      NOLD=NC-1
      IF(NOLD)21,21,22
   21 NOLD=40+NOLD
   22 U=SYMB(NOLD)
      J=NC-KTD-1
      IF(J)10,10,11
   10 J=40+J
   11 JI=J-1
      IF(JI)12,12,13
   12 JI=40+JI
   13 CONTINUE
      UPAST=SYMB(J)
      UOLD=SYMB(JI)
C  PREDICTOR
   35 CM2=CM2*B+B*GM*(1./CE-1.)*UOLD  +GM*(1.-B/CE)*UPAST
C  MODEL
      CM1=CM1*B+GM*(1.-B)*U
C  LOADPREDICTOR
      D=CM2-CX
      P=D+ALPHA*TS*(KTD+BETA)*(D-DOLD)
      DOLD=D
C  CONTROL

      E=R-CM1+P
      SUM=SUM+E
      U=KC*(E+TS/TI*SUM)
      U=U+USS
C    SETS OUTPUTLIMITS
      IF(U-OUTL)23,23,24
   24 U=OUTL
   23 CONTINUE
      IF(U-1.)26,25,25
   26 U=1.
   25 CONTINUE
C  STORES NEW U
      SYMB(NC)=U
      JNEW=JS+NC-1
      WRITE(38'JNEW)SYMB(NC)
      NC=NC+1
      IF(NC-40)15,15,16
   16 NC=1
   15 CONTINUE
      U=U-USS
      RETURN
      END
```

```
      SUBROUTINE ANPRE(U,CX,CXO,DK,KC,KI,TS,R,A,B,CE,
     + GM,NC,KTD,JS,USS,OUTL)
      REAL KC,KI
      DIMENSION SYMB(40)
C  SYMB=STORAGE FOR PAST U VALUES
C  NC=CURRENT STORAGE FOR U
C  J=STORAGE KTD+1 SAMPLING TIMES BACK
      READ(38'JS) (SYMB(I),I=1,40)
      NOLD=NC-1
      IF(NOLD)21,21,22
   21 NOLD=40+NOLD
   22 U=SYMB(NOLD)
      J=NC-KTD-1
      IF(J)10,10,11
   10 J=40+J
   11 JI=J-1
      IF(JI)12,12,13
   12 JI=40+JI
   13 CONTINUE
C   CALCULATES DK FOR BUMPLESS TRANSFER ON FIRST PASS
      IF(DK)30,31,30
   31 DK=(CX-GM*USS)/GM
      U=0.
      RETURN
   30 CONTINUE
C  PREDICTOR
      CM=B*CXO+GM*(1.-B/CE)*(SYMB( J )+DK)+GM*B/CE*(1.-CE)*
     + (SYMB( JI )+DK)
      CXO=CX
C  INTEGRAL TERM
      DK=DK+KI*TS*(CX-CM)
C  PREDICTED OUTPUT
      IF(KTD)6,6,14
   14 CONTINUE
      SUM=0.0
      DO 7 L=1,KTD
      NP=NC-L
      IF(NP)17,17,27
   17 NP=40+NP
   27 CONTINUE
      SUM=SUM+B**(L-1)*(SYMB( NP  )+DK)
    7 CONTINUE
      CP=CX*CE*B**KTD+GM*(1.-B)*SUM+GM*(1.-CE)*B**KTD*(SYMB( J )+DK)
      GOTO 8
C  FOR FRACTIONAL DEADTIME
    6 CP=CX*CE+GM*(1.-CE)*(U+DK)
C  CONTROL
    8 PK=R*(1.+1./(KC*GM))
      U=KC/(1.+KC*GM*(1.-A))*(PK-A*CP)-DK
C   SETS OUTPUTLIMITS
      IF(U-OUTL)23,23,24
   24 U=OUTL
```

```
   23 CONTINUE
      IF(U-1.)26,25,25
   26 U=1.
   25 CONTINUE
C  STORES NEW U
   JNEW=JS+NC-1
   SYMB(NC )=U
   WRITE(38'JNEW)SYMB(NC)
   NC=NC+1
   IF(NC-40)15,15,16
16 NC=1
15 CONTINUE
   U=U-USS
   RETURN
   END
```

```
   SUBROUTINE PICO(U,X,R,KC,TI,TS,SUM,USS,OUTL)
   REAL KC
   ERR=R-X
   SUM=SUM+ERR
   U=KC*(ERR+TS/TI*SUM)+USS
C  SETS OUTPUTLIMITS
   IF(U-OUTL)1,1,2
 2 U=OUTL
 1 IF(U-1.)3,4,4
 3 U=1.
 4 U=U-USS
   RETURN
   END
```

APPENDIX G

TYPICAL STEADY STATE OPERATING CONDITIONS OF THE DISTILLATION COLUMN

The steady state operation of the distillation column before and after control runs could be verified by performing a mass balance around the column using program DASS. The program also provides a means to ensure that constant operating conditions are used over longer periods of time. Appendix G shows the report generated for typical steady state conditions. For details on the program the reader is referred to Liesch (18).

STEADY STATE DATA
RUN NO AP#31
15/04/76

FEED FLOW	18.03G/SEC	BOTTOM PROD	9.06G/SEC
REFLUX FLOW	15.71G/SEC	TOP PROD	8.76G/SEC
STEAM FLOWW	14.73G/SEC	COOL WATER	242.92G/SEC
FEED PLATE	4	FEED COMP	50.00WT% MEOH *
DIST COMP	96.63WT% MEOH	BOTTOMS COMP	5.00WT% MEOH
FEED INLET	71.8DEG C	REFLUX INLET	59.8DEG C #
STEAM TEMP	106.1DEG C	PRESSURE	-29.0KPA

MATERIAL BALANCE

	FLOW (G/SEC)	COMP (WT PCT)	METHANOL (G/SEC)	WATER (G/SEC)
FEED	18.03	50.00	9.01	9.01
BOTTOM PRODUCT	9.06	5.00	0.45	8.61
TOP PRODUCT	8.76	96.63	8.47	0.29
CLOSURE ERROR-PC	-1.0		-0.9	-1.1

ENERGY BALANCE

	ENTHALPY IN (KJ/SEC)	ENTHALPY OUT (KJ/SEC)
COOLING WATER	13.83	36.94
REFLUX	2.80	2.85
TOP PRODUCT		1.59
FEED	4.71	
STEAM	39.70	6.53
BOTTOM PRODUCT		3.47
TOTAL	61.05	51.40
HEAT LOSS		9.6

Loop inoperable

* Entered off-line

STEADY STATE CONDITIONS BASED ON 20 POINTS
RUN NO AP#31 15/04/76

FEED FLOW	= 18.033	G/SEC	DEV= 0.0285
REFLUX FLOW	= 15.710	G/SEC	DEV= 0.1061
STEAM FLOWW	= 14.739	G/SEC	DEV= 0.1908
BOTTOM PROD	= 9.067	G/SEC	DEV= 0.1718
TOP PROD	= 8.768	G/SEC	DEV= 0.2421
COOL WATER	=242.925	G/SEC	DEV= 5.0941
DIST COMP	= 96.637	WT% MEOH	DEV= 0.1216
BOTTOMS COMP	= 5.000	WT% MEOH	DEV= 0.0000
FEED COMP	= 50.000	WT% MEOH	DEV= 0.0000
PRESSURE	=-29.072	KPA #	DEV= 0.6830
COND LEVEL	= 18.476	CM	DEV= 0.0443
REB'R LEVEL	= 49.127	CM	DEV= 1.8997
DIFF PRESS	= -4.268	KPA #	DEV= 0.1703
REB'R O'HEAD	= 91.9	DEG C	DEV= 0.1439
PLATE 1 TEMP	= 81.3	DEG C	DEV= 0.3450
PLATE 2 TEMP	= 75.4	DEG C	DEV= 0.2368
PLATE 3 TEMP	= 159.9	DEG C	DEV= 0.2084
PLATE 4 TEMP	= 72.0	DEG C	DEV= 0.1010
PLATE 5 TEMP	= 67.7	DEG C	DEV= 0.1001
PLATE 6 TEMP	= 65.2	DEG C	DEV= 0.1065
PLATE 7 TEMP	= 63.7	DEG C	DEV= 0.1072
PLATE 8 TEMP	= 62.4	DEG C	DEV= 0.0925
COND TEMP	= 60.8	DEG C	DEV= 0.1017
STEAM TEMP	= 106.1	DEG C	DEV= 0.1539
COND'T TEMP	= 105.0	DEG C	DEV= 0.1730
REFLUX TEMP	= 49.4	DEG C	DEV= 0.1069
FEED TEMP	= 35.8	DEG C	DEV= 0.1028
BOTTOMS TEMP	= 57.1	DEG C	DEV= 0.1072
REB'R TEMP	= 91.8	DEG C	DEV= 0.1632
FEED INLET	= 71.8	DEG C	DEV= 0.1256
REFLUX INLET	= 59.8	DEG C	DEV= 0.5574
COL O'HEAD	= 62.7	DEG C	DEV= 0.0942
WATER INLET	= 13.6	DEG C	DEV= 0.0755
WATER OUTLET	= 36.3	DEG C	DEV= 0.1509

Loop inoperable

APPENDIX H

T-X DIAGRAMS FOR THE METHANOL-WATER SYSTEM

For a binary mixture the thermodynamic relationship between the composition and its boiling point at a given pressure can be represented in a T-X diagram. Fig. H-1 shows a comparison of T-X curves for the methanol-water system at different pressures with experimental data from the column. The literature data were calculated from partial pressure data reported in the Handbook of Chemistry and Physics*. The pressure P at the location of the temperature probe could not be measured, but it could be calculated from the atmospheric pressure $P_{Atm.}$, the pressure drop ΔP in the column and the hydrostatic pressure P_{Hydro} of the liquid in the reboiler:

$$P = P_{Atm.} + \Delta P + P_{Hydro} \qquad (H.1)$$

ΔP was measured and found to be 25 ± 5 mm Hg, depending on the operating conditions. The liquid level in the reboiler was controlled, but not recorded. Estimated values are 50 ± 10 cm resulting in a hydrostatic pressure of approximately 35 ± 7 mm Hg. Considering the atmospheric pressure of roughly 700 mm Hg in Edmonton the pressure P at the location of the temperature probe was 760 ± 12 mm Hg. Thus the liquid at the temperature probe location was not at its boiling point, as can be seen from Fig. H-1. Presumably this was due to the fact that the temperature probe was located close to the point where liquid from the column enters the reboiler.

* Handbook of Chemistry and Physics, 57th Edition, p. D-179 and D-192

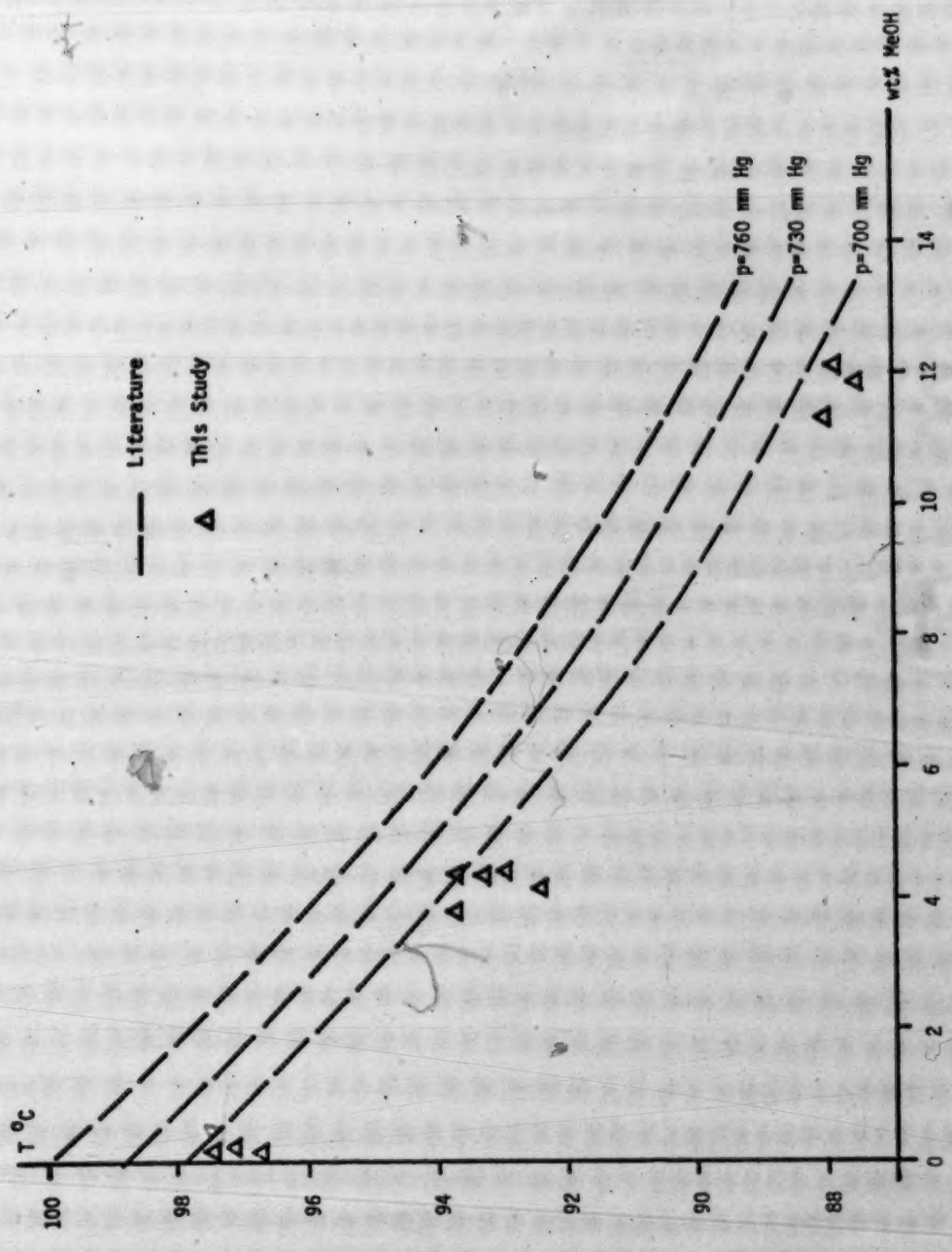

Fig. H-1 : T-X Diagram for the Methanol-Water System

Fig. H-1 also provides a means to estimate the changes in composition that can be expected at constant temperature due to variations in pressure. If atmospheric pressure changes of ± 15 mm Hg are considered, total pressure changes due to different atmospheric and operating conditions could be as high as ± 27 mm Hg. This would result in composition errors of up to ± 1% at constant temperature.